KINGSTON
UNIVERSITY

# Intrinsically Conducting Polyaniline Blends

A Thesis Submitted in Partial Fulfilment of the
Requirements of Kingston University for the
Degree of Doctor of Philosophy

**by**

**Zaid Kahtan Abbas**

Materials Research Group
School of Pharmacy and Chemistry
Penrhyn Road
Kingston upon Thames
Surrey
KT1 2EE

**March 2009**

## Abstract

The project involved the production of conductive polyanilines and their blending with elastomers to make new conducting rubbers. Conductive elastomers already have commercial applications such as antistatic coatings, artificial muscles, sensors and electromagnetic screening. These have been based on carbon black or metal fillers, or more recently conducting polymer powders incorporated into natural or synthetic rubbers. A number of polyaniline-rubber blends have been reported in the literature. A key aim of this project was to improve the compatibility, mechanical, thermal stability and electrical properties of this type of blend through different mixing methods such as solution and thermo-mechanical with more systematic mixing procedures and better optimised mixing conditions.

The first part of the work was to optimise the synthesis of conducting polyanilines (PAni), polyanisidines (PoAnis), and copolymers of the latter two, in the presence of a variety of protonating agents under a range of conditions, in order to study the influence of the synthetic conditions on the physical, chemical and morphological characteristics of the polymers. PAni/PoAnis products were prepared via solution polymerisation (simple oxidation at low pH) or via emulsion polymerisation using sulfonic acids (surfactants). Syntheses yielded the emeraldine salts (ES), which were either kept as such, or deprotonated using ammonia solution. There were noticeable differences in the behaviour of the two families of polymers.

PAnis display better conductivity and a higher thermal stability than PoAnis due to their less hindered structure. These differences in physical characteristics tend to fade when the compounds are synthesised using a protonic surfactant such as dodecylbenzenesulfonic acid (DBSA). Here, the surfactant-induced order of the final polymeric particles becomes dominant over that of the pendant methoxy-group of PoAnis. Scanning electron microscopy (SEM) revealed the strong influence of the protonic acid used for the synthesis on the shapes of the final particles. Hence, PAni-DBSA has a monoclinic appearance and rhombic shape particles while PAni-β-naphthalenesulfonic acid (β-NSA) has a "flakey" morphology. It was shown that a very small quantity of *co*-monomer could change drastically the physical characteristics of PAni; hence, when anisidine (Anis) is added to the aniline-acid complex, a different crystalline structure is achieved.

The chosen polymer (PAni-DBSA) was matched with two individual elastomers, one based on an ethylene oxide *co*-polymer and the other on a nitrile butadiene *co*-polymer, both of which had suitable solubility parameters. The polymers were solution-blended and studied for compatibility by means of microscopy, electrical conductivity measurements and thermal analysis.

Blends of poly (epichlorohydrin-*co*-ethylene oxide) rubber (Zeon Hydrin® C2000L) and polyaniline doped with dodecylbenzenesulfonic acid (PAni-DBSA), containing different weight fractions of PAni, were cast from solution. Solubility parameters for both PAni-DBSA and Hydrin® were calculated and found to be comparable, favouring some degree of miscibility. Conductive transparent films were formed by casting onto PTFE substrates. Conductivities of the cast films were found to be in the region of $10^{-7}$ S.cm$^{-1}$ for 1wt% PAni-DBSA. Electrical conductivities increased with the proportion of PAni-DBSA, showing a percolation threshold as low as 1wt%, with highest conductivity achieved at 50wt%. Decomposition steps of conductive blends were investigated using thermogravimetric analysis (TGA) and differential scanning calorimetry (DSC). The thermal stability of the

blends was influenced by the ratio of PAni-DBSA to Hydrin®. The effect of composition on the glass transition in the blends was determined using thermomechanical analysis (TMA).

Thin films of the blends of dodecylbenzenesulfonic acid (DBSA) doped polyaniline (PAni) and pure grade of Poly[(acrylonitrile-co-butadiene)/poly vinylchloride] (Zeon Nipol® DN171) were prepared via co-dissolution, at varying ratios of conducting filler (0.5-50)wt %. The electrical conductivity correlated with the concentration of PAni-DBSA. At a percolation threshold of 0.9% (wt/wt), an increase in electrical conductivity of approximately eight orders of magnitude was observed, with a recorded conductivity of $1.21 \times 10^{-4}$ $S.cm^{-1}$ for the most conductive blend (consisting of 50wt% PAni). Characterisation by UV-visible spectroscopy indicated the retention of the doped state of the conductive PAni-DBSA in each elastomer blend. Morphological studies by optical microscopy, showed the presence of PAni-DBSA agglomerate networks (or interpenetrating networks) at higher concentrations; however, at lower concentrations of PAni-DBSA, the dispersion and encapsulation of the conductive species was observed. Due to the double phase morphology of Nipol® DN171, the encapsulating phenomenon was attributed to the presence of the thermoplastic (poly vinylchloride). Solubility parameter calculations confirmed the compatibility of PAni-DBSA with the constituents of the Nipol® DN171 elastomer. This was supported by the infrared spectrum, which shows the presence of functional groups specific to the reacting components of each blend. Thermal studies, performed by DSC and TGA, indicated an increased thermal stability with increasing concentration of the elastomer.

## List of Papers and Conferences

- Zaid K. Abbas, Stephen J. Barton and Peter J. S. Foot. Intrinsically Conductive Polymers and Elastomers "Towards the Elasticity of Conducting Polymers". *European Postgraduate Industry Tour* (Royal Society of Chemistry), Germany& UK (2005).

- Zaid K. Abbas, Stephen J. Barton and Peter J. S. Foot. Towards the Conductivity of Elastomeric Materials "Conductive Blends of Polyaniline and Ethylene Oxide Copolymer". *Material Research conference Proceeding* (Institute of Materials, Minerals and Mining), London, United Kingdom 5-7 April (2006).

- Zaid K. Abbas, Stephen J. Barton, Peter J. S. Foot, H. Morgan. Conductive Polyaniline/Poly(Epichlorohydrin-*co*-Ethylene Oxide) Blends Prepared in Solution. *Polymers & Polymer Composites*, **15** (2007) 1.

- Zaid K. Abbas, Stephen J. Barton, Peter J. S. Foot. The Synthesis and Evaluation of Conducting Polyaniline/Poly[(Acrylonitrile-*co*- Butadiene)/Poly vinylchloride] Blends. Manuscript drafted (2008).

## Acknowledgment

I would like to express my sincerely thank to my research supervisors Dr. Stephen Barton and Prof. Peter Foot for their invaluable help, guidance, encouragement and friendship during both the practical work and the preparation of this thesis. I wish to thank Kingston University for providing me with research facilities and for funding this project. All my thanks to the Polymer Centre at London Metropolitan University who gave me the opportunity to carry out the thermal mixing of the conducting polymer with the elastomer.

I am also indebted to my colleagues, past and present, in laboratory (EM211) and laboratory (GO1) for their discussions and constructive comments particularly Bassem Sabagh, Cyrille Allais, Moayad Almasri, Hugh O'Malley, Baljet, Kevin and Wendy.

The research presented in this thesis wouldn't have been possible without the assistance of the technical staff. I would like to thank particularly Mrs J. Falla and Mr P. Stovell from the spectroscopy laboratory, Richard Giddens for the countless hours he spent with me looking at my samples under the scanning electron microscope and Simon DeMars for his help and advice on thermal analysis.

Finally, I would like to dedicate this thesis to my family in recognition of all their help, encouragement and support throughout my education.

## Table of Content

# List of Figures and Tables

## List of Abbreviations and Symbols

### Chemicals and Products

| | |
|---|---|
| APS | ammonium peroxydissulfate |
| β-NSA | beta-naphthalenesulfonic acid |
| CSA | camphorsulfonic acid |
| DBSA | dodecylbenzenesulfonic acid |
| EB | emeraldine base |
| ES | emeraldine salt |
| $FeCl_3$ | iron (III) chloride |
| $H_2O$ | de-ionised water |
| HCl | hydrochloric acid |
| MeSA | methanesulfonic acid |
| $NH_3$ | ammonia |
| NMP | N-methylpyrrolidinone |
| p-TSA | para-toluenesulfonic acid |
| Nipol DN171 | poly[(acrylonitrile-*co*-butadiene)/poly vinylchloride] |
| PAni | polyaniline |
| PoAnis | polyanisidine |
| Epi-EO | poly(epichlorohydrin-*co*-ethylene oxide) |
| THF | tetrahydrofuran |

### Units

| | |
|---|---|
| wt % | weight percentage |
| A | ampere |
| Å | Ångstrom |
| g | gram |
| h | hour |
| l | litre |

| | |
|---|---|
| M | metre |
| M | molar |
| mol | mole |
| ° | degree (angle) |
| °C | degree Celsius |
| S | siemens |
| V | volt |
| v/v | volume per volume |
| w/v | weight per volume |
| w/w | weight per weight |
| Ω | ohm |
| nm | nanometre |
| µm | micrometre |

**Symbols**

| | |
|---|---|
| σ | conductivity ($S.cm^{-1}$) |
| λ | wavelength (nm, Å…) |
| pH | potential Hydrogen |
| $M_W$ | molecular weight ($g.mol^{-1}$) |
| A | absorbance |
| θ | Bragg angle (°) |
| Ø | diameter (m) |
| d | layer spacing (Å) |
| L | domain length (Å) |

# CHAPTER 1

# INTRODUCTION

*In the first part of this Chapter, following generalities on polymers, a review is presented of some principles and theories, which detail the important aspects of conjugated polymers with regards to the electronic structure and bonding of the polymer chain. Fundamental issues related to their processibility. This thesis is especially concerned with a family of conducting polymers called polyaniline (PAni). Hence, their development, preparation and typical properties will be reviewed in the second part of this chapter. Particular attention is given to the emeraldine form of polyaniline and its transition to conductive behaviour upon protonation with acid species. Aims of the present research are outlined at the end of this chapter.*

# 1 Introduction

## 1.1 The Nature of Polymers

### 1.1.1 Polymers: From a Structural Perspective

The simple image of a chemical reaction is that under certain conditions, two reactants ***A*** and ***B*** react to form a new compound ***C***. Some compounds are capable of reacting with themselves; in which case, C can be a finite molecule (ring forming reactions) or in other cases a molecule that could carry on reacting with another molecule of the starting material. This type of compound is called a ***monomer***, and if extensive reaction is favoured, it will be converted into a short chain of the same monomer units forming an ***oligomer*** and eventually to a much larger molecule of n repeat units called a ***polymer***. The process in which this reaction takes place is called ***polymerisation***. The term "polymer" is derived from the Greek words: '***poly***' meaning many, and '***meros***' meaning parts. The key feature that distinguishes polymers from other molecules is the repetition of many identical, similar, or complementary molecular subunits (monomer) in these chains.

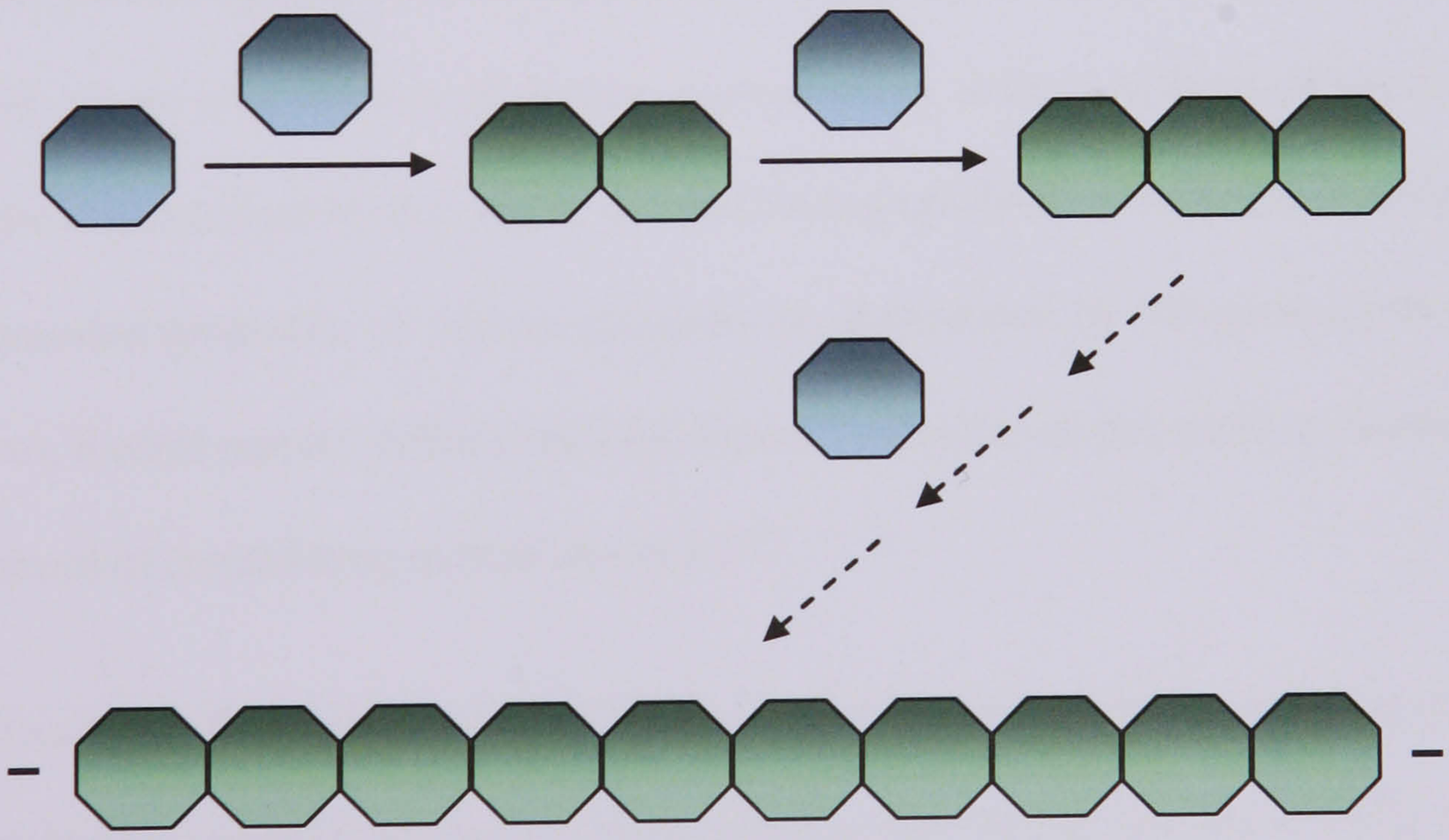

Figure 1 Basic view of the polymerisation reaction.

### 1.1.2 The Classification of Polymers

There are three types of classifications that are commonly used in order to distinguish between various polymers or polymer configurations, and these are based on their ***skeletal structures, monomer chemical type*** or their ***micro-structure***.

The skeletal structure of a polymer may be further classified as (a) ***linear***, (b) ***branched***, or (c) ***crosslinked or networked*** as shown in the illustrative diagrams Figure 2

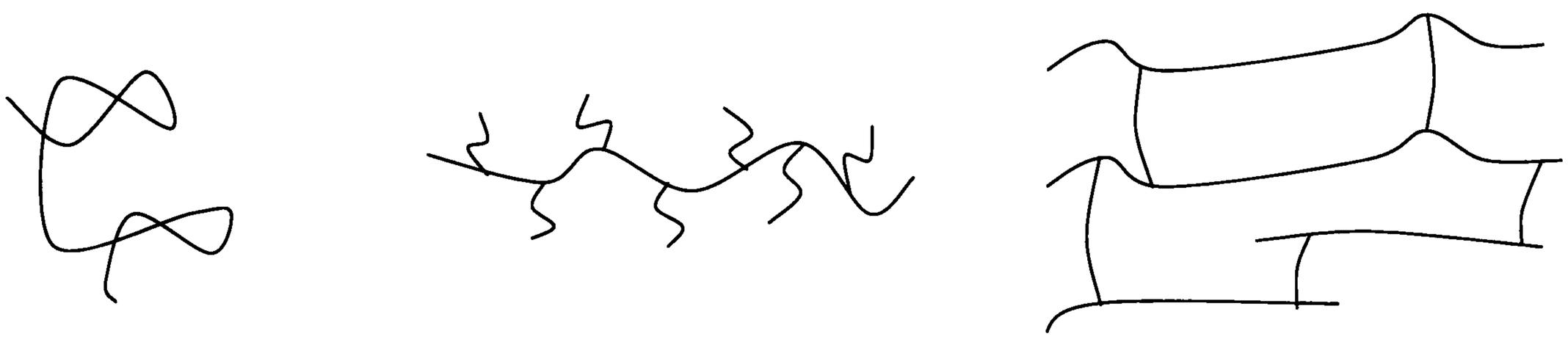

(a) (b) (c)

Figure 2 Representation of polymer type.

Monomers when arranged in a long chain form linear polymers. Branched polymers comprise long chain monomer arrangements with covalently bonded side chains or branches at various junction points. Cross-linked or network polymers involve the connection of the monomer of one chain to that of another corresponding chain by a series of junction points, which are characterised by the degree of crosslinking involved. In addition, it is obvious that the impressive properties of various polymers are determined by variations in their skeletal structures. Recent reports indicate the high thermal stabilities of polymers as characteristic of the presence of crosslinking in their structures [1].

The second classification of polymers which is based on the monomer chemical type, are (a) ***Homopolymers*** and (b) ***Copolymers***. Homopolymers are formed as a result of the reaction of one type of monomer specie (A), while copolymers consist of two or more monomer species (A, B and C represent hypothetical monomers) as shown in Figure 3.

-A-A-A-A-A-A-A-A-A-

(a)

-A-B-C-A-B-C-A-B-C-A-B-C-

(b)

Figure 3 Representation of (a) homopolymer, (b) copolymer.

Copolymers may be classified further into four categories as illustrated in (Figure 4). These classifications are based on the arrangements of the different species of monomers (A and B) in the polymer chain [2].

(I) **Alternating copolymers** -A-B-A-B-A-B-A-B-A-B-A-B-A-B-A-

(II) **Block copolymers** -A-A-A-A-B-B-B-B-A-A-A-A-B-B-B-

(III) **Random copolymer** -A-A-B-B-B-A-B-B-A-B-A-BB-A-B-

(IV) **Graft copolymers**

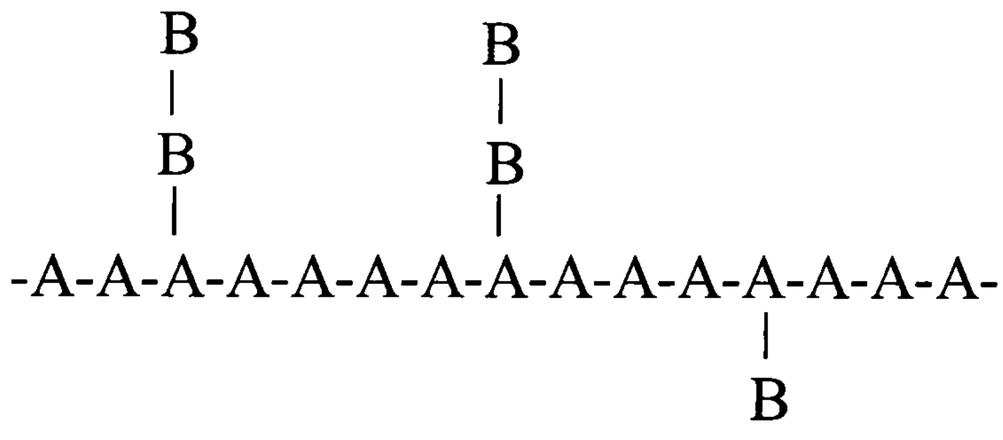


Figure 4 Schematic representation of (I) Alternating, (II) Block (III) Random, and (IV) Graft copolymers.

In addition, it is important to emphasise the fact that both block and graft copolymers exhibit properties which are unique to each of the constituent homopolymers, in contrast to random and alternating copolymers. These special properties arise due to the chemical linkages formed within each sequence of homopolymers and thereby promoting cooperative interactions between the polymer chains [3].

The microstructure (that is, the microscopic arrangements of the polymer chains) also plays an important role in determining their mechanical properties. The microstructure of polymers can be described as ***amorphous*** or ***semi-crystalline***. Amorphous polymers do not possess any order within their structures, and therefore the arrangements of the chains are of a random nature. Conversely, polymers with structures which are partially organised are referred to as semi-crystalline polymeric materials. Both amorphous and semi-crystalline polymers have been studied over the years with their mechanical properties as the main focal point [4,5,6].

### 1.1.3 Polymerisation Processes

Polymers can be prepared via two common methods of synthesis [7], ***step growth*** (condensation) and ***chain growth*** (addition) reactions.

#### *1.1.3.1 Step Growth (Condensation) Polymerisation*

This type of polymerisation proceeds as the name suggests in a stepwise reaction, and in general can be shown as:-

$$A\text{-}A + B\text{-}B \longrightarrow \text{-}[\text{-}A\text{-}A\text{-}B\text{-}B\text{-}]\text{-}$$

In general condensation polymerisation involves the elimination of small molecules (e.g. the reaction of an alcohol and an acid resulting in elimination of water), or it contains functional groups as a part of the polymer chain. Any polymer made this way increases in size and hence molecular weight very slowly as in the first stages of the polymerisation, most of the monomers will react to form dimers which then continue to react with any remaining monomers to produce trimers and tetramers etc. An example of condensation polymerisation is the reaction between 1,4-benzenedicarboxylic acid and 1,4-butanediol to produce polyethylene terephthalate (polyester) and water.

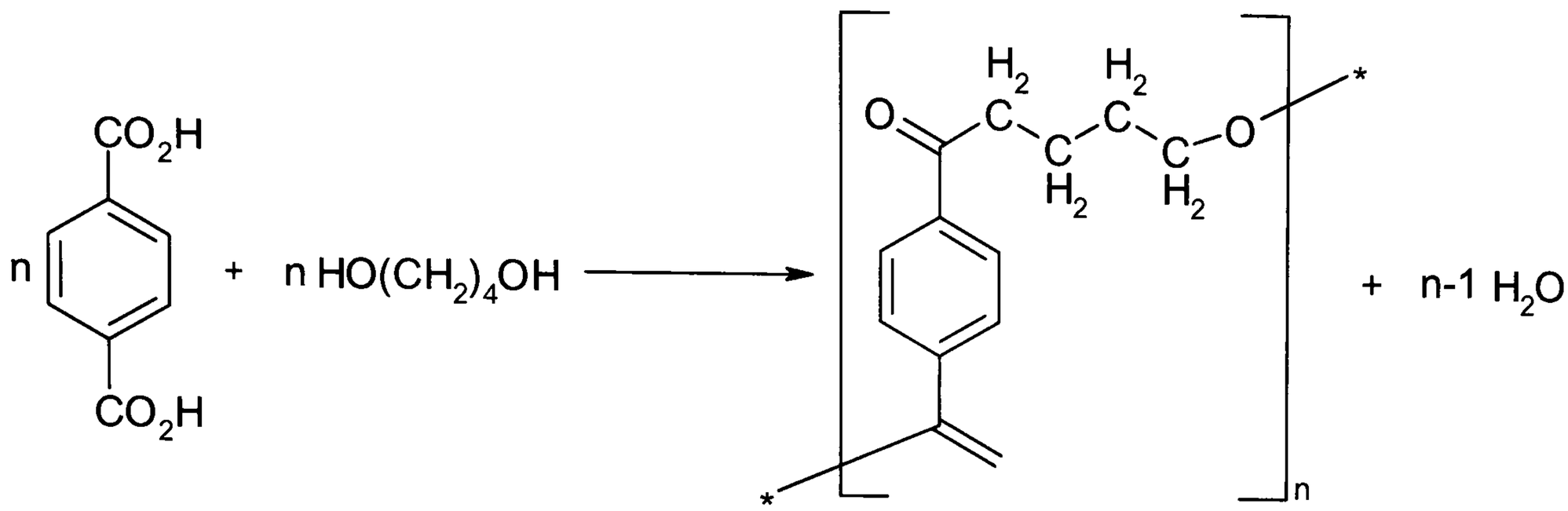

Figure 5 Example of condensation polymerisation.

### *1.1.3.2 Chain Growth (Addition or Free Radical) Polymerisation*

This method is sometimes used in the manufacture of conducting polymers. Addition polymerisation consists of three distinct steps: ***initiation***, ***propagation*** and ***termination***. An initiator reacts with a monomer to produce a radical species which can then react with another monomer extending the chain. The growth of the chain terminates either when the monomer is exhausted or when two free radicals react, removing the polymers, ability to grow. Chain polymerisation can be generalised as seen below and is most commonly observed in vinyl polymers such as poly (vinyl chloride).

| | |
|---|---|
| **Initiation** | $I \rightarrow I^*$, $I^* + M \rightarrow I\text{-}M^*$ |
| **Propagation** | $I\text{-}(\text{-}M\text{-})^*n\text{-}1 + M \rightarrow I\text{-}(\text{-}M\text{-})^*n$ |
| **Termination** | $I\text{-}(\text{-}M\text{-})^*n + T \rightarrow I\text{-}(\text{-}M\text{-})^*n - T$ |

Addition polymerisation has the advantage over condensation polymerisation due to a quicker reaction producing a greater yield. The rate of molecular weight increase in these reactions depends on the rate of initiation, propagation and termination. In many cases after initiation, the polymerisation proceeds very quickly to form a high molecular weight polymer. This is an advantage when the polymer is insoluble in the reaction solution.

## 1.2 Conducting Polymers

### 1.2.1 Historical Review: Polymers from Insulator to Conductor

Synthetic polymers were first produced in the late 19th century, but were not developed for industrial use until the 1940's and 50's. These polymers had many potential uses, due to their ease of fabrication, low cost of production, plasticity and toughness. They also possessed high electrical resistance and were therefore used mainly as insulators in electrical applications.

The term 'electrical conduction' is usually assigned to metals or alloys. Polymers with the inherent properties of semiconductors and metals are a relatively recent development. These new materials, also known as "organic synthetic metals", combine the conductive properties of metals and have the added advantages of being light weight, easy to handle and low cost of production [8,9]. The award of the Chemistry Nobel Prize in 2000 to Shirakawa, MacDiarmid, and Heeger recognised the discovery of conducting polymers.

Intrinsically conducting polymers (ICP's) conduct because the electrons are delocalised in the conjugated structure. This in turn brings insolubility and infusibility to the polymers, resulting in poor processibility. A number of different methods have been developed to improve the processibility of conducting polymers. These methods include block copolymerisation [10], increase of chain flexibility via incorporation of flexible centres in the main chain [11], side

chain substitution by the addition of different side groups to the polymer backbone [12], use of processible precursor polymers [13], and the formation of polymer blends [14].

### 1.2.2 Classification of Conducting Polymers

Conducting polymers are usually categorised into two main groups based on their ***electric transport***. The first group includes polymers that exhibit ionic conduction. They are often called '***polymer electrolytes***' or '***polymer ionics***'. Polyethylene oxide, in which lithium ion is mobile, is a typical example. The second group of ***intrinsically conducting polymers*** or ***conjugated polymers*** are those materials that exhibit electronic conduction [15].

### 1.2.3 Common Structure of Conducting Polymers

The principal structural feature of conducting polymers is the conjugation of carbon $p_z$ orbitals. In other words, there is an alternation of single bonds and double bonds in a carbon-carbon chain. The structures of some common conducting polymers are shown in Figure 6.

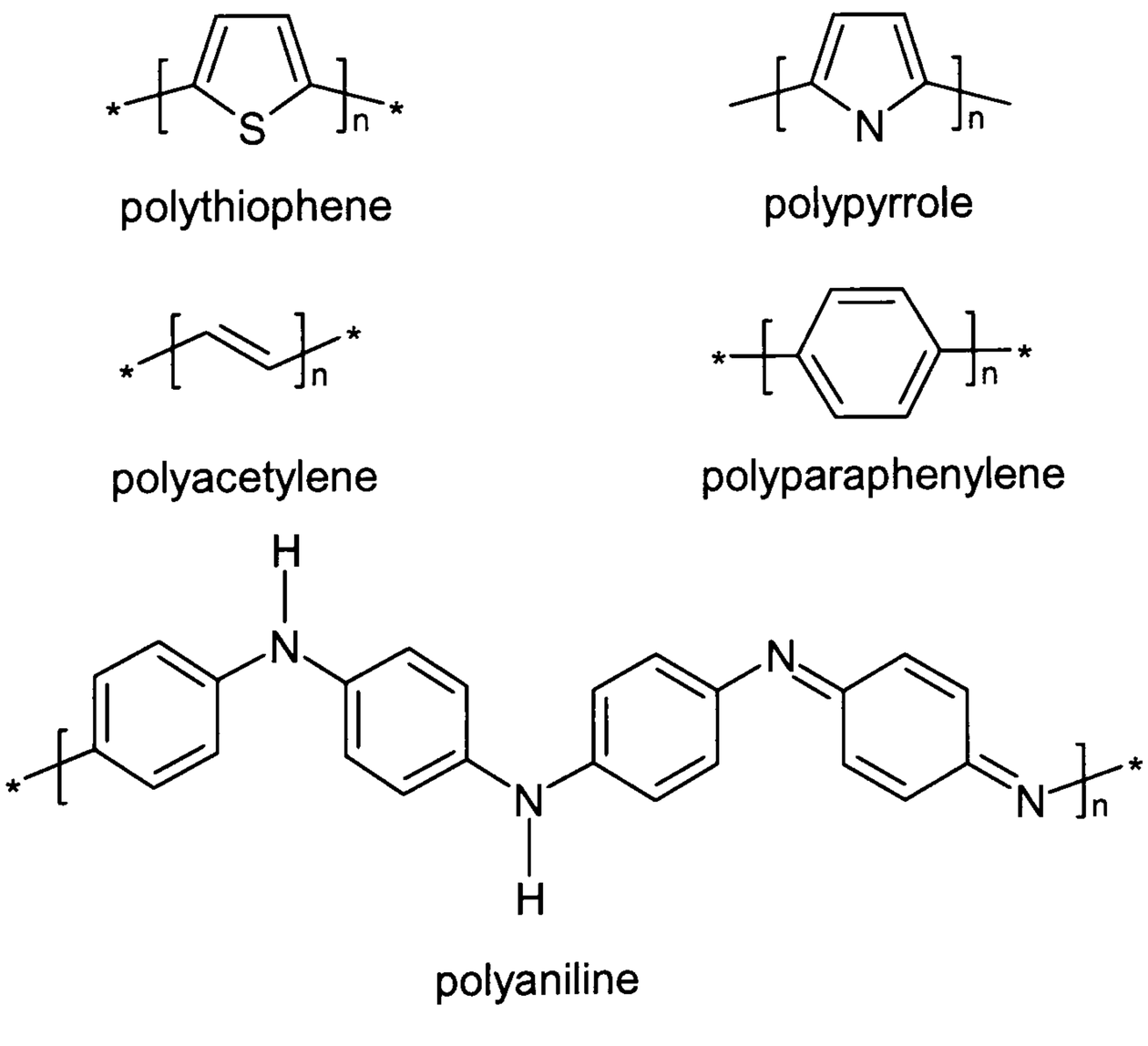


Figure 6 Structures of some examples of conjugated polymers.

### 1.2.3.1 Polyacetylene

Polyacetylene has been the most theoretically [16] and experimentally studied conducting polymer, owing to its simplistic conjugated structure and high conductivity ($10^4$-$10^6$ S.cm$^{-1}$), which is comparable to that of a metal [17]. Most research on polyacetylene has been focussed on the ***'Shirakawa' type***, which is synthesised via the Ziegler-Natta polymerisation of acetylene [18,19]. In the late 1950's polyacetylene was synthesised as a black powder by Natta [20]. It was found that this polymer had the characteristics of a semi-conductor, with conductivity between $10^{-9}$ and $10^{-1}$ S.cm$^{-1}$, depending on how the polymer was synthesised [21].

In 1967, when a postgraduate student of Shirakawa at Tokyo Institute of Technology attempted to synthesise polyacetylene, a silvery film was produced, and upon investigation it was found to be a semiconductor with a similar degree of conductivity to the black powders previously synthesised [22]. Shirakawa continued the investigation of the conducting polymer, by exposing a thin film of polyacetylene to halogens, resulting in a billion-fold enhancement of its conductivity [23]. Undoped polyacetylene was described as silvery, insoluble and intractable, with conductivity similar to that of semi-conductors [24]. but upon the introduction of an oxidising agents such as iodine to the polymer, there was a change in the colour from silver to gold and an enhancement in the conductivity to $10^4$ S.cm$^{-1}$ [25].

Polyacetylene is formed as two isomers, ***(E)*** and ***(Z)***, of which the *(E)* form is the more conducting and thermodynamically stable. The relative proportions of the two isomers depend upon the reaction temperature, solvent and the nature of the catalyst. By varying the catalyst concentration and the solvent, it is possible to obtain polyacetylene as a gel, powder, or thin film [26].

Polyacetylene produced by this method has two main disadvantages: the electrical conductivity decays rapidly upon exposure to air and the polymer is entirely intractable. The polymer has a low stability in air, specifically when oxidised [18], due to the fact that oxygen reacts with it to form carbonyl, hydroxyl and epoxide groups, which break the conjugated π-system that is so important to conducting polymers [27]. The Shirakawa synthesis was modified by the 'Naarmann process', which resulted in an improvement in its environmental stability [28]. In addition, this process yields materials with the highest known electrical conductivity per unit weight [28].with the exception of superconductors.

### *1.2.3.2 Polyheterocycles as Conducting Polymers*

The synthesis of polyacetylene in the highly conducting doped form created a surge of investigations into the synthesis and characterisation of these materials [29]. In the 1980's polyheterocycles were found to have more stability in air than polyacetylene, and despite the fact that their conductivities were not as high as polyacetylene, interest in this area increased.

Electrodeposition of free standing films of polypyrrole from organic media [30] opened the way to intensive research into polyheterocyclic and polyaromatic conducting polymers [31]. The electrochemical oxidation of these resonance-stabilised aromatic molecules has become one of the principal methods of preparing conjugated, electronically conducting polymers. At present, a wide range of polyheterocycles have been synthesised and characterised: such systems include polyaniline (PAni) [32], polythiophene (PT) [33], polypyrrole (PPY) [34], polyfuran (PFU).

Although the polymers mentioned above share many structural similarities, they have a wide range of conductivity values depending on the doping concentration, the nature of the doping, the temperature of the synthesis reaction, the nature of the oxidant, the alignment of the polymer chains and the purity of the samples.

## 1.3 Requirements for Intrinsic Conductors

### 1.3.1 Electronic Structure of Conjugated Polymers

The principal feature of conducting polymers is a π-π* band structure. The overlap of bonding orbitals produces the valence band. Non-bonding states form the conduction band. For instance, extended overlap of π-bands forms the valence band and π* bands the conduction band. The bands are separated by a bandgap. The energy of the bandgap determines the conductivity of materials (Figure 7). ***Conductive*** (overlapping bands), ***intrinsically semiconductive*** (< 1 eV) and ***insulating*** (> 3-5 eV).

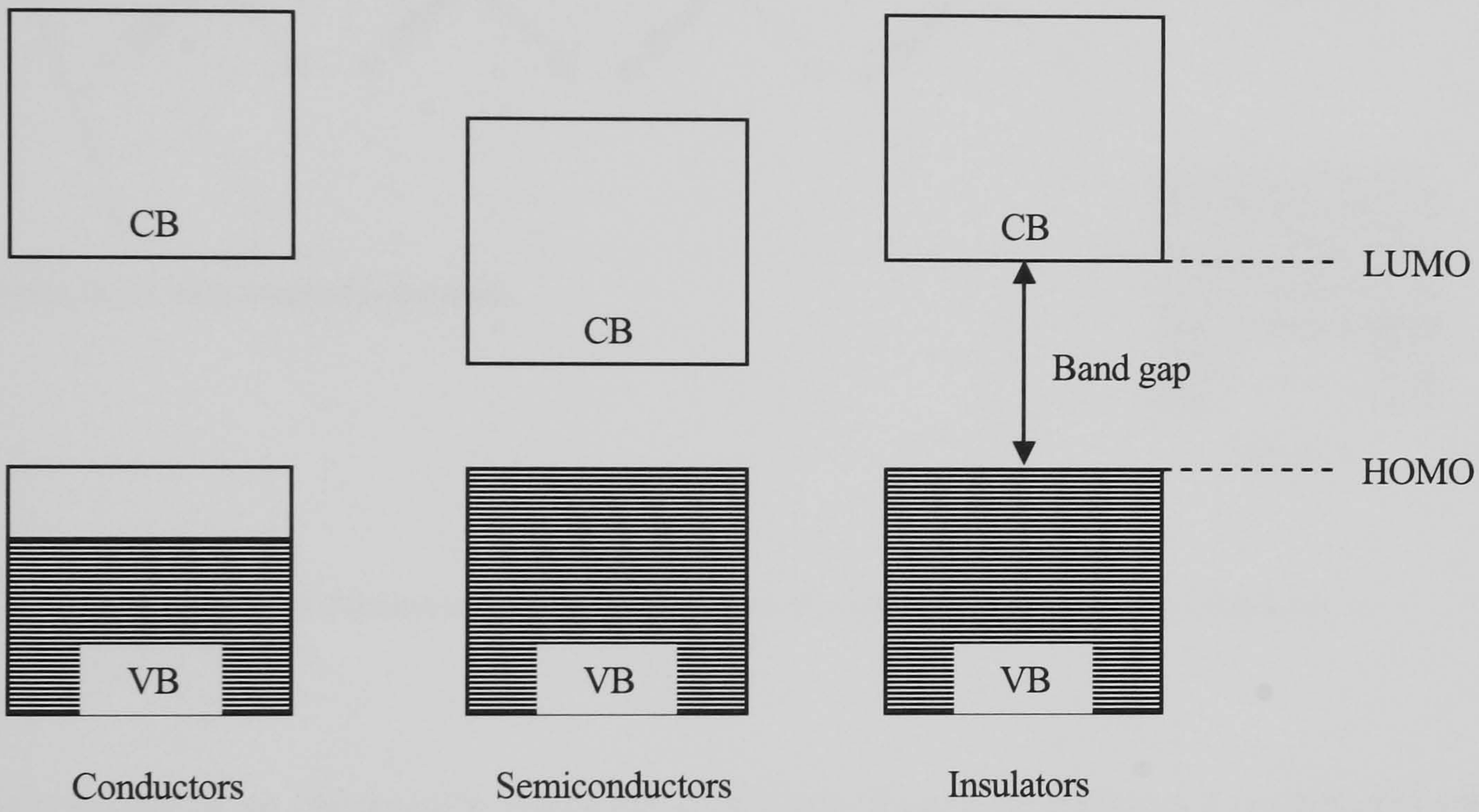


Figure 7 Energy band structure of conductors, semiconductors and insulators.

In the general concept of polymers (saturated polymers), the molecular orbitals responsible for C-C interaction are of the $sp^3$ sigma hybridized orbitals. In this type of hybridisation, all four electrons of the valence band for the carbon are used up in sigma bonds; therefore it is unsuited for extensive orbital overlap. This fact serves to localise the electrons between the bonding carbons, and results in the inability of the electrons to contribute to the conduction process. In terms of simple band theory, this type of bonding generates a large energy gap between the valence band and the conduction band, giving the polymer the characteristics of

a good insulator. This is illustrated in Figure 8 for polyethylene which is known to be an excellent insulator.

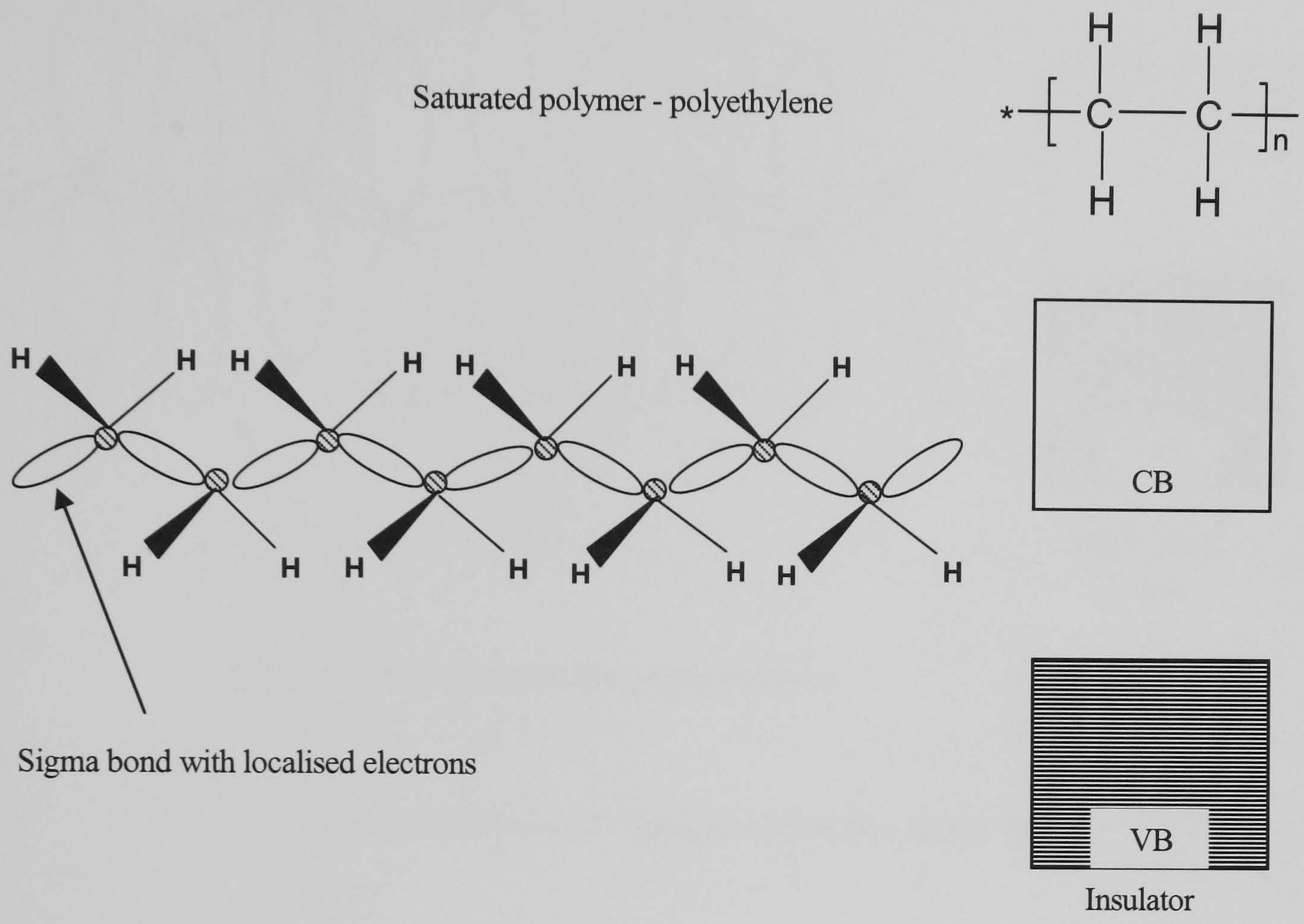


Figure 8 Saturated backbone structure of electrically insulating polyethylene.

The creation of an electrically conductive polymer therefore, requires a continuous system of atomic orbitals that can allow the formation of delocalised electronic states. This type of molecular array can be found in polymers that contain conjugated unsaturated bonds along their backbone. In this system, chemical bonding leads to one unpaired electron per carbon atom. Moreover, π-bonding, in which the carbon orbitals in the $sp^2p_z$ configuration and in which the $p_z$ orbital is oriented perpendicular to the polymer backbone and capable of overlapping with its neighbours (Figure 9), results in electron delocalisation along the backbone of the polymer.

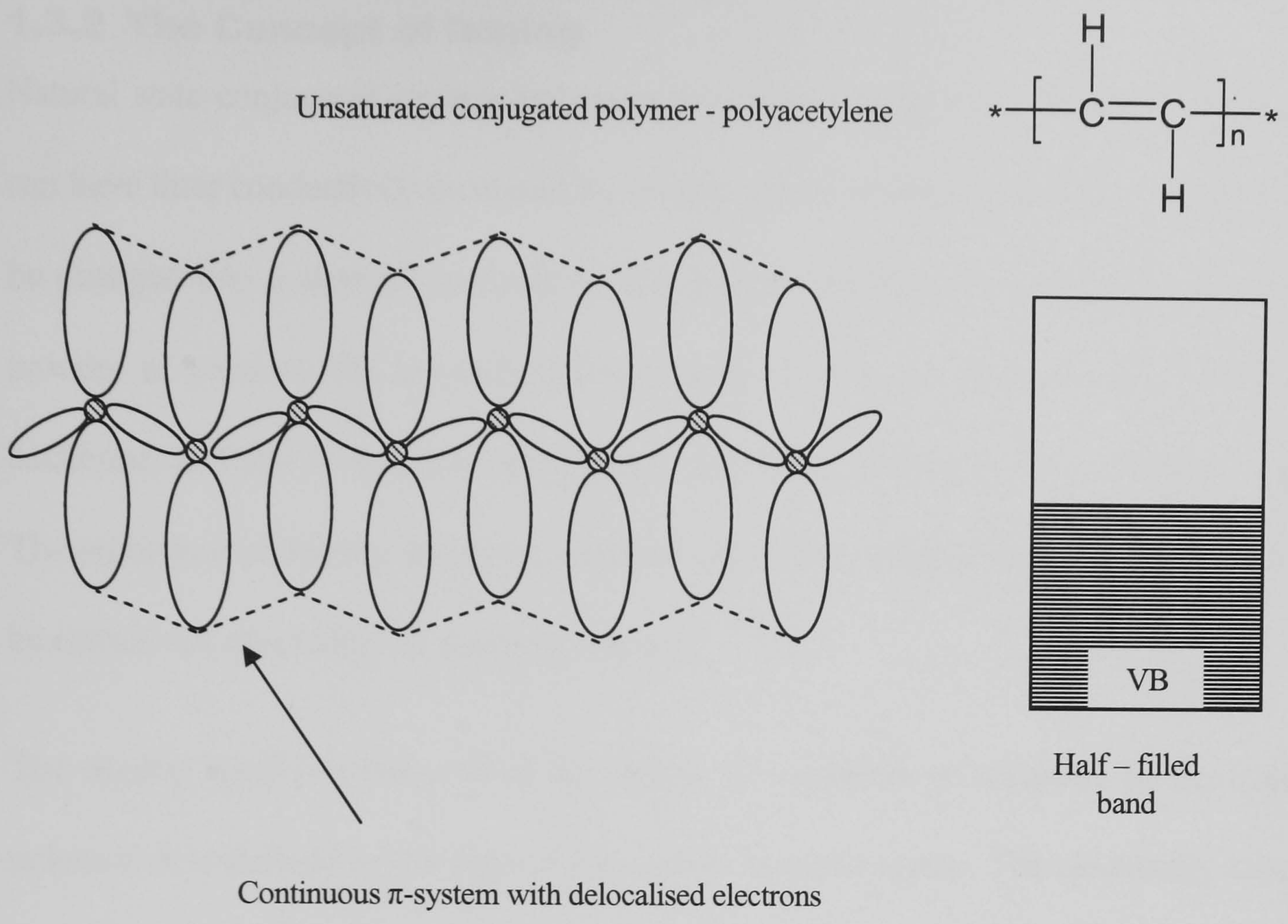


Figure 9 Unsaturated conjugated polymer – polyacetylene.

This electron delocalisation supplies a "highway" for charge mobility along the backbone of the polymer chain. Intrinsically conducting polymers (ICP's) have a relatively small energy gap between the highest occupied energy band (valence band) and the lowest unoccupied energy band (conduction band), allowing excited electrons to reach the energy level of the conduction bands.

### 1.3.2 The Concept of Doping

Natural state conjugated organic polymers are either insulators or semiconductors but they can have their conductivity increased by several orders of magnitude if the pure polymer can be changed into a state of conduction. This process is known as doping. It is a reversible process to produce the original polymer with little or no degradation of the polymer backbone, and can be tuneable according to the extent of doping in the backbone structure. The procedure of doping, involving a dopant counterion which stabilise the doped state, may be carried out chemically or electrochemically.

The doping level is a measure of the degree of oxidation or reduction of the conducting polymer. It is defined as the ratio of charges to monomer units. The electrically conducting form is obtained when the polymer is doped and the electrical conductivity is strongly dependent upon the polymer's doping level; this is normally higher for electrochemically formed polymers than for chemically formed polymers.

#### *1.3.2.1 Redox Doping*

All conjugated polymers, and most of their derivatives, undergo either p-type (oxidation) and/or n-type (reduction) doping, which can be carried out using chemical and/or electrochemical processes, and in which the number of electrons associated with the backbone changes during the doping process.

### p-Type Doping

This type of doping takes place when a conjugated polymer is partially oxidised and it can be accomplished through either chemical or electrochemical means. In this type of doping, electrons are removed from the backbone of the polymer which becomes partially positively charged. Electrochemical doping is achieved by attaching a film of the organic polymer to the positive terminal of a Direct Current (DC) power source such as the (anode) of an electrochemical cell containing electrolyte such as $LiClO_4$. Some electrons from the polymer are removed generating a positively charged network stabilised by the associated anions.

### n-Type Doping

Conjugated polymers can conduct electricity in an electron rich state. This type of doping can be achieved by partial reduction of the backbone $\pi$-system of an organic polymer either by a chemical or electrochemical process. This occurs by inserting electrons into the backbone of the conjugated polymer.

#### *1.3.2.2 Non-Redox Doping*

This type of doping differs from redox doping, in that the number of electrons associated with the polymer backbone does not change during the doping process. The non conductive form of polyaniline (emeraldine base) was the first example of the doping of an organic polymer to produce an environmentally stable polysemiquinone radical cation. The highly conducting form of polyaniline will be discussed further in the later stages of this chapter.

#### *1.3.2.3 Charge Generation Involving No Dopant Ions*

In certain types of conjugated polymers, charge production can be achieved without the need of any dopant ion. In this case, it can be accomplished by exposing the polymer to photons or injecting charges into the polymer backbone.

### Photo-Conduction

Photo-carrier generation doping involves a polymer being exposed to radiation of a higher energy than that of its band gap. This radiation causes the electrons to hop across the conduction band and become free, resulting in the presence of partial positive and negative charges that require constant exposure to be reformed into charged solitons when they collide.

### Charge-Injection

Charge Injection can be achieved using a metal/insulator/semiconductor (MIS) configuration. The MIS system involves a metal and a conducting polymer separated by a thin layer of a high dielectric strength insulator. The insulator molecules will align themselves at the metal/insulator interface in the direction of the electric field, which consequently loads the insulator/semiconductor interface with an opposite partial charge. This enables the conjugated polymer to gain an excess charge by either removing (oxidation), or inserting (reduction) electron density from/to the insulator/semiconductor interface.

## *1.3.2.4 Charge Carriers and Mechanism of Conduction in ICPs*

Intrinsically conducting polymers can be prepared via chemical and electrochemical polymerisation. In this reaction, conjugated monomer is polymerised and charge carriers are generated via doping. These charge carriers differ depending on the degree of doping and the structure of the polymer.

### Solitons

The general structure of ICPs is an alternating sequence of single and double bonds. The degeneracy of the ground state of polyacetylene depicts structural defects in the polymer backbones, leading to a change in bond alternation (Figure 10). At the defect site, a single unpaired electron exists, although the overall charge remains zero, forming a new energy

level at mid-gap (a non-bonding orbital). This defect state, known as a '***neutral soliton***', is singly occupied, possessing a spin of ½. The soliton energy level can accommodate zero, one or two electrons and thus the soliton may also be positively or negatively charged, giving the unusual property of separating spin and charge, with neutral solitons possessing spin, but no charge, and charged solitons having no spin. Neutral and charged solitons are not localized on one carbon atom, but spread over about fifteen carbon atoms [35].

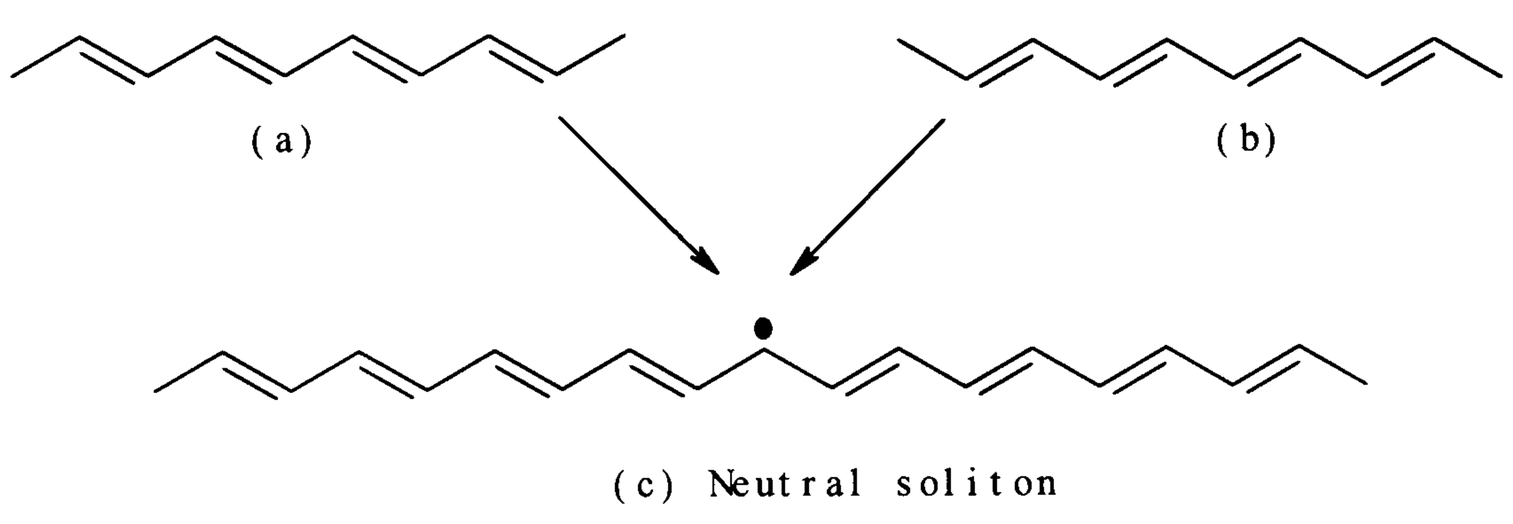


Figure 10 Structural representation of a bond alternation defect (neutral soliton) at a phase boundary between the two degenerate phases of polyacetylene.

The p-type doping will be considered as an example. Reductive doping can be explained in a similar way. The initial oxidation of trans-polyacetylene generates a radical cation. Since it has no preference in bond alternation, the positive charge and the unpaired electron can move independently along the polymer chain. Further oxidation of polyacetylene forms polymeric dications as illustrated in Figure 11.

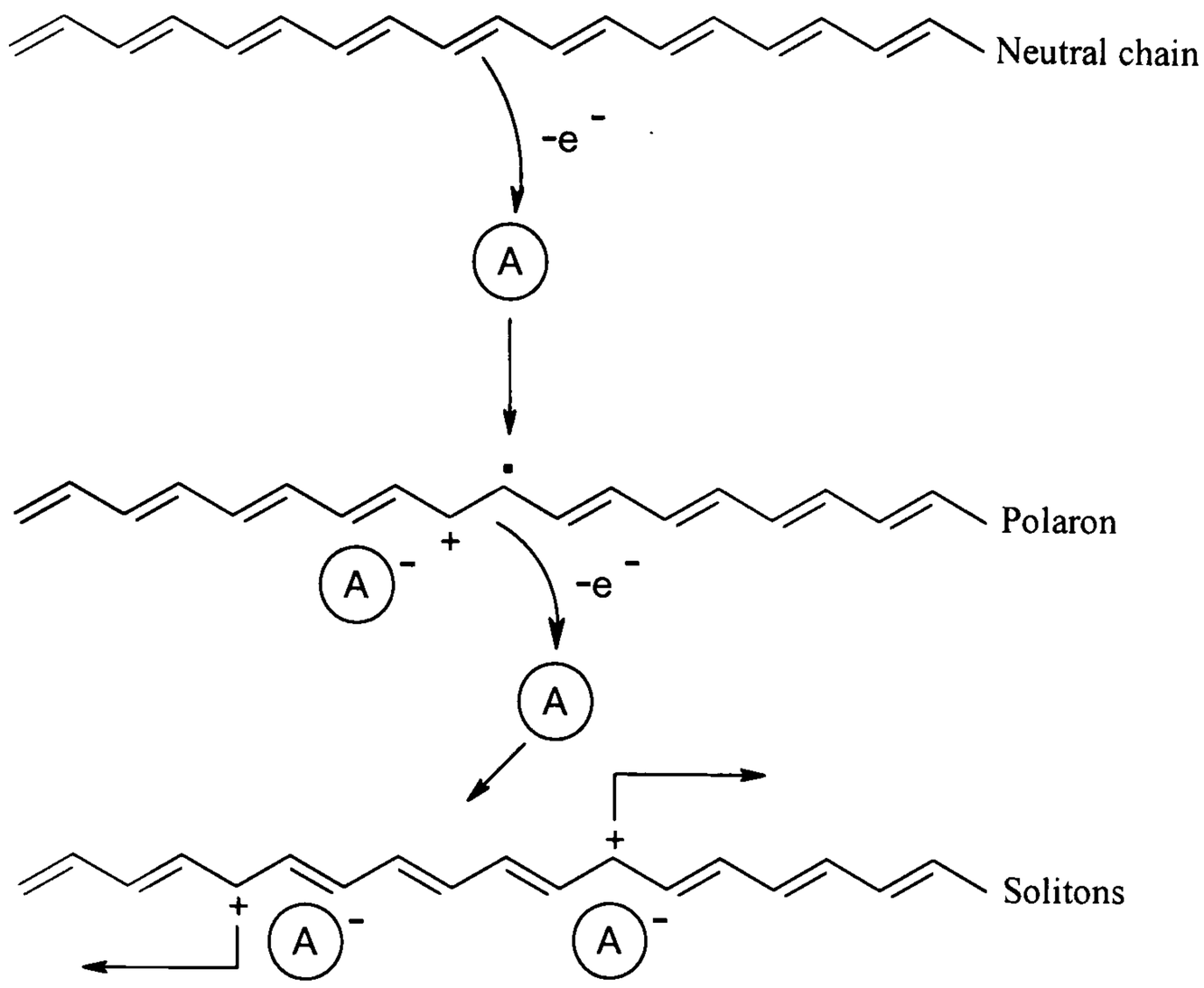


Figure 11 Oxidation of polyacetylene and the formation of polaron and solitons states.

Since the ground state structure of the polymer is twofold degenerate, the charge cations are not bound to each other by high energy bonding and can freely separate along the polymer. This generates two equivalent resonance forms, creating domain walls between the two opposite phases of bond alternation. In solid state physics a charge associated with a boundary or domain wall is called a ***charged soliton***, because it has the properties of a solitary wave which can move with only slight deformation and energy dissipation [36].

## Polarons and Bipolarons

Most ICPs possess a nondegenerate ground state with a preferred sense of bond alternation. Polypyrrole is an example of nondegenerate ground state polymer that has an aromatic configuration with long bonds between the aromatic rings. The other type of bond alternation is the quinoid configuration which is characterized by shortened bonds between the quinoid rings (Figure 12). The quinoid geometry can be considered as an excited state configuration of the aromatic structure.

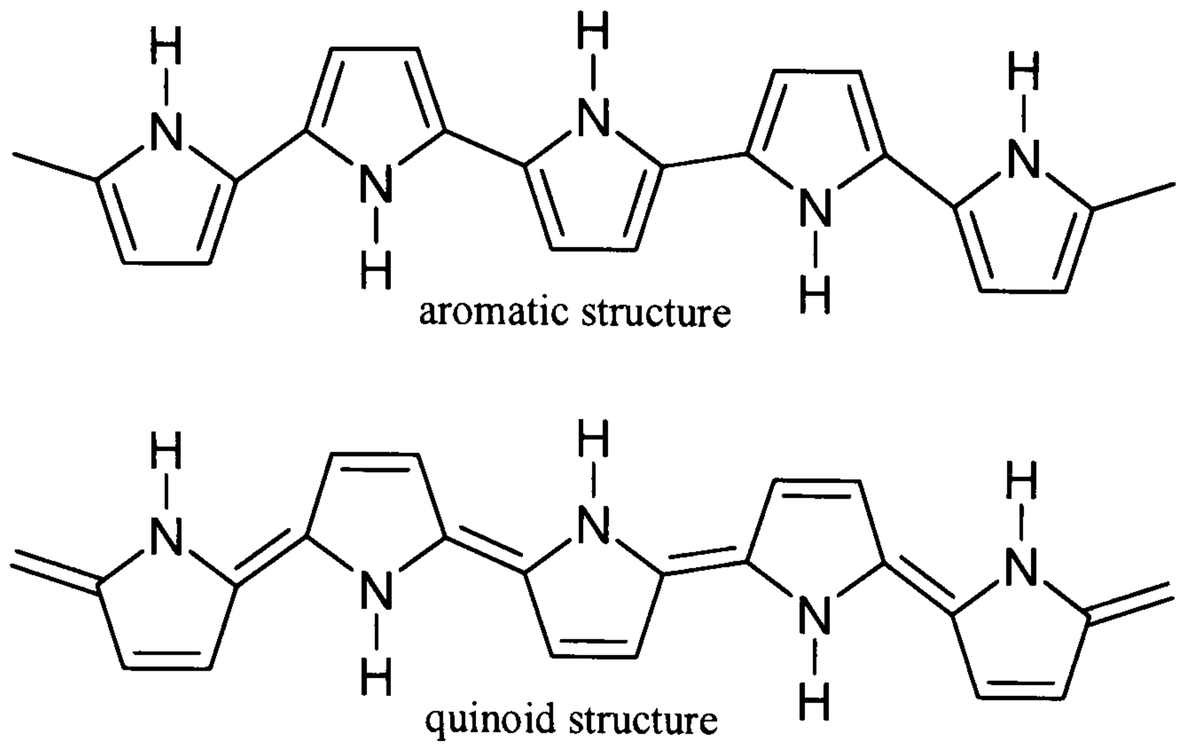


Figure 12 Senses of bond alternation of polypyrrole: aromatic and quinoid structure.

The degeneracy of the ground state has an important effect on the nature of the charged species that can be obtained via oxidative or reductive doping. Oxidation of polypyrrole generates a radical cation, where the positive charge and the free radical of the initially formed radical cation cannot move independently. The nature of the chain segment between the positive charge and the unpaired electron is that of a quinoid configuration, which confines the charge and spin density to a single self-localized structural deformation that is mobile along the chain (Figure 13). This combination of a charged site coupled with unpaired electron associated with lattice deformation is called a ***polaron***.

Upon further oxidation of a nondegenerate polymer chain two things can happen. A second electron can be removed from a different segment of the polymer chain creating a new polaron, or the unpaired electron of the previously formed polaron is removed. The latter produces a spinless di-cation confined to a single lattice deformation on the chain, which is called a ***bipolaron*** [35]. Bipolarons can also originate from an attractive interaction between the lattice deformations of two polarons in which their unpaired electrons form a bond on a doubly oxidized polymer chain (Figure 13). The latter also results in a single lattice deformation. At higher doping levels, bipolarons may also combine to form 'bipolaron bands' within the gap [37].

Although these charge carriers are responsible for electrical conductivity in conjugated polymers, many other structural imperfections are present in all polymers and these defects need to be considered.

Conduction by polaron or bipolaron motion is now generally considered to be the dominant mechanism of intrachain transport. Conductivity is not only a result of charge transfer along the chain, but is also due to electron hopping between chains and between different conjugated segments of the same chain. In addition to these processes which act at a molecular level, bulk conductivity values are also dominated by electron transfer between grain boundaries and variations in morphology [38,39].

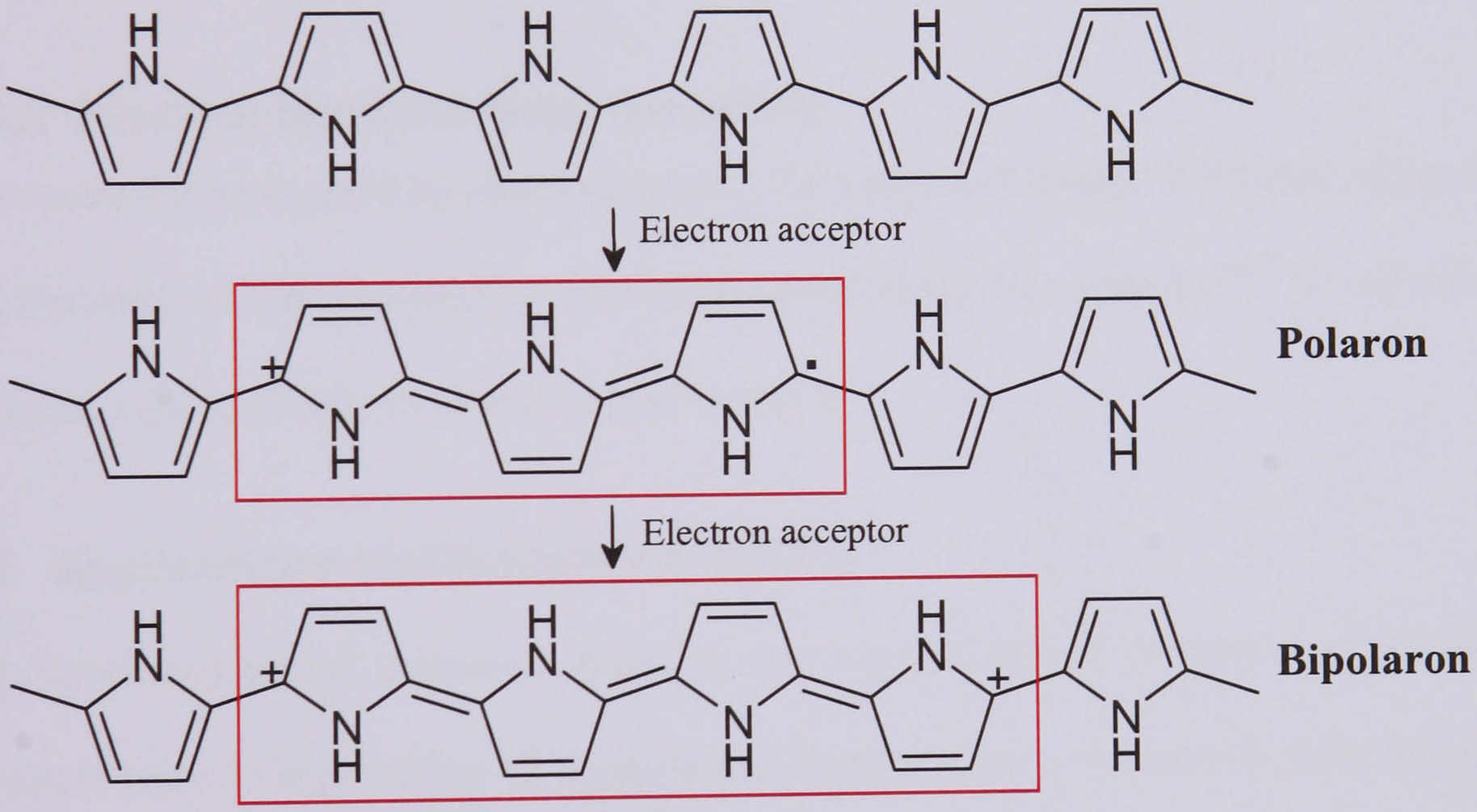


Figure 13 oxidation of polypyrrole and the formation of polaron and bipolaron.

## 1.4 Synthesis of Conducting Polymers

Conducting polymer synthesis can be classified in two main groups:

### 1.4.1 Chemical Polymerisation

This method is relatively simple, involving monomer, oxidant and dopant in an organic or aqueous solvent. In some special cases, the dopant can act as an oxidant. The polymerisation usually occurs in the range of temperatures 20 – 80°C and the product is obtained after filtration and drying. The mechanism proposed assumes that the radical cation is formed in the bulk of solution by oxidation of the monomer. The coupling between radical and monomer and its oxidation produces a bi-radical cation. Coupling and oxidation continue until the polymer chain becomes insoluble.

### 1.4.2 Electrochemical Polymerisation

This method is more used by electrochemists. The polymer deposits on the electrode surface. The thickness of film, morphology and other properties can be controlled [40] by adjusting the potential, current density or reactant concentrations.

## 1.5 Applications and limitations of ICPs

The novel and varied chemical, electrical and electrochemical properties of conducting polymers have a large variety of applications. In many cases, conducting polymers offer a unique combination of properties that make them attractive alternatives for certain materials currently in use in the industry. In addition, these materials have low density, and high mechanical flexibility in comparison with their metallic counterparts. There are however disadvantages which severely limits the use of conducting polymers for certain applications. Many conducting polymers previously synthesised, have been formed as intractable, insoluble films or powders which could not be further manipulated to form more ordered materials and controllable structures. In conjugated polymers, the structural characteristics

give rise to the electrical and optical properties. Planar conjugated backbones, also severely limit the ways in which the polymer can be processed, resulting in limitations in their applications.

The major driving force behind much of the research into conducting polymers has been the potential commercial applications of them. The recent improvements in processibility have greatly enhanced the prospective uses of conducting polymers. Some of these applications include rechargeable batteries, corrosion-inhibiting paints, EMI shielding, electrochromic displays and photovoltaic cells, and these are discussed below

### 1.5.1 Rechargeable Batteries

A widely acknowledged use of conducting polymers is in battery devices [41]. The reversible switching between the two redox states of conducting polymers has allowed the materials to be used as electrodes in rechargeable batteries, the advantage being that the polymer electrodes should have a longer lifetime than their metal counterparts. This is due to the dopant ions which are involved in the delivery and storage of the charge. These ions are an integral part of the electrodes themselves, thus reducing mechanical wear associated with dissolution and redeposition of electrode material in traditional batteries.

### 1.5.2 Electrochromic Displays

Optical properties of conducing polymers have now become an important area of materials research, since during their electrochromic switching, distinct changes in the optical properties can occur. Polythiophene and polyaniline have both been investigated for their uses as display devices. In electrochromic displays reversible colour changes are induced by the application of a suitable electrode potential.

A lot of polymeric and crystalline organic conductors show non-linear optical properties and this behaviour is thought to result from the interaction of intense electromagnetic fields with the delocalised π electron system.

### 1.5.3 Photovoltaic Cells

Photovoltaic cell technology based on conducting polymers has become an area of increased scientific interest [42] since polymer photovoltaics offer great technological potential as a renewable, alternative source of electrical energy.

Solar power is currently harvested a variety of methods, but the most familiar method involves the use of silicon-based solar cells. These inorganic solar cells have been highly optimized and can operate with efficiencies of greater than 12%. The use of solar-based power has been hindered because of high manufacturing costs, difficulties in tailoring the cells to various applications, and the inherent physical rigidity of silicon.

Organic photovoltaic (OPV) cells can overcome these problems because of their inherent property of being easily manipulated into the many spatial arrangements of an organic molecule. Their synthetic flexibility allows the properties of the solar cells to be tuned to particular applications. The ability to add solubilising groups to organic molecules also allows for the use of new and less costly techniques, such as inkjet printing. Finally, organic materials tend to have good mechanical flexibility. The combination of lower cost and better adaptability should provide an enhancement in the feasibility of solar power [43]. The main disadvantage of OPV is that although these polymers can absorb sunlight, the energy conversion efficiencies fall below those required for effective solar cells. Efficiencies up to a relatively low 4.8% are reported for this type of organic solar cell.

### 1.5.4 Corrosion-Inhibiting Paints

Steel plates when exposed to brine or acidic conditions can undergo corrosion; this process can be inhibited by the use of a thin layer of polyaniline [44,45]. The polyaniline is involved in the mechanism that reduces corrosion, by forming a thin, uniform layer of unhydrated iron oxide that acts as a barrier to the rusting process [46].

### 1.5.5 EMI Shielding

With the rapid advances of computer and telecommunication technologies, there is increased interest in shielding of electromagnetic radiation, mainly in the radio and microwave frequency ranges. The common shielding techniques focus on the use of typical metals such as copper or aluminium and their composites, which have disadvantage due to their heavy weight, limited mechanical flexibility, corrosion, and difficulty of tuning the shielding efficiency.

Conducting polymers are promising candidates for shielding electromagnetic radiation and reducing or elimination of electromagnetic interference (EMI) because of their relatively high conductivity and dielectric constant and ease of control of these properties through chemical processing [47,48].

### 1.5.6 Light Emitting Diodes

Organic and polymer light emitting diodes (LED) are undoubtedly revolutionary approaches in the area of information displays. The advantages of LED are as follows: wide angle of visibility, reduced power consumption, high image quality, low operational temperatures and small size. A polymer LED is a sandwich formed by a high work function transparent conducting anode (composed of indium tin oxide film or polyaniline), and a low work function metal cathode on both sides of the active emitting layer based on an organic luminescent material or conjugated polymer. The active layer is separated from anode and

cathode by hole and electron transmission films respectively. When direct voltage is applied to the device, holes injected at the anode, and electrons at the cathode meet to combine within the illuminating layer and cause electroluminescence. The above-mentioned structure can be simplified.

## 1.6 Project Materials

### 1.6.1 Polyaniline (PAni): from Discovery to Present

#### *1.6.1.1 Concise History of Polyaniline*

In 1835, the intrinsically conducting polymer, polyaniline, was first described as ***aniline black***, based on the process of oxidation that resulted in its formation [49]. Subsequently, Fritzche continued the uncertain analysis of the products acquired by the chemical oxidation of this aromatic amine [50]. Research and studies encompassing over two decades led to the oxidation of aniline with potassium dichromate as the oxidising agent, by Perkin in 1856. This resulted in the formation of a black precipitate which was probably a mixture of aniline black and polyaniline [51,52].

Perkin proceeded by the extraction of a dye (purple coloured) called mauveine which is in fact the first commercially synthesized dyestuff. In 1896, as the pure aniline was further oxidized, pseudomauveine was obtained [52], which implies that in the course of the oxidation of aniline, a soluble protonated phenazinium structure is formed. Prior to this discovery, in 1862, at the college of London Hospital, a partially conductive substance was synthesized by the anodic oxidation of aniline in aqueous sulfuric acid by Letheby [53].

Nonetheless, it was not until the twentieth century that the accepted mechanism of the synthesis and structure of polyaniline was made explicit. Organic chemists started investigating the nature of "aniline black" and its intermediate products [54]. In 1907 and 1909, Willstatter considered aniline black to be an eight-nuclei chain compound with an

indamine structure [55,56]. Green and Woodhead proposed a linear octameric structure, of the quinone-imine type in the para-position, for the product obtained by the chemical oxidation of aniline [57]. It is only recently in the 1980's that great interest has been shown in synthetic organic metals such as polyaniline and its structure finally defined [58,59,60,61].

### *1.6.1.2 Basicity and Reactivity of Aniline*

Aniline is a very weak base, with a $pK_b = 9.38$. Amines are transformed into their salts by aqueous mineral acids and liberated from their salts by aqueous hydroxides. They are therefore more basic than water and less basic than a hydroxide ion.

$$\underset{\text{Stronger base than water}}{ArNH_2} + H_3O^+ \longrightarrow ArNH_3^+ + \underset{\text{weaker base}}{H_2O}$$

$$ArNH_3^+ + \underset{\text{Stronger base}}{OH^-} \longrightarrow \underset{\text{weaker base}}{ArNH_2} + H_2O$$

Aniline is a weaker base than ammonia due to that fact that the lone pair of electrons on the nitrogen atom is partially shared with the ring, and are therefore less available for sharing with a hydrogen ion. Moreover, in aniline the nitrogen atom is bonded to a $sp^2$ hybridised carbon atom but, more importantly, the unshared electron pair on nitrogen can interact with the delocalised $\pi$-orbitals of the nucleus as illustrated in Figure 14. Also widely known is the fact that the $-NH_2$ group (electron donating) behaves like a powerful activator and ortho, para director in electrophilic aromatic attack.

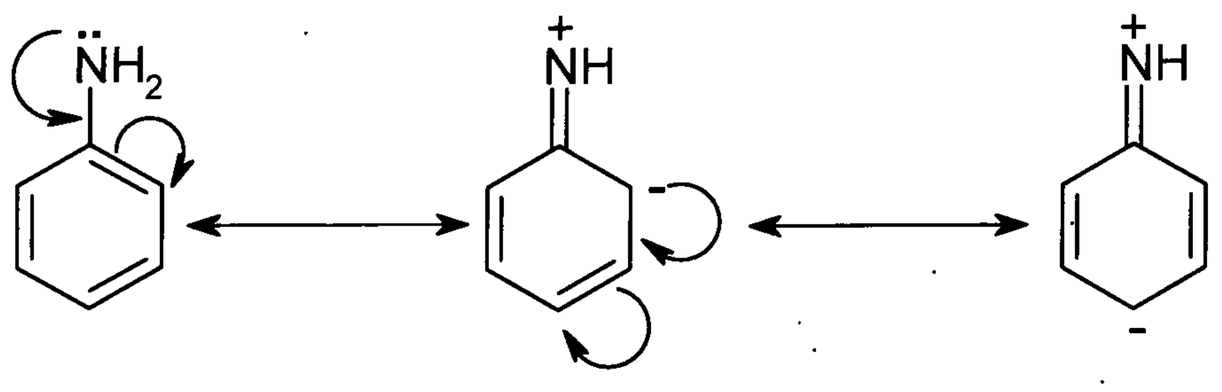


Figure 14 Delocalisation of the electron pair along the ring.

### 1.6.1.3 Polyanilines: A Novel Class of Conducting Polymers

Polyaniline (PAni) is probably the most important industrial organic conducting polymer today. This is due to its facile synthesis and processing, environmental stability and low cost. In addition, PAni has two attractive properties: intrinsic redox state and reversible doping/de-doping of acid/base; thus this material can potentially be used for future applications in fields such us supercapacitors [62], batteries [63] and microwave absorbing systems [64].

### 1.6.1.4 Polyaniline: From a Structural Perspective

Since the resurgence of interest in PAni, there has been a great deal of uncertainty and confusion about its structure. In the 1980's MacDiarmid's investigations [65,66] resulted in the formulation of a proposed structure for polyaniline together with a modification of its classification based on the older beliefs. As previously stated, Green and Woodhead [57] gave various arbitrary names to PAni, but were unaware of the polymer's real structure, presuming it to be an octameric molecule.

PAni exhibits a much greater complexity of properties and structures than most other conductive polymers, due to the fact that the nitrogen atoms in the polyaniline structures inhabit primary sites in the chain backbone. This heteroatom (nitrogen atom) plays a key role in controlling the properties of the system since there is no continuous carbon-carbon chain. Indeed, polyaniline can take various forms, such as the reduced or oxidised forms as illustrated in Figure 15 or salt form and base form, and therefore shows different colours.

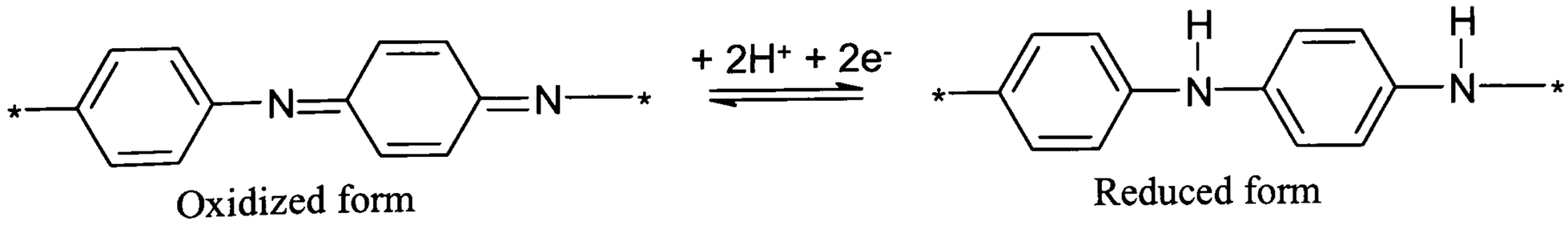


Figure 15 Redox forms of polyaniline.

Polyaniline is considered to be a family of three polymers, depending on the oxidation state.

***Leucoemeraldine***, also known as poly (paraphenyleneamine) is the fully reduced form and has the simplest backbone as illustrated in Figure 16. This polymer has a white to light brown colour and behaves as an insulator because of its unconjugated backbone. The polymer is unstable with respect to oxidation in air.

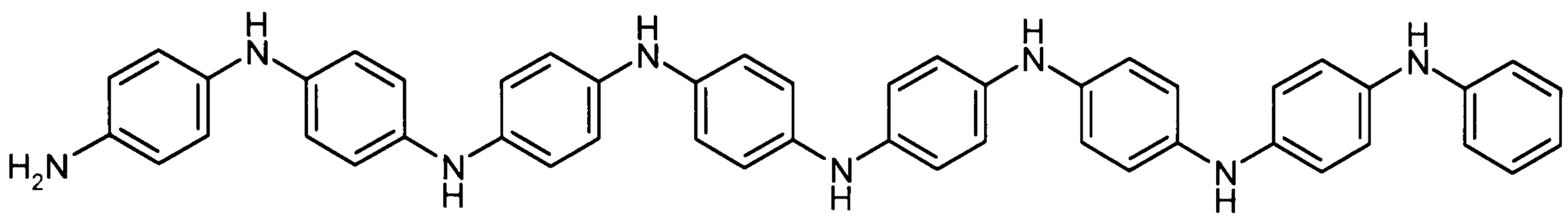

Figure 16 Structure of Leucoemeraline.

***Pernigraniline***, also called poly (paraphenyleneimine) is the fully oxidised form as illustrated in Figure 17, with all the nitrogens present in the quinonediimine form. Furthermore, a susceptibility of the quinoid sites in its structure to hydrolysis makes it difficult to synthesise in aqueous media. This polymer is the most optically interesting material because the system is fully conjugated and strongly coloured. Pernigraniline is a weak semiconductor because of the difficulty of delocalisation of any charge on nitrogen atom amongst other resonance structures.

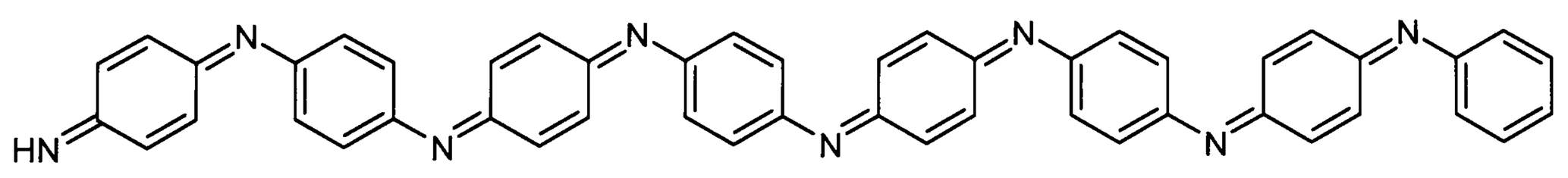

Figure 17 Structure of Pernigraniline.

***Emeraldine base*** or poly (paraphenyleneamineimine) is a term that refers to a 50% oxidised polymer as illustrated in Figure 18. Since the nitrogen atom bridging the neighbouring phenyl rings can exist either as the oxidised or imine (-N=) form, or as the reduced or amine (-NH-)

form, the ring can have either a benzoid or quinoid structure [67], in what is formally a benzenamine-quinonediimine polymer.

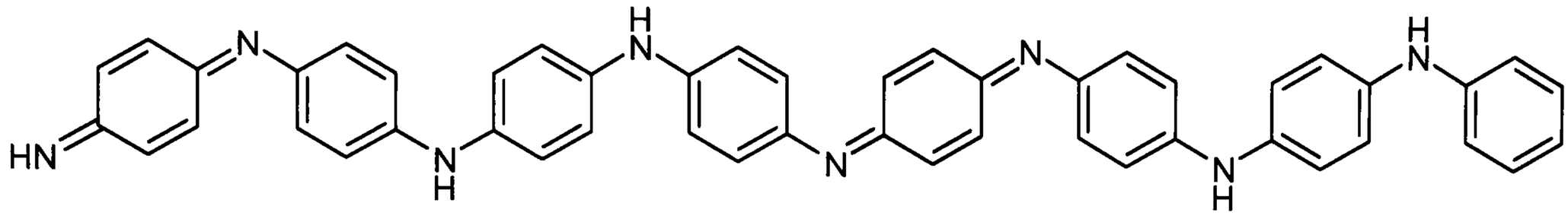

Figure 18 Structure of Emeraldine Base.

Therefore, PAni can be illustrated as having four benzene ring repeat units Figure 19.

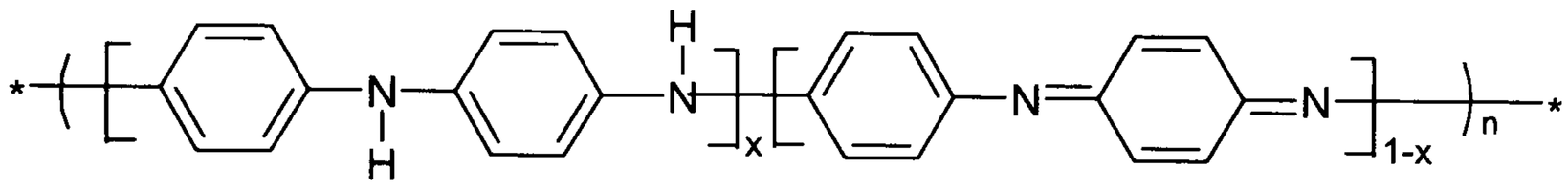

Figure 19 Structure of Polyaniline repeat unit.

### *1.6.1.5 The Distinctive Doping Method of Polyaniline*

Polyaniline is unusual amongst ICPs in that its electronic properties are governed by two parameters [55,68,69]: the oxidation level as discussed in section 1.6.4 and the protonation level.

This means that it can be changed from an insulating state to a highly conducting one through appropriate oxidation and protonation steps. Despite the fact that the three oxidation states of polyaniline mentioned previously produce polymers that are electrical insulators, emeraldine base produces a salt form when treated with acid of pH<3. This protonation is accompanied by an increase in the electrical conductivity of the material by a factor in the region of $10^{11}$.

The degree of protonation can be controlled by variation of the pH of the acid, with lower pH values causing higher levels of protonation. It is widely known that the maximum doping level occurs when half of the nitrogen sites on the chain are protonated.

The transition to conductive behaviour that occurs with acid doping is extremely interesting for two reasons. Firstly, the emeraldine base form of the polymer is not strictly conjugated,

i.e. alternation of single and double bonding does not extend along the entire length of the polymer repeat unit, as it does in the pernigraniline structure. Secondly, the process of protonation does not change the number of electrons on the chain, like the oxidative doping of polyacetylene, polythiophene and polypyrrole. The chemistry of polyaniline involves oxidation/reduction reactions as well as protonation/deprotonation achieved either individually or all together [55,70,71,72,73].

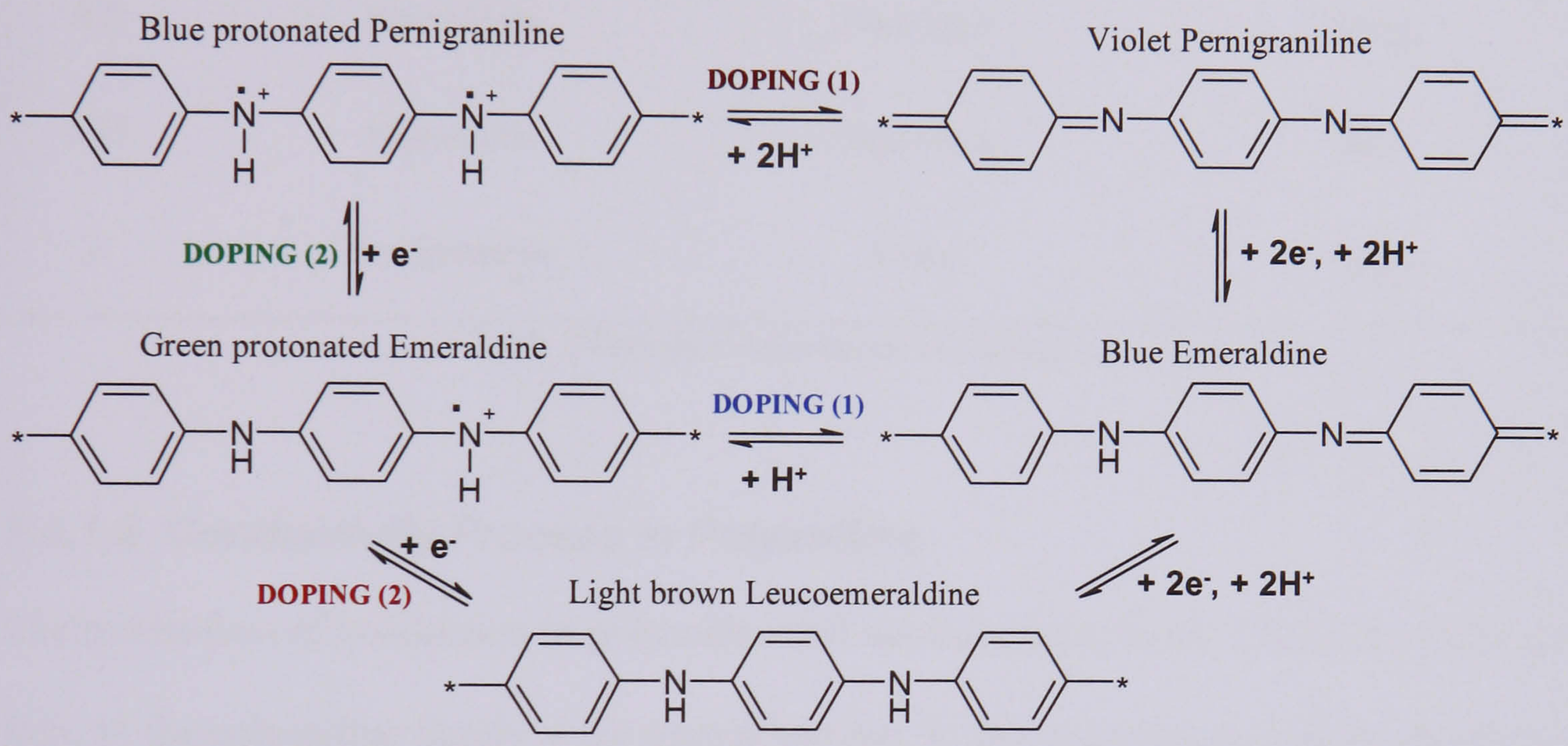


Figure 20 Doped and Undoped forms of polyaniline: (1) chemical (protonation) & (2) Oxidative.

The five forms of polyaniline may be partly or completely protonated with a protonic acid to give the corresponding "salt". In both cases, either one or both nitrogen atoms in a repeat unit may be protonated, depending on the pH of the medium to which the polymer has been exposed. A series of compounds can be formed according to the different oxidation and protonation levels. Their approximate compositions, along with their names and colours are listed in Table 1.

It is well known that emeraldine salt is a good electronic conductor because of the possibility of the combination of charge and its delocalisation amongst the possible resonance forms of its structure. The conjugation leads to strong visible absorption and a green colour Treatment

of protonated polyaniline with aqueous alkali results in de-protonation and the insulating. emeraldine base form is recreated.

| X | Name | Base Form | Protonated Form |
|---|---|---|---|
| 1 | Leucoemeraldine | Light brown | Pale yellow |
| 0.75 | Protoemeraldine | Violet | Light green |
| 0.5 | Emeraldine | Dark blue | Green |
| 0.25 | Nigraniline | Blue-black | Blue |
| 0 | Pernigraniline | Violet | Purple |

Table 1Various compositions of polyaniline.

### *1.6.1.6 Conductivity Process in Polyaniline*

The mechanism of conduction in polyaniline still not fully understood. The most conductive form in the polyaniline family is the emeraldine salt. In this polymer, the charge transport is presumably dominated by hopping involving the polaronic species. Once protonation of the emeraldine base has occurred, geometrical relaxation immediately follows, resulting in quinoid and benzoid forms as illustrated in Figure 21. This results in the formation of a bipolaron which has a relatively high energy and therefore, is short-lived. Redistribution of the radical cation results in a polaron which is more stable as a charge carrier [74].

The stability of the polaronic structure is attributed to a number of factors involving a reduction in Coulombic repulsion [75], and gain of resonance energy [76].

Studies have shown [54,77] the doped form of polyaniline is a strongly paramagnetic material, therefore the bipolaronic structure, which is diamagnetic, does not dominate, suggesting the

conversion of the initially formed bipolaron into separate polarons, resulting in a delocalised half-filled polaron band.

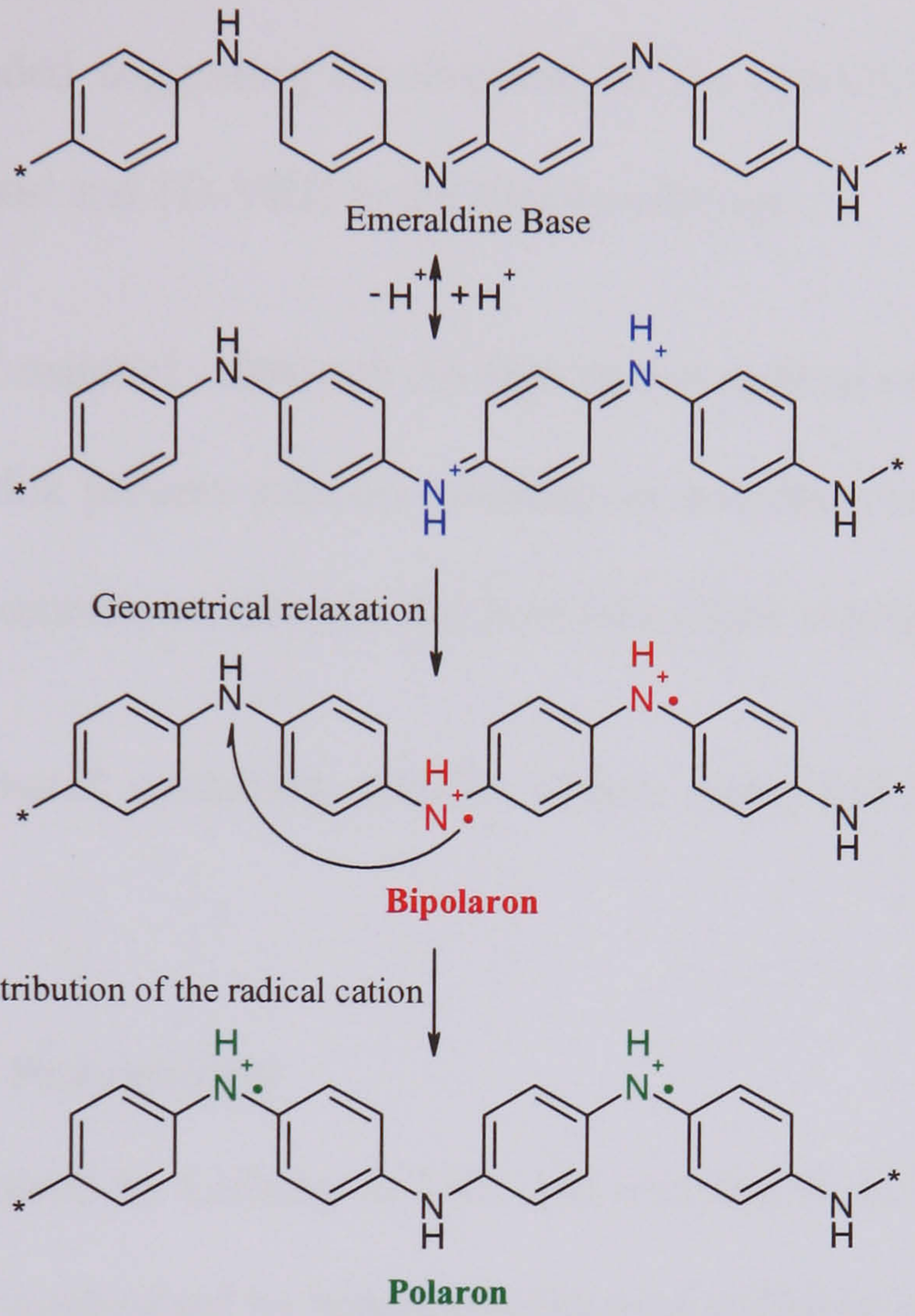


Figure 21 Polyaniline charge carriers: Bipolarons and Polarons.

During recent years, the conversion from semiconductor to metal has been explained but still not completely understood, and there is no evidence that the energy of the emeraldine salt is lower than that of the semiconductor. Theoretical and experimental investigations have shown a particular interest in understanding the mechanism of the charge transport of conducting polyaniline (ES), and these studies concluded:

- Charge transport of conductive polyaniline is dominated by hopping of the polaron species; this can be explained involving the Quasi-1D VRH model.

- Wang et al. [78] proposed, from their observation that the emeraldine salt consists of coupled parallel chains that form metallic bundles. These bundles are the crystalline region of conducting polyaniline in which the electron wave function is three dimensionally extended suggesting involvement of the 3D-VRH model in the intra bundle charge transport and 1D-VRH in the inter bundle one.

- The P-type nature of material - although the protonation method of polyaniline has been explained as non redox process with no oxidation or reduction to the backbone of the polymer, the charge carriers are cationic and therefore, relate to p-type doping.

- PAni is a granular metal, containing metallic islands embedded in a sea of insulating matrix.

#### *1.6.1.7 Synthesis of Polyaniline*

Polyaniline was first prepared by Letheby in 1862 and was known as Aniline black. In this method, the polymer was synthesised by anodic oxidation of aniline in an aqueous solution of sulphuric acid. PAni and its derivatives can be synthesised by both chemical and electrochemical methods. Studies have been carried out to understand the relationship between the conditions of the reaction, both chemical and electrochemical, and the resulting materials properties.

In this study, chemical synthesis of polyaniline was investigated. This method is based on oxidative coupling which involves the oxidation of the aniline monomers to form a radical cation followed by coupling to form a di-cation. Repetition leads to the desired polymer. The polymerisation was carried out using acidic conditions. This kind of synthesis is straightforward, and provided aniline is in contact with both oxidant and acid, the polymerisation is expected to occur.

## Chemical Polymerisation

The typical method of synthesizing polyaniline is the oxidation polymerisation which can be carried out in a solution containing the monomer (aniline or its derivative) and an oxidant such as ammonium persulfate (APS) in an acidic medium. Three common acids used are (hydrochloric acid (HCl), dodecylbenzenesulfonic acid (DBSA) and toluenesulfonic acid (TSA). The preparation can be carried out either in solution or emulsion at low temperature (typically $0^{o}C$), to prevent the formation of low crystallinity polymer.

The mixture becomes coloured during the polymerisation (oligomer formation) and yields a dark blue/green precipitate depending on the degree of oxidation of the polymer obtained (emeraldine salt). The stable emeraldine base can be prepared by immersing the doped polymer in ammonia solution.

### Influence of Polymerisation Conditions

Four main factors can affect the route of the reaction and the nature of the final polymer, as described below:

#### a) Nature of the Medium

The ideal solvent for oxidative polymerisation should have the following characteristics: Low ionic strength, a degree of volatility, and be non-corrosive. Hydrochloric acid is the choice as a medium for polymerisation due to its volatility. If a non-volatile acid such as (sulphuric acid) is employed, a thin film of concentrated sulphuric acid would be left on the surface of the emeraldine salt particles after the removal of the water in a vacuum. This film may react, at least in part, either reversibly or irreversibly with the polymer, and if an attempt is made to remove the free acid through washing with water, complete or partial deprotonation of the emeraldine salt may occur (depending on the washing conditions).

The concentration of the acid medium should not exceed 1M; the reason being that a high acidity accelerates hydrolysis of the polymer backbone. Therefore, the conductivity of polyaniline can be affected by two parameters: the nature of, and the concentration of the acid medium.

**b) Concentration of the Oxidant**

Ammonium persulfate is the most commonly used amongst many oxidants such as potassium dichromate, sodium vanadate, hydrogen peroxide, and ceric sulphate etc. for the polymerisation of aniline in acidic media.

According to the literature, when the initial mole ratio r of oxidant/monomer is higher than 1.15, the result is an over-oxidation of the polyaniline with a concomitant decrease in conductivity [79] and yield of the polymer. However, when r is less than 1.15, the yield of the polymer increases with a basically unaltered elemental composition, degree of oxidation, and conductivity of the resulting polymer.

**c) Duration of the Reaction**

Commonly, chemical polymerisations of aniline are carried out over a period of 10-90 hours [74], but Heeger and his co-workers found that long polymerisation times did not, in fact, favour the synthesis of high molecular-weight polyaniline. He concluded that the oxidation of aniline at various polymerisation times had a reaction yield almost the same over periods from 1-24 hours. However, reduced viscosities were observed at polymerisation times exceeding four hours: these results indicated that the polymerisation occurred rapidly and was essentially completed in four hours [80]. Thus, the duration of the polymerisation has only a limited influence on the yield, conductivity and elemental composition.

**d) Temperature of the Medium**

The process of chemical polymerisation contains two steps as illustrated in Table 2. Furthermore, the rate of the polymerisation reaction varies with temperature in the range of 0-80°C, while the total enthalpy of the reaction remains almost constant ($\Delta H$ = 372 kJ/mole). The temperature is dependent on the concentration of the oxidant

| Step Type | Speed | Dependence on |
|---|---|---|
| Endothermic | Slow | Temp., r, pH |
| Exothermic | Fast | Temp., r |

Table 2 Endo and exothermic steps in the synthesis of polyaniline.

## Electrochemical Polymerisation

The mechanism of this polymerisation is similar to that of the chemical synthesis. Compared to chemical synthesis, the electrochemical approach has definite disadvantages such as the high cost of polymerisation and lower yields than the chemical method. Therefore, the electrochemical synthesis of PAni is not of primary interest to this study.

It still a very elegant way to produce conducting polyaniline since this method has its advantages [44,81], such as purity of the product and easy control of the thickness of polymer deposited on working electrode. In addition, the doping level can be controlled by varying the current and potential with time; synthesis and deposition of polymer can be realised simultaneously.

Electrochemical polymerisation can be carried out in three ways: (1) potentiostatic method (constant potential); (2) galvanostatic method (constant current); (3) potentiodynamic method (potential scanning or cyclic voltammetry).

Typical electrochemical techniques include a three-electrode cell which contains a working electrode (WE), a reference electrode (RE) and a counter electrode (CE) or an auxiliary electrode (AE). Many types of materials can be used as working electrodes. The most commonly used WEs are gold, nickel, platinum, palladium, copper [49], indium-tin oxide coated glass plates and stainless steel [82], Semi-conducting materials, such as n-doped silicon [83], gallium arsenide [84], cadmium sulphide, and semi-metal graphite are also employed for the growth of polymer films. The reference electrode (RE) is typically a saturated calomel electrode (SCE) or Ag/AgCl electrode. The CE or AE is usually made of a platinum wire or foil. Electrochemical synthesis can be done in aqueous or organic solutions.

### *1.6.1.8 Polymerisation Mechanism of Polyaniline*

Since the discovery of "Aniline Black", a wide range of methods have been used for the synthesis of polyaniline leading to the formation of a range of products whose nature and properties differ greatly. As a result of the many studies carried out on PAni and its derivatives, a vast number of polymerisation mechanisms have been proposed by a variety of authors. In keeping with the views of most authors, the first step in the synthesis of PAni is the formation of the anilinium cation by dissolving the aniline in a strong protonic acid. This involves ionically binding the nitrogen lone pair of the aniline and the labile proton of the acid. Although this reaction is fast and the equilibrium shifted towards the formation of the anilinium cation, the presence of short-lived aniline molecules is expected.

The addition of the oxidant to the solution involves removing an electron from either the free aniline or from the anilinium cation (Figure 22) with immediate release of a proton. This leads to the termination of the initiation process by forming the reactive anilinium radical cation which is the main criteria for achieving the polymerisation.

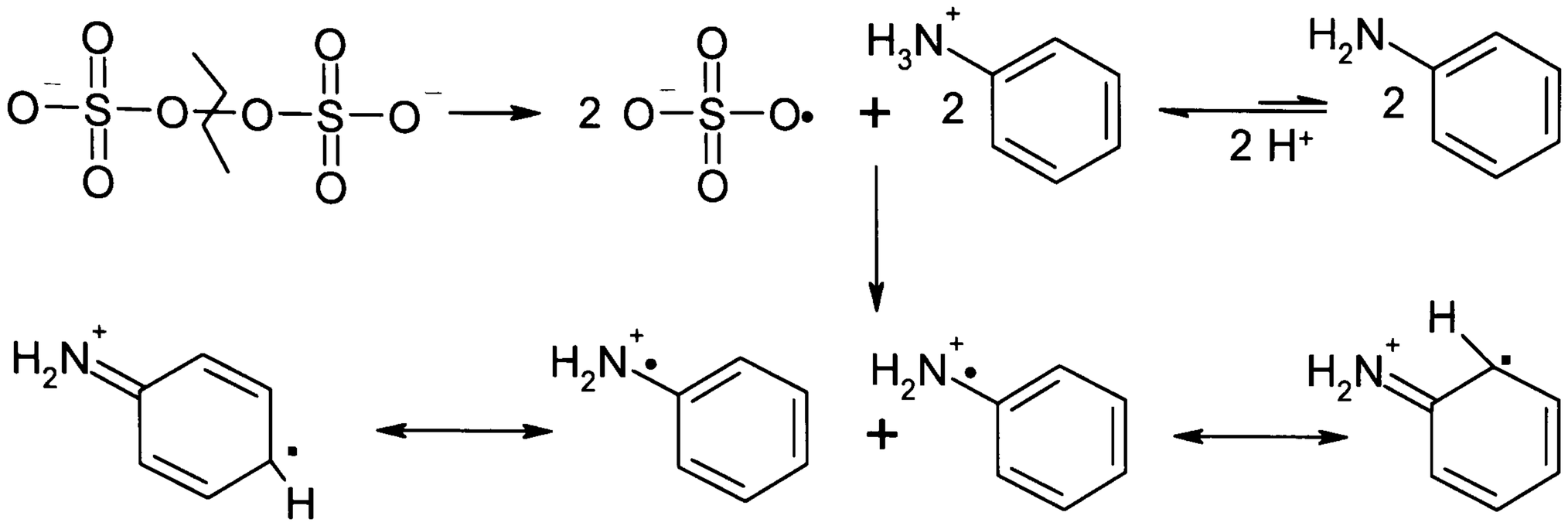

Figure 22 Formation and resonance forms of the anilinium radical cation.

It should be noted that upon direct oxidation of aniline, the anilinium radical cation will be formed. Therefore, the polymerisation of aniline would be achievable without use of the protonic acid. This type of reaction has been always unfavourable for polymerisation however, since the end product is a small chain oligomers or/and diazobenzene Figure 23. Thus it is very likely that the oxidised species is the anilinium cation.

Mohilner [85] was the first to ascertain that in sulphuric acid medium, the oxidation of aniline predominantly resulted in para-coupled chains Figure 23. However, para coupling is not exclusive; radical cation coupling at the ortho position Figure 23 may lead to the formation of an ortho-coupled dimer/oligomer [86,87]. However, in view of steric effects, the ortho product would be less stable than the para coupling. An intermediate product of the oxidation of aniline has been identified by FT-IR spectroscopy, this being P-aminodiphenylamine (PADPA).

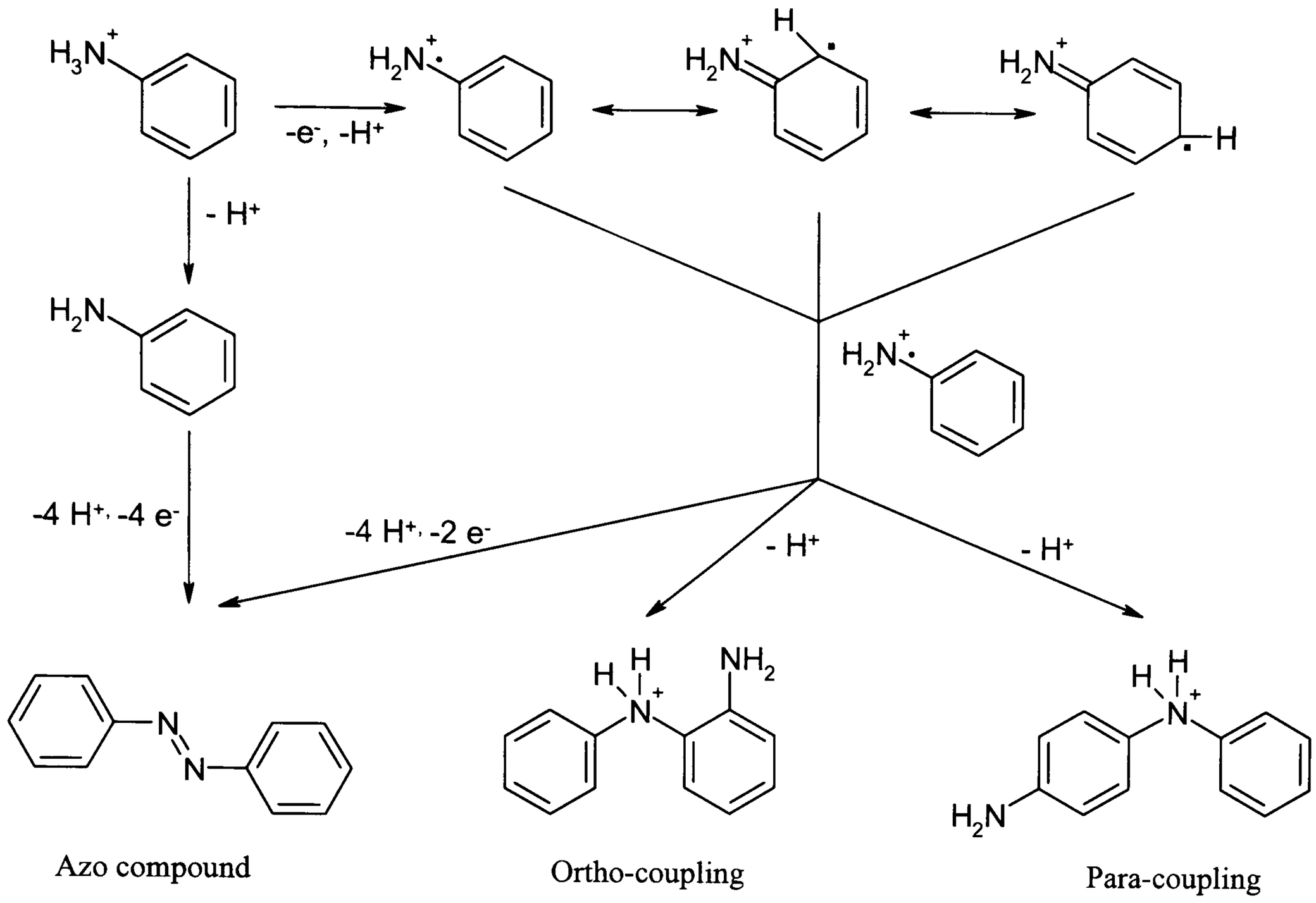


Figure 23 Proposed coupling configurations of the anilinium radical cation.

It is possible that an azo-compound could be formed but this type of reaction is more likely to occur starting with oxidation of aniline instead of the anilinium cation. Moreover, this reaction is not favoured at low pH [67], and the possibility of coupling two nitrogen radicals is low.

The radicals formed stabilise themselves by delocalisation of the electron within the benzene ring of the molecule. The polymerisation starts, and dimers can be formed Figure 24. Upon further oxidation, these dimers will be reactivated and are likely to react with aniline monomers or dimers.

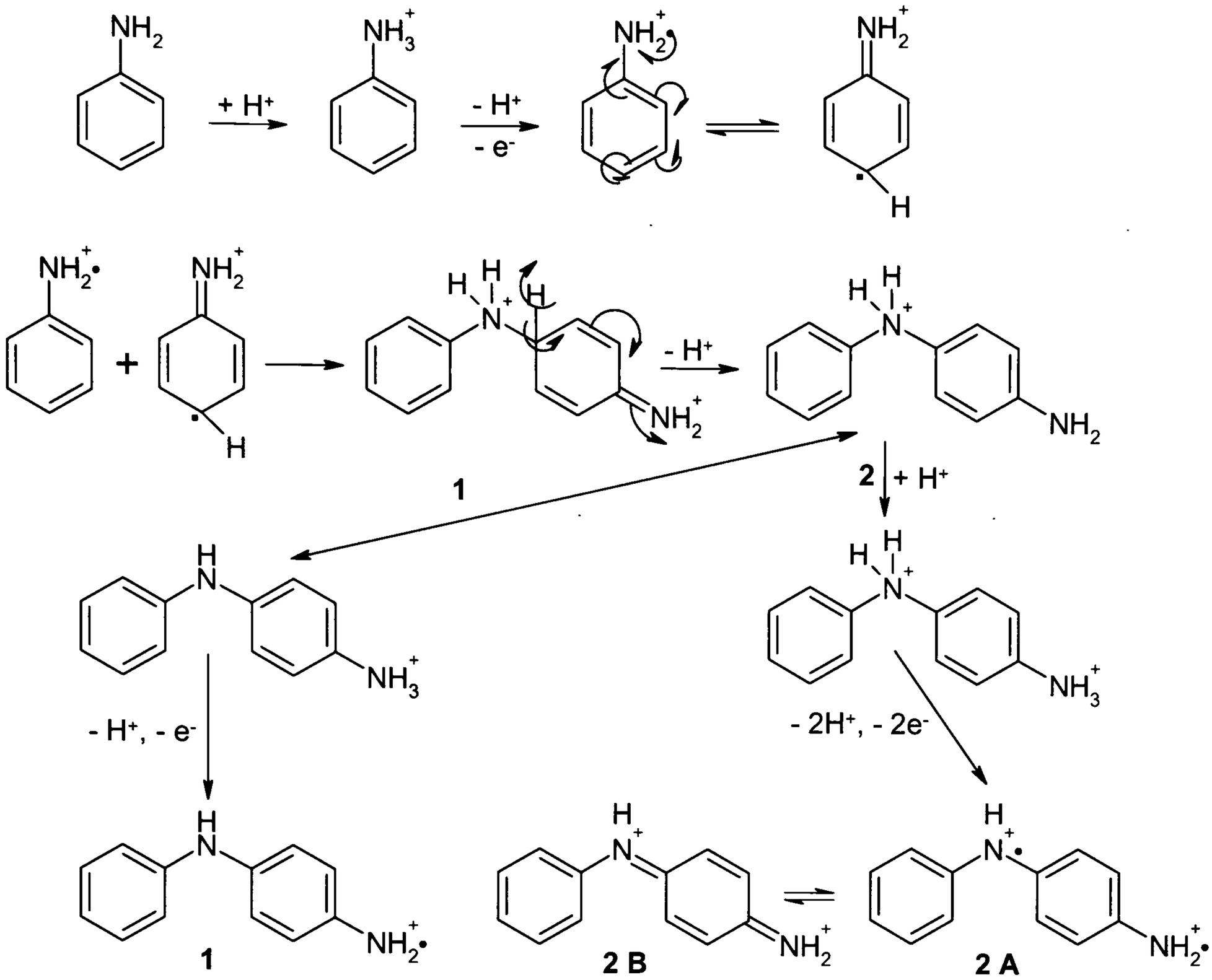


Figure 24 Dimerisation reaction of the anilinium radical cation.

Dimers 1 and 2A are obtained after further oxidation while dimer B is a rearrangement of dimer 2A and has lower oxidation potential than aniline. The polymer achieved at the end of this polymerisation is known to be fully conjugated with alternating para-coupled quinoid and benzoid rings. Moreover, this polymer is protonated at the imine sites of the quinoid ring; the reaction can be illustrated in Figure 25.

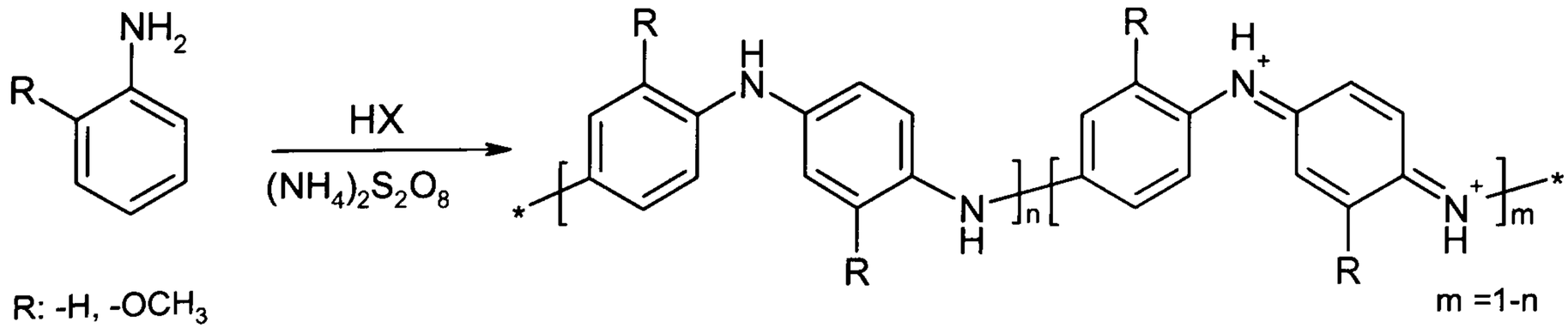


Figure 25 General synthesis route of protonated polyaniline.

### *1.6.1.9 Physical and Chemical Properties of Polyaniline*

**Low solubility** is one of the disadvantages of the polyemeraldine hydrochloride salt (PAni-HCl). Most polyanilines doped with small size dopants have this drawback. Thus, many methods have been attempted to enhance the solubility of PAni salts in conventional organic solvents and it has been shown that this drawback can be overcome by using other dopants instead of HCl and $H_2SO_4$, either during chemical/electrochemical polymerisation of aniline or by doping polyaniline base in aqueous solution. For instance, long-chain functionalized protonic acids such as dodecylbenzene sulfonic acid (DBSA) [88,89], camphorsulfonic acid (CSA) [90,91], Toluenesulfonic acid (TSA) and β- Naphthalenesulfonic acid (see Figure 26) are also sometimes employed. Large dopant or polymeric acids such as polyacrylic acid [92,93] have also been used as dopants of PAni.

On the other hand, introducing functional substitutions of hydrogen atom either in the aniline ring in various positions or in the nitrogen of the amino group is another important method used to improve the solubility of PAni. The usual substituents are – R or –OR (R = alkyl). Some of these groups allow the modified polymers to be more soluble in organic solvents, (e.g. groups such as $–OCH_3$ and $–OC_2H_5$), but also reduces the conductivity of the polymer to as low as $10^{-1} \sim 10^{-3}$ $S.cm^{-1}$. N-substituted PAni dissolves in some organic solvents [94,95] but has reduced thermal stability compared with PAni [96]. 'Self-doped' PAni, whose substitution is an acidic group like $–SO_3H$, -COOH etc, has better solubility [90,97] but lower thermal stability[98,99].

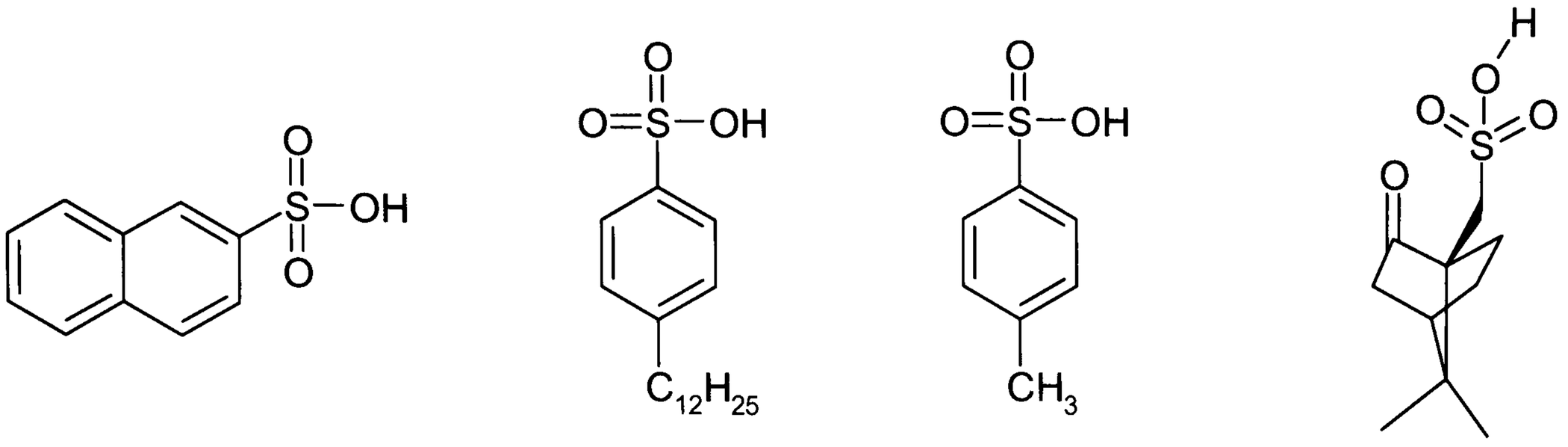


Figure 26 Sulfonic acids used as polyaniline dopants.

**Good thermal stability** is an attractive property of PAni. It is recognized that PAni has good temperature stability up to 400°C in $N_2$ [100,101]. Counter ions in the PAni chains influence the thermal properties of PAni. For example the introduction of $-SO_3H$ in the aniline ring can weaken the thermal stability of polyaniline [93,94]. Many studies reported the change of PAni structure during heating at high temperature. Several cross-linking structures resulting from degradation of PAni during heating were proposed. It is reported controversially that cross-linking started at around 200°C [96,102,103,104,105].

"**Anion effects**" [106] are often referred to as the strong influence of counter ions on the properties of PAni. These effects affect polymeric morphology and thermal stability, extent of electropolymerization, and the electrochemical response [107]. The growth rate of a PAni film is apparently dependent on the type of anion as well [108]. Wang et al [109] observed that the reaction rate followed the order: $H_2SO_4 > H_3PO_4 \approx HF > > HBF_4 \approx HClO_4 > HCl$. A similar order in reaction rate was reported by several groups, e.g. $H_2SO_4 >> HCl \approx HNO_3 >> HClO_4 > HBF_4 > CF_3CO_2H$ by Zotti et al [110]; $H_2SO_4 >> HCl \approx HNO_3 >> HClO_4 \approx CF_3CO_2H$ by Desilvestro and Scheifele [111]; and $H_2SO_4 > > HCl \approx HNO_3 > HClO_4$ by Nunziante et al. [112] and Duic et al [113]. In summary, anion effects can be classified into two types from two groups of counter ions. One contains $BF_4^-$, $ClO_4^-$, and $CF_3COO^-$, which

results in a compact structure with fibres; while the other consists of $SO_4^{2-}$, $NO_3^-$ and $Cl^-$ anions, leading to an open granular structure. Tang et al [114] studied the anion effect on the over-oxidation of PAni.

**Low processibility** is the major drawback of polyaniline and results in its limited use for industrial applications. Hence there is a vast volume of research occurring in this area to try and overcome this disadvantage. One outcome of this research is the idea of blending polyaniline with other materials, such as rubbers to try and improve its processibility.

### 1.6.2 Rubber (Elastomers)

The term "rubber" is often used to describe the naturally occurring polymer while "elastomer" is used when referring to synthetic materials; however the two terms are often used interchangeably. They refer to molecules with an irregular structure, weak intermolecular attractive forces and a very flexible backbone. Elastomers generally have low initial modulus in tension, but when stretched they stiffen. Since these polymers exist above their glass transitions at room temperature, their chain can undergo high local mobility but this mobility can be restricted, typically by the introduction of a few cross-links into the structure. In the absence of applied stress, molecules of elastomers usually have coiled shapes. Consequently, elastomers possess the ability to stretch and retract rapidly on the removal of the imposed stress [1].

#### *1.6.2.1 A Synopsis of the Development of Rubber*

The discovery of rubber in the 18$^{th}$ century has played an important role in our domestic lives. The increase in its popularity was due to its use as a waterproofing agent, and in 19$^{th}$ century, the production of waterproof shoes was realised [115]. The chief source of rubber is the milky fluid (latex) obtained from the rubber tree (*havea brasiliensis*), which is prevalent in the Brazilian Amazon forest. Latex consists of cis-1,4-polyisoprene and various proteins in

the form of a colloidal suspension [116]. There are two classes of rubber, namely, natural and synthetic rubber. The latter is a form of elastomer which regains its original shape after undergoing plastic deformation. Conversely, natural rubbers are obtained directly from latex. The need for synthetic rubbers became apparent during the Second World War as the high demand for natural rubbers in the military and the automobile industry could not be met [115,117]. Synthetic rubbers are made by polymerisation and are used for various purposes around the world.

### *1.6.2.2 Epichlorohydrin-Ethylene Oxide (Epi-EO)*

EPI-EO is a synthetic rubber copolymer made from epichlorohydrin and ethylene oxide monomers. This elastomer is halogenated linear aliphatic polyethers. The presence of the ether oxygen group has two opposing effects:

(i) Increase in chain flexibility which depresses the $T_g$ (and $T_m$ if the polymer is crystallisable).

(ii) Increase in polarity and hence interchain attraction that will increase the $T_g$ and $T_m$.

The relative effect of these two factors depend on the ether group concentration i.e. the value of R in a polymer of type

$$\sim(CH_2)_R\sim O\sim$$

The $T_m$ is at a minimum with a $CH_2/O$ ratio of 3-4. Copolymerisation of two ethers will usually inhibit crystallisation so that rubberiness will depend on the much lower $T_g$ rather than $T_m$. The introduction of chlorine atoms onto the main chain improves oil resistance and increase interchain attraction, thus raising the $T_g$ and, in the case of crystalline polymers, the $T_m$. However, if the chlorine is incorporated into a side chain such as in a $\sim CH_2Cl$ group, the chain separating effect of the side group will more than offset the interchain attraction effect

of the halogen, leading to a decrease in the transition points. If the polymer is substantially atactic there will be no crystallisation and the $T_g$ may be so low that the polymer is rubbery at room temperature.

The copolymerisation of epichlorohydrin with a less polar monomer such as ethylene oxide markedly depresses the $T_g$ and thus enables the rubber to be used at a much lower temperature. The somewhat high $T_g$ of the homopolymer influences several other properties. These include resilience which is very low at normal room temperatures and low permeability which is much less than for butyl or nitrile rubber, both of which are outstanding in this respect. The chlorine content (about 38.4% for homopolymer and 25% for the normal copolymer) has a notable effect in improving oil resistance and increasing flame retardancy. The absence of double bonds results in these rubbers having excellent resistance to ozone, weathering and heat resistance.

Other than its vulcanisation issues, epichlorohydrin elastomers are known for their excellent balance of properties for engineering applications particularly in automotive and marine areas. The presence of oxygen atoms in the polymer backbone imparts flexibility, while saturation in the polymer chain provides superior ozone resistance. As epichlorohydrin elastomers contain about one third by mass of chlorine (chloromethyl groups) and is polar, it has a very good resistance to oils and fuels (with the exception of polar brake fluids). Because of the existence of highly polar and dense chloromethyl groups, epichlorohydrin elastomers also have excellent permeation resistance. Hydrin® rubber is currently undergoing research into ionic conductivity and there have been promising positive results when salts have been integrated into the copolymer matrix of EPI-EO [118].

### *1.6.2.3 Poly [(acrylonitrile-co-butadiene)/poly vinylchloride]*

Poly[(acrylonitrile-co-butadiene)/poly vinylchloride] is a pre-plasticised nitrile elastomer, commercially known as Nipol® DN171. It consists of acrylonitrile butadiene rubber or nitrile rubber [40 wt% of nitrile butadiene rubber (NBR), copolymerized with 30 wt% of acrylonitrile (ACN)], blended with 30 wt% of poly vinylchloride (PVC). In addition, it is synthesised in the form of light-amber coloured slabs via mechanical mixing. Nitrile rubber (NBR), is a copolymer of nitrile butadiene rubber and acrylonitrile, which is highly flexible, thermally stable, and highly resistant to chemical attack [119]. Conversely, poly(vinyl chloride) (PVC), is a thermoplastic polymer, whose structure is semi-crystalline in nature; in order words, its structure possesses both amorphous and crystalline regions. Unlike, NBR (whose properties depend on the content of acrylonitrile), PVC possess very good mechanical properties, which depends on the bulky chlorine group on each monomer unit in the polymer chain. However, under light and heat, it readily dissociates with the evolution of gaseous HCl (by dehydrochlorination). This instability can be prevented by adding stablisers, which involves the mixture of PVC with various additives. These additives help to increase the flexibility of the polymer chain, by acting as an internal lubricant [1, 3]. Therefore, the blending of such plasticized PVC with NBR (in this case, it consist of 30 wt% ACN), should result in an increased impact strength, and polarity of the blended elastomer (as a result, of the combination of the properties of both constituents). This type of elastomer (Nipol® DN171) may be considered as possessing a two phased morphology.

## 1.7 Definition of Polymer Blends and Blending Methods

Blends in general terms are mixtures of two or more substances, and the same is true of polymer blends and composites [120,121]. A mixed polymer is called a blend if there is no covalent bonding occurring between the two polymers and it is homogeneous. It can be referred to as a composite only if the components are heterogeneous and immiscible. There

are three different routes by which it is possible to mix polymers. The first is via a synthetic method. The polymerisation occurs either inside the polymer matrix or in the presence of it, so it could be called a "one beaker reaction". The second method is a "co-dissolution"; this involves both of the substances, (in most common cases a conducting polymer and a host polymer) to be dissolved in the same solvent then mixing the two solutions and allowing the solvent to evaporate to form a blended solid. The third method is "dry blending", this can be achieved by mixing the two polymers mechanically then moulding them in a hot press or extruder.

### 1.7.1 Blends of Electrically Conductive Polymers

As discussed in section 1.6.9, the mechanical limitations of conducting polymers may be overcome by incorporating the polymers in blends or composites with a host substrate. The substrate can either be electrically insulating or conducting. In the case of insulating substrates, sufficient concentration of the conducting polymer is required to achieve a percolation threshold for an insulator-to-conductor transition [122]. The percolation threshold is theoretically predicted to be at a volume fraction of 0.154 for globular agglomerates in a three dimensional insulating medium [114] and 0.183 for randomly packed hard spheres [123]. In reality, the percolation threshold is strongly influenced by the size and shape of the conducting species, as well as by processing methods such as solution casting, compression and injection moulding, chemical modification, or chemical deposition.

#### *1.7.1.1 Conducting Elastomers*

Conducting rubber has been known since the latter part of nineteenth century. It was not of primary interest until about 1930, when several patents explained the use of conducting compounds for the prevention of corona discharge in cables[124]. Most of the early work employed large quantities of graphite or other coarse carbon blacks or even powdered metals

to produce conductivity and the resultant material tended to have very poor physical properties. The introduction of acetylene black and other conductive blacks however led to the production of a material which had mechanical properties almost comparable to those of insulating elastomers.

The principal use of conventional conducting elastomers is to dissipate electrostatic charges which are developed whenever two dissimilar surfaces are separated either with or without rubbing. The development of conducting elastomers usage as antistatic materials appeared in the late 1930s, when the surgical world was worried about the frequency of explosions in operating theatres, many of which occurred due to static electricity sparks igniting ether vapours.

Antistatic materials have since been used in many circumstances where explosive vapours, liquids or powders are being handled, and for vehicles and aircrafts, where static charges can be generated by the tyres or acquired in flight.

The use of conducting elastomers for heating purposes was the subject of research since 1940s, but there were considerable problems associated with a change in resistance upon flexing. Conducting silicone rubbers show promising results in resolving this difficulty[124]. These materials have also been used in the field of electronics in order to reduce the size and weight of many electrical devices, such as connectors, switches, thermostats and internal mountings[125].

A combination of conductive polymers (rigid) and elastomers (flexible) in flexibility hybrid systems, could possess enormous advantages over metals such as malleability, ability to absorb mechanical shock, low density, wide range of electrical conductivity and corrosion

resistance properties[124]. These characteristics are highly advantageous in the production of viable commercial applications.

On the other hand, elastomer blends cannot be produced with such high conductivities as metals and they commonly have lower mechanical strength than metals.

### *1.7.1.2 Conductive Polyaniline Blends*

Conventional conducting elastomers (prepared by filling elastomers with carbon black, metallic powders or fibres coated with metals) if compared with novel conducting elastomers have some significant disadvantages. Carbon black has relatively poor conductivity which results in a high percolation threshold [126] and the conductivity values are not higher than $10^{-8}$ $S.cm^{-1}$. Carbon black-elastomers have a shielding effectiveness of 40-50dB only with about 40 wt% of loaded filler[127]. In the case of metal powders it has been found that to achieve adequate shielding[127], there must be a high (>55 wt %) fraction of metal in the elastomeric blend, which produces a heavy and less malleable composite. Metal fibres tend to have complicated manufacturing issues which can limit their suitability. All conventional composites containing metal powders are susceptible to oxidation; hence their conductivities are subject to reduction[128].

In order to overcome the problems of these conventional conducting elastomers, this PhD study has concentrated on intrinsically conducting elastomers as they can be more easily manipulated and have greater conductivity, potentially with a low percolation threshold. Also, investigations into the orientation of polyaniline chains have demonstrated a threefold increase in conductivity when the chains were stretched and aligned compared to randomly dispersed chains [129].

Novel electrically conductive elastomer blends may be expected to have a combination of good electrical properties of the intrinsically conductive polymers with good mechanical properties of elastomers. They should be considered for sophisticated applications such as electromagnetic interference shielding (EMI), gas separation membranes and superior corrosion-inhibiting coatings. These conductive materials are also expected to have good processibility and could potentially processed with the conventional elastomer processing machines, e.g. internal mixer injection moulder and a single or twin screw extruder.

## 1.8 Aim of the Project

PAni is viewed by many as a wonder molecule whose properties render it unique in the family of conducting polymers. The important characteristics of the polymer are its:

- Tuneable conductivity
- Multiple oxidation states
- Electrochromic behaviour

Research on conducting polymers and polyanilines has been ongoing for many years at Kingston University and is a principal area of expertise in the Materials Research Group. One of the main focuses of past research has been to try and find ways of producing uniform conducting films and coatings by incorporating the conducting polyaniline in a plastic matrix. The present project is divided into two parts:

The first part of this project investigated the influence of various parameters such as different acid dopants and the use of substituted anilines co-monomers on the chemical structure, electrical properties, thermal degradation, physical characteristics, and morphology of the polymer.

Österholm [130] was one of the first to study the influence of a surfactant sulfonic acid on the structure of the polymer. The use of surfactant molecules in the synthesis yields materials

which differ in their physical characteristics compared to those prepared via precipitation polymerisation. Emulsion polymerization brings uniformity in the sizes and shapes of the PAni particles.

Using substituted aniline as a *co*-monomer also changes the physical and chemical characteristics of the final compounds. Hence, 2-methoxyaniline (anisidine) [131] which brings increased electron density to the polymer along with a saturated pendant group, was studied.

The aim was to produce polyaniline particles of different size and shapes and to study the mechanisms which lead to these structures.

The second and the main objective of this project was to prepare and investigate various polyaniline blends and their properties. Non-blended polyaniline and its derivatives have enormous potential as viable alternatives to traditional metals in a wide variety of applications, due to their high electrical conductivities. Nevertheless, their poor processibility has made them particularly difficult to handle and thus restricts other potential applications. Therefore, the combination of conductive polyaniline and the elastomeric materials should create an ideal blend. Normally, in order to achieve the target of an ideal blend, both the selected elastomer and the conductive polymer must have comparable solubility parameters, to favour compatibility and therefore blends will be prepared through different mixing methods (i.e. solution and thermo-mechanical) with more systematic mixing procedures and better optimised conditions. Two elastomers (i.e. Epi-EO and Nipol®DN171) will be used as the host matrix and an intrinsic electrically conductive polymer (i.e. PAni-DBSA) as the conductive filler, through solution mixing (for the fundamental study i.e. compatibility of the mixing components) and thermo-mechanical (for larger scale application purposes). No literature works have been reported to date relating to the study of electrical properties of Epi-EO/PAni-DBSA blends or thermoplastic rubber such as Nipol®DN171 with PAni-DBSA.

In this study, polyaniline was synthesised via chemical oxidative polymerisation. The synthesis involved the addition of oxidant to aniline dissolved in aqueous hydrochloric acid solution resulting in PAni-HCl powder. PAni-HCl was first dedoped and then reprotonated with a suitable functionalised protonic acid (DBSA), in order to induce processibility in THF and compatibility with both Epi-EO and Nipol®DN171. The compatibility or miscibility of the blended elastomer (Nipol® DN171 rubber) with the electrically conducting polyaniline (polyaniline doped with DBSA), should be enhanced (due to the plasticization effect of the PVC), coupled with an improved processibility, and mechanical properties. Although, there are no literature reports detailing studies of any kind on a two phased elastomer blended with conducting polyaniline, polymer blends of its constituents (NBR and PVC, individually) with PAni-DBSA have been investigated with promising outcomes [119,132].

Electrically conductive blends were produced by combining an elastomeric material such as Hydrin or Nipol®DN171 with varying amounts of PAni-DBSA. It was decided to prepare blends by a co-dissolution method which required both polymers to be soluble in common solvents such as THF. This method had not previously been used to make Hydrin or Nipol®DN171-based conductive blends. The polymers were solution blended and studied for compatibility by means of infrared spectroscopy (IR), ultraviolet-visible (UV-Vis) spectroscopy. Electrical conductivity measurements were carried out using two and four probe methods. Thermal analysis was undertaken using differential scanning calorimetry (DSC), thermogravimetric analysis (TGA), thermomechanical analysis (TMA). The characterisation of the blends using the above techniques allowed the study and evaluation of the polyaniline blends in greater detail.

CHAPTER

# 2

# EXPERIMENTAL WORK

*This chapter reports on general procedures regarding sample preparation, blending processes and materials handling.*

*Methods of synthesis of different polyanilines are assessed and compared in the first part of the chapter. The chosen monomers, aniline and o-anisidine, are polymerised using two systems: Solution and emulsion polymerisation. The second part of the chapter will be concerned with the preparation of conductive polyaniline blends which was undertaken by co-dissolution and thermal blending processes.*

# 2 Experimental

## 2.1 Polyaniline and Its Derivatives

Since the discovery of "Aniline Black", a wide range of methods have been used for the synthesis of polyaniline, leading to the formation of a range of products whose nature and properties differ greatly. Polyaniline can be prepared either by chemical or electrochemical polymerisation of aniline. The present study involved trying to produce PAni using synthetic routes that could be easily scaled-up for eventual industrial production. Electrochemical polymerisation was thus discarded from the project. In addition, the solubility of the prepared polymers was also an important consideration, which led us to consider sulfonic acid polymerisation routes. The first step in the synthesis of PAni is the oxidation of aniline to form a radical cation which is the main criteria for achieving polymerisation.

## 2.2 Chemicals and Raw Materials

Aniline monomer 99% (Sigma-Aldrich), o-Anisidine monomer 99% (Sigma-Aldrich) both purified by vacuum distillation, ammonium persulfate 98% (Sigma-Aldrich), 4-dodecylbenzenesulfonic acid (DBSA) 90% (Fluka), p-toluenesulfonic acid monohydrate (p-TSA ) 98% (Aldrich), β-naphthalenesulfonic acid (β-NSA) 70% (Aldrich), methanesulfonic acid (MeSA) 99% (Aldrich), (+/-)-10-camphorsulfonic acid (CSA) 98% (Aldrich), hydrochloric acid (GPR, 36.5 - 38%), 33% ammonia solution (VWR), methanol (VWR), tetrahydrofuran (THF) (VWR), chloroform ($CHCl_3$) (VWR), trans-decalin (VWR), n-hexane (VWR), cyclohexane (VWR), xylene (VWR)

## 2.2.1 Polyaniline

### *2.2.1.1 Solution Polymerisation (using a strong acid medium)*

Polyaniline and its derivatives are generally synthesised using a strong protonic acid medium such as aqueous HCl, $H_2SO_4$, or $HClO_4$. As mentioned in section (1.7.1.8) the polymerisation involves proton-transfers to and from the monomer, dimer, oligomer, and polymer molecules.

Synthesis of PAni-HCl at Different Oxidant Ratio

The oxidant/monomer ratio plays a key role in governing the final physical properties of the particles prepared [49]. Not only has it an effect on the yield of the polymer, but also it has a variable effect on the oxidation state of the final particles, and therefore their chain length, doping level, conductivity etc.

A series of experiments was set up to study the significance of the initial mole ratio of ox/mon on conductivity, and the physical properties of the polymeric particles. The experimental conditions of the synthesis were derived from Armes [79] in a study of the optimum reaction parameters for the polymerisation of aniline using APS as initiator.

| Sample ID | Compound name | Synthetic method | % Yield |
|---|---|---|---|
| Z-0001 | PAni-HCl | OX:MON = 0.25:1 | 21.6% |
| Z-0002 | PAni-HCl | OX:MON = 0.5:1 | 40.5% |
| Z-0003 | PAni-HCl | OX:MON = 0.75:1 | 55% |
| Z-0004 | PAni-HCl | OX:MON = 1.08:1 | 87.3% |
| Z-0005 | PAni-HCl | OX:MON = 1.25:1 | 88.7% |
| Z-0006 | PAni-HCl | OX:MON = 1.5:1 | 88.3% |

Table 3 PAni-HCl synthesised at different oxidant: monomer ratios.

10ml of aniline was dissolved in 150ml of 1M hydrochloric acid and pre-cooled to 0°C. The aniline solution was added to solutions of varying concentrations of ammonium persulfate in 110ml of 1M hydrochloric acid in order to produce the desired range of oxidant/monomer initial mole ratio r. This range is illustrated in Table 3. A few drops of ferric chloride were added to the polymerisation mixture as a catalyst. In each case an intermediate pink colour was observed, the intensity of which increased with r. The pink colour remained for approximately one minute, with the reaction solution gradually turning from blue to green over a period of several minutes. The oxidant was added drop-wise over a period of 35 minutes. The addition of the oxidant caused a sudden increase in temperature, dependent on the ratio of oxidant to monomer. The polymerisation mixture was then cooled and maintained at 0°C until the end of the polymerisation reaction, while the pH was adjusted to be between 0-0.5 by the addition of concentrated HCl. The mixture was left for five hours to complete the polymerisation. The reaction solutions were then filtered and washed with 500ml of 1M hydrochloric acid. The colour of the filtrates was reddish-pink due to the presence of soluble aniline oligomers. These filtrates were then dried under vacuum for 24 hours and finally, left in a vacuum oven to dry for a further 24 hours at a temperature of 40°C.

## Synthesis of PAni-HCl

Conductive emeraldine salt PAni-HCl was synthesised by oxidative chemical polymerisation using aqueous HCl as an acidic medium. The wide use of HCl can be attributed to a various factors such as:

- High reactivity leading to fast syntheses
- High yield
- High conductivity of the synthesised polymer
- Low cost

Most of the work on conductive blends and composites of polyaniline has been carried out on

particles synthesised using a standard method.

Compound Z-0007 was prepared by dissolving 100ml (1.097mole) of aniline in 1500ml of 1M HCl and leaving it to stir using a mechanical stirrer. The solution was cooled and the temperature maintained at 0°C aided by an ice bath. Separately 187.8g (0.822mole) of $(NH_4)_2S_2O_8$ were dissolved in 1100ml of 1M HCl and left to cool in an ice bath with the aid of a magnetic stirrer. After 1 hour 45 minutes the oxidant was added drop wise; during the addition of oxidant the temperature rose. After 20 minutes, the colour changed from dark blue to emerald. The reaction was allowed to proceed for 5h from the addition of the first drop of oxidant. The end product was PAni-HCl. It was then washed with 5L of 1M HCl, and the filtrates were pink in colour. A 5g portion of the PAni-HCl sample was removed and dried in an oven at 40°C for 24 hours and retained for characterisation.

## Preparation of PAni-Base (Neutral Polymer)

Emeraldine base (Z-0008) was prepared by de-protonating the wet emeraldine salt (PAni-HCl) in 0.5M aqueous ammonia solution (5250ml) with 24 hours stirring. After that, the final product was washed using 8L of distilled water and filtered under vacuum for 24h. Drying was carried out in a vacuum oven at 50°C.

## Doping the EB with HCl at Different pH

Polyaniline prepared using conventional routes can be easily deprotonated and then re-protonated with HCl. A series of doped emeraldine base samples was prepared using a variety of HCl concentrations. The method used to prepare compounds (Z-0009-Z-0012) is as follows: 5g of emeraldine base was placed in a 500ml beaker to which 250ml volumes of varying concentrations of HCl were added. These solutions were then stirred until the specified pH of the system was reached; see Table 4.

| Sample ID | Compound name | Concentration HCl (mole/L) | pH |
|---|---|---|---|
| Z-0009 | PAni-HCl | 1 | 0 |
| Z-0010 | PAni-HCl | 0.1 | 1 |
| Z-0011 | PAni-HCl | 0.01 | 2 |
| Z-0012 | PAni-HCl | 0.001 | 3 |

Table 4 Protonation of EB with HCl at different pH.

The samples were filtered and dried in the vacuum oven at 40°C, to remove excess water.

## Doping the EB with Different Dispersing Agents

A batch of polyaniline doped HCl (Z-0007) was prepared and then fully deprotonated using ammonia solution as described above. The resulting base was protonated with a range of different dispersing agents, which included DBSA, TSA, NSA, CSA and MeSA. Solutions containing 200ml of $H_2O$ and dispersing agent were prepared, and to this, portions of 5g of EB (with equivalent molar ratio to the dispersing agent) were added. The relative amount of dispersing agents used is described in Table 5. The mixtures were left to stir for 24 hours at room temperature. These samples were then washed with 700ml of methanol and left to dry for 24 hours at 40°C so the filtrates were protonated. The end product was a green coloured powder in each case.

| Sample ID | Dispersing agents | Amount Used (g) |
|---|---|---|
| Z-0013 | DBSA | 29.86 |
| Z-0014 | p-TSA | 15.66 |
| Z-0015 | β-NSA | 24.49 |
| Z-0016 | MeSA | 10.1 |
| Z-0017 | CSA | 19.12 |

Table 5 protonation of the EB with various dispersing agents.

### *2.2.1.2 Emulsion Polymerisation*

An important benefit of emulsion polymerisation is to obtain particles with a uniform morphology. The polymer chains may increase in order throughout the backbone structure and the aggregates and particles are expected to show a decrease in their average size.

PAni-DBSA via Emulsion Polymerisation in Water

The emulsion polymerisation of PAni-DBSA in $H_2O$ was carried out in accordance with the method outlined by Haba [133] which involved a two step process, namely:

a) The creation of anilinium-DBSA complex with needle-like structures which are formed by the combination of the monomer and the DBSA acid.

b) The initiation of polymerisation occurs by the addition of APS to the complex. The reaction mechanism is thought to be similar to that of the conventional method for the preparation of polyaniline. The bulky nature of the surfactant molecules leads to an increase in viscosity of the reaction medium, meaning the process of polymerisation is somewhat slower; thus the molecules transport is slower than it would be if the reaction occurred in

solution. Consider the diagram below (Figure 27), which is a representation of the DBSA micelle in water.

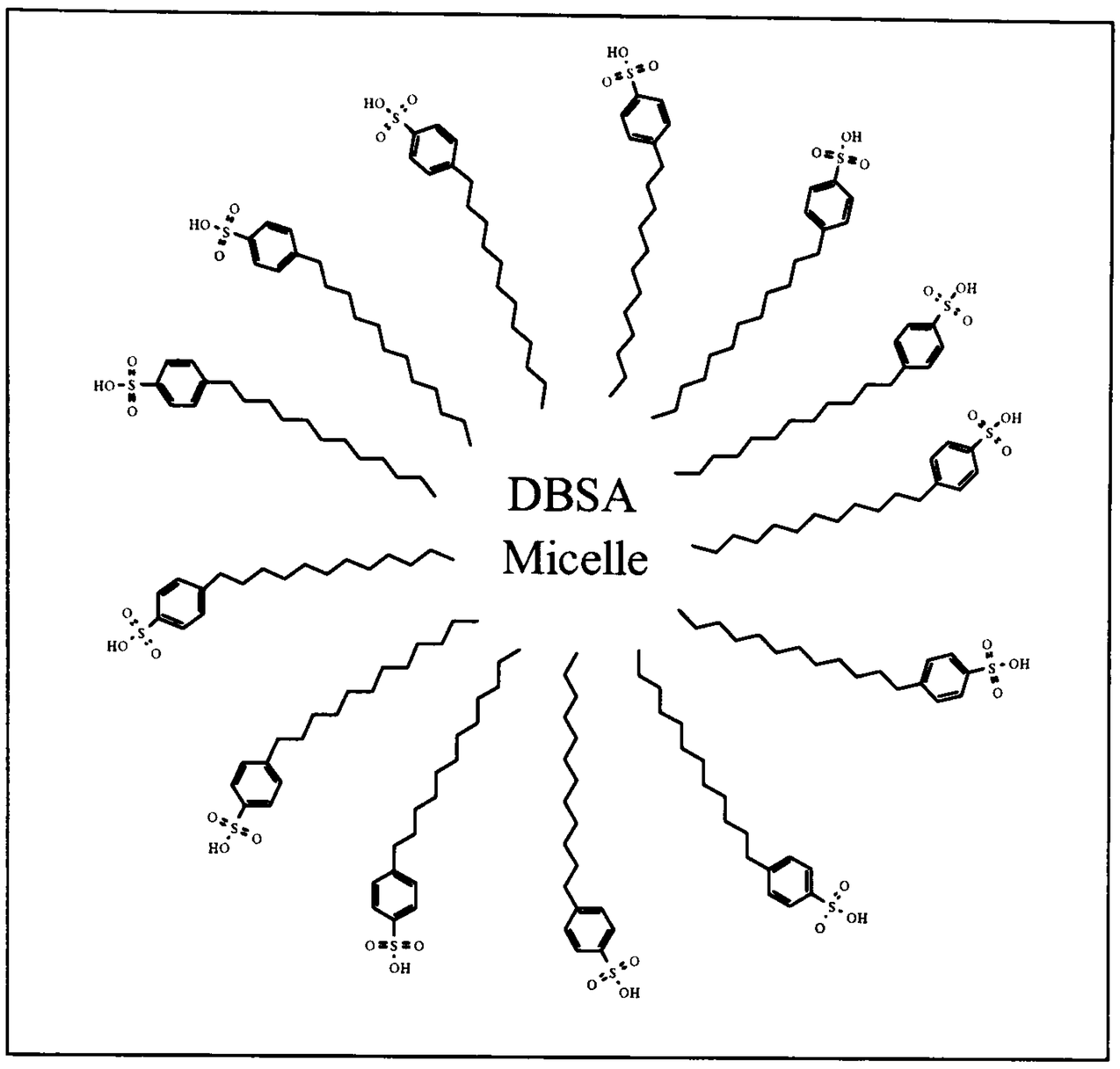


Figure 27 DBSA micelle in water.

The hydrophilic sulfonic acid heads surround the micelle, solubilised by the water molecules, and the hydrophobic tails of the surfactant point towards the centre of the micelle away from the solvent These interactions occur mainly from Van der Waals forces between the long alkyl chains inside the structure which may cause higher stability, leading to elliptically shaped micelles; therefore when the aniline and the later oxidant are added to the reaction system, partial fragmentation of the DBSA micellar structure occurs as illustrated in the following reaction diagram (Figure 28).

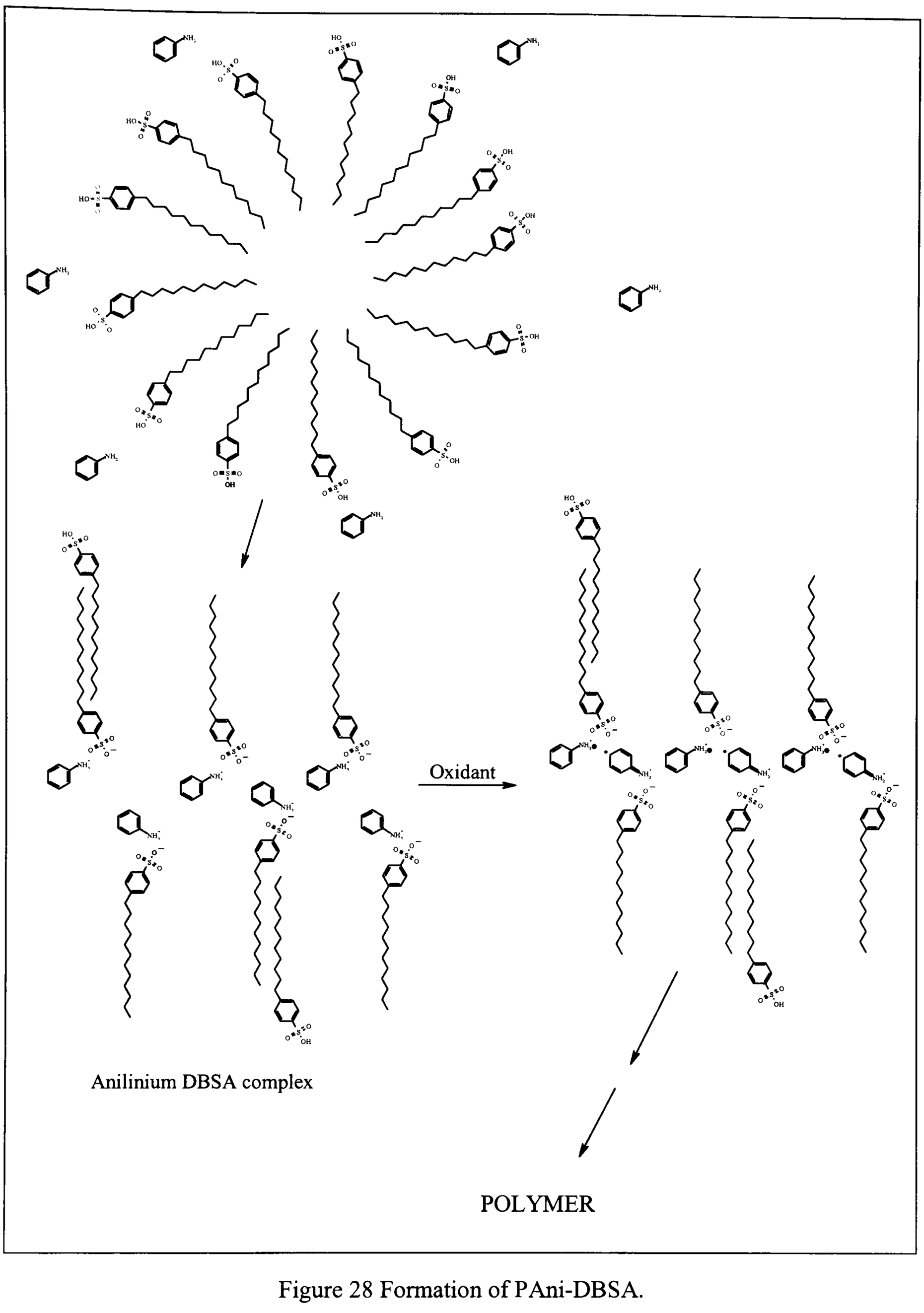


Figure 28 Formation of PAni-DBSA.

As the polymer chains grow the formation of another type of micelle possibly occurs along with remaining DBSA micelles, consisting of polymeric cores surrounded by a double layer of DBSA molecules as seen in Figure 29.

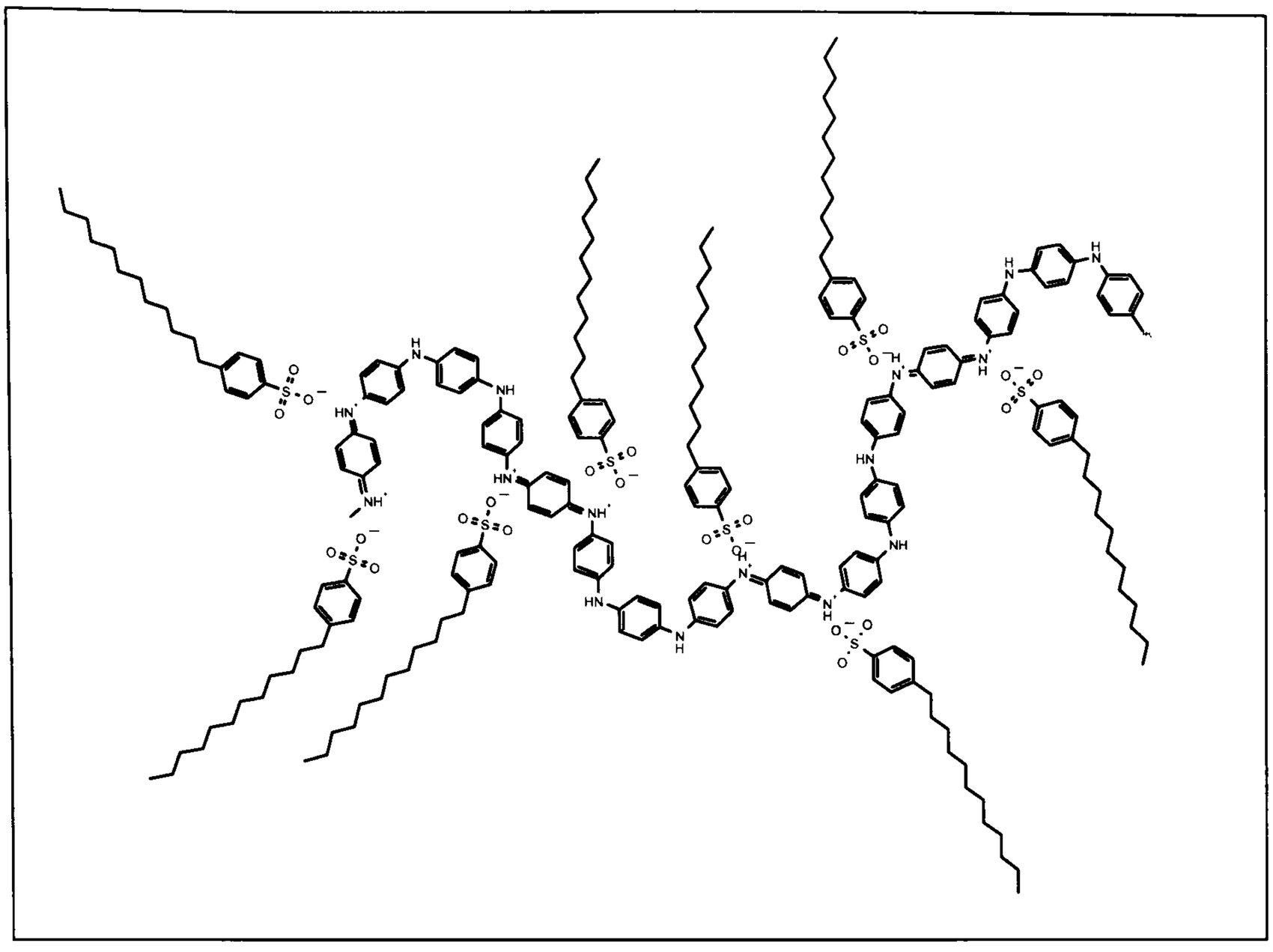

Figure 29 PAni-DBSA polymeric micelle.

For Compound Z-0018, 66.30g (0.1646moles) of DBSA was weighed and dissolved in 400ml of water and stirred mechanically. It was important that the DBSA was fully dissolved in $H_2O$, to allow ion exchange to occur. This was then cooled with an ice bath, and 10ml (0.1097mole) of aniline was added to the mixture. The dispersion turned white upon formation of insoluble anilinium-DBSA complex. After stirring for approximately two hours under these conditions, 18.80g (0.0823moles) of APS initiator was dissolved in 100ml of water and placed in ice bath. The initiator was then placed in a separating funnel and slowly added (over a period of one hour) into the polymerisation bath which already contained monomer and surfactant. It was noted that on the addition of the oxidant the temperature rose. The suspension turned from white to purple, blue and finally emerald over the course of an hour.

The reaction was continued for eight hours. Methanol 1.5 litres was added to the PAni–DBSA aqueous dispersion to precipitate the doped PAni powder (methanol: PAni dispersion

volume ratio was 1:1). The precipitate was filtered, washed with methanol and dried in a vacuum oven at 40°C for 48 hours.

## PAni-DBSA via Emulsion Polymerisation in a Water-Organic Solvent System

Österholm *et al* [130] and the following year Yang [88] reported a direct one step emulsion polymerisation route to conducting PAni-DBSA using binary solvent mixtures. In this project various water-organic solvent mixtures were chosen in conjunction with the aniline monomer to form a host of colloidal structures, as depicted in Figure 30.

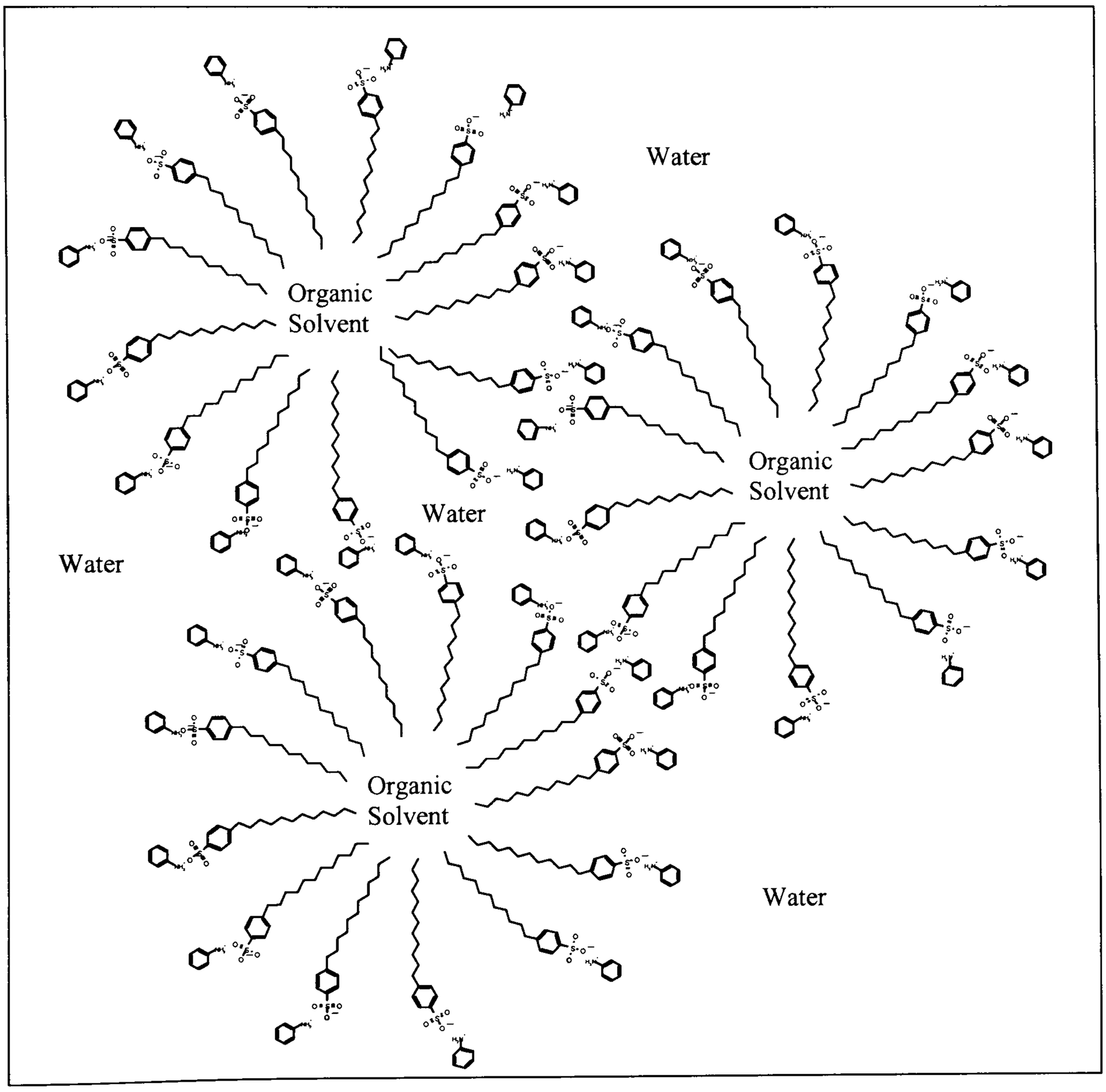


Figure 30 DBSA micelles in a water/organic solvent system.

It can be seen from the scheme that the organic solvent is trapped within the micelle structure, due to the hydrophobic tail of the chosen surfactant.

The varying water-organic solvents typically had common water: organic ratio of 4:1 respectively. A typical reaction method is outlined below:

The ammonium persulfate (12.33g) was dissolved in (100ml) of deionised water. Separately 39.81g of DBSA was dissolved in a mixture of (300ml) $H_20$ and (100ml) of the organic solvent (Table 6); then the oxidant was added dropwise and the polymerisation was carried out over an 8h period. Precipitation occurred by breaking the micelle structure, and this process was achieved by adding methanol to the system followed by washing and filtration of the sample.

| Sample ID | Compound name | Organic solvent | % Yield |
|---|---|---|---|
| Z-00019 | PAni-DBSA | Trans-Decalin | 35% |
| Z-0020 | PAni-DBSA | n-Hexane | 30% |
| Z-0021 | PAni-DBSA | Cyclohexane | 29% |
| Z-0022 | PAni-DBSA | Xylene | 37% |
| Z-0023 | PAni-DBSA | Chloroform | 31% |
| Z-0024 | PAni-DBSA | THF | 27% |

Table 6 Synthesis of PAni-DBSA in water / organic medium.

## Synthesis of Polyaniline Doped with β-NSA, CSA, TSA, MeSA

For the synthesis of doped polyaniline with various dispersing agents, the method undertaken is similar to that described in section 2.2.2.1, with just alteration of the dispersing agent (see Table 7). In the case of PAni-NSA, microtubules of diameter 100 micro metres were obtained by a simple reaction route [134], first the aniline and β-naphthalenesulphonic acid (β - NSA) were mixed, resulting in a "needle-like" product. The anilinium salt was then oxidised by dropwise addition of a solution of APS in water. The mixture was stirred for 8h and washed with methanol and vacuum dried for 48h at 40°C.

| Sample ID | Dispersing agent | Amount used (g) | % Yield |
|---|---|---|---|
| Z-0025 | β –NSA | 48.97 | 42% |
| Z-0026 | CSA | 38.24 | 44% |
| Z-0027 | P-TSA | 31.31 | 46% |
| Z-0028 | MeSA | 10.68 | 57% |

Table 7 Preparation of PAni using various dispersing agents.

## 2.2.2 Polyanisidine

The family of polyanisidine compounds were prepared following the methodology used in the preparation of polyaniline in section (2.2.1.1) and (2.2.1.2).

### *2.2.2.1 Solution Polymerisation*

Owing to polyanisidine's greater solubility with respect to polyaniline, it was decided to synthesise a variety of polyanisidine compounds with differing dispersing agents via precipitation polymerisation, with a view to improve their solubility in common organic solvents. In this method, PoAnis-HCl (Z-0029) was synthesised via oxidative polymerisation of anisidine in a similar procedure to that undertaken for PAni-HCl. Neutralisation was achieved using ammonia solution, forming PoAnis base (Z-0030) (Table 8 shows an overview of the different quantities of constituents used in this preparation of the PoAnis), finally, PoAnis base was protonated using a variety of dispersing agents. See Table 9.

| Reagent | Amount |
|---|---|
| Anisidine Monomer | 100ml |
| Oxidant | 187.8g |
| HCl 1M | 2600ml |
| Ammonia solution 0.5M | 3000ml |

Table 8 Synthesis summary of PoAnis via precipitation polymerisation.

| Sample ID | Compound name | Amount Used (g) |
|---|---|---|
| Z-0031 | PoAnis-DBSA | 22.27 |
| Z-0032 | PoAnis-TSA | 11.68 |
| Z-0033 | PoAnis-NSA | 18.27 |

Table 9 PoAnis with different dispersing agents.

The first synthesis of PoAnis was described by Macinnes in 1988, however the actual description of synthetic conditions were derived by S.P. Armes, in the study the optimum reaction parameters for the polymerisation of PAni-HCl using APS as oxidant.

### *2.2.2.2 Emulsion Polymerisation*

Emulsion polymerization of PoAnis family was carried out in $H_2O$ in accordance with the method outlined in section (2.2.1.2). This involved the combination of anisidine with a host of dispersing agents namely DBSA, TSA, CSA, NSA and MeSA, followed by addition of APS oxidiser. Table 10 below describes the family of polyanisidines prepared using different dispersing agents. The mole ratios of monomer, oxidant, and dispersing agent used in the synthesis of PoAnis were similar to those of the PAni dispersed compounds.

| Reagent | Amount |
|---|---|
| Anisidine monomer | 10ml |
| Oxidant APS | 15.18g |
| Distilled water | 500ml |
| Methanol for washing | 1.5L |

Table 10 Synthesis summary of PoAnis via emulsion polymerisation.

| Sample ID | Dispersing agent | Amount Used (g) | %Yield |
|---|---|---|---|
| Z-0034 | DBSA | 48.24g | 53% |
| Z-0035 | TSA | 25.30g | 43% |
| Z-0036 | CSA | 30.90g | 38% |
| Z-0037 | β-NSA | 39.57g | 29% |
| Z-0038 | MeSA | 8.63ml | 50% |

Table 11 Preparation of PoAnis using various dispersing agents.

### 2.2.3 Co-Polymerisation of Aniline/o-Anisidine

The co-polymerisation of aniline and 2-ethoxyaniline by Kim *et al* was an ideal starting point for the synthesis of polyaniline/o-polyanisidine co-polymers and blends. Following the reported method, it was decided to combine o-anisidine monomer with a monomer of aniline in varying molar ratios. The mixtures consisted of 5ml (0.0549mol) aniline and 6.2ml (0.0549mol) of anisidine which comprised a 50:50 molar ratio co-polymer, then 7.5ml (0.0824mol) of aniline with 3.1ml (0.0275mol) of anisidine which represents 75:25 molar ratio, and finally 2.5ml (0.0275mol) aniline with 9.3ml (0.0824mol) anisidine was employed to give a molar ratio of 25:75. The various monomer ratios were then added to a known concentration of dispersing agents i.e. DBSA, TSA, CSA, β-NSA and MeSA. Similar methods to the formation of the homopolymers (as seen in section 2.2.1.2, 2.2.2.2) were

employed for the co-polymerisation of aniline/o-anisidine. The following tables show the differing molar ratios of aniline to anisidine which include varying dispersing agents.

| Sample ID | Compound name | Amount used (g) | % Yield |
|---|---|---|---|
| Z-0039 | PAni: PoAnis -DBSA | 59.86 | 70% |
| Z-0040 | PAni: PoAnis-NSA | 49.09 | 64% |
| Z-0041 | PAni: PoAnis -CSA | 38.33 | 65% |
| Z-0042 | PAni: PoAnis -TSA | 31.39 | 67% |
| Z-0043 | PAni: PoAnis -MeSA | 10.7 | 62% |

Table 12 Preparation of 50:50 molar ratio of aniline-anisidine *co*-polymer.

| Sample ID | Compound name | Amount used (g) | % Yield |
|---|---|---|---|
| Z-0044 | PAni: PoAnis-DBSA | 59.86 | 59% |
| Z-0045 | PAni: PoAnis-NSA | 49.09 | 43% |
| Z-0046 | PAni: PoAnis-CSA | 38.33 | 64% |
| Z-0047 | PAni: PoAnis-TSA | 31.39 | 75% |
| Z-0048 | PAni: PoAnis-MeSA | 10.7 | 54% |

Table 13 Preparation of 75:25 molar ratio of aniline-anisidine *co*-polymer.

| Sample ID | Compound name | Amount used (g) | % Yield |
|---|---|---|---|
| Z-0049 | PAni: PoAnis-DBSA | 59.86 | 59% |
| Z-0050 | PAni: PoAnis-NSA | 49.09 | 42% |
| Z-0051 | PAni: PoAnis-CSA | 38.33 | 48% |
| Z-0052 | PAni: PoAnis-TSA | 31.39 | 71% |
| Z-0053 | PAni: PoAnis-MeSA | 10.7 | 48% |

Table 14 Preparation of 25:75 molar ratio of aniline-anisidine *co*-polymer.

## 2.3 Polymer Blends

### 2.3.1 Blends Prepared via Co-dissolution Method

#### *2.3.1.1 Chemicals and Raw Materials*

Aniline monomer (99 wt%, Sigma-Aldrich), ammonium persulfate [APS] (98 wt%, Sigma-Aldrich), 36.5-38 wt% HCl solution (GPR), 33 wt% ammonia solution (GPR), 90 wt% DBSA solution (GPR, Fluka), Tetrahydrofuran (GPR), Methanol (GPR), poly(epichlorohydrin-*co*-ethylene oxide) elastomer (Zeon Chemicals). Poly[(acrylonitrile-*co*-butadiene)/poly vinylchloride] Nipol® DN171 (Zeon chemicals). All types of rubber (Hydrin rubber and the thermoplastic rubber) were washed with methanol for 24 hours using Soxhlet extraction in order to remove chemical additives, prior to drying and use for making blends.

#### *2.3.1.2 PAni-DBSA/poly (Epichlorohydrin-co-ethylene oxide) Blends*

Preparation

5g of PAni-DBSA (Z-0013) was dissolved in 500ml of THF and left for 10 days with continuous stirring. PAni-DBSA solution was then filtered and the residual filtrate was weighed to quantify un-dissolved polymer. The weight of dissolved polymer was 1.7g in 460ml; hence the concentration of polymer in THF was 0.37% (w/v).

10g of the host polymer (epichlorohydrin-ethylene oxide copolymer) was dissolved in 500ml of THF and left for 10 days with continuous stirring. All of the copolymer was dissolved. Hence, the concentration of copolymer in THF was 2% (w/v).

Blends of PAni-DBSA and C-2000L in THF were obtained by adding a known quantity of the conducting polyaniline solution to appropriate amounts of copolymer solution as indicated in Table 15.

The mass of PAni-DBSA in 20ml of polymer solution was equal to 0.074g. Hence the preparation of a 1:1 mass-ratio blend was achieved by adding 3.7ml of C-2000L solution.

| Film no. | Ratio of PAni-DBSA to rubber (%) | Ratio of PAni-DBSA to rubber | Volume of PAni-DBSA solution (ml) | Mass of PAni-DBSA (g) | Volume of rubber solution (ml) | Mass of rubber (g) |
|---|---|---|---|---|---|---|
| F-0001 | 50 : 50 | 1:1 | 20 | 0.074 | 3.7 | 0.074 |
| F-0002 | 67.7:33.3 | 2:1 | 40 | 0.148 | 3.7 | 0.074 |
| F-0003 | 75:25 | 3:1 | 60 | 0.222 | 3.7 | 0.074 |
| F-0004 | 80:20 | 4:1 | 80 | 0.296 | 3.7 | 0.074 |
| F-0005 | 83.4:16.6 | 5:1 | 100 | 0.37 | 3.7 | 0.074 |
| F-0006 | 40:60 | 1:1.5 | 20 | 0.074 | 7.4 | 0.148 |
| F-0007 | 30:70 | 1:2.33 | 20 | 0.074 | 8.621 | 0.172 |
| F-0008 | 20:80 | 1:4 | 20 | 0.074 | 14.8 | 0.296 |
| F-0009 | 16.6:83.4 | 1:5 | 20 | 0.074 | 18.5 | 0.37 |
| F-0010 | 14.28:85.71 | 1:6 | 20 | 0.074 | 22.2 | 0.444 |
| F-0011 | 12.5:87.5 | 1:7 | 20 | 0.074 | 25.9 | 0.518 |
| F-0012 | 11.1:88.9 | 1:8 | 20 | 0.074 | 29.6 | 0.592 |
| F-0013 | 10:90 | 1:9 | 20 | 0.074 | 33.3 | 0.666 |
| F-0014 | 9:91 | 1:10 | 20 | 0.074 | 37 | 0.74 |
| F-0015 | 5:95 | 1:19 | 20 | 0.074 | 70.3 | 1.406 |
| F-0016 | 2.5:97.5 | 1:39 | 20 | 0.074 | 144.3 | 2.886 |
| F-0017 | 1:99 | 1:99 | 20 | 0.074 | 366.3 | 7.326 |
| F-0018 | 0.75:99.25 | 1:132.3 | 20 | 0.074 | 489.5 | 7.344 |

Table 15 The cast films and composition (by ratio) of each elastomeric blend.

A series of different mass-ratio blends were prepared (as shown in Table 15) by mixing a constant amount of copolymer solution with increasing amounts of the conductive polymer solution (0.074–0.296g). Table 15 illustrates the preparation of blends by increasing the amount of C-2000L (0.074–7.34g) and keeping the amount of PAni-DBSA constant.

Fifteen slides (25 x 25mm) of PTFE sheets were cut, rinsed with distilled water and left to dry at room temperature. The slides were aligned next to each other and labelled accordingly.

Six individual layers of the blends were cast to make films. This was carried out on each slide by slowly distributing exactly 1ml of the blend which was then left to dry for 30mins. The films were covered to assure slow, even evaporation of solvent, as fast evaporation can lead to cracks in the film and damage its uniformity and homogeneity.

It was observed, for mass ratios of conducting polymer solution greater than the Hydrin rubber solutions, cracks were occurring in the films. This phenomenon could be due to the fact that the pure conductive polymer does not have the required elasticity to form uniform and homogenous films.

### 2.3.1.3 PAni-DBSA/Poly [(acrylonitrile-co-butadiene)/poly vinylchloride] Blends

Preparation

PAni-DBSA (10g) was dissolved in THF (920ml) by stirring for a period of 10 days. The mixture was filtered, leaving behind the undissolved PAni-DBSA (8.90g).

| Film no. | Ratio of PAni-DBSA to rubber (%) | Ratio of PAni-DBSA to rubber | Volume of PAni-DBSA solution (ml) | Mass of PAni-DBSA (g) | Volume of rubber solution (ml) | Mass of rubber (g) |
|---|---|---|---|---|---|---|
| F-0001 | 50 : 50 | 1 : 1 | 30 | 0.036 | 1.80 | 0.036 |
| F-0002 | 40 : 60 | 1 : 1.5 | 30 | 0.036 | 2.70 | 0.054 |
| F-0003 | 25 : 75 | 1 : 3 | 30 | 0.036 | 5.40 | 0.108 |
| F-0004 | 20 : 80 | 1 : 4 | 30 | 0.036 | 7.20 | 0.144 |
| F-0005 | 15 : 85 | 1 : 5.7 | 30 | 0.036 | 10.30 | 0.205 |
| F-0006 | 10 : 90 | 1 : 9 | 30 | 0.036 | 16.20 | 0.324 |
| F-0007 | 5 : 95 | 1 : 19 | 30 | 0.036 | 34.20 | 0.684 |
| F-0008 | 1 : 99 | 1 : 99 | 30 | 0.036 | 178.20 | 3.564 |
| F-0009 | 0.75 : 99.25 | 1 : 132.3 | 30 | 0.036 | 237.60 | 4.752 |
| F-0010 | 0.5 : 99.5 | 1 : 199 | 30 | 0.036 | 358.20 | 7.164 |

Table 16 The cast films and composition (by ratio) of each elastomeric blend.

Table 16 shows the composition of each elastomeric blend prepared, and their corresponding cast film number.

The concentration of the solution was 0.12% (w/v), based on the amount of PAni-DBSA (1.10g) that dissolved. Nipol® DN171 (10g) was dissolved in THF (500ml) by stirring for 10 days. The concentration of the mixture was 2% (w/v), due to complete dissolution of the Nipol® DN171 rubber in the THF. Several blends of PAni-DBSA and Nipol® DN171 rubber were prepared by mixing the stock solutions in varying ratios.

Cast films were prepared using microscope glass slides (x10) and PTFE sheets (x10). On the PTFE sheets (25 x 25mm), six layers (1ml each) of the PAni-DBSA/Nipol® DN171 rubber blends were deposited and the solvent (THF) allowed to gradually evaporate by placing beakers over the sheets at room temperature for 24h. Additionally, three layers (1ml each) of the blends were cast in the same manner on microscope glass slides (25 x 25mm).

### 2.3.2 Blends Prepared via Thermal Blending Method

For practical commercial applications, all rubber compounds (either natural or synthetic) which are mixed and shaped into blanks for further processing (e.g. moulding and extruding) must be vulcanised by one of many systems such as sulfur vulcanisation, sulphurless vulcanisation, resin vulcanisation (epoxy and phenolic resins), peroxide vulcanisation (for saturated rubbers that cannot be crosslinked by sulphur) and irradiation vulcanisation (e.g. electron beam, gamma and X-ray radiation). During the vulcanisation, the following changes occur:

a) The long chains of the rubber molecules become crosslinked by reactions with the vulcanisation agent to form three-dimensional structures. This reaction transforms the soft, weak viscous material into a strong elastic product.

b) The rubber also loses its tackiness, becomes insoluble in solvents and more resistant to deterioration normally caused by heat, light and ageing processes.

It was decided to produce the vulcanised elastomer blends by thermo-mechanical mixing, using a temperature controlled internal mixer.

An internal mixer is a closed mixing device. It has a pair of counter-rotating rotors and moveable steel ram (to force compound ingredients into the rotors' grasp) in order to perform the mixing. The rotors are encased by a heavy metal jacket with a hopper at the top to feed in the ingredients, and a door at the side of the rotors to let the mixed materials out. There are also drilled channels in the walls of the mixing chamber and in the cores of both rotors, where water can pass through to control the mixing temperature. Mixing can occur between the rotors or between the mixing chamber walls and the rotors.

### 2.3.2.1 Chemicals and Raw Materials

Aniline monomer (99 wt%, Sigma-Aldrich), ammonium persulfate [APS] (98 wt%, Sigma-Aldrich), 36.5-38 wt% HCl solution (GPR), 33 wt% ammonia solution (GPR), 90 wt% DBSA solution (GPR, Fluka), methanol (GPR), poly(epichlorohydrin-*co*-ethylene oxide) C-2000L (Zeon Chemicals). Hydrin rubber was washed with methanol for 24 hours using Soxhlet extraction in order to remove chemical additives. The curing system known as Zisnet-FET was supplied by Zeon Chemicals, Wales, and stearic acid powder was supplied by Omya. (Stearic acid was used to control the degree of splitting and tearing of the Hydrin rubber during mill-mixing. Another advantage of using stearic acid is to reduce the degree of surface bloom in vulcanisates fabricated from the Hydrin mixes). The accelerator used in conjunction with Zisnet-FET was diphenyl guanidine (DPG), supplied by Omya. DPG was supplied under the trade name DPG 75; this was 75% active material in a polyethylene binder.

### 2.3.2.2 Effect of Crosslinking Agent with Epi-EO

Compounding

For this section of the project it was decided to investigate the advantages of adding higher proportions of crosslinking agent than has been recommended in the literature. Therefore four different mixes (crosslinking agent 1.6%, 2.4%, 3.2%, 4%; see Table 17) were prepared using a 300cm$^3$ Francis Shaw Intermix (Manchester, United Kingdom). The internal mixer was set to operate at a rotor speed of 50 revolutions per minute, under a ram pressure of approximately 0.70MPa. The fill factor used was 70% and the batch masses were approximately 250g. The discharge temperatures were all within 50$^o$C ± 5.

| Batch No | Epi-EO (g) | Stearic Acid (g) | DPG (g) | Zisnet-FEt (g) |
|---|---|---|---|---|
| B-001 | 247 | 2.47 | 1.24 | 3.95 |
| B-002 | 241 | 2.41 | 1.9 | 5.78 |
| B-003 | 234 | 2.34 | 2.6 | 7.5 |
| B-004 | 228 | 2.28 | 2.96 | 9.12 |

Table 17 Representation of different amounts of crosslinking materials in the vulcanisates.

All the mixes were prepared according to the protocol outlined in Table 18. At the end of mixing each sample was refined on a 0.45m two-roll mill operating at an even speed of 15 revolutions per minute with roller surface at 50°C (the two roll-mill gap was adjusted to 4-5mm); the whole operation took about 11 minutes.

| Time elapsed (min) | Stage of mixing |
|---|---|
| 0 | Addition of raw Epi-EO |
| 3 | Addition of stearic acid |
| 4 | Addition of DPG and Zisnet-FET |
| 6 | Sweep and cross-cut from each side of a sheet of rotating rubber |
| 9 | Six time end-roll on a tight nip, allow to band for one minute |
| 11 | Sheet off at a thickness 4-5 mm |

Table 18 Mixing schedules of mixes with different combination of factors.

Each batch was sheeted out at approx 4-5mm thickness. Material loss due to mixing was less than 2%, and this percentage loss is considered quite acceptable for mixing operations as far as elastomers are concerned.

## Vulcanisation

The determination of the vulcanisation characteristics was carried out on a Monsanto Oscillating-disc rheometer. It was maintained at a temperature of 150°C and set so that it would operate at strain amplitude of ±3° of arc. The extent of crosslinking was indicated by the difference between the maximum torque and minimum torque and the vulcanisation time was indicated by the plateau which occurred when the curing process was complete. It was noticed that in the case of Hydrin rubber vulcanization, the curing time changed (between 38-45min), with respect to the ratio of crosslinking agent used. A Bradley and Turton steam press was used for the moulding process. For each mix, a set of square plates was used for moulding; the sample was sandwiched between the two plates and compression moulded on a steam press at 150°C and a pressure of 80psi. The moulding times quoted, were those corresponding to values recorded by the rheograms of the respective mixes. Then, the post curing process was carried out by passing cold water through the system till room temperature was reached, which allowed sufficient time for vulcanisates to obtain a state of thermal equilibrium.

### *2.3.2.3 PAni-DBSA/Poly (Epichlorohydrin-co-ethylene oxide) Blends*

From the initial studies described in section 2.3.2.2 (Effect of Crosslinking Agent with Epi-EO) it was discovered that 4% of the crosslinking material was the optimum ratio required for effective crosslinking of the rubber. As a result this percentage was universally used in all blending experiments. Following the acquisition of this information, it was decided to introduce the conductive filler in varying ratios. The procedure is out lined below.

## Compounding

Vulcanised Epi-EO/PAni-DBSA blends with different compositions of PAni-DBSA wt%: Epi-EO wt% (i.e. 1:99, 5:95, 10:90, 20:80, 30:70, 50:50; see Table 19) were prepared by

using an internal mixer (Francis Shaw Intermix). A fill factor of 70% was used in order to perform the blending in the mixer (with free total volume, 90cm$^3$). The starting temperature of each mixing was 50°C and the mixer rotor speed was 50rpm.

| Sheet no | Mass ratio | Epi-EO (g) | PAni-DBSA (g) | Stearic acid (g) | DPG (g) | Zisnet-FET (g) |
|---|---|---|---|---|---|---|
| S-001 | 1:99 | 226 | 2.26 | 2.26 | 2.9 | 9 |
| S-002 | 5:95 | 218 | 10.9 | 2.18 | 2.8 | 8.7 |
| S-003 | 10:90 | 208 | 20.8 | 2.08 | 2.7 | 8.32 |
| S-004 | 20:80 | 191 | 38.2 | 1.91 | 2.48 | 7.64 |
| S-005 | 30:70 | 177 | 53.1 | 1.77 | 2.03 | 7.08 |
| S-006 | 50:50 | 154 | 77 | 1.54 | 2 | 6.16 |

Table 19 Different compositions of vulcanised Epi-EO/PAni-DBSA blends.

The mixing procedure was carried out according to the schedule outlined in Table 20.

| Time elapsed (min) | Stage of mixing |
|---|---|
| 0 | Addition of raw Epi-EO |
| 1 | Addition of PAni-DBSA |
| 3 | Addition of stearic acid |
| 4 | Addition of DPG and Zisnet-FET |
| 6 | Sweep and cross-cut from each side of a sheet of rotating rubber |
| 9 | Six time end-roll on a tight nip, allow to band for one minute |
| 11 | Sheet off at a thickness 4-5 mm |

Table 20 Stages of mixing Epi-EO/PAni-DBSA blend using internal mixer and two roll-mills.

## Vulcanisation

The vulcanisation behaviour of poly(epichlorohydrin-*co*-ethylene oxide) blends, containing 5%, 20% and 50% were examined using a Monsanto Oscillating-disc rheometer S100 at a temperature of 150°C and blend duration of 60 minutes. The information obtained from this test was used as a guideline for the vulcanisation of Epi-EO/PAni-DBSA blends using the hot press moulding.

Appropriate amounts of each blend were cut from the sheet and fed into a 1mm thick square (100 x 100mm) stainless steel mould while it was soft and warm. The mould containing the blend was set for the hot-pressing process with a curing temperature of 150°C, pressure 80psi and duration 35 minutes. The post-curing was carried out by passing cold water through the system till room temperature was reached, which allowed sufficient time for vulcanisates to obtain a state of thermal equilibrium.

CHAPTER

# 3

# Methods &Techniques of Characterisations

*This chapter introduces the reader to several areas of sample characterisation. It outlines a basic description of the techniques employed for the characterisation and study of these compounds and blends. The techniques used are as follows:*

*Infrared spectroscopy (IR), Ultraviolet-Visible (UV-Vis), DC conductivity, thermal techniques including thermogravimetry (TG) and differential scanning calorimetry (DSC), morphological studies using Scanning electron microscopy (SEM), X-Ray Diffraction (XRD) and Optical microscopy, measurement of the vulcanisation behaviour of the Epi-EO rubber using a Rheometer and determination of the tensile strength and elongation at break using a tensile tester.*

# 3 Methods & Techniques of Characterisations

## 3.1 Infrared Spectroscopy

### 3.1.1 Introduction

The infrared portion of the electromagnetic spectrum extends from the red end of the visible spectrum out to the microwave region. It includes radiation with wave numbers ranging from 14,000 to 20cm$^{-1}$. However, the spectral range of greatest chemical use is the mid-infrared region (200 – 4000cm$^{-1}$).

Infrared radiation can induce response from chemical bonds. The frequencies at which there is absorption of IR radiation can be correlated directly to the bonds present within the compound in question. Each inter-atomic bond may vibrate in several different modes (stretching or bending) and individual bonds may absorb at more than one IR frequency. Stretching absorptions usually produce stronger peaks than bending; however the weaker bending absorptions can be useful in differentiating similar types of bonds.

### 3.1.2 IR Apparatus

The infrared spectra of the conducting polymers and each of the blends were obtained using a Perkin Elmer Spectrum One infrared spectrophotometer coupled with Universal ATR (Attenuated Total Reflectance) Sampling Accessory (crystal: Diamond/ZnSe) to allow easy recording of the traces for the dark polymer powders. The absorption peaks were recorded between (650-4000cm$^{-1}$).The raw spectral data were converted to Microsoft Excel files on the Spectrum 3.01 software and analysed in Excel.

## 3.2 Ultraviolet-Visible Spectroscopy

### 3.2.1 Introduction

Ultraviolet/visible spectroscopy involves the absorption of ultraviolet/visible light (190< $\lambda$<800 nm) by a molecule causing the promotion of an electron from a ground electronic state to an excited one. There are several types of electronic transitions available to a molecule including: $\sigma$-$\sigma^*$ (e.g. alkanes), $\sigma$-$\pi^*$ (e.g. carbonyl compounds), $\pi$-$\pi^*$ (e.g. alkenes, carbonyl compounds, alkynes, azo compounds), n-$\sigma^*$ (e.g. oxygen, nitrogen, sulfur, and halogen compounds), n-$\pi^*$ (e.g. carbonyl compounds).

Transitions from the highest occupied molecular orbital (HOMO) to the lowest unoccupied molecular orbital (LUMO) require the least amount of energy and are therefore the most frequently observed.

### 3.2.2 UV-Vis Apparatus

Polymers were dissolved in NMP or THF and their spectra recorded on a Varian CARY100 SCAN spectrophotometer against THF or NMP using quartz cuvettes (1cm path length) . The absorbance was measured between 190 and 900nm, in order to determine whether the PAni-DBSA had become dedoped by the constituents of Epi-EO or the Nipol® DN171 in each elastomeric blend. UV-Visible traces were converted to Excel files using the CARYWIN 1.90 Software and treated in Excel.

## 3.3 DC Conductivity Measurements

### 3.3.1 Introduction

Electrons are one of the most common energy-conversion sources used nowadays. To transfer electrons from one point to another, one needs to use a material that can accept a large electron density. These materials, such as metals, are known as conductors. However,

for some applications, compounds are required whose electron density is low or nil; these compounds are known as semi-conductors and insulators respectively.

### 3.3.2 D.C. Conductivity Apparatus

The conductivity of the polymer samples was estimated using the van der Pauw four-probe method. Discs (13mm Ø) of compressed dry powders were prepared using standard 13 mm dies (90 $kg.mm^2$ uniaxial pressure, under vacuum). Their thicknesses were measured accurately using a digital calliper (average of 6 readings) and assumed to be homogeneous and uniform. The pellet was placed in a PTFE holder with four metallic contact screws. Three electrical measurements were recorded before the pellet was rotated through 90 degrees, and a further three were taken.

Moreover, the electrical resistance of the cast films of PAni-DBSA and Epi-EO rubber blends or PAni-DBSA and Nipol® DN171 rubber blends, at various ratios, were measured using a Keithley 617 programmable electrometer and a Keithley 224 programmable current source, under computer control. The standard two and four probe van der Pauw techniques were employed. PAni-DBSA rubber blends were cast on 25mm x 25mm PTFE sheet. Fine copper wires (length 5cm) were attached to each of the four corners of the cast film using a quick-drying silver paint. Two-probe electrical resistance measurements were performed for the less conductive cast films ($\sigma < 10^{-9}$ $S.cm^{-1}$), e.g. cast films of pure Epi-EO and Nipol DN171, by coating the opposite faces of each cast film with equal widths (5mm) of quick-drying silver paint.

Measurements were taken following the scheme depicted in Figure 31, and with the sample turned through 90 degrees.

The resistance readings were not always totally concordant with each other for the pellets tested. Readings at 0 and 90° gave resistance values varying between 2-2.5% compared to the mean value used for the conductivity calculation.

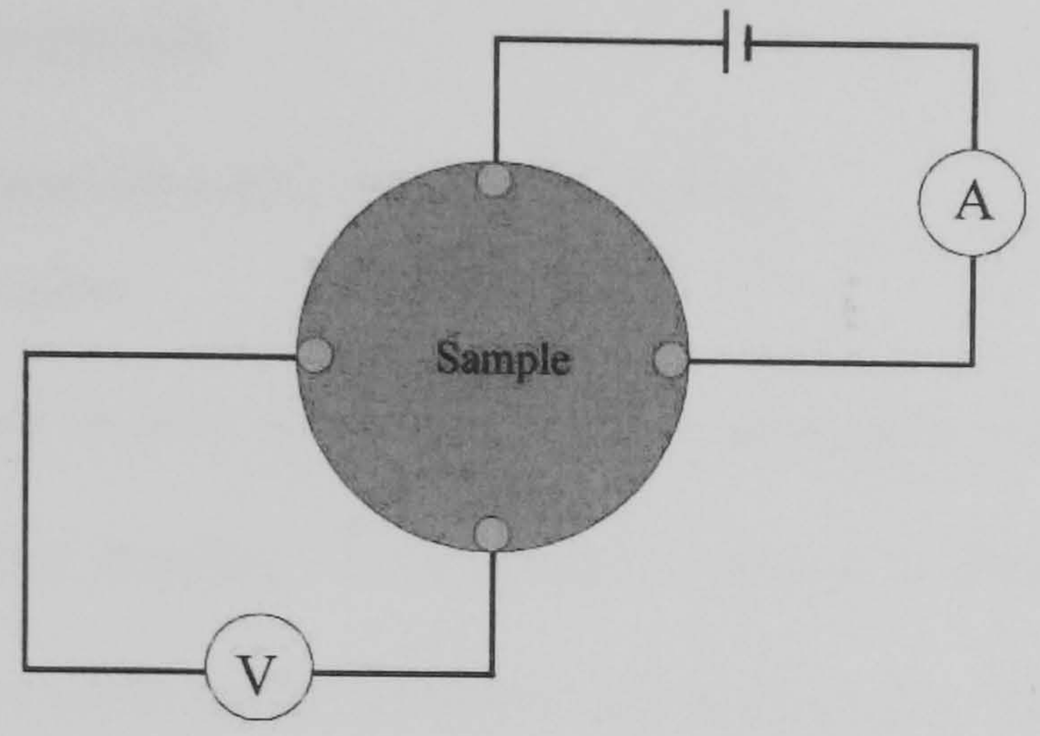


Figure 31 DC conductivity measurement set-up.

Electrical conductivities as measured by the four probe technique were calculated using the van der Pauw equation

$$\sigma = \frac{2\ln 2}{(R_1 + R_2)\pi df}$$

Where σ is electrical conductivity ($S.cm^{-1}$), R1 and R2 are two average readings of measured resistance for the pellet in the case of PAni-DBSA powder and the cast film for the blend in its two different contact configurations (Ω), d is thickness of the sample (cm), and f is a geometric factor (approximately 1 for symmetrical contacts on circular pellets or square-shaped plaques).

Electrical conductivities as measured by the two probe method were calculated by using the equation below

$\sigma = \left(\frac{1}{R}\right)\left(\frac{L}{A}\right)$, Where σ is the electrical conductivity ($S.cm^{-1}$), R is the measured resistance of the cast blend (Ω), L is electrode spacing distance (cm) and A is the cross sectional area ($cm^2$) of the cast film between the electrodes.

## 3.4 Thermal Analysis

### 3.4.1 Thermogravimetric Analysis (TGA)

#### *3.4.1.1 Introduction*

When polymers are heated substantially, they eventually undergo decomposition. This process may involve breaking of backbone bonds as a direct or indirect result of the temperature they are subjected to, releasing volatile products. Thermogravimetry can be used to study changes in sample weight as a function of time at a given heating rate or at constant temperature (isothermal TGA). The analysis is usually performed under nitrogen, argon, or in the presence of air.

#### *3.4.1.2 TGA Apparatus*

Polymer powders were placed in a platinum crucible on a Mettler M3 balance operated on the null-balance principle. A pair of photodiodes was used to register the displacement of the balance beam. A Mettler TC 10A low thermal resistance furnace was used to heat the samples at 10 and 20°C/min from 30 to 600°C under $N_2$ atmosphere. The oven temperature was monitored by a thermocouple located close to the sample boat. The raw data were processed using the Mettler Graphware TA72PS2 software package, exported from Qnix to MS-DOS, and re-plotted using Excel.

### 3.4.2 Differential Scanning calorimetry (DSC)

#### *3.4.2.1 Introduction*

DSC is a technique in which the difference in heat flow to the sample and to a thermally-stable reference, are monitored against temperature. It has the ability to detect thermal

transitions including endothermic or exothermic changes and glass transitions. Therefore it was employed to study the various transitions in the polymers and the blends that had been prepared.

#### *3.4.2.2 DSC Apparatus*

The cast films of each elastomer blend (of the conducting polymer PAni-DBSA and Epi-EO or the Nipol® DN171, at selected ratios) and that of the pure grade of Epi-EO or Nipol® DN171 were analysed, using a Mettler Toledo 822e differential scanning calorimeter. A sample cell (40μL aluminium pan), containing the material to be analysed, and a reference cell (blank pan) were heated at a rate of $10^{o}C.min^{-1}$ under a nitrogen ($N_2$) atmosphere, from $30-450\,^{o}C$.

## 3.5 Morphological Studies

### 3.5.1 Scanning Electron Microscopy Analysis

#### *3.5.1.1 Introduction*

Scanning Electron Microscopic Analysis is a powerful tool for determining micro- and nano-morphological patterns of materials, rendering the observation of single clusters and even particles of the polymeric material possible. The basic principle is similar to that of a normal optical microscope, except that the light reflected by a material in a normal microscope is replaced by an electron beam focussed on a metal-coated sample. As the beam strikes each point on the specimen, various responses are produced due to sample-electron-interactions. Several of these responses (secondary electrons, backscattered electrons) can be collected by suitable detectors, amplified, and displayed in the viewing tube, and an "image" is formed.

#### *3.5.1.2 SEM Apparatus*

The samples were placed on aluminium stubs, using double-sided sellotape, and gold-coated using a Polaron E5175 gold sputter coater evacuated with an Edwards double-stage high

vacuum pump. All particle size estimation analyses were performed on a JEOL-6310 scanning electron microscope (SEM), operated at 15kV accelerating voltage, controlled by ISIS 200 software. The samples were then observed with various high magnifications, mainly 500x, 1000x, 5000x and 10000x.

## 3.5.2 Powder X-Ray diffraction analysis

### *3.5.2.1 Introduction*

When an atom is excited by the removal of an electron from an inner shell, it usually returns to its normal state by transferring an electron from some outer shell to the inner shell with consequent emission of energy as X-rays; that is, photons of high energy and short wavelength (0.154 nm for CuKa radiation) that can be used to detect the presence of elements in samples. They are also a useful source of radiation for analytical studies such as X-ray absorption and in the present study, X-ray diffraction analysis. The latter is a powerful tool for determining crystal parameters of materials. In this technique, a monochromatic beam of X-rays is aimed at the surface of the material studied, which is rotated to give a wide range of angles of incidence and diffraction.

The angles of the diffraction peaks in an x-ray diffraction pattern are directly related to the atomic distances. The atoms, and/or molecules, in a powder, can be viewed as forming different sets of planes in the crystal. For a given set of lattice planes with an inter-plane distance d, the condition for a diffraction (peak) to occur can be simply written as:

$d = \lambda/2.\sin\theta$ (Bragg's law)

Where $\theta$ is the diffraction angle and $\lambda$ is the x-ray wavelength. The peak positions, intensities, widths and shapes can all provide information about the structure and morphology of the material.

#### *3.5.2.2 X-Ray Diffraction Apparatus*

X-ray diffraction studies of PAni powders were performed on a Bruker AXS generator, combined with a D8 Advance automatic goniometer (Average speed 0.033degree.$s^{-1}$). The XRD patterns were obtained with CuKα radiation (0.154nm), produced by the bombardment of a copper target (40kV, 25mA) and filtered, using a nickel filter. The system was controlled via a Bruker XRD manager software package, and the diffractograms were analysed by Bruker EVA evaluation software and exported as data to Excel for plotting.

### 3.5.3 Optical Microscopy

#### *3.5.3.1 Introduction*

The morphology of PAni-DBSA blends was studied using a compound optical microscope. This microscope contains multiple lens components in both objective and eyepiece assemblies. These multi-components are designed to reduce aberrations, particularly chromatic aberration and spherical aberration.

#### *3.5.3.2 Optical Microscope Apparatus*

PAni-DBSA blends were analysed and studied with an Olympus BX51 optical microscope (magnification 200X) linked to a computer by a video converter for digital image capture. Blend films were obtained by casting the solution onto glass substrates and allowed to evaporate to form a thin transparent film.

## 3.6 Mechanical properties study

### 3.6.1 Measurement of Vulcanisation Behaviour of Epi-EO Rubber

#### *3.6.1.1 Introduction*

The vulcanisation behaviour of Zisnet-FET vulcanised Epi-EO rubber containing 1.6 wt%, 2.4 wt%, 3.2 wt% and 4 wt% of the crosslinking agent was measured using a Monsanto moving die rheometer (100S) at a temperature of 150°C and duration of 60min. Information

from this test was used as a guideline for the vulcanisation of Epi-EO/PAni-DBSA blend test pieces with hot-press moulding.

#### *3.6.1.2 Rheometer Apparatus*

A moving die type rheometer was used in this work. It is a modification of the Mooney viscometer, but unlike the Mooney, the non-vulcanised sample is compressed between two heated platens forming a sealed cavity and by an applied oscillating force. The platens are maintained at a desired vulcanisation temperature while one platen oscillates. The stationary platen is equipped with a torque transducer, which records the induced torque as time and vulcanisation progress. The sample is thus subjected to an oscillatory shearing action of constant amplitude. Oscillation of the platens does not result in the destruction of the sample. As vulcanisation proceeds, the torque required to shear the rubber increases and a curve of torque versus cure time is generated. Since the platens are straining the rubber, the torque value is directly related to the shear modulus of the rubber.

### 3.6.2 Tensile Properties Measurements

#### *3.6.2.1 Introduction*

Tensile property testing was carried out according to British Standards Institution (BSI) requirements. The test was performed in a controlled atmosphere with room temperature 23 ± 2 and relative humidity 50 ± 5%. Six test pieces of each raw material or blend were used to repeat each test in order to define the final result as the mean value of a total of six measurements.

#### *3.6.2.2 Tensiometer Apparatus*

The tensiometer is usually loaded with a sample between two grips that are adjusted manually to apply force to the specimen. The measurements taken are force and extension and a tensiometer gives the load extension curve directly rather than the stress strain curve.

A tensile tester (Tinius Olsen H10K-S) was used to measure two tensile properties, tensile strength and elongation at break with constant straining rate (5mm/sec). Test pieces in standard dumb-bell shape were used here. Tensile strength is defined as the maximum tensile stress recorded in extending the test piece to breaking point, and elongation at break is defined as tensile strain (expressed as a percentage increase of the test length, produced by tensile stress) at the breaking point.

CHAPTER

# 4

# RESULTS & DISCUSSION

*The previous chapter of this thesis was concerned with the description of methods and techniques of characterisation. In order to assess the chemical and physical properties of the prepared polymers and PAni-DBSA blends, several characterisation methods were employed and the findings obtained by these methods are presented in this chapter.*

*The first part of the chapter will only explore the characterisation of conducting polyanilines (PAni), polyanisidines (PoAnis), and their copolymers, in the presence of a variety of protonating agents.*

*The second part of this chapter will deal with PAni-DBSA blends. In this chapter studies of the properties of these blends will be discussed, such as solubility parameters, IR and UV-Vis spectroscopy, thermal analysis, morphological studies, measurements of electrical conductivity and mechanical properties of the blends.*

# 4 Results & Discussion

## 4.1 Conductive Polyaniline and Its Derivatives

### 4.1.1 Infrared Spectroscopy

Infrared (IR) characterisation of PAni is an important way of identifying the various natures of chemical bonds present in the structure. Upon closer inspection of specific areas of the spectrum, links can be made between the degree of oxidation of the polymer and its conductivity. The common bands and their assignments for PAnis as reported in the literature [96,135,136,137,72] are given in Table 21.

| Wavenumber ($cm^{-1}$) | Assignment |
|---|---|
| 3450-3200 | N-H str. |
| ~2350 | Aliphatic C-H str. |
| ~1600 | Quinoid (N=Q=N) str. |
| ~1500 | Benzoid str. |
| ~1290 | C-N str. |
| ~1140 | Polaron band of –N=Q=N- / C-H bend |
| ~825 | C-H o/P bend (1,4) |

Table 21 PAni IR absorptions.

#### *4.1.1.1 PAni and PoAnis via Precipitation Polymerisation*

<u>Polyaniline Salt ES and Emeraldine Base EB</u>

The main striking difference between the two spectra is the broadness of the peaks for ES, as seen in Figure 32. This is due to higher electronic displacement within the ES conjugated system. Doping usually increases the hydrophilicity of the polymers; water of hydration of the counter chlorine ion is present ($3815cm^{-1}$) and it accounts for the broad, high wavenumber, end of the spectrum [137]. Peaks in the region of $3000cm^{-1}$ can be attributed to

N-H stretching while the peak at 2668cm$^{-1}$ in the ES is due to vibrations of the iminium cation [138].The peaks relevant to quinoid and benzoid stretching vibrations are seen around 1582 and 1497cm$^{-1}$ respectively and, as mentioned in the literature [139,140], their wavenumbers decrease with doping to 1563 and 1479cm$^{-1}$ respectively, due to the lower electron density and bond strength in the polymer (especially in the quinoid structure where doping occurs). The C=N stretching region of aromatic imines lies between 1400 and 1300cm$^{-1}$; the medium peak at 1332cm$^{-1}$ is shifted to 1295cm$^{-1}$ in the salt, with a pronounced appearance of a shoulder at 1244cm$^{-1}$ [89] for the C-N$^{+}$ stretching, which is linked to conductivity.

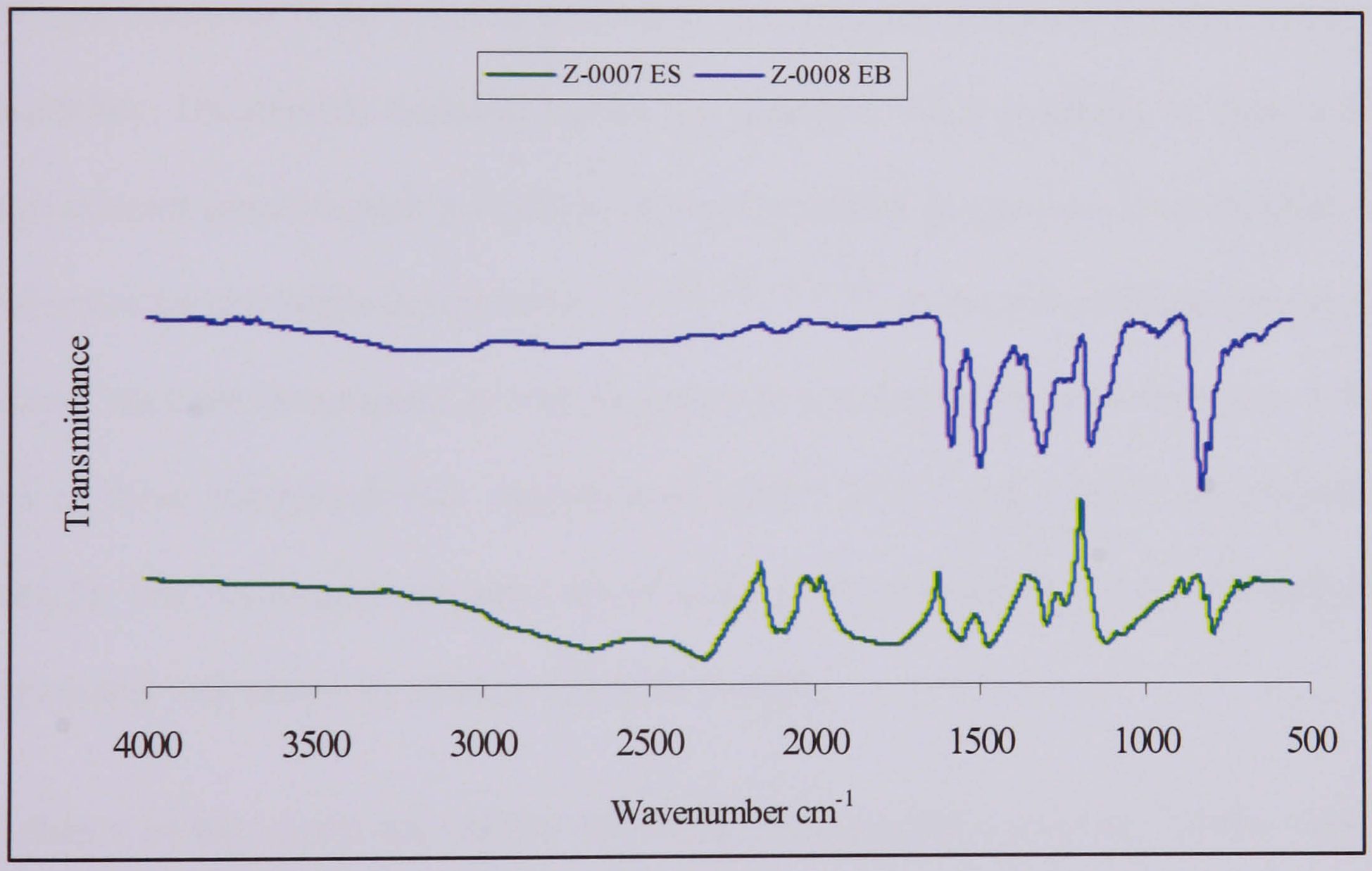


Figure 32 IR spectra of emeraldine salt and emeraldine base.

The peak seen at ca. 1165cm$^{-1}$ results from the bipolaronic structure (C-H out of plane (o/p) bending) in the conjugated backbone, and is hence also related to conductivity [139, 141,142]. The wavenumber of this peak is shifted down for the salt [143] and it is rather broad due to greater electronic delocalisation. Peaks in the region of 950cm$^{-1}$ can be assigned to C-H in plane (i/p) bending vibrations of the aromatic backbone. Lower wavenumber peaks are

mostly attributed to benzene substitution bending modes: the peaks at 822 (base) and 876cm$^{-1}$ (salt) refer to the para-substituted rings. The 790cm$^{-1}$ peak of the salt stands in the region ascribed to meta-substituted rings. However, for the polaron band, the para-substituted absorption band is shifted to a lower wavenumber for the same reasons as mentioned above. Hence it is reasonable to think that the salt's 790cm$^{-1}$ peak would relate to ortho-substituted benzene rings, which is in accordance with mechanistic considerations developed in the introductory chapter. Finally the band at 510cm$^{-1}$ is also due to C-H o/p bending for 1, 4-disubstituted benzene rings.

## Polyaniline and Polyanisidine Bases

The major drawback in the possible application of conjugated polymeric systems lies in their intractability. Unsaturated macromolecules are generally rather insoluble in most solvents though pendant moieties such as methoxy, ethoxy, and alkyl groups have been attached to the monomer to try and tackle this problem [137, 144, 136 , 145, 146]. In the course of the present study, anisidine has been investigated as well as aniline as a monomer for polymerisation. Infrared traces of these compounds (see experimental section 2.2.1.1 and 2.2.2.1) are presented in Figure 33. The two spectra presented are of bases prepared by oxidative polymerisation and deprotonated with ammonia solution (Z-0030, Z-0008).

The shapes of the curves are similar. However, the expected absorptions of the methoxy-group of PoAnis are observed as reported in the literature [145]. Hence for compound Z-0030, a shoulder is present at 2950cm$^{-1}$ due to aliphatic C-H stretching in O-$CH_3$. Quinoid and benzoid ring stretching vibrations are seen at the same wavenumbers, leading to the conclusion that their position in the spectrum is not influenced by the methoxy- group [146].

Bands around 1310cm$^{-1}$ are relevant to C-N stretching and are quite weak due to the relatively small electronic displacement in EB. For PoAnis, peaks consistent with aralkyl ethers (1270-1230cm$^{-1}$ - aryl-O, and 1167-1020cm$^{-1}$ - alkyl-O) are seen. An obvious example is the strong peak around 1215cm$^{-1}$ for Ar-O stretching.

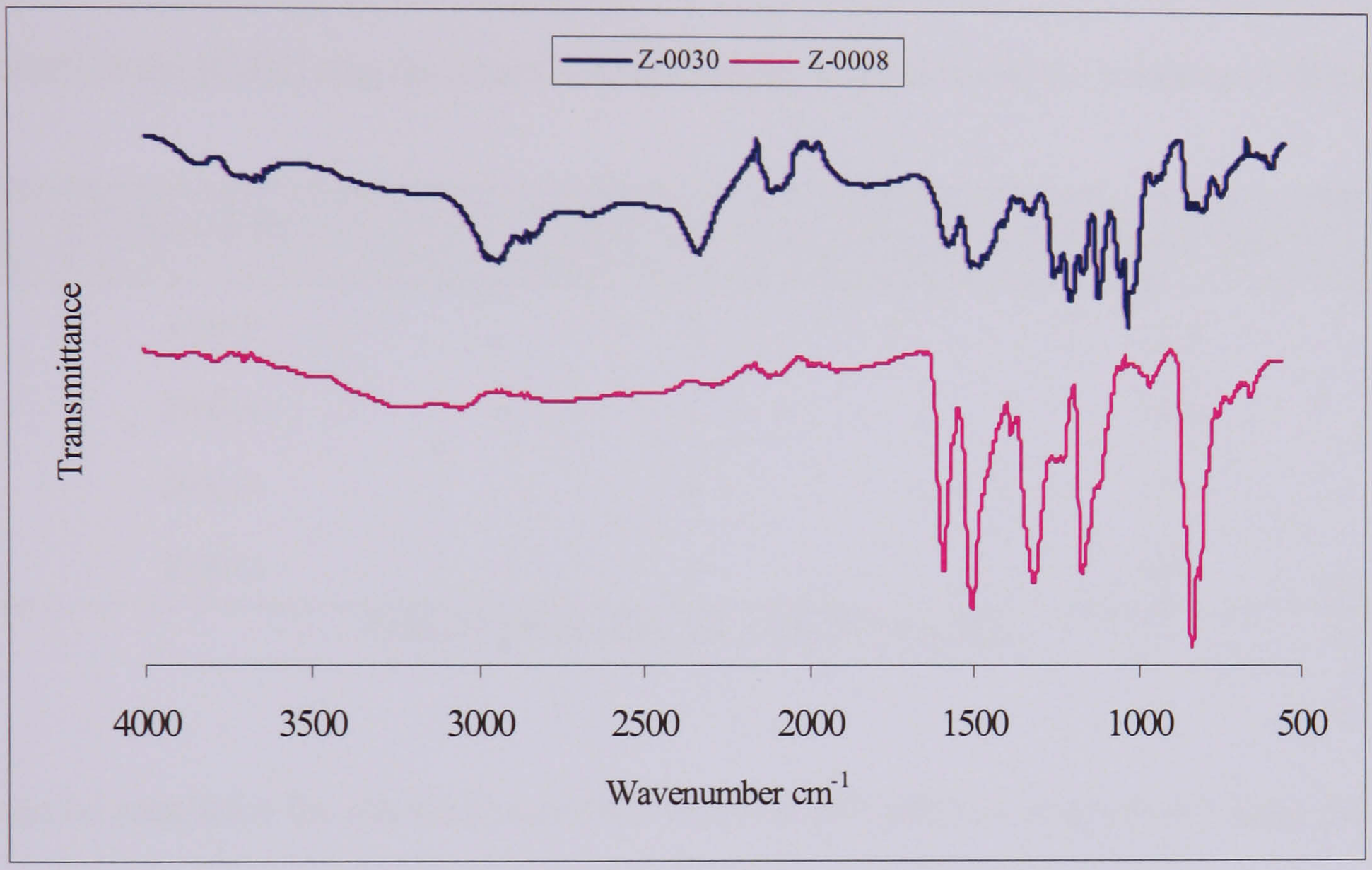


Figure 33 IR spectra of PAni and PoAnis bases.

The strong peak expected at 1167cm$^{-1}$ competes with the expected polaron band and is hence not clearly detectable in PoAnis. The peaks at 850cm$^{-1}$ for Z-0030 are assigned to C-H out of plane bending of 1,2,4- trisubstituted benzene rings [147,148], whereas those at 822 cm$^{-1}$ in Z-0008 and Z-0030 represent the same vibrational mode for 1,4-disubstituted rings [149, 148,140]. The vibration at 790cm$^{-1}$ present in Z-0030, Z-0008 is due to the 1,2- disubstituted terminal rings o/p bending [137].

## PAni-HCl at Different pH

Table 22 shows the change in the frequency of the $C_6H_4$ ring absorbance. As can be seen, the frequency of this absorbance decreases as the protonation level increases (pH decreases). If the protons interact and partly depopulate the π-system of the polymer; the frequency of this mode may decrease with increasing protonation since the C-C bond order (and hence, force constant) in the ($C_6H_4$) ring decreases with decreasing population of the bonding π orbitals.

| Sample ID | pH | IR frequency ($cm^{-1}$) |
|---|---|---|
| Z-0009 | 0 | 1554 |
| Z-0010 | 1 | 1558 |
| Z-0011 | 2 | 1576 |
| Z-0012 | 3 | 1585 |

Table 22 Effect of the pH on the IR frequency.

As can be seen from the classical resonance forms of polyaniline salt given in Figure 34, it is to be expected that positive charge will be transferred in part from the N to the π system of the ($C_6H_4$) rings. This will result in a partial delocalization of positive charge along the backbone of the polymer chain. The charge will naturally tend to be pinned close to the anion, $A^-$and delocalization will become less extensive as the distance from the $N^+$ atom increases.

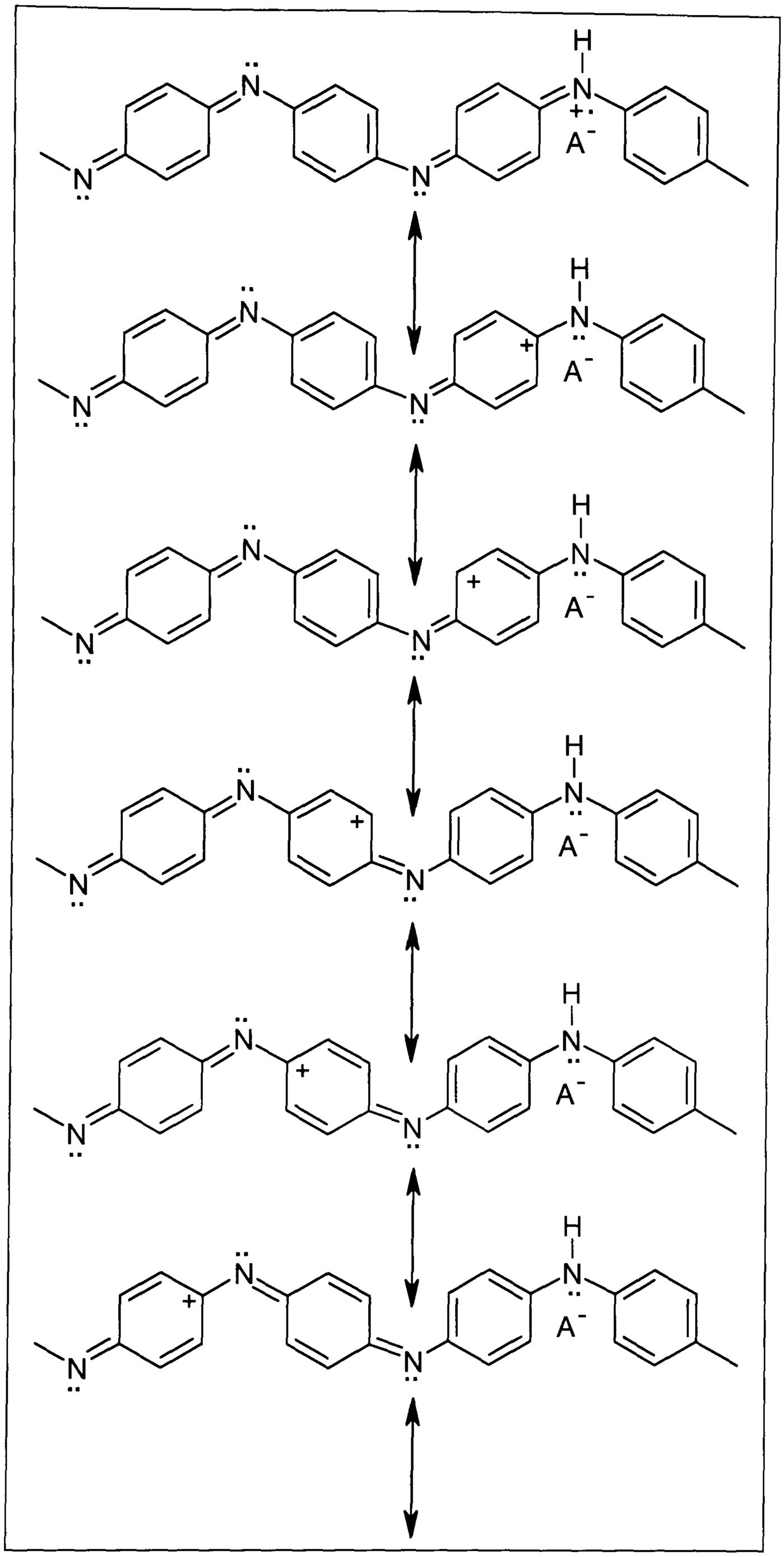

Figure 34 Representation of the delocalised positive charge from N to pi system.

## PAni at different oxidant/monomer ratios

It is known that oxidative polymerisation of aniline leads to the formation of the "quasi" ES in which roughly half of the nitrogen atoms are present as secondary amines (-N-B-N-) and

half as imines (-N=Q=N-) [148]. IR stretching bands of these two forms are characteristic of the polymer and their investigation [135,136,143,148] has led to the conclusion that they could give information about the degree of oxidation of different PAnis.

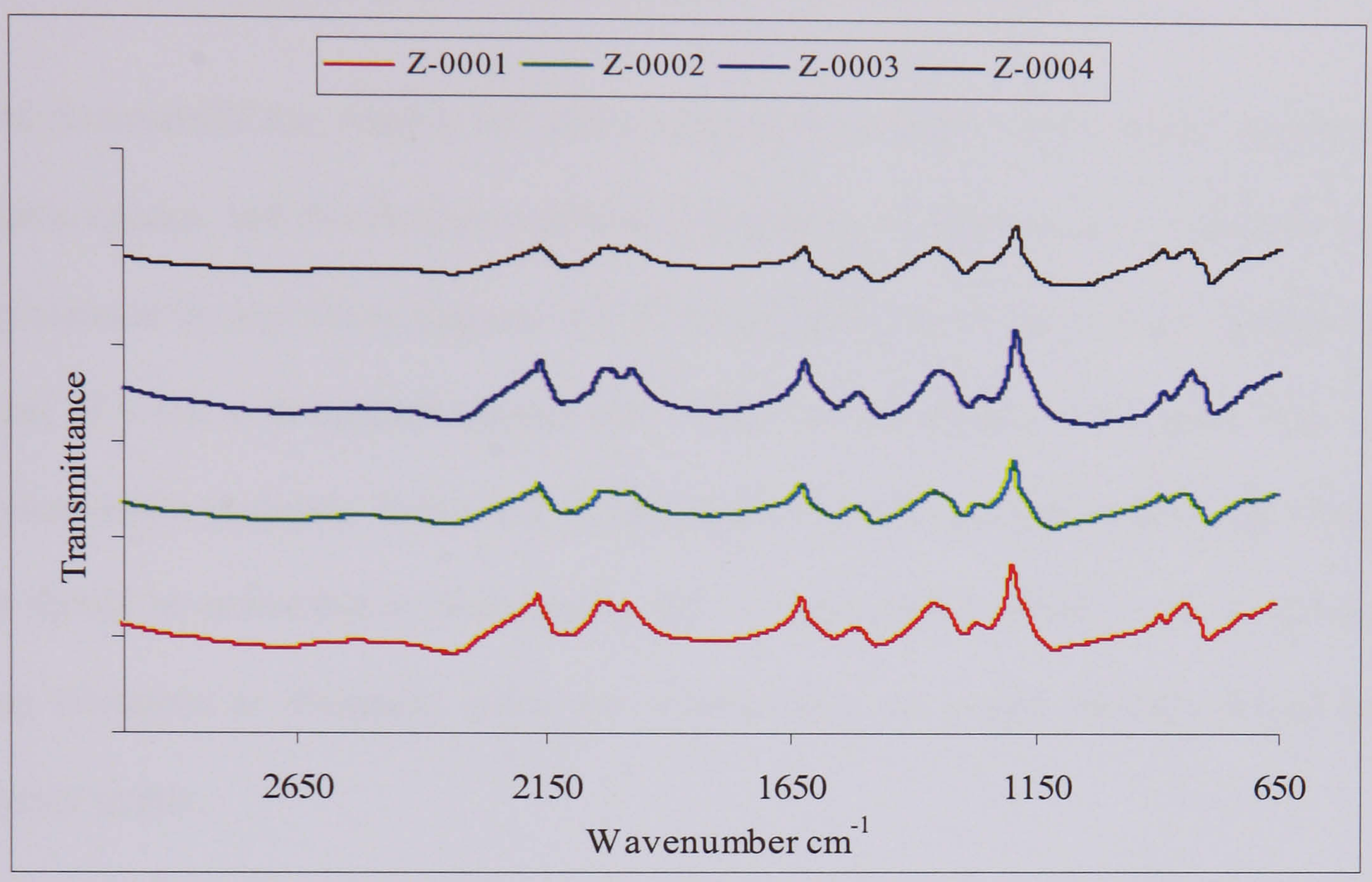


Figure 35 Infrared study of different oxidant: monomer ratios PAnis.

The first feature to be noted is the difference between spectra of protonated polymers and those of deprotonated PAni. The bands are, as mentioned earlier, much broader and bands of CH o/p bending [136] are seen at 1800 and 2000cm$^{-1}$ due to the greater electronic delocalisation of the structures. Although the monomer:oxidant ratio varies for the different polymers, it is reasonable to say that the spectra look very similar and that the ratios of the peaks for quinoid and benzoid stretching are comparable. The shapes of the spectra are similar to those previously reported[143]. Hence, it is possible to conclude that the degree of oxidation of these polymers is similar. A small difference can be noted though for Z-0003 in its relatively bigger and broader absorption around 1135cm$^{-1}$ which suggests greater electronic delocalisation and hence higher inherent conductivity.

### 4.1.1.2 PAni and PoAnis Doped with Sulfonic Acids

When EB is doped with a sulfonic acid, its infrared spectrum varies in two ways. Firstly, as a result of doping, some peaks are shifted and their relative intensity varies; secondly, new peaks characteristic of the presence of the dopant in the backbone appear.

In the protonated PAni, roughly half of the nitrogen atoms in the crude product are present as cationic species, and this electronic deficiency improves its conducting behaviour via charge displacement through the conjugated core of the polymer. The actual structure of the polymer is that of a salt with pendant counter-ions, which are the anions of the acids used in the polymerisation processes. In the case of surfactants, the salts may have specific IR vibrations that should be noticeable in their spectra. For a deprotonated polymer, one would expect these vibrations to disappear, since the counter-ion is no longer ionically bound to the polymer matrix.

PAni-Sulfonic acids from Emeraldine Base

Various sulfonic acids solutions were added to the non-conductive form of polyaniline (EB) Z-0008. When doping is achieved in solution, free imine sites are readily available to the dopant molecules. As the base is protonated, it becomes less soluble and particle aggregation starts to occur. The spectra of PAni doped sulfonic acids are similar in appearance to the EB but some peaks are stronger and broader, suggesting a higher degree of delocalisation in the backbone. This method of doping does not allow many dopant molecules to get fixed on the polymeric backbone, but inspection of the infrared data reveals that the dopants managed to protonate the free imine sites of the polymer aggregates. The presence of dopants in the backbones causes the peak at ca. 1240cm$^{-1}$ to become slightly stronger, as well as one at 1300cm$^{-1}$ (Figure 36). The polaron peak is broader than that found in the base as a result of the doping; overtones of C-H o/p bending 1900-2200cm$^{-1}$ start to appear but remain weak.

The presence of dopant anions is confirmed by the changed wavenumbers of the quinoid and benzoid vibrations which would not be shifted down in the case of partial or de-doped PAnis. Due to the general broadening of the spectra, it is difficult to see any specific peaks for each of the different dopants used; however peaks around 1030-1000cm$^{-1}$ are seen for all the samples, leading us to the conclusion that the doping process was successful in every case. Moreover, small C-H stretching vibrations appear as shoulders over the major vibrations around 3000cm$^{-1}$ between N-H and N-H$^{+}$ stretching. A further band at 1740cm$^{-1}$ is seen in Z-0015 (doped with β-NSA) which could be assigned as ring rocking vibrations for the naphthalene moiety.

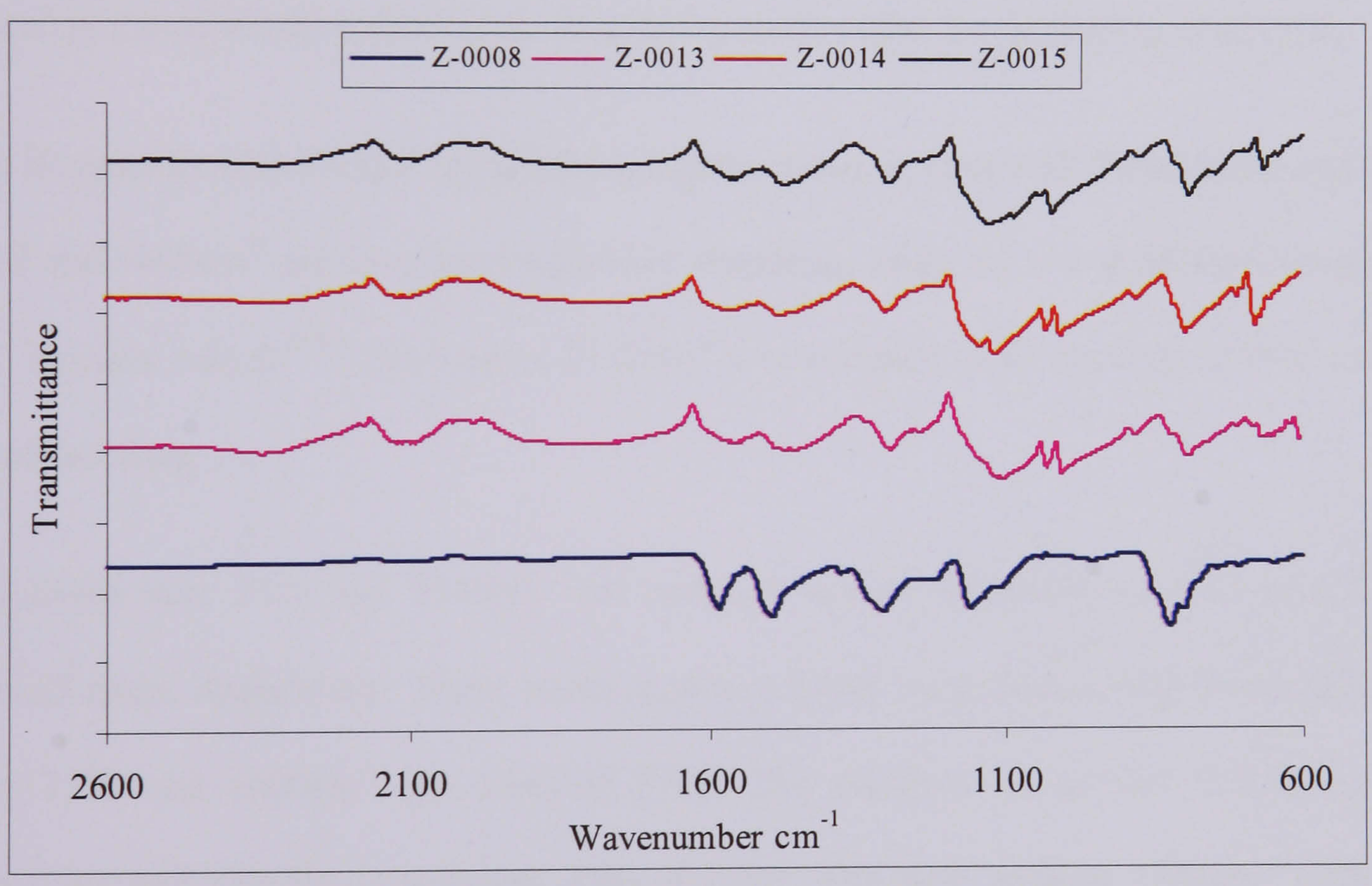


Figure 36 Infrared spectra of PAni-sulfonic acid from precipitation.

T he peak at 1244cm$^{-1}$ which appeared as a shoulder to the 1300cm$^{-1}$ peak for Z-0013, is now a strong one. The polaron related peak is now stronger and merged with one of the S=O stretching peaks for which smaller bands between 1050 and 1000cm$^{-1}$ are also seen. A peak appears at 1660cm$^{-1}$ which was only barely seen in Z-0013; however, it is not reported in the

literature. Two assignments may be suggested to interpret this vibration, either due to DBSA's benzene C=C skeleton and/or CH out-of-plane vibrations.

## PAni-Sulfonic acids by Emulsion Polymerisation Pathway

The main difference between the spectra of the polymers synthesised via emulsion polymerisation and those prepared via doping of the EB is the overall broadness of the peaks which is probably due to the presence of DBSA within the core of the polymer. It has also been shown [150,151,88] that emulsion polymerisation yields a more ordered polymer in which presumably electronic delocalisation is enhanced compared to the more conventional solution preparation using HCl as a protonic acid and dopant. This assumption is reasonable when related to the observation about peak broadening made earlier for the doping in solution.

The IR spectra of (Z-0018) PAni-DBSA sample is shown in Figure 37. Peaks in the region of 3212 and 3408cm$^{-1}$ are associated with N-H stretching, while the one at 2660cm$^{-1}$ is due to the iminium cation [138].The band at 2112cm$^{-1}$ was assigned to an overtone of C-H (out of plane) bending.

The bands near 1447 and 1546cm$^{-1}$ are assigned to C=C stretching of the benzoid and quinoid rings, respectively. These bands appear at lower wavenumber than those observed near 1500 and 1600cm$^{-1}$ for undoped PAni. The presence of quinoid and benzenoid vibrations indicates the emeraldine state of PAni. The peak seen at 1291cm$^{-1}$ with the pronounced appearance of a shoulder at 1242cm$^{-1}$ [89] for C-N$^{+}$ stretching is characteristic of the conducting PAni-ES form. The band around 1102cm$^{-1}$, referred to as an electronic band by MacDiarmid and co-workers [152], was considered a measure of the degree of electron delocalisation in the polymer chain. Bands at 1027 and 1000cm$^{-1}$ correspond to the S=O stretching vibration. The band at 790cm$^{-1}$ was attributed to the out of plane bending of C-H

and the 878 $cm^{-1}$ band was considered to be evidence of the formation of para-linked polyaniline.

Figure 37 shows an example of PAni prepared using β-NSA as a protonic acid, Z-0025 being the salt of the polymer. The peak at 3215$cm^{-1}$ is assigned to the N-H stretching. The characteristic band at 2118$cm^{-1}$ can be assigned to the vibration of the naphthalene moiety (>CH stretching). The spectrum of PAni-β-NSA shows the expected quinoid and benzoid vibrations in the regions of 1565 and 1485$cm^{-1}$, C-N stretching at 1303$cm^{-1}$ and a polaron band at 1137$cm^{-1}$ together with the absorption at ca. 1085$cm^{-1}$ assigned as CH i/p bending of 1,2,4 trisubstituted aromatic rings [136,72] or S=O stretching [145]. The peak at 1026$cm^{-1}$ is also assigned to S=O stretching.

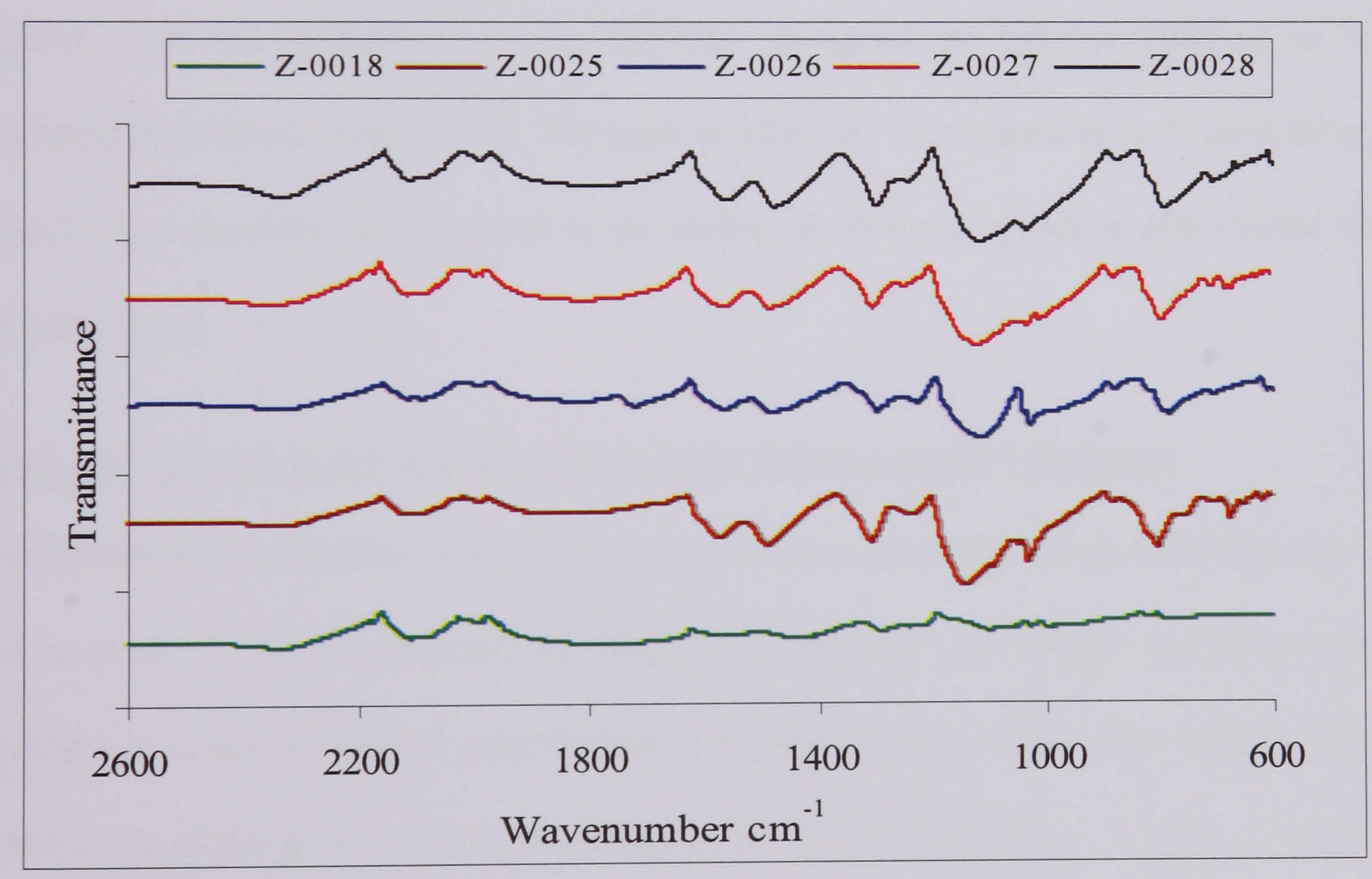


Figure 37 Infrared spectra of PAni-sulfonic acid from emulsion.

In many aspects, the PAni-CSA spectrum resembles that of PAni-DBSA[153]. The main difference between the spectra of the last two polymers is the presence of the C=O stretching vibration around 1740$cm^{-1}$ in Z-0026 [154]. It is also interesting to note that the second strong

>C=O stretching vibration present at 1421cm$^{-1}$ in the spectrum of the acid salt is only barely seen as a very tiny shoulder on that of the polymer. Peaks relevant to S=O stretching are also seen around 1000cm$^{-1}$.

Infrared spectra of these materials (Z-0027 and Z-0028) are also very similar to other sulfonic acid prepared PAnis. Within the spectra of the polymers, amongst the usual peaks for PAni, one would expect peaks relevant to both aromatic (which may blend within the peaks assigned to the aromaticity of the polymer itself) and sulfonic group vibrations. Figure 37 shows spectra of PAnis prepared via emulsion polymerisation using both acids.

The spectra of both polymers show the expected quinoid and benzoid vibrations in the regions of 1558 and 1478cm$^{-1}$, C-N stretching at 1297cm$^{-1}$ and a polaron band at 1118cm$^{-1}$ together with the absorption at ca. 1085cm$^{-1}$ assigned as CH i/p bending of 1,2,4-trisubstituted aromatic rings [72,136]. The peak at 1034cm$^{-1}$ is assigned to S=O stretching. For PAni-TSA, a shoulder has appeared in the region of 1006cm$^{-1}$ which is also caused by the S=O stretching.

## (PAni-*co*-PoAnis)-Sulfonic acid by Emulsion Polymerisation Pathway

Copolymerisation of aniline and o-methoxyaniline was also performed, following the work of Kim et al. [155,156]. As expected, the spectra are generally very similar, and the copolymer spectrum is closer to that of pure PoAnis than that of pure PAni. The assignments and observations of the general bands are similar to those presented above. A gradual increase in the size of the peak based around 1211cm$^{-1}$ relevant to Ar-O stretching is seen with increase of o-methoxyaniline content, the peak being totally absent from the pure PAni spectrum. This peak builds up until it overtakes the 1300cm$^{-1}$ peak of C=N stretching. As mentioned by Motheo et al. [157], a symmetrical stretching peak of the C-O-C moiety at 1026cm$^{-1}$ is seen in the products. These results confirm the effective copolymerisation of the two monomers.

### 4.1.2 Conductivity Measurements

The conductivity σ of a material can be simply viewed as a measure of its electron transfer capacity. It equals the current density per unit electric field and is expressed in S.I. units Siemens/metre (or more commonly in Siemens/centimetre), ($S.cm^{-1}$) [158].

$$\sigma = \frac{2\ln 2}{(R1 + R2)\pi df}$$

Where σ is electrical conductivity ($S.cm^{-1}$), R1 and R2 are two average readings of measured resistance (Ω), d is thickness of the sample (cm), and f is a geometric factor (approximately 1 for symmetrical contacts on circular pellets or square-shaped plaques).

PAni, depending on its degree of oxidation and of doping, can have a conductivity comparable to insulators or metals; EB is known to be an insulator with a conductivity value of ca. $10^{-10}$ $S.cm^{-1}$, and doped films of PAni-CSA from m-cresol [159,160,161] have reached conductivities of 200-400 $S.cm^{-1}$. It has been shown that in its pristine form, if all the charge carriers contributed to electrical conduction, this value would rise to a staggering $10^5$ S. $cm^{-1}$ [162] and would be comparable to that of metallic copper.

The present study was aimed at producing such types of highly conducting PAni based materials; therefore most of the compounds prepared were partially or totally protonated forms of the ESs obtained from the syntheses. For production of blends with good electrical properties (see section 4.2), the dispersed materials should have a high conductivity.

### 4.1.2.1 Influence of oxidant/aniline ratio

For PAni-HCl at different Ox/Mon mol ratios, we can see that the polymer yield and conductivity were strongly affected by the oxidant/aniline ratio (Table 23). The optimum yield was obtained with a ratio of 1.25, whereas the maximum conductivity was obtained with a ratio of a 0.75. it appears that when the ratio of Ox/Mon is high, chain scission may occur, leading to lower conductivity. On the other hand, reaction yield increases with the use of larger amount of oxidant. By increasing the amount of oxidant in the reaction medium, the concentration of radical cation will be larger, and consequently the polymer chains will be shorter and the conductivity will be lower.

| Sample ID | Ox:Mon ratio | Conductivity S/cm | % Yield |
|---|---|---|---|
| Z-0001 | 0.25:1 | 5.2±0.2 | 21.6% |
| Z-0002 | 0.5:1 | 7.4±0.2 | 40.5% |
| Z-0003 | 0.75:1 | 9.9±0.2 | 55% |
| Z-0004 | 1.08:1 | 8.7±0.2 | 87.3% |
| Z-0005 | 1.25:1 | 3.3±0.2 | 88.7% |
| Z-0006 | 1.5:1 | 0.7±0.2 | 88.3% |

Table 23 Effect of the oxidant/aniline ratio.

In addition, according to Geniès et al., the use of larger amounts of oxidant induces polymer degradation. Improvement in yield is explained by the fact that, in the presence of larger amount of oxidant, aniline monomer is more easily oxidised, producing insoluble oligomers.

### 4.1.2.2 Doping the EB with HCl at Different pH

The experiments here were designed to study the sensitivity of the conductivity of the EB to the pH of the aqueous HCl solution. HCl was added in order to lower the pH from 12 to 0. It was found that when HCl was added to the base, the latter underwent an insulator- metal transition involving an increase in conductivity of $10^{10}$. In principle it should be possible to non-redox dope a conducting polymer (EB) by adding protons, which may interact with the base and hence partly depopulate the pi system with concomitant increase in conductivity of the polymer.

| Sample ID | Compound name | Conductivity S/cm | pH |
|---|---|---|---|
| Z-0008 | PAni-Base | $2.6 \times 10^{-8}$ | 12 |
| Z-0009 | PAni-HCl | 11 | 0 |
| Z-0010 | PAni-HCl | 10 | 1 |
| Z-0011 | PAni-HCl | $1.2 \times 10^{-2}$ | 2 |
| Z-0012 | PAni-HCl | $4.3 \times 10^{-5}$ | 3 |

Table 24 Effect of pH on the conductivity.

### 4.1.2.3 Doping the EB with Different Dispersing Agent

Table 25 gives the conductivity values obtained for the solution polymerised samples of emeraldine salts (pressed pellet). The PAni-HCl exhibited a maximum conductivity value of 9.9 $S.cm^{-1}$ compared to the conductivity values of PAni-dispersing agents. Conductivities of pressed pellet samples have previously been reported to be $3.3\times10^{-1}$ $S.cm^{-1}$ for PAni-HCl and $1.1\times 10^{-4}$ $S.cm^{-1}$ for PAni-DBSA [163], which are much smaller than these results. Pure PAni-HCI and PAni-MeSA showed the highest conductivities, probably due to the small size of $Cl^-$ and $CH_3SO_3^-$ ions within the matrix. TSA, NSA, CSA and DBSA are bulky dopants that may interrupt the conductive

pathways between the polymer chains. However, this deficiency is compensated to some extent by the improved self-organisation, thermal stability and processibility caused by using the larger dopants. It is thought that DBSA dopant molecules are selectively bonded to the iminic nitrogens of PAni via proton transfer, whereas any "free" DBSA molecules are expected to be strongly hydrogen bonded to the aminic nitrogens and to other hydrogen bonding acceptors [164].

| Sample ID | Compound name | Conductivity (S/cm) |
|---|---|---|
| Z-0013 | PAni-DBSA | $(4.1\pm0.2)\times10^{-1}$ |
| Z-0014 | PAni-TSA | $(11.5\pm0.2)\times10^{-1}$ |
| Z-0015 | PAni-NSA | $(14.7\pm0.2)\times10^{-1}$ |
| Z-0016 | PAni-MeSA | $(27.3\pm0.2)\times10^{-1}$ |
| Z-0017 | PAni-CSA | $(8.8\pm0.2)\times10^{-1}$ |

Table 25 Conductivities of full protonated polyaniline.

### *4.1.2.4 Conductivity of Polyaniline 'As Synthesised'*

Chemical synthesis of PAnis in acidic conditions yields the most conducting form of the polymer because the ES is almost in its theoretical 1:1 benzoid: quinoid conformation (ca. 42% of the nitrogens are protonated [59]). Conductivities of polymer samples were measured to determine any influence of the type of protonic acid used on the conductivity of the bulk material.

| Sample ID | Compound name | Conductivity (S/cm) |
|---|---|---|
| Z-0018 | PAni-DBSA | $(16.7\pm0.2)x10^{-1}$ |
| Z-0025 | PAni-NSA | $(2.6\pm0.2)x10^{-1}$ |
| Z-0026 | PAni-CSA | $(27.9\pm0.2)x10^{-1}$ |
| Z-0027 | PAni-TSA | $(72.7\pm0.2)x10^{-1}$ |
| Z-0028 | PAni-MeSA | $(70.3\pm0.2)x10^{-1}$ |

Table 26 Conductivity of some as prepared polyaniline.

PAnis prepared by precipitation from HCl solution have lower conductivities than those prepared via emulsion polymerisation, probably due to molecular order induced by the sulfonic acids and more homogenous protonation of PAni achieved by the *in situ* doping through the emulsion polymerisation route.

It can also be noted that small dopant molecules such as p-TSA or MeSA seem to achieve more efficient doping than the more bulky conjugated ones such as DBSA and NSA or non-conjugated ones such as CSA. The lower values of conductivity of the present doped PAni systems might be due to the bulky nature of the dopant, which disrupts the efficient packing of the molecules.

It is well known that the water solubility of these organic sulfonic acids decreases in the order: MeSA>p-TSA>DBSA>CSA>β-NSA; this means that most strong acidic medium occurred in the case of MeSA. As a result, the strong acidity and smaller molecular size of MeSA would favour the formation of a less-doped reduction state of PAni during the oxidative polymerisation. But for p-TSA, the lower acidity than that of MeSA would cause the more oxidative state of PAni; this may be because emeraldine type structure is predominant in PAni-p-TSA. In contrast with other organic sulfonic acids, DBSA, CSA and

β-NSA have larger molecular size and lower solubility in water due to their longer alkyl chains. The lower water solubility would lower the hydrogen ion concentration, which would favour the formation of the oxidised form of PAni, but a separation of the oxidant (APS) from monomer (anilinium complex) would be caused by the steric hindrance of longer alkyl chain length of these sulfonic acids, which was also of benefit for the less-doped state of PAni during the oxidative polymerization.

### 4.1.2.5 Conductivity of Polyanisidines

The study of the relationship between the product conductivity and the dispersing agents focused on two methods, solution polymerisation and emulsion polymerisation.

All conductivity results for PoAnis prepared using the precipitation method are listed in Table 27, apart from those for PoAnis-MeSA, PoAnis-CSA and PoAnis-Base, because these products were very gelatinous, which made measurements difficult and extremely inaccurate. In the case of polyanisidine base, the sample showed a higher resistance than the upper limit of the electrometer (150GΩ).

| Sample ID | Compound name | Conductivity (S/cm) |
|---|---|---|
| Z-0029 | PoAnis-HCl | $(6.8\pm0.2)\times10^{-2}$ |
| Z-0031 | PoAnis-DBSA | $(0.2\pm0.2)\times10^{-2}$ |
| Z-0032 | PoAnis-TSA | $(1.5\pm0.2)\times10^{-2}$ |
| Z-0033 | PoAnis-NSA | $(1.2\pm0.2)\times10^{-2}$ |

Table 27 Conductivity results of doped PoAnis.

In terms of conductivity, TSA appears to be a better dopant of PoAnis base than NSA and DBSA. This could be due to the fact that bulky dopants such as DBSA may hinder the intermolecular charge-transport by generating excessive distances between the polymer chains.

Contrary to the observations made in section 4.1.2.4, the conductivities of PoAnis are lower than those of their PAni counterparts. This may be due to the higher electron density (from the methoxy group) of the polymer containing anisidine.

Based on the results obtained for PoAnis-HCl, PoAnis was prepared in the presence of different dispersing agents (MeSA, TSA, NSA, CSA, DBSA), using the same conditions.

However, there was no precipitation of the product after 4h. Since the reaction medium containing dispersing agents such as TSA, DBSA, CSA, NSA was more viscous, the diffusion of the reactants was slower and, consequently, the reaction rate in the presence of any of the mentioned acids is also lower. Thus, a period of 8h was necessary to obtain the product (PoAnis-dispersing agent).

| Sample ID | Compound name | Conductivity (S/cm) |
|---|---|---|
| Z-0034 | PoAnis-DBSA | $(0.7\pm0.2)\times10^{-2}$ |
| Z-0035 | PoAnis-TSA | $(7.7\pm0.2)\times10^{-2}$ |
| Z-0036 | PoAnis-CSA | $(2.8\pm0.2)\times10^{-2}$ |
| Z-0037 | PoAnis-β-NSA | $(1.4\pm0.2)\times10^{-2}$ |
| Z-0038 | PoAnis-MeSA | $(4.8\pm0.2)\times10^{-2}$ |

Table 28 Conductivity values of synthesised PoAnis via emulsion polymerisation.

The conductivity values obtained for TSA (see Table 28) were higher than those obtained with other dispersing agents. Once again, the intermolecular spacing could be the determining factor here. The intermolecular distances created by the structure of the dispersing agent have increased the spaces between polyaniline backbones, making interchain proton hopping more difficult.

Polyanisidines prepared by precipitation from HCl solution have lower conductivities than the ones prepared via emulsion polymerisation, probably due to molecular order induced by the sulfonic acid salts.

### 4.1.2.6 Conductivity of Polyaniline Copolymer with Respect to O-anisidine Ratio

Some observations have already been made about the difference in conductivities between polyanilines and polyanisidines. Figure 38 shows the influence of co-monomer ratios on conductivity for compounds protonated with different dispersing agents.

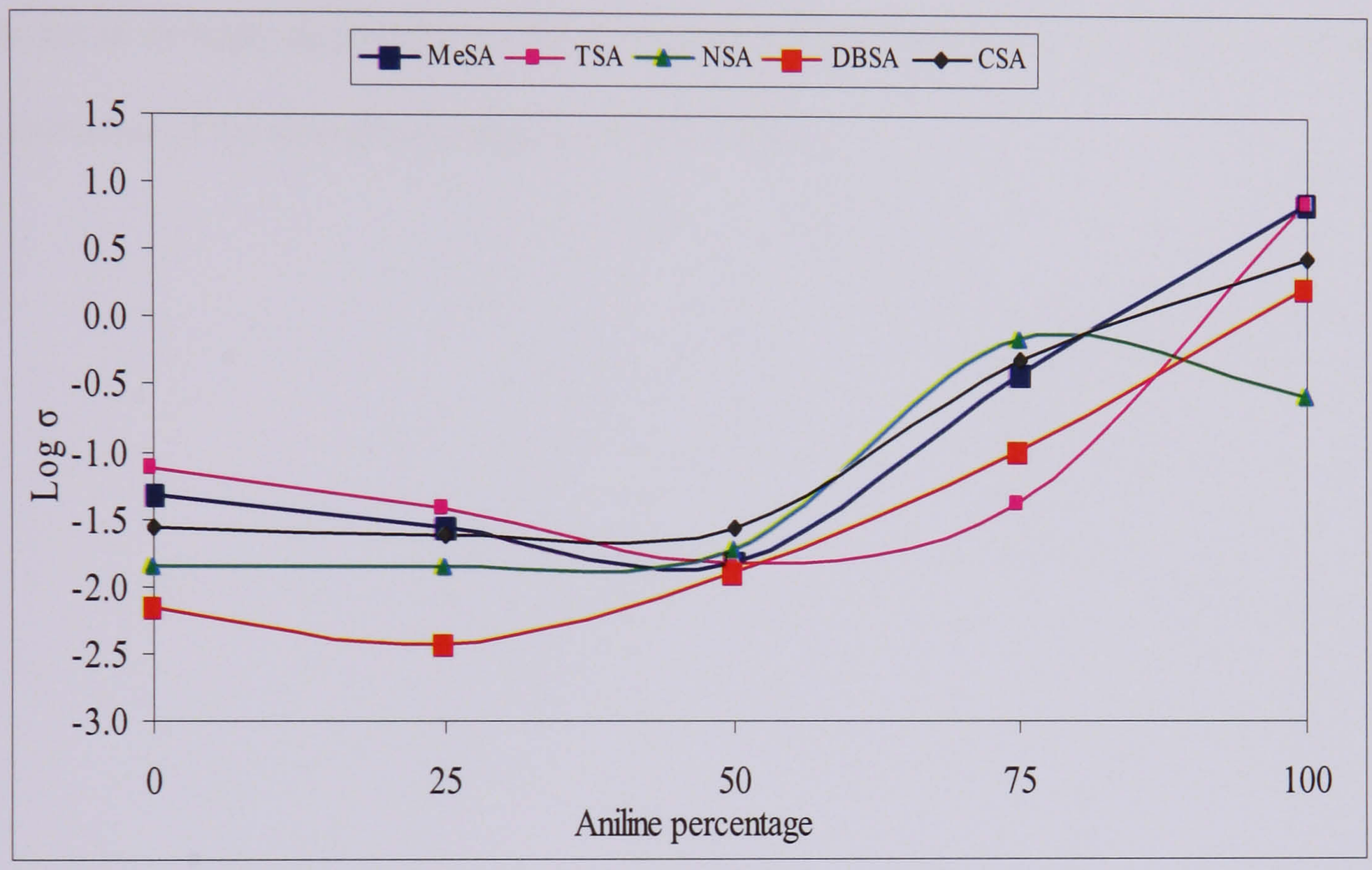


Figure 38 Conductivity of poly aniline-*co*-anisidine with respect to the monomer ratio.

The conductivities of the five samples tend to decrease as the ratio of anisidine increases, in accordance with reported results [157] [155], due to the decreased chain planarity caused by the methoxy-side-groups. The methoxy group donates electronic density to the conjugated ring which renders the amine moiety of *o*-methoxyaniline more likely to bind to a free proton from the acidic medium than that of aniline. When aniline is in excess however, after the first block of PoAnis is created and while the concentration of free anisidinium radical cations or oligomeric radical cations decreases in the reaction mixture, anilinium radical cations are inserted in the structure, creating a localised alternating copolymer before terminating the chains with a block of pure aniline. It is thought that the shorter length of this alternating

polymer may explain the increase in conductivity for the compounds prepared in solution. The alternating co-polymer structure is most probably the form of the polymer where the loss of planarity due to the pendant side groups is highest, explaining the lower (or comparable) conductivity of compounds prepared at 25 and 50% aniline loadings. When the reaction is carried out in a strongly dispersing medium such as DBSA, the shape of the final polymer particles is strongly dependent on the arrangement of the surfactant molecules, over-ruling the influence of the side groups attached to the chain.

### 4.1.3 Thermogravimetric Analysis

Thermal degradation of polymers is an important area of study. Polymers find applications in fields where heat is present, and should preferably display the same characteristics over a suitable temperature range. TGA is a very simple technique in which samples are gradually heated and their weight loss monitored over a period of time. PAni materials usually display three steps in their degradation process in nitrogen (2 for EB) which have been ascribed to:

**1. Loss of solvent and small molecules** ca. 80-150°C [101, 165,166] The polymers and especially doped polymers usually carry water/solvent molecules, either hydrogen bonded to the polymer or hydrating the dopant anions which are difficult to remove by conventional drying. Upon sufficient heating of these materials, the small molecules are evaporated from their structure.

**2. Loss of dopant anions** ca. 150-350°C [165,167] Upon stronger heating, dopant anions start vaporising and leave the polymeric backbone. The degradation of the latter may also start at the high end of this temperature range.

**3. Backbone degradation** ca. 350- 650°C [101,165 ,166] Upon reaching high temperatures, the polymer backbone starts to break down via oxidation reactions until complete destruction of the material occurs. Little or no residue is found at temperatures over 600 °C in the presence of air. These reactions are either internal or oxygen induced radical degradations and can be outlined as follows [165].

| | | | |
|---|---|---|---|
| Polymer | ⟶ | P• | Initiation |
| $P• + O_2$ | ⟶ | $PO_2•$ | |
| $PO_2• + PH$ | ⟶ | $PO_2H + P•$ | |
| $2\ PO_2H$ | ⟶ | $PO• + PO_2• + H_2O$ | Chain branching |
| $PO_2H$ | ⟶ | $PO• + •OH$ | |
| $PH + •OH$ | ⟶ | $P• + H_2O$ | |
| $2\ PO_2•$ | ⟶ | Inert products | Termination |
| $PO_2• + P•$ | ⟶ | $PO_2P$ | |
| P• | ⟶ | P-P | |

Many studies of PAni stability under an argon or nitrogen flow [96, 101, 142, 150,168 , 167, 169] have shown that the absence of oxygen in the oven retards the decomposition of the polymer and residues. It has been shown by Cataldo [96] that EB heated at 20°C/min under nitrogen has a weight loss at 800°C of less than 25 %.

### *4.1.3.1 Thermogravimetric Analysis of PAni-HCl and EB*

To be familiar with the general patterns of degradation and thermal behaviour of polyanilines, it is necessary to study doped and dedoped polyaniline. Dedoped PAni was obtained by converting the pristine doped polymer into its base form using a dilute solution of ammonia. The thermal stabilities of PAni-HCl, EB, PoAnis-HCl and PoAnis-Base were assessed by heating the samples at 20°C/min between 30 and 650°C. Plots are presented in Figure 39.

The TGA thermogram of PAni-HCl shows the expected three step weight loss behaviour. The obvious and only major difference between the two polymers is the presence of dopant (HCl) in Z-0007. The first weight loss step (37-144°C) of PAni-HCl not only represents the release of water but also free molecular acid left over at the end of the synthetic processes. Various authors have reported and characterised the release of free acids [170,171].

The second weight loss step (165-330°C) indicates mostly the loss of ionic HCl bound to the polymer chain as protonating dopant acting as a counter ion for the positively charged nitrogen. The final step (465-650°C) of degradation represents the breakdown of the backbone of the polymer.

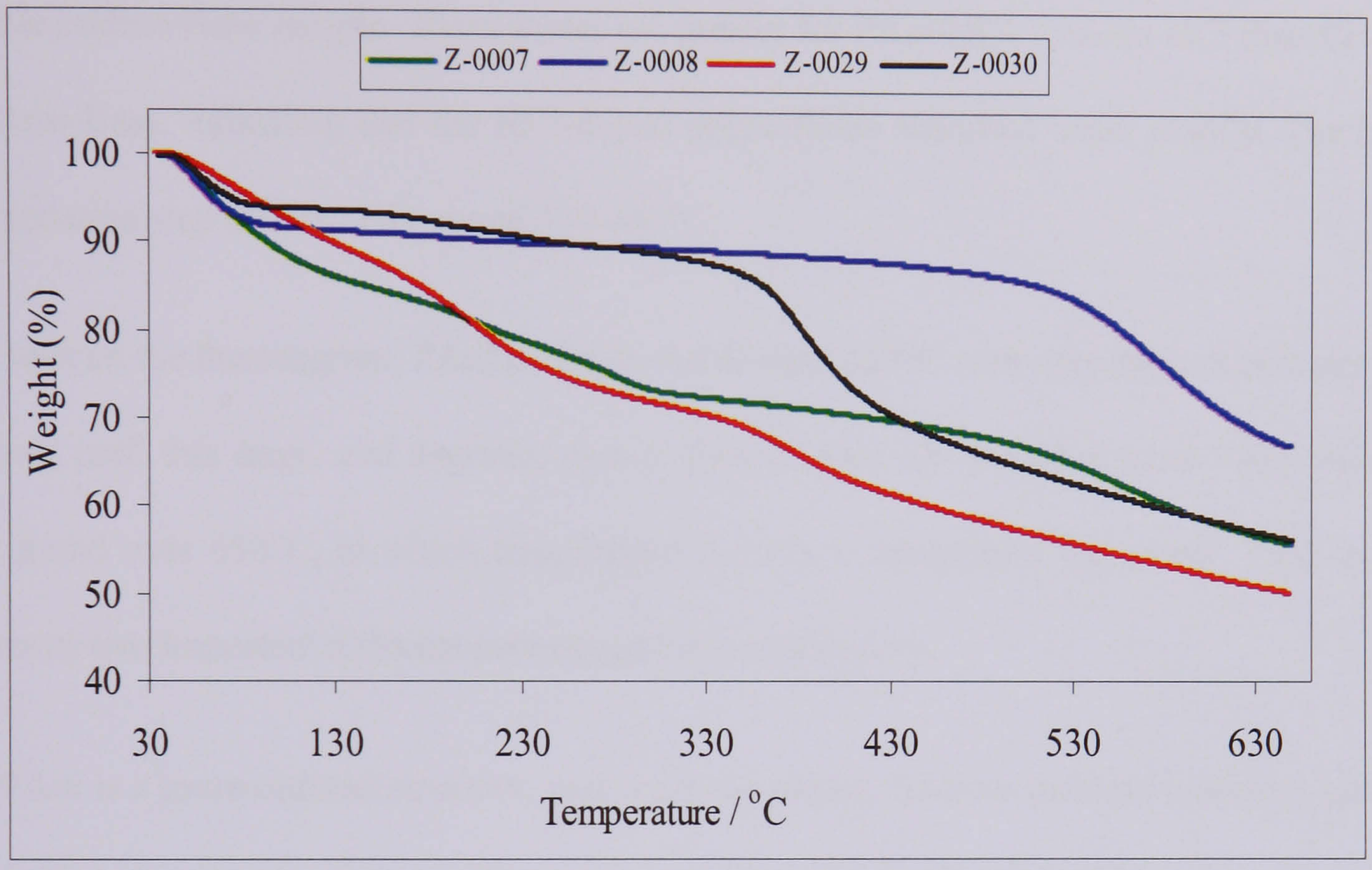


Figure 39 TG plots for PAni and PoAnis prepared using HCl as protonic acid and deprotonated using ammonia solution at a heating rate of 20°C/min under $N_2$.

For EB, the degradation patterns show differences from PAni-HCl. The first step represents the release of water (42-87°C), which is a normal phenomenon with all types of hydrophilic polymers. The main degradation step occurs in the range 517-631°C and involves the degradation of the polymer backbone through a succession of chain scissions via breaking bonds and formation of radicals. These radicals can be then degraded further, ultimately to the point where the molecular weight of the product is low enough for sublimation to occur.

For PoAnis-HCl, the first weight-loss observed up to 133°C could be due to loss of residual water molecules/moisture present from the polymer matrix. The second stage observed within the temperature range of 142–294°C could be related to removal of dopant molecules

from the polymer structure. The weight-loss observed after the removal of the dopant molecules (328-423°C) corresponds to the complete degradation and decomposition of the polymer main chain.

The small fractions of weight loss below 90°C are attributed to the loss of moisture in the Polyanisidine-Base sample. These losses are greater for PAni-HCl, PoAnis-HCl than EB and PoAnis-Base, indicating that the HCl-doped polyanilines absorbed water readily. The main degradation step occurs in the range 339-463°C.

As seen on the thermogram, PAni is clearly stable until 465°C with only the loss of water and dopant until this stage, and degrades slower than PoAnis. On the other hand PAni residues are found over 650°C, at which temperature PoAnis is completely vaporised. One should reiterate two important differences between PAni and PoAnis.

- PAni is a more ordered structure, and is almost planar, whereas pendant methoxy- groups in PoAnis introduce a steric effect causing torsion of the polymer backbone.

- Polyanisidine is more likely to undergo radical coupling than polyaniline due to the mesomeric effect from the methoxy- group towards the ring.

Taking these two remarks into account, it is possible to formulate a hypothesis for the difference of degradation behaviour of the two structures. PoAnis being a less ordered structure and containing pendant methoxy-groups, upon heating it would start degrading more rapidly than PAni. During the degradation process, as the chains break and radicals are formed, these reactive poly(oligo)-anisidine radicals are more likely to undergo a faster degradation than the less reactive poly(oligo)-aniline radicals, explaining the different observations made.

### 4.1.3.2 Thermogravimetry of Sulfonic Acids Doped PAni and PoAnis

The sulfonic acid doped PAni samples were investigated and as for insoluble polyanilines discussed previously, the soluble polymers present a three-step weight loss. Figure 40 represents the thermograms of polyanilines doped with different dispersing agents. Among the three steps of decomposition, the first and the last steps are quite distinct and exhibit rapid weight loss with respect to the temperature, while the middle or second step is less conspicuous, involving gradual weight loss extending over a broad temperature range (150-420°C). However, as can be seen in Figure 40, a peak due to loss of dopant is not seen for PAni-DBSA.

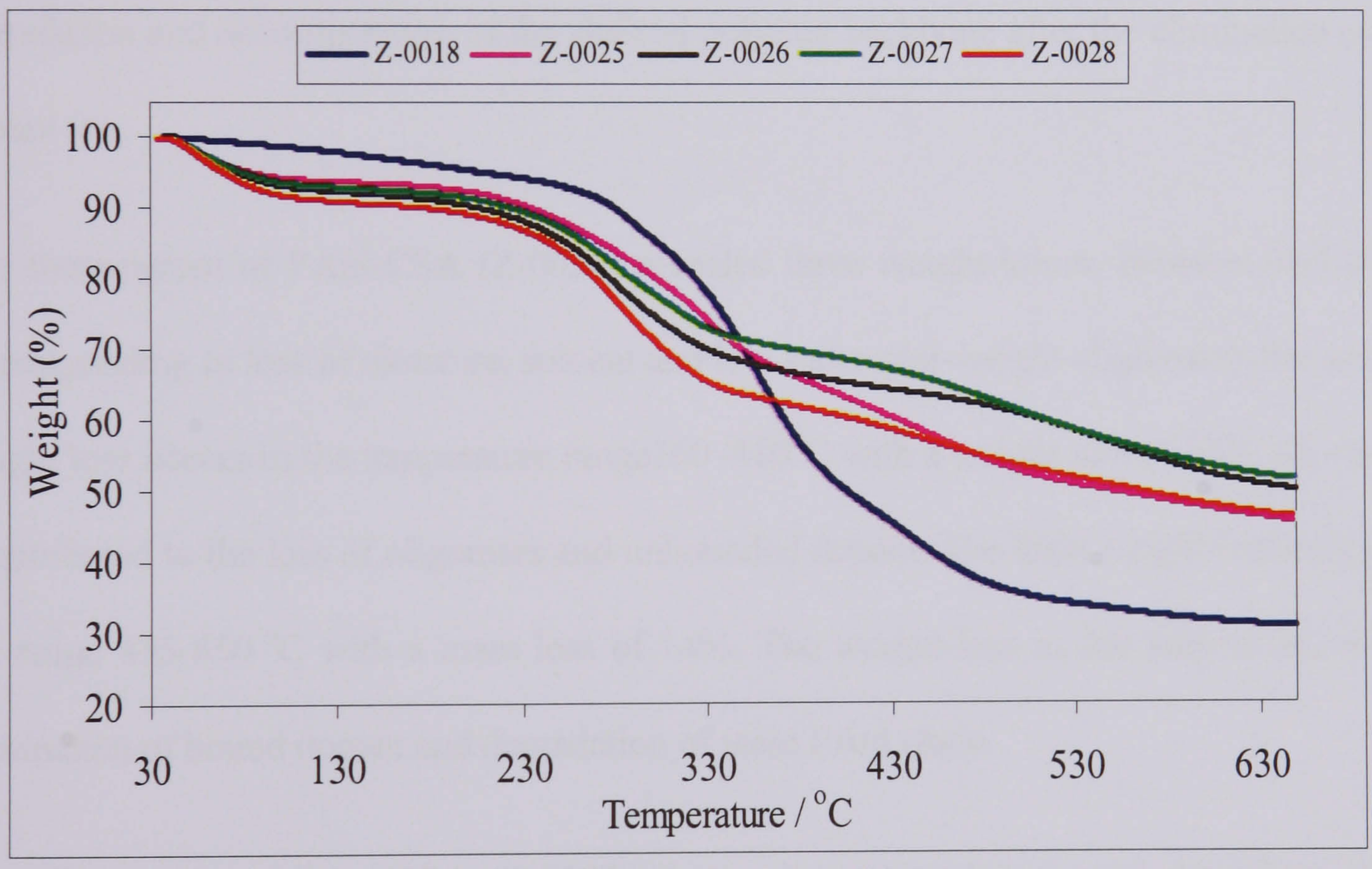


Figure 40 TG plots of sulfonic acids doped PAni at a heating rate of 20°C/min under $N_2$.

The first weight loss from 40-120°C is attributed mainly to the loss of free water/ moisture present in the polymer matrix. The weight loss values range from 0.7% for PAni-DBSA to 9% for PAni-MeSA. The polymer matrix of PAni-MeSA is more hydrophilic than those of the other polyanilines studied which would explain the greater water content and hence weight loss.

The TGA thermogram of PAni-DBSA (Z-0018) shows a two-step weight loss. The first step occurs in the range 78-75°C with a weight loss of 0.7% which is attributed to the expulsion of water molecules from the polymer. The second-step occurs between 264-477 °C with a weight loss of 55%, which is attributed to chain scission and dopant degradation.

For PAni-NSA (Z-0025), it is observed that the polymer exhibits a three-step decomposition pattern, the first step in the decomposition pattern between 42-113°C (6%) being due to the removal of free water molecules present in the polymer matrix. The second loss starting from 186 and continuing to 420 °C (31%) is mainly caused by loss of the dopant ion from the polymer chains (thermal dedoping). The third step starting at 428°C is accounted for by the degradation and decomposition of the skeletal polymer backbone after the elimination of the dopant ion.

The thermogram of PAni-CSA (Z-0026) revealed three weight losses, between 38-118 °C (corresponding to loss of moisture, solvent and low molecular-weight oligomers); the second weight loss occurs in the temperature range160 -416°C with a weight loss of 26% which can be attributed to the loss of oligomers and unbounded dopant. The third weight loss occurs in the range 435-650 °C with a mass loss of 14%. The weight loss in this step is due to the elimination of bound dopant and degradation of main PAni chain.

The TGA curve of PAni-TSA (Z-0027) shows three mass losses, and according to the literature these can be assigned to water loss, TSA loss and polymer chain degradation. PAni-TSA was stable until 153-370 °C (22%), when loss of dopant was occurred, followed by degradation of the main chain at 425 °C (16%).

The thermogravimetric analysis of PAni-MeSA (Z-0028) indicates three weight losses, the first weight loss occurs in the range of 44-119 °C (9%), which is due to loss of water. The

second weight loss occurs between 165-387 °C (29%), which is attributed to the loss of low molecular weight substances, and dopant (MeSA) from the PAni chain. The third weight loss between 394-524 °C (9%) is due to the degradation of the main chain of PAni.

Figure 41 displays the thermal profile of PoAnis doped with DBSA, TSA, CSA, NSA and MeSA. From the figure, it is observed that the polymer exhibits a three-step decomposition pattern similar to that of unsubstituted polyaniline.

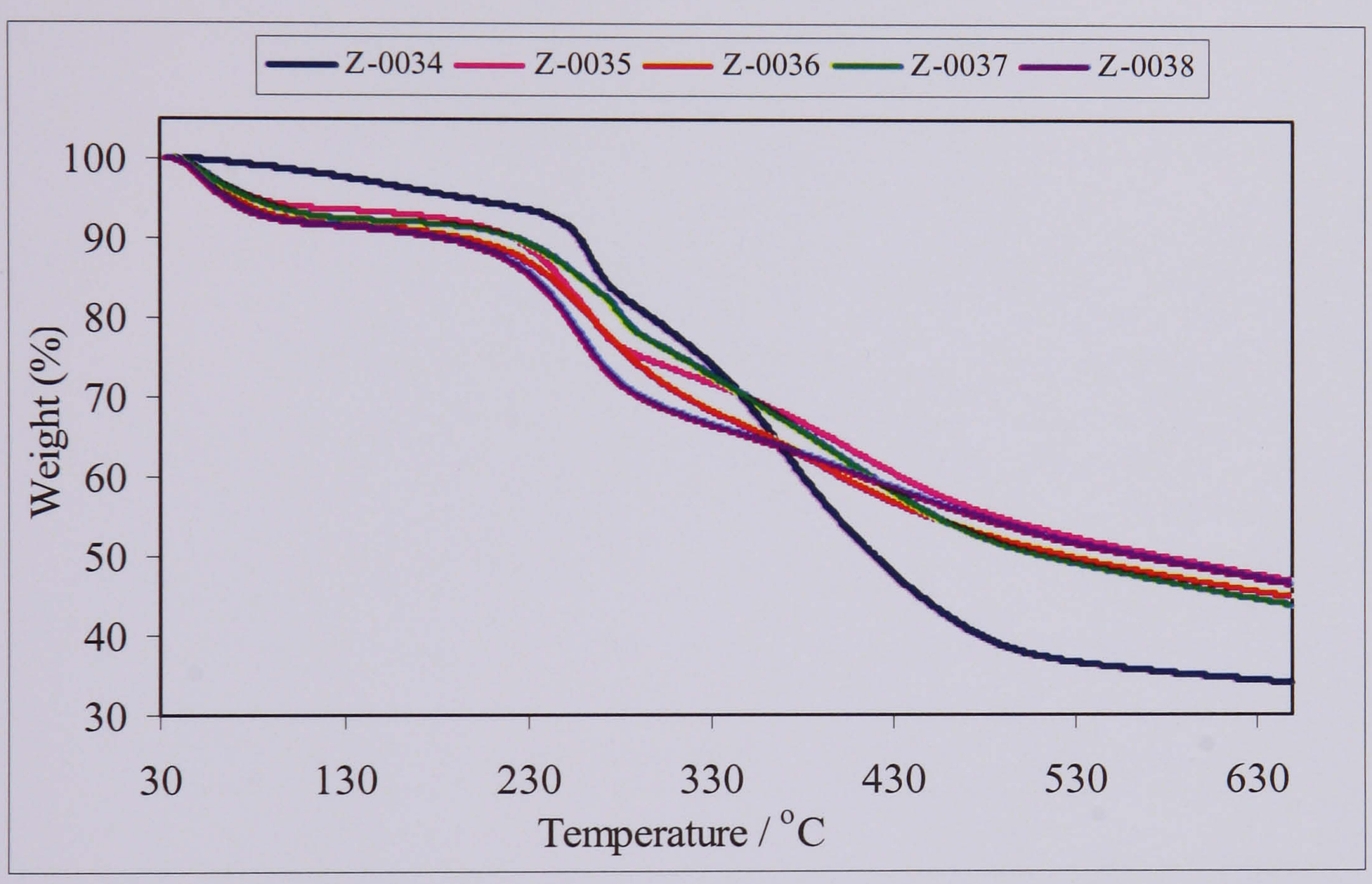


Figure 41 TG plots of sulfonic acids doped PoAnis at a heating rate of 20°C/min under $N_2$.

For the sulfonic acid doped PoAnis, rapid weight loss is observed in the third step of decomposition over the temperature range between 350-500 °C. This is mainly because of the presence of the methoxy substituent present on the benzene rings of the polymer backbone. The steric effect rendered by this flexible methoxy group and loosening of the polymer skeleton would require less energy to undergo a complete breakdown of the polymer chains. Thus, the incorporation of substituent on the benzene ring reduces the thermal stability of the resulting polymers because of the formation of defects in the polymer chains, which favours

the early degradation and decomposition of the polymer matrix. Major weight loss is observed between 200-450 °C in sulfonic acid doped polyanisidines. On comparison of the weight losses in the third step of decomposition, it is observed that 50% of the original weight is stable up to 390 °C in MeSA-doped PoAnis, TSA-doped PoAnis is stable up to 330 °C, NSA-doped PoAnis is stable up to 355 °C, CSA-doped PoAnis is stable up to 365 °C, whereas in DBSA-doped PoAnis it is only stable up to 310°C. Therefore, MeSA-doped PoAnis is thermally the most stable sulfonic acid doped polyanisidine.

### 4.1.4 Physical and Morphological Characterisation

In this section, scanning electron microscopy was one of the main tools used to find chemical routes yielding elongated particles that were clearly seen with high magnification pictures. Although fibrillar morphology was reported earlier in the case of electrochemical preparation of ES (PAni-$HClO_4$) [172], polymers prepared via chemical solution polymerisation are best described as granular materials [173,174]. Research began in the nineties aimed at controlling the size and shape of these materials via chemical routes. To date, production of fibres [130], "template free" microtubules [175], "rice grain" particles [79], and coral-like networks [176] of PAni has been achieved by different groups.

Along with SEM analysis, the crystallinity of the polymers was analysed by X-ray diffraction using a powder diffractometer. When a polycrystalline sample is placed in a diffractometer, sharp peaks are seen at angles at which there is reflection of the incident beam. The size and position of these peaks are specific to the crystal observed and the size of the interplanar spacing (d) and crystalline domain (L), (equivalent to the diameter for spherical particles) are made possible, by use of the Bragg and Scherrer equations respectively:

$d = \lambda/2.sin\theta$ **Bragg equation**

$L = 0.9\lambda/\Delta(2\theta).cos\theta$ **Scherrer formula**

Where:
$\lambda$:Wavelength of the X-Ray source (1.542 Å)
$\theta$: Bragg angle
$\Delta(2\theta)$: FWHM (full width at half maximum)

Studies have shown that PAni (EB from PAni-HCl) is an almost amorphous compound while its hydrochloride salt displays some crystallinity [70,177,178]. It has also been shown that after dissolution of EB and film casting/stretching, more ordered structures can be obtained. In this chapter, we present the different morphologies encountered during the research and try to

relate them to the preparative conditions. The samples for SEM were not ground, in order to preserve macroscopic as well as microscopic and nanoscopic morphologies, whereas for XRD, basic pestle and mortar grinding was used to obtain a flat powder sample.

#### *4.1.4.1 PAni-HCl*

PAni and PoAnis prepared via conventional chemical routes were observed under the electron beam. The morphologies are in accordance with those of granular materials encountered in previous studies.

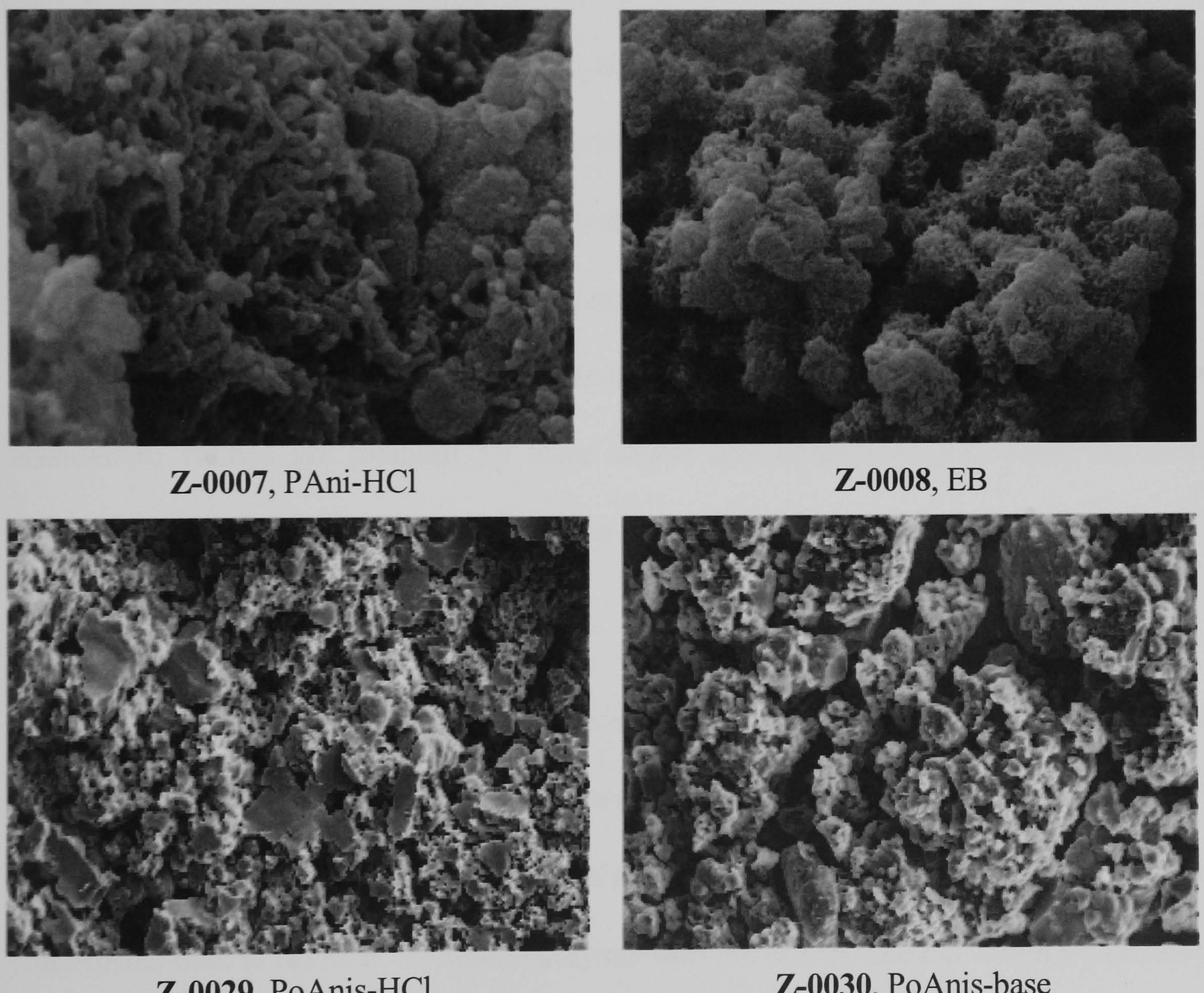

**Z-0007**, PAni-HCl **Z-0008**, EB

**Z-0029**, PoAnis-HCl **Z-0030**, PoAnis-base

Figure 42 SEM photographs for PAni-HCl obtained via solution polymerisation.

The photographs presented in Figure 42 show the different type of morphologies for PAni and PoAnis. It can be found from Figure 42 (a) that Z-0007 has mixed regions of fibrillar mat

and globular morphologies with no microscopic size uniformity. Z-0008 has a coral-like morphology that is quite homogeneous, porous but apparently composed of fibrillar units.

The a-synthesised HCl salt of PoAnis (Z-0029) showed signs in the charging of electron beam of the SEM; the highly charged regions are clearly electrically isolated from the aluminium substrate. This is consistent with the much lower conductivity of the PoAnis salt compared with PAni salt (by a factor of $10^4$ times). The particles are loose and porous agglomerates with no obvious structure or features. Large particles appear as lumps of 10–100μm along with smaller clusters of ca. 0.1–5μm in diameter; the larger lumps are probably formed upon drying the polymers and are not relevant to the actual aggregation process. Remembering the different steps in the formation of PoAnis and PoAnis base, it can be proposed that the large clusters correspond to the first-reacted polymer chains which aggregate in solution via van der Waals attractions and electrostatic double layer forces. When the particles become big, they precipitate as a salt. At this point in time, unreacted anisidinium cations get oxidised by these chains and become free to react, but since concentration of monomer is less, the reaction is slow and yields shorter chains which will in turn precipitate as small clusters of particles.

It appears from the X-ray diffraction patterns presented in Figure 43 that the degree of crystallinity of PAni and PoAnis powders are relatively low. Since the four polymers exhibit the same amorphous pattern, a comparison of the areas under curves indicates that PAni-base and PoAnis-base is the most crystalline polymer than the others. The EB exhibits three main reflections, at $2\theta = 15°, 20°, 25°$ and a fourth small reflection at $2\theta = 10°$.

PAni-HCl exhibits its typical reflections at similar angles. Small deviations are obtained due to different unit cell dimensions, stemming from the presence of dopant. PAni-HCl exhibits four main reflections, at $2\theta = 9.5°, 15°, 22°, 27°$ and a fifth small reflection at $2\theta = 28°$. The

peak at $2\theta = 28^{\circ}$, is dominant for most polyaniline samples, and is thought to relate to the broad range of co-facial repeat distances between the monomer units. The peak at $2\theta = 27^{\circ}$ is attributed to the periodicity perpendicular to the polymer chain, the peak located at $2\theta = 22^{\circ}$ may be ascribed to the periodicity parallel to the polymer chain, while the peak at $2\theta = 9.5^{\circ}$ may be caused by the scattering along the orientation parallel to PAni chains.

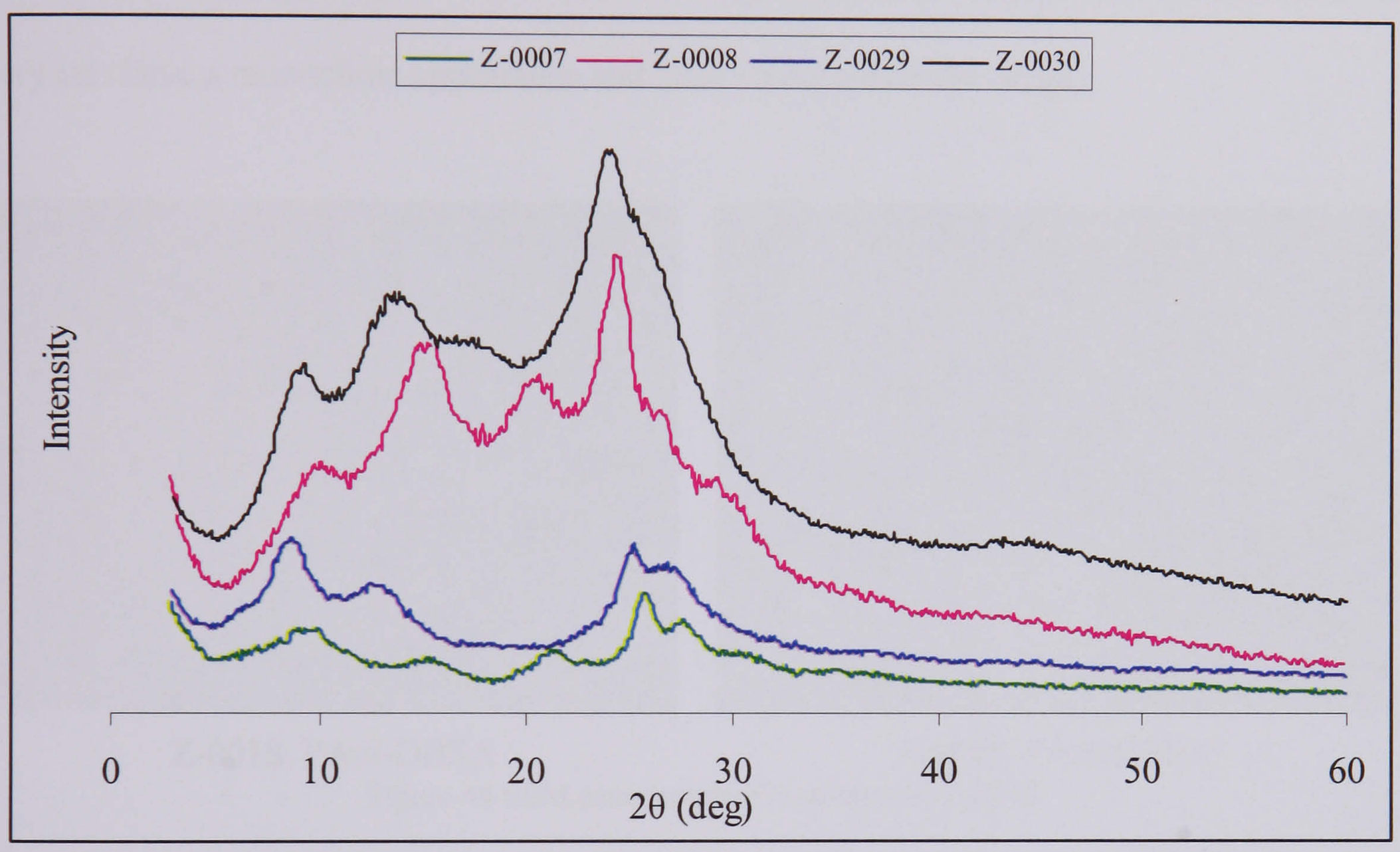


Figure 43 XRD pattern for PAni-HCl, PoAnis-HCl, EB and PoAnis-Base.

The X-ray diffraction patterns for the PoAnis powder and its base obtained through the solution polymerisation method are shown in Figure 43 Bragg diffraction peaks of $2\theta = 8^{o}$, $12.5^{o}$, $25.5^{o}$, $27^{o}$ can be found in the XRD patterns of the PoAnis salt. This XRD patterns are similar to those of electrochemically prepared PoAnis salts [179,180]. The peak at the lowest angle ($2\theta = 8^{o}$) is considered to relate to the distance between two stacks in the 2D stacking arrangement of polymer chains with intervening dopant ions between stacks; this reflection is due to the ordering of PoAnis caused by protonation with acids. The peak at $2\theta = 25.5^{o}$ represents the characteristic distance between the planes of benzene rings in adjacent chains.

### 4.1.4.2 PAni-Sulfonic Acids

PAni-DBSA, as it contains one of the most studied surfactant counterions for emulsion polymerisation of aniline, PAni-DBSA was used in the present research as a reference compound. This polymer shows (see Figure 44) well developed crystalline particles, probably based largely on very low molecular weight polymer, and a matrix of more amorphous looking material which may be a high molecular weight material. A number of crystals have a monoclinic appearance and others have a rhombic shape.

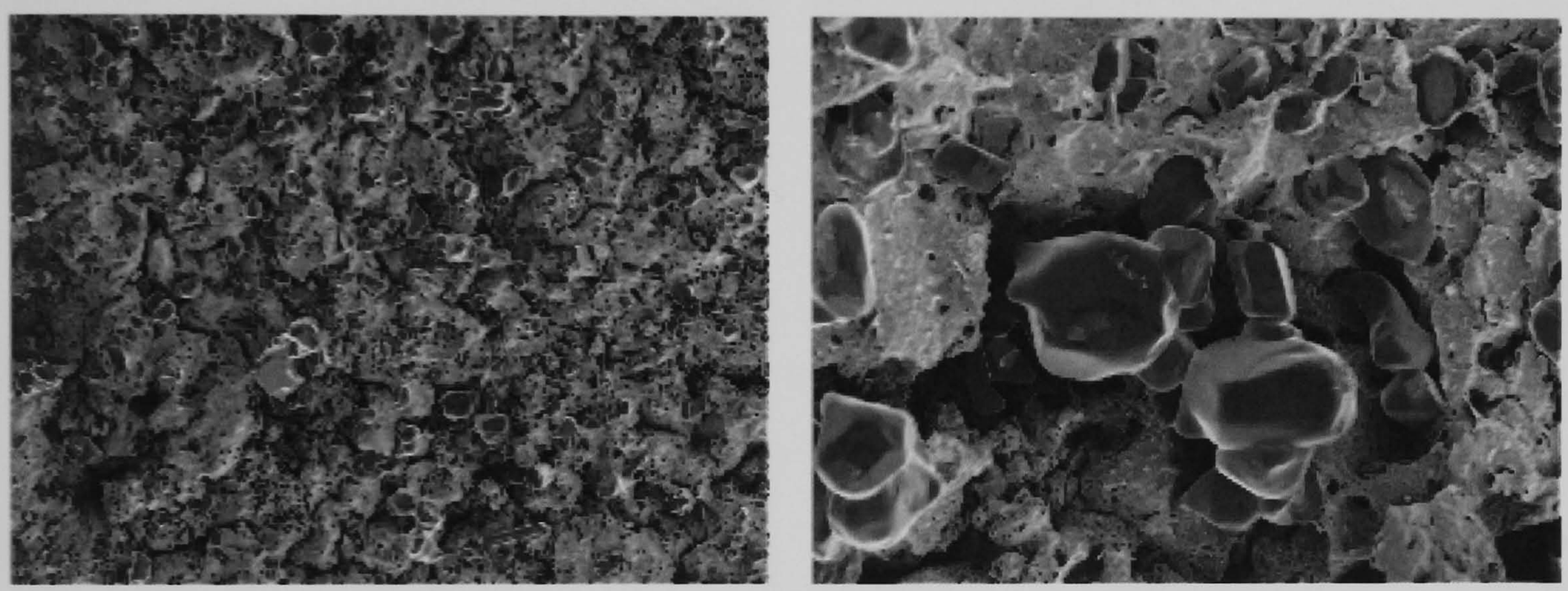

**Z-0018**, PAni-DBSA **Z-0018**, PAni-DBSA

Figure 44 SEM photographs for compound Z-0018.

It was studied the influence of other well-known sulfonic acids (CSA, β-NSA, p-TSA and MeSA) on the particle size, shape and crystallinity of intrinsically doped PAnis. Most of the compounds appear amorphous (Figure 45) without clearly ordered structures. PAni -NSA has been widely described as being a blend of fibrillar, tubular, and even micro spherical morphologies [175,181,182,183]. Here, the compound studied was prepared at Ox:Mon ratio 0.75.The observed morphology was somewhat different to that previously reported in the literature. Z-0025 displays a fine layered flakey structure with pronounced crystalline regions which often have a hexagonal appearance, but there is also some amorphous material present as indicated by the X-ray diffractometry. Upon closer inspection, some holes are seen in the

material which leads to the consideration of the hypothesis of an initial formation of large tubules thin walls. These tubules would be very fragile and break upon compression, giving the overall morphology of a flaky structure.

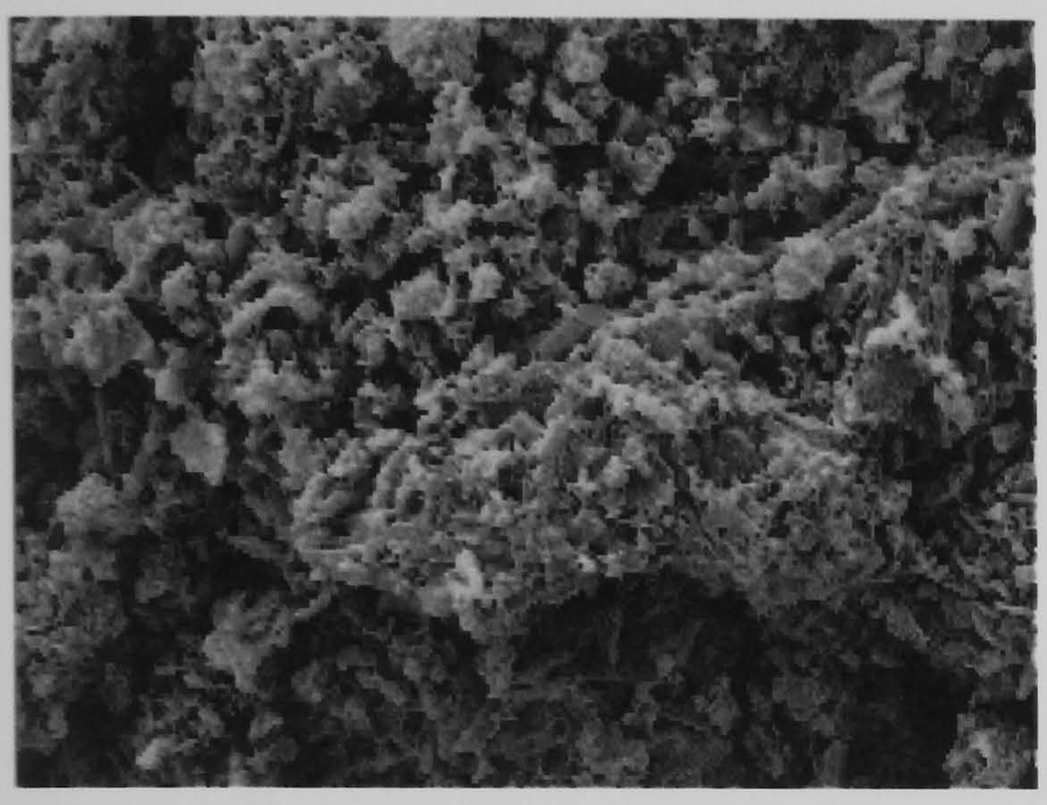

**Z-0025**, PAni-NSA

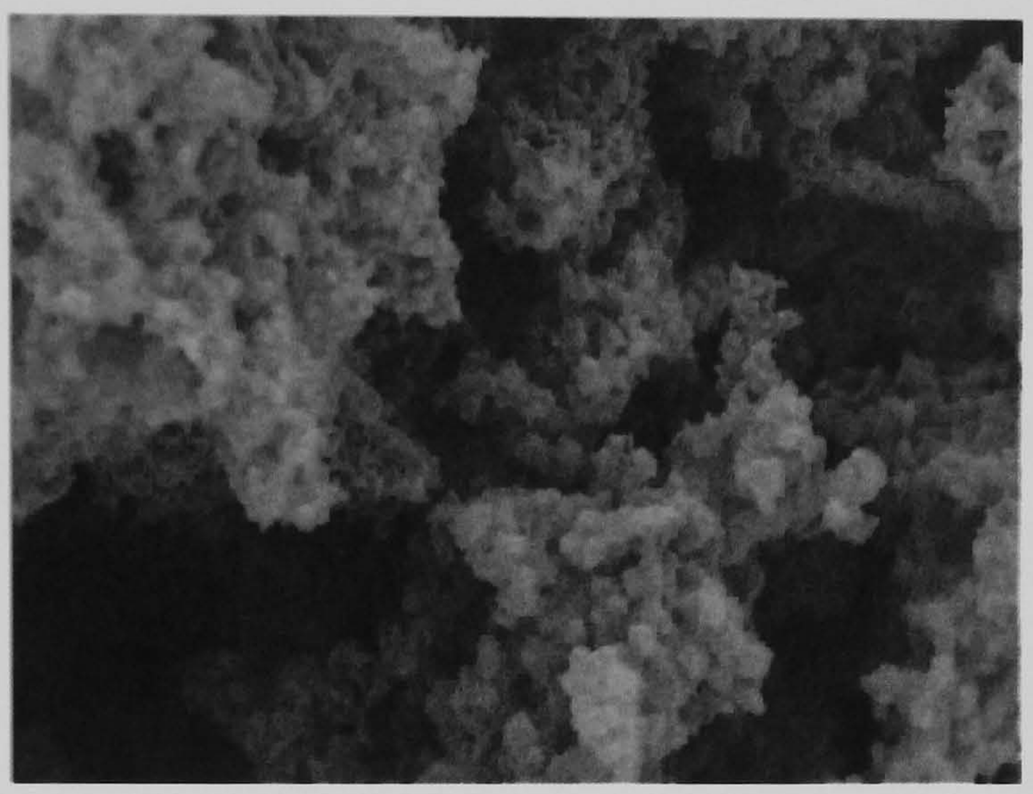

**Z-0026**, PAni-CSA

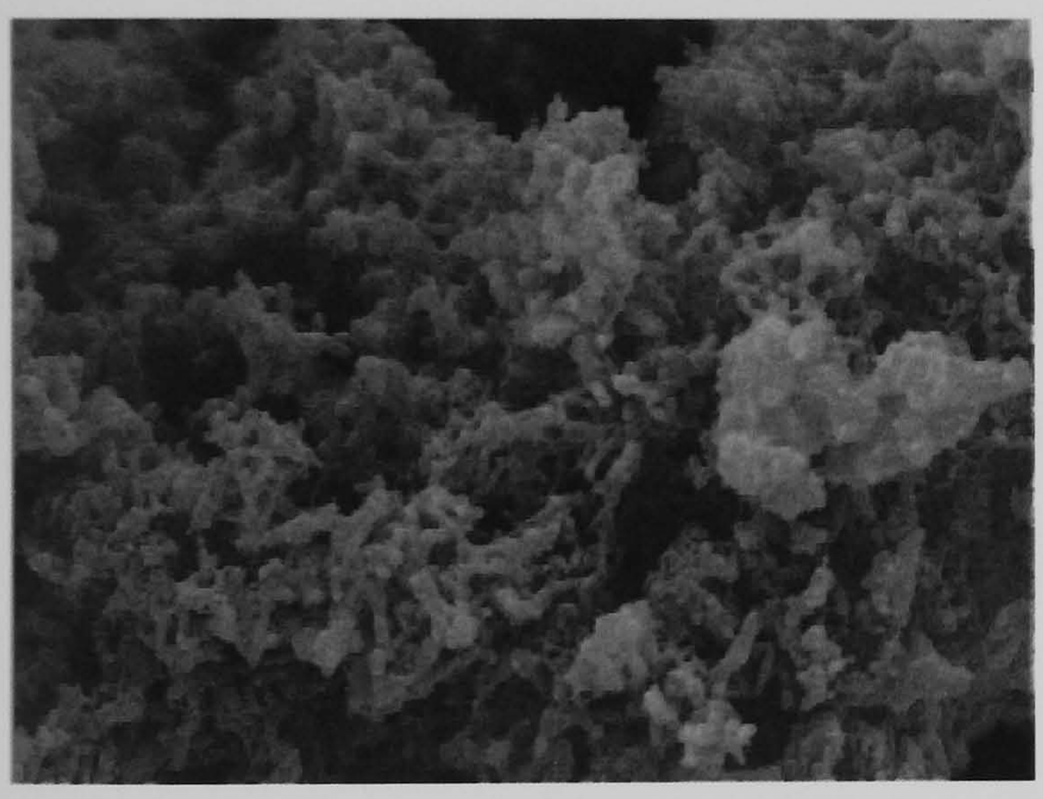

**Z-0027**, PAni-TSA

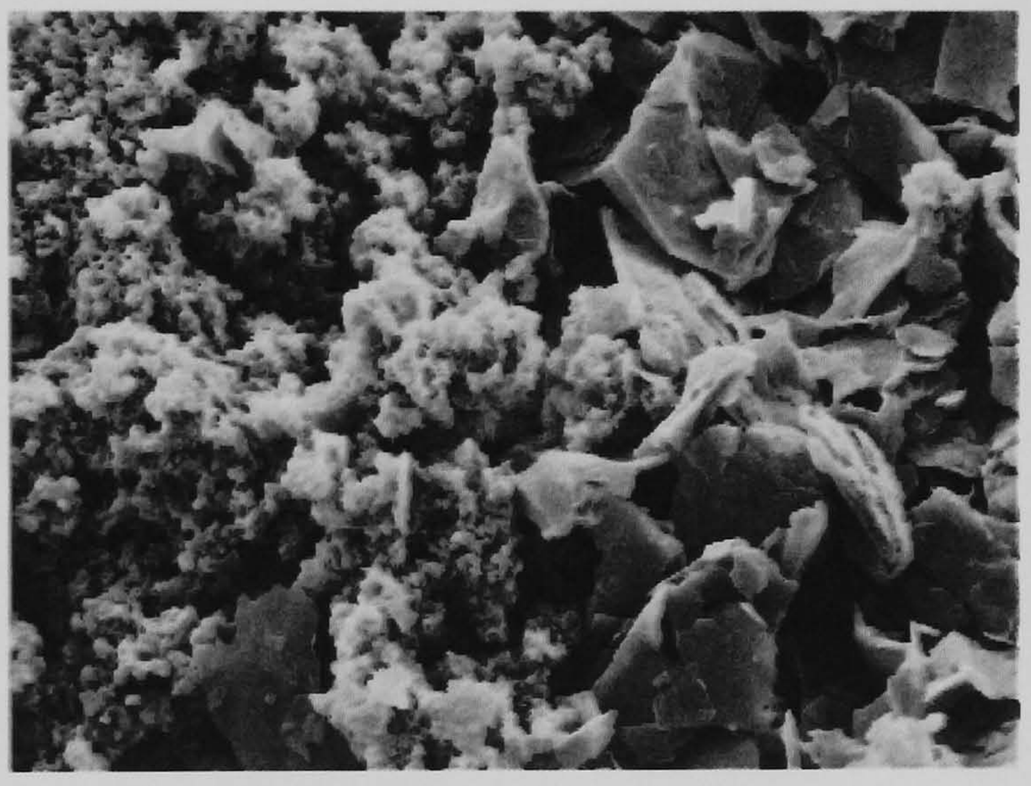

**Z-0028**, PAni-MeSA

Figure 45 SEM photographs for Sulfonic acids doped PAni.

The morphology of PAni-CSA shows very porous structures of small agglomerated particles, not particular crystalline in appearance with a typical size of 150nm.

The morphology for PAni-p-TSA is similar to that of PAni-HCl, fibre-like with a nano-scale globular appearance, probably due to the fact that p-TSA is a small molecule and hence not an effective surfactant. The polymerisation can be then seen as a precipitation and not a dispersion one, as for PAni-DBSA/β-NSA. Z-0027 has a very porous and fibrillar structure

which is para crystalline. The fibres may contain aligned chains which are not in perfect registry and so only a single sharp peak is observed in the XRD at 3.4A° corresponding to the interchain spacing. PAni-MeSA has a mixture of two regions, the first one being agglomerated very small amorphous particles and the second phase being larger plate-like particles, apparently with low crystallinity as well, since just a few of these particles seem to have crystalline edges.

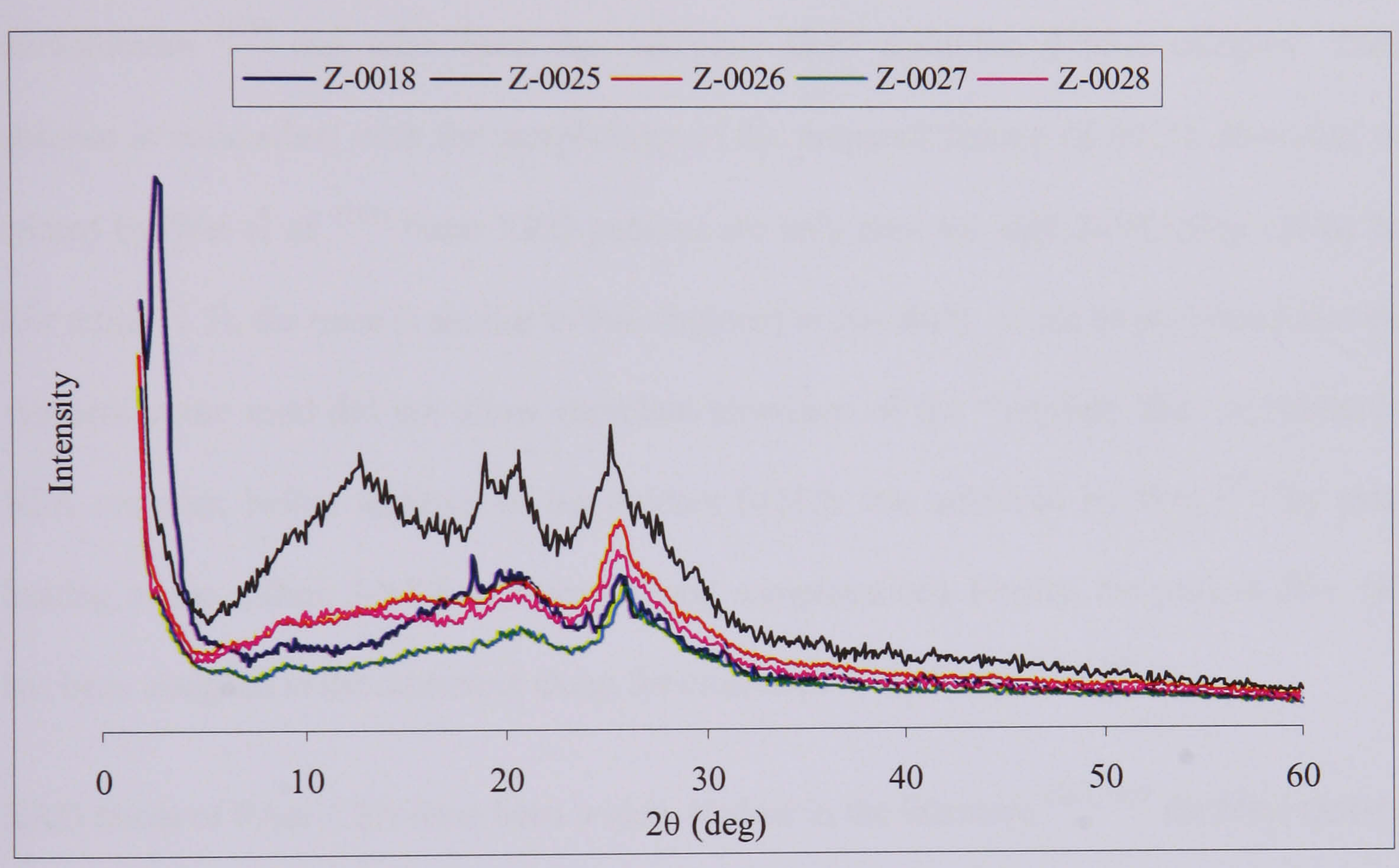


Figure 46 XRD pattern for Sulfonic acids doped PAni.

XRD patterns for these compounds are presented in Figure 46. They are in accordance with partially-crystalline polymers. It is clear from the spectra that all samples had two broad peaks at approximately $2\theta = 20^{o}$ and 25 °. the peak centred at $2\theta = 20^{o}$ was ascribed to periodicity parallel to the polymer chain and the one at $2\theta = 25^{o}$ was due to the periodicity perpendicular to the polymer chain. The amorphous background absorption centred at 25° is similar to that reported in the literature [184]. PAni-DBSA was found to have a partially crystalline structure, probably because of the bulky and anisotropic dopant present in the lattice causing some self-organisation. In addition to the common reflections, there is an

additional strong peak at $2\theta = 2.5^{o}$, which is indication of an interlayer repeat distance of alkyl tails of counter-ions that function as spacers between parallel planes of stacked PAni backbones.

The XRD pattern of PAni-β-NSA is that of a rather amorphous polymer, contrarily to reported literature [175, 181, 182] where sharp peaks were observed rising above the two main reflections centred around 20 and 25°. These sharp peaks are characteristic of PAni microtubules [175] and arise from the "template like" anilinium β-NSA complex. Their absence is concordant with the morphology of the prepared sample (Z-0025). However, as related by Wei *et al.* [181] these XRD patterns are only seen for high β-NSA:Ani ratios; for low ratios (1.5), the trace is similar to that observed in this study. It can be postulated that the synthetic route used did not allow complete formation of the "template like" anilinium β-NSA complex before addition of the oxidant (which was achieved by Wei [181] by prior heating of the aniline β-NSA mixture for total complexation). Finally, the peak at $2\theta = 12°$ has been assigned to the scattering along the orientated PAni chains [185,175].

XRD traces of PAni-CSA have been widely studied in the literature [186, 187] for films derived from EB. Intrinsically doped PAni-CSA (Z-0026) has a similar pattern to the previously reported values, with reflections having interplanar distances of 6.2, 4.6, and 3.6A° (5.9-6.1, 4.3, and 3.5A° [187, 188]). The large peaks at ca. 4.3° and 9.6° observed in films of PAni-CSA from m-cresol by Djurado [188], Rannou [161], and Winokur [189] but are not clearly seen in Z-0026. Emulsion-prepared PAni-CSA does not yield a very crystalline compound. Conductivity measurements lead us to think that in this type of preparation, CSA was not a good dopant, while it is very efficient when used as with secondary dopant (m-cresol). It could be due to the saturated structure of CSA that not offering strong interactions with the unsaturated growing polymer to effectively dope the chains in water. On the other hand,

when both the polymer and CSA are in solution in m-cresol, reaction occurs quickly and a very conductive layered structure (crystalline) is achieved.

### *4.1.4.3 PoAnis-Sulfonic Acids*

Figure 47 shows the SEM images of the PoAnis arrays prepared with different dispersing agents as dopants. It is found that the size and the morphology of PoAnis strongly depend on the kind of dopant.

The morphology of PoAnis-DBSA shows a large number of well developed fibrillar para-crystalline features protruding from a majority amorphous phase. The XRD only shows one sharp crystal peak at 3.4A$^{o}$ corresponding to the interchain packing distance in the fibril. In the case of TSA doped PoAnis, the SEM image gives the impression of several coexisting phases, one (probably of low molecular weight) with signs of crystallinity and the second like a typical amorphous thermoplastic of high molecular weight. The second phase in particular seems to show the imprint of soluble particles that may have been dissolved during the washing process. When CSA is introduced, the PoAnis product consists of a platelet structure, (typically 5-10μm in diameter and 0.5-2μm thickness), together with amorphous aggregates of globules of 1-2μm in diameter. The SEM photo suggests that the platelets are becoming very crystalline but the XRD data revealed only two crystalline peaks at $2\theta = 21^{o}$, 24.5$^{o}$ on a substantial amorphous background.

For PoAnis-NSA, the SEM image shows a porous structure, apparently made of interconnected rag-like material, the morphology resembles thin sheets of polymer with a uniform thickness of about 0.5μm but torn into random sized pieces. The layered structure may be due to the self-organising effect of the flat NSA anions, while PoAnis-MeSA morphology displays agglomerated particles with semi-porous morphology, the diameter of these particles being in the region of 150-300nm.

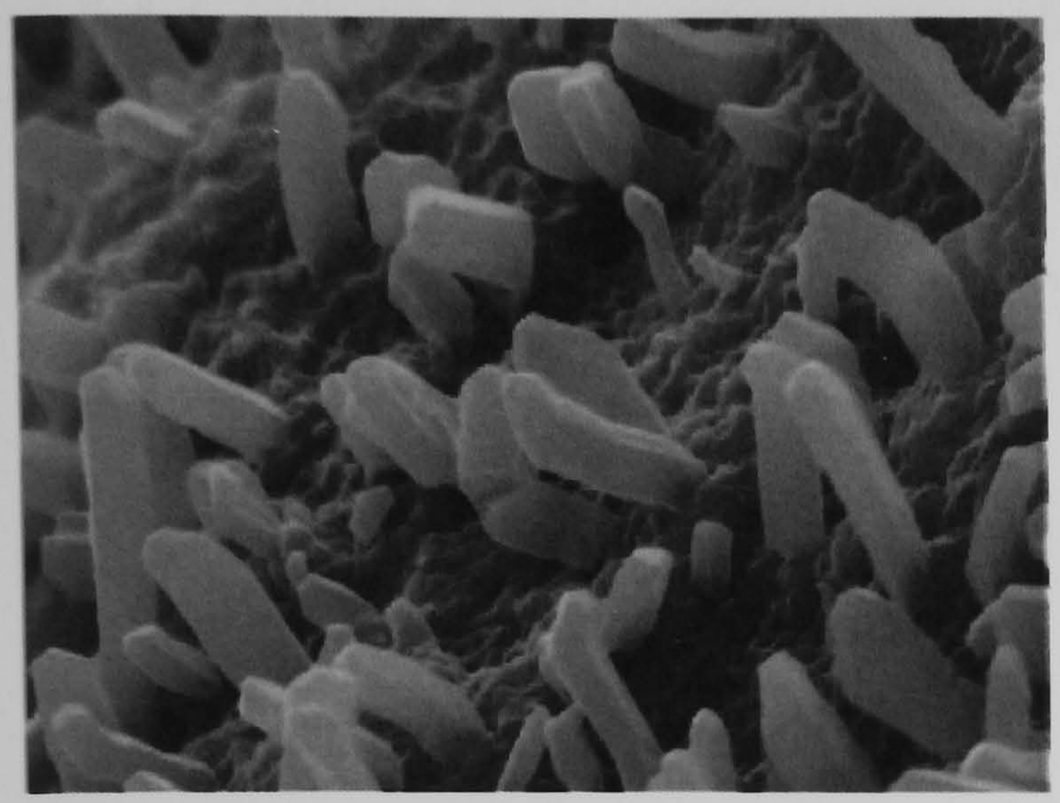

**Z-0034**, PoAnis-DBSA

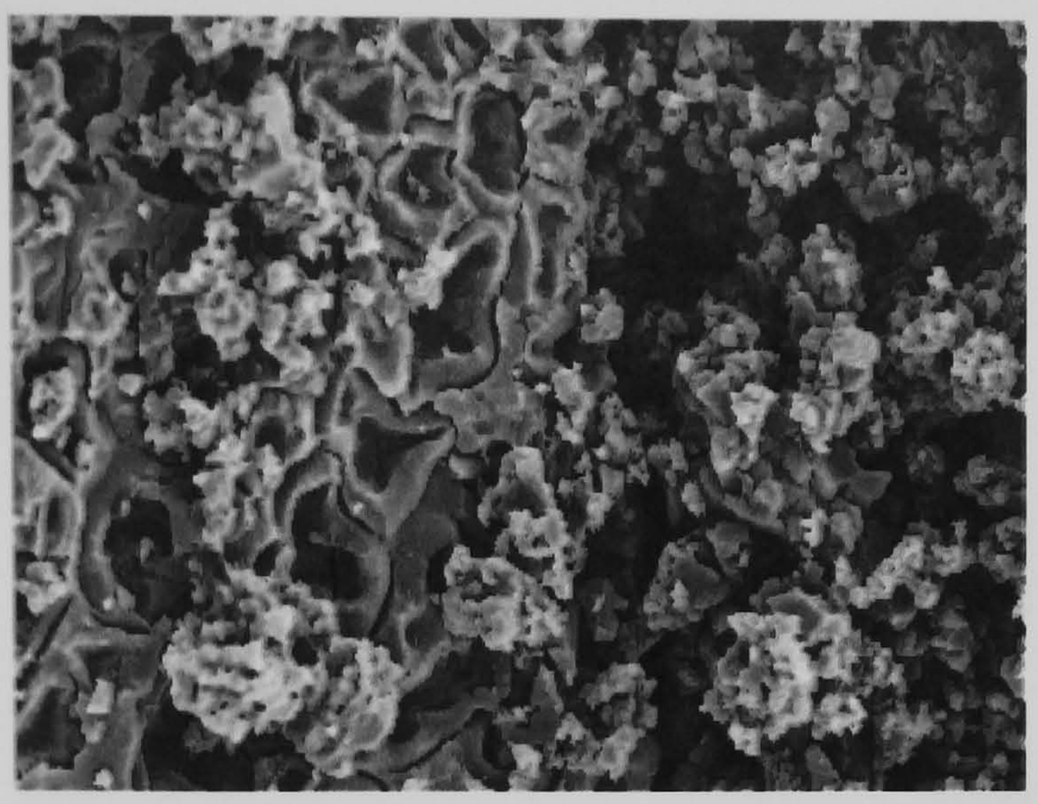

**Z-0035**, PoAnis-TSA

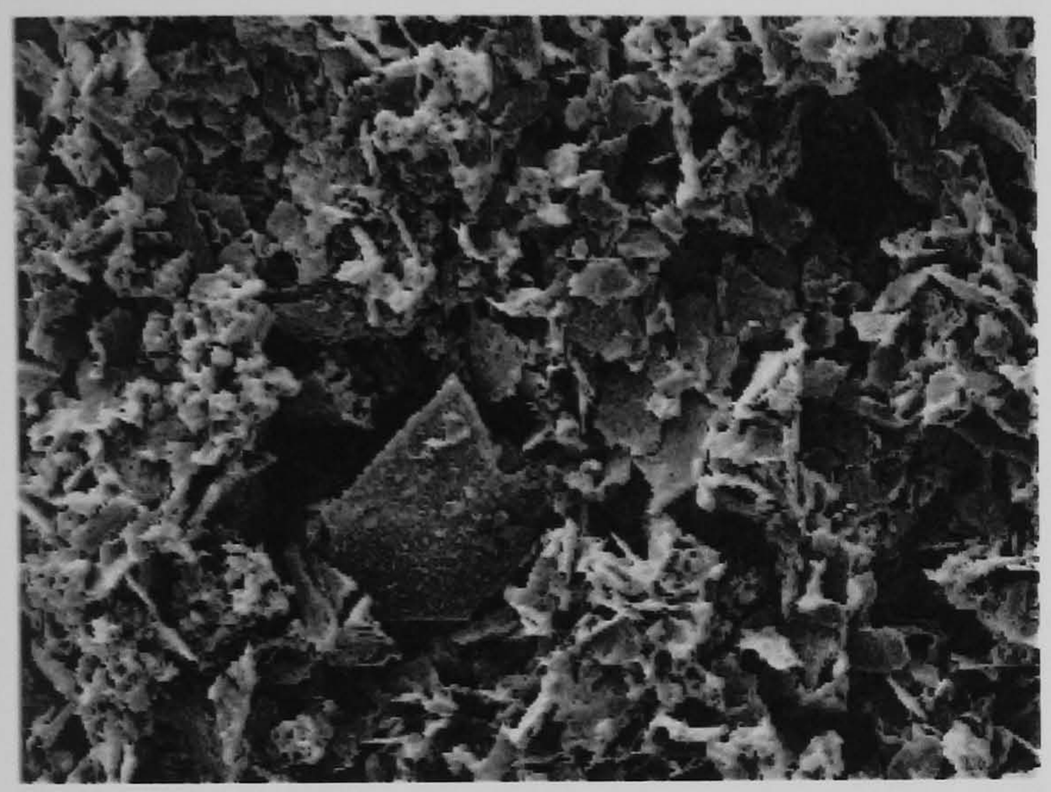

**Z-0036**, PoAnis-CSA

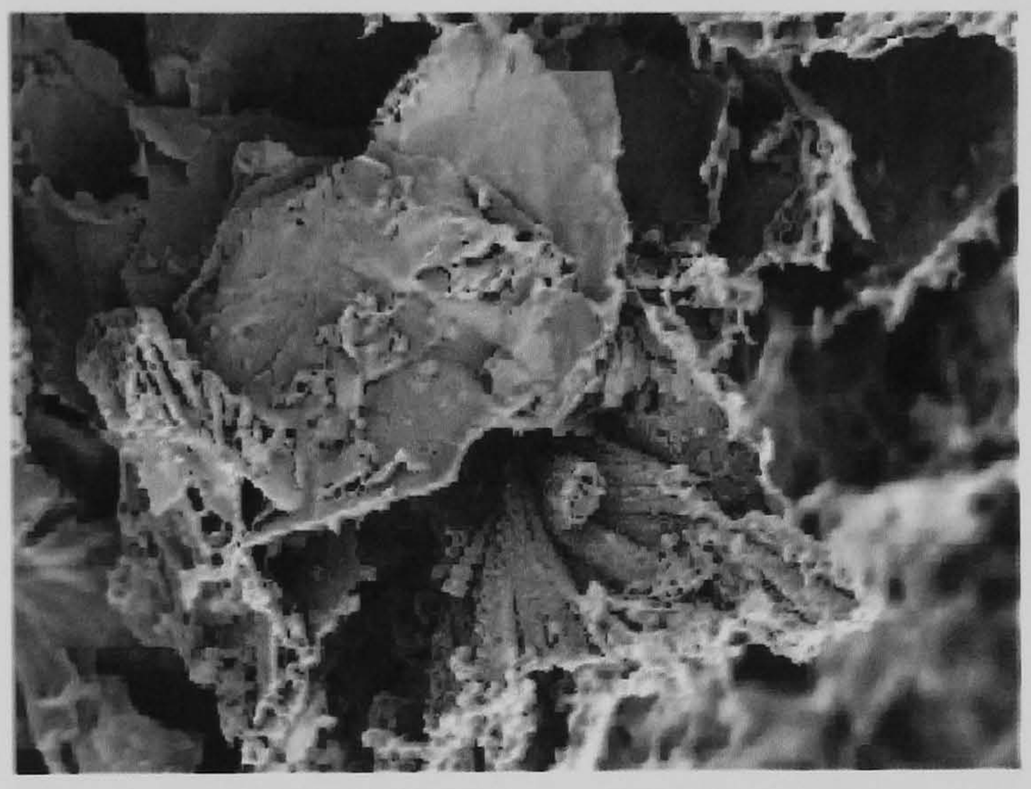

**Z-0037**, PoAnis-NSA

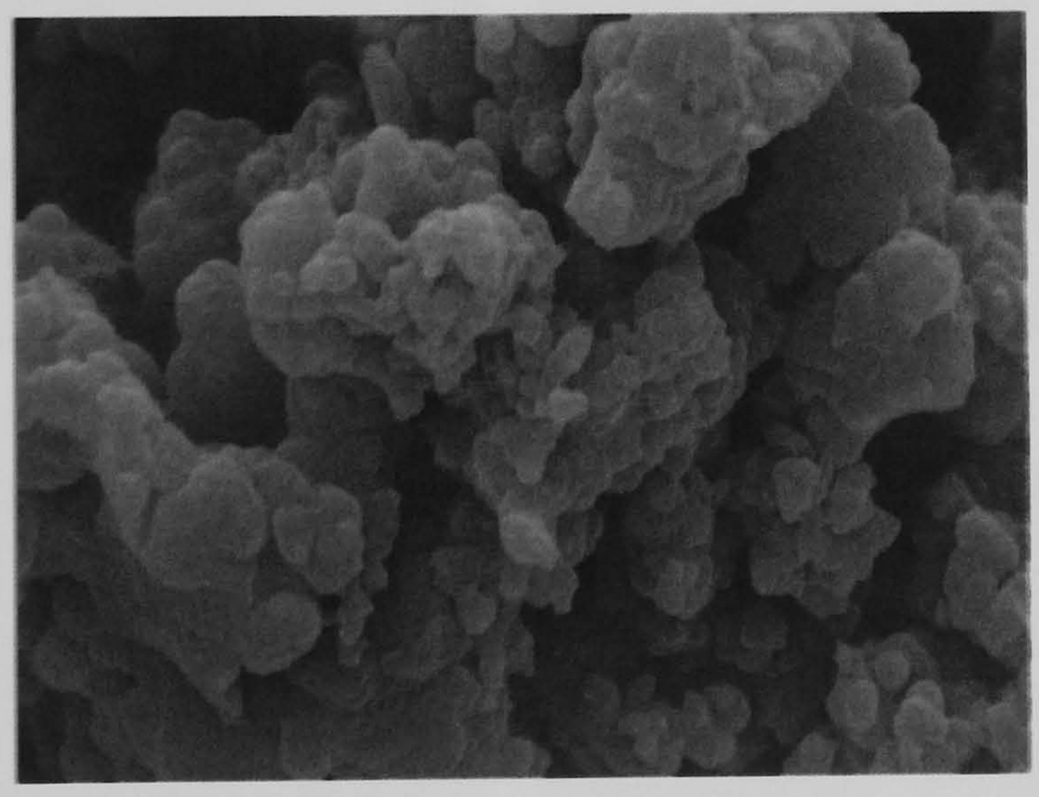

**Z-0037,** PoAnis-MeSA

Figure 47 SEM photographs for Sulfonic acids doped PoAnis.

### 4.1.4.4 *Influence of co-monomer ratio*

We present results for poly(aniline-*co*-anisidine) compounds prepared in acidic media with a Ox:Mon ratio of 0.75. Figure 48 presents SEM images of six representative samples.

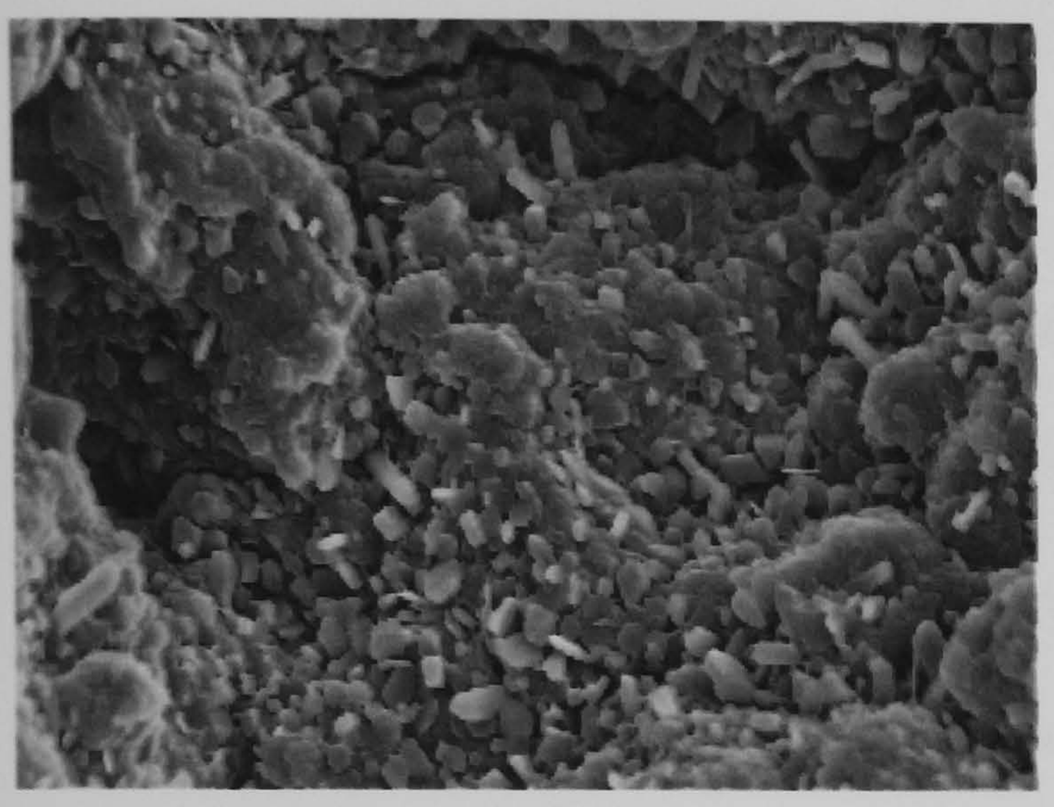

**Z-0039**, PAni:PoAnis-DBSA (50:50)

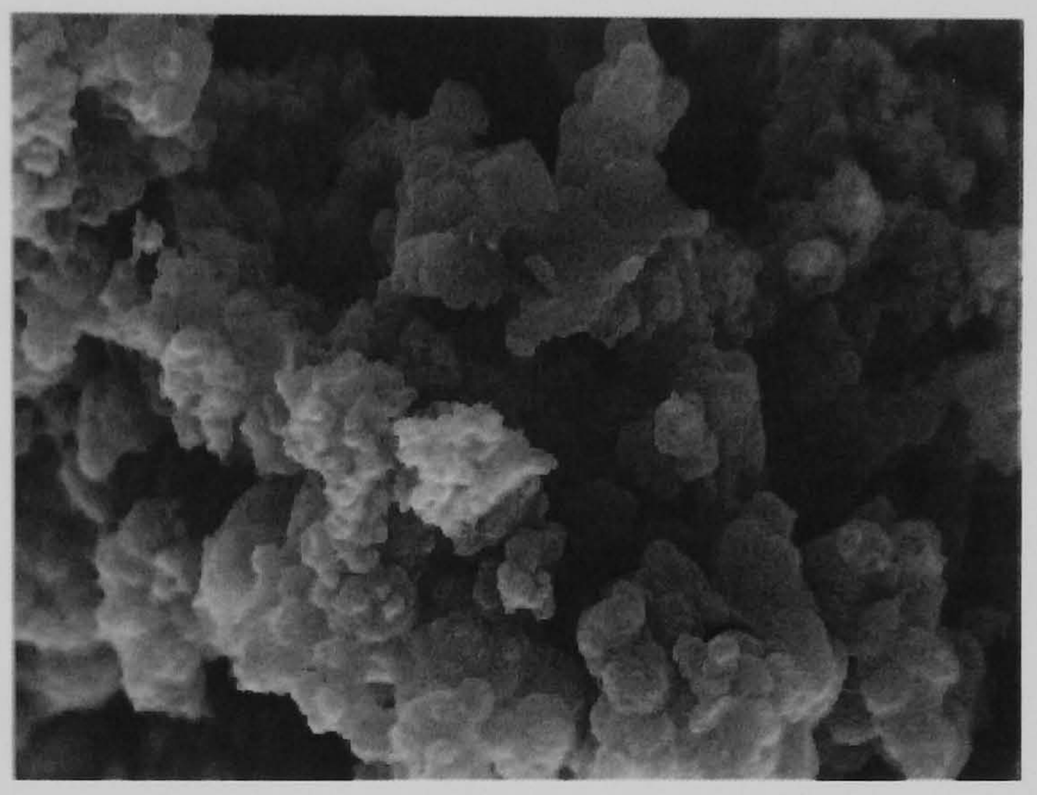

**Z-0042**, PAni:PoAnis-TSA (50:50)

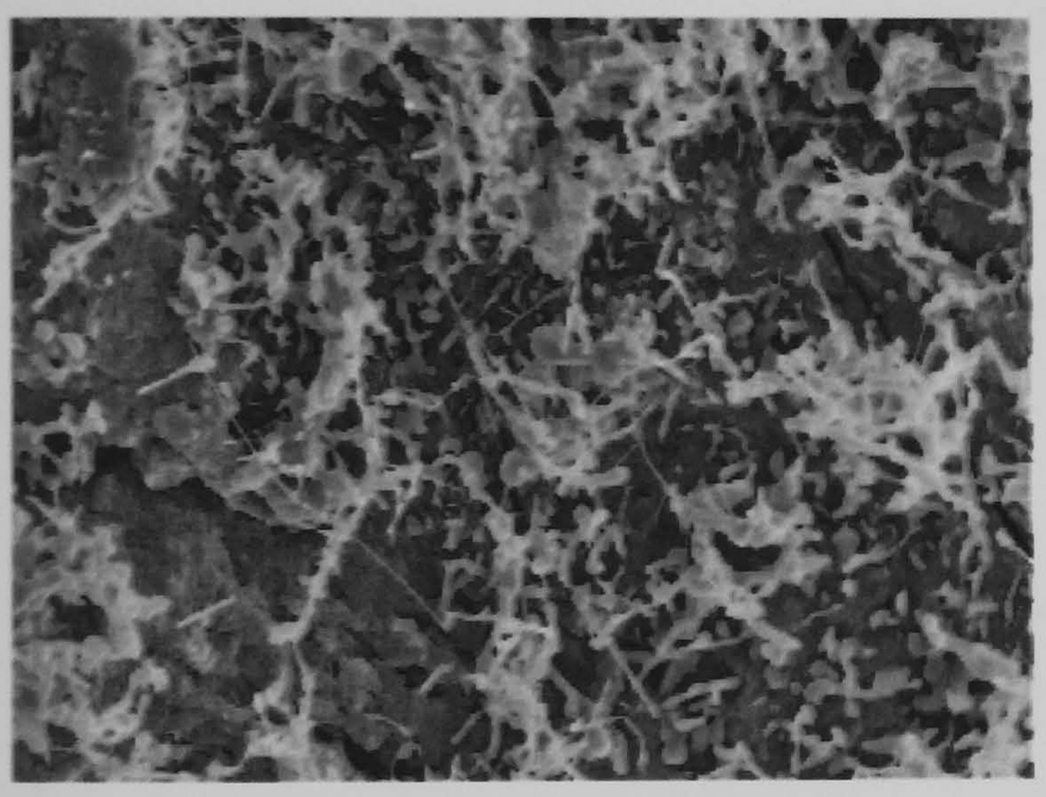

**Z-0044**, PAni:PoAnis-DBSA (75:25)

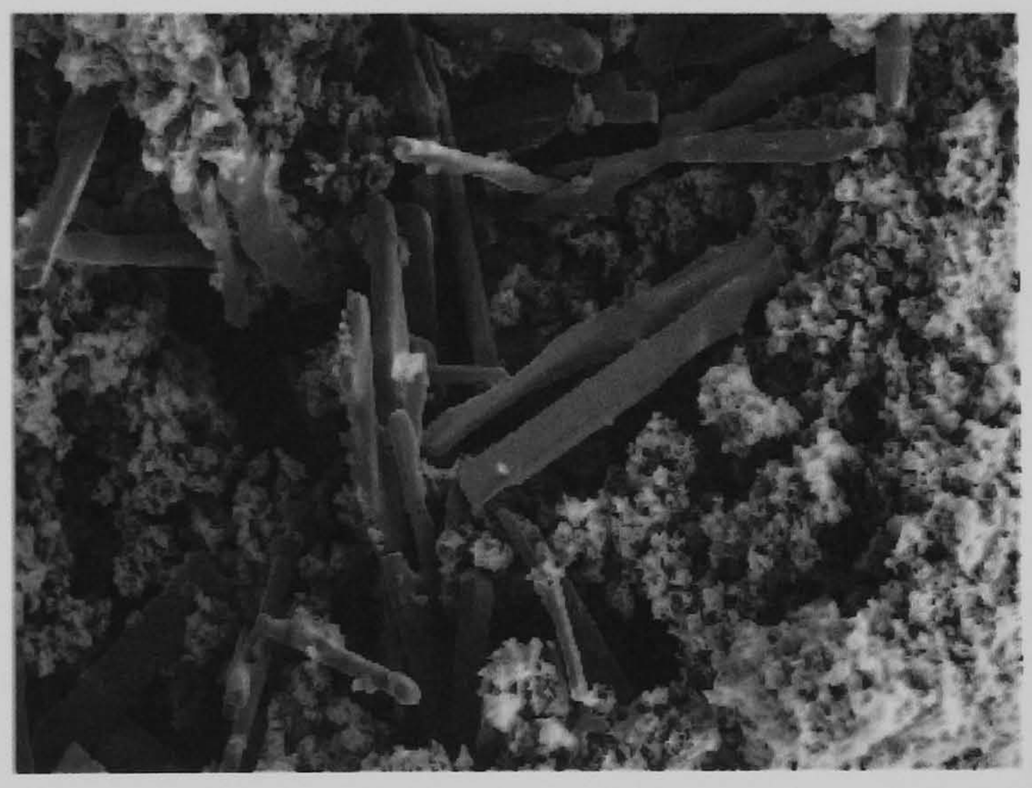

**Z-0047**, PAni:PoAnis-TSA (75:25)

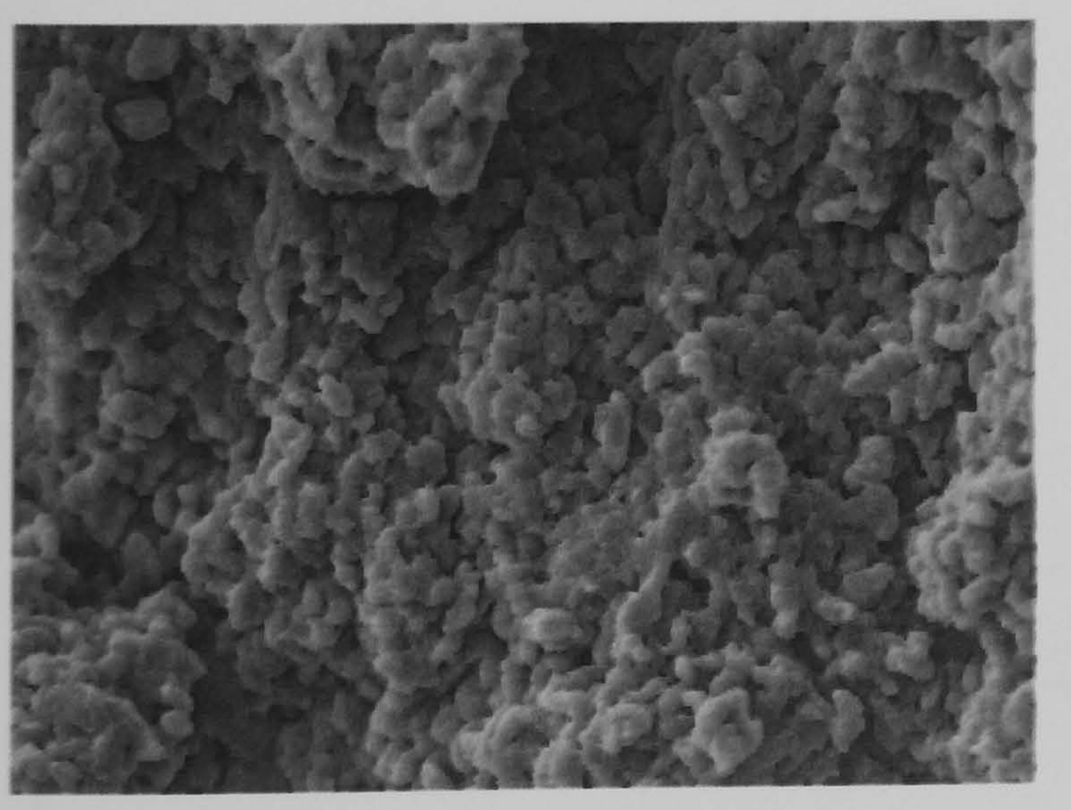

**Z-0049,** PAni:PoAnis-DBSA (25:75)

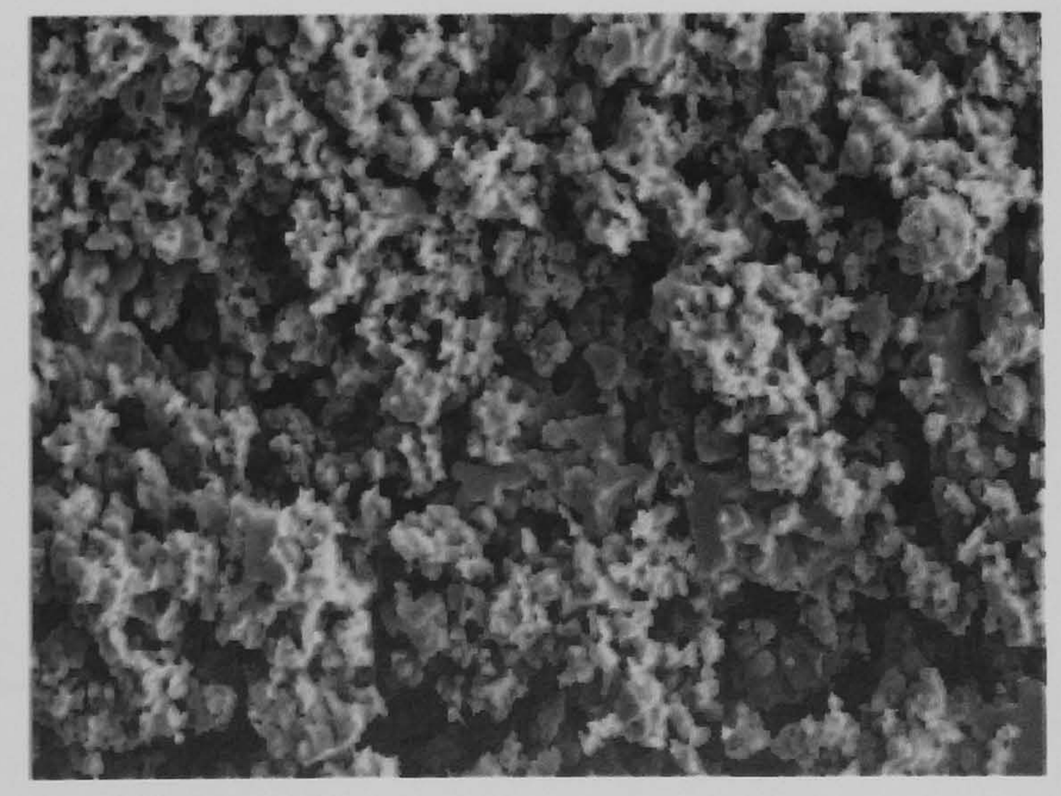

**Z-0052,** PAni:PoAnis-TSA (25:75)

Figure 48 Poly(aniline-*co*-anisidine) at different molar ratios SEM observation.

The morphology of Z-0039 consists of a majority phase with a compact amorphous structure and a crystalline phase consisting of well-developed prismatic crystals (3-5μm long and 1-2μm in diameter). XRD shows a few sharper lines due to this crystalline phase.

At a ratio (75:25) of Ani:Anis, the product is composed of an entangled network (Ø ~ 50nm) which contains short fibres with large beads like small tadpoles. When the ratio (25:75) of Ani:Anis is introduced, the copolymer is netlike with an interpenetrating structure. Indeed, the morphology of Z-0049 shows a compact structure with partly-developed crystallinity. There are relatively few well-formed crystals, but the XRD diffractogram shows sharp peaks at $2\theta = 25^{o}$ corresponding to the interchain packing.

It is found that the copolymer prepared with varying amounts of aniline using DBSA as a dopant exhibit different morphologies, which leads to the conclusion that the process of aggregation is different in all cases, and primarily related to the co-monomeric interactions more than the DBSA ones.

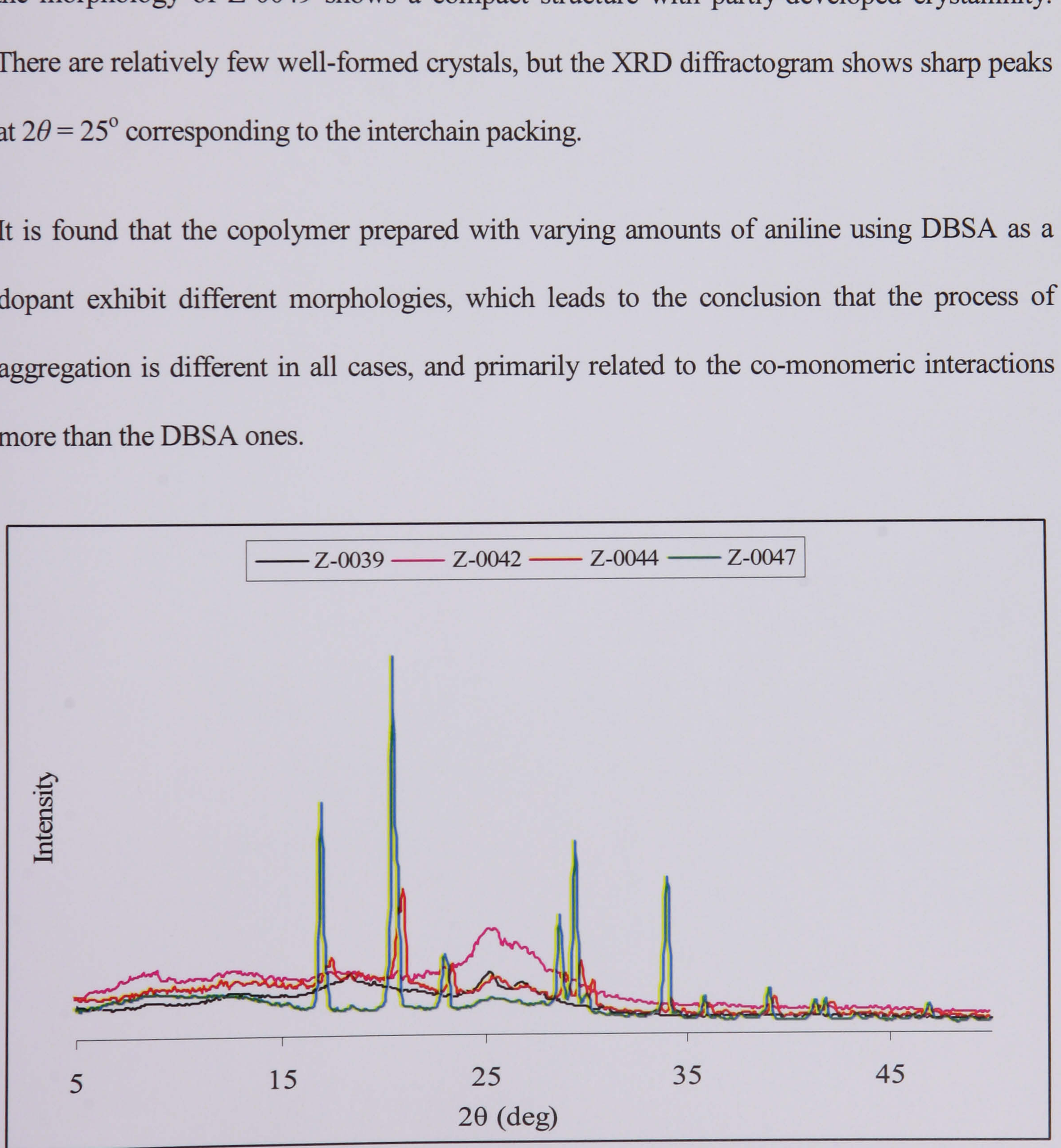


Figure 49 XRD pattern for samples of DBSA or TSA doped poly(aniline-co-anisidine).

The morphology of PAni:PoAnis-TSA (which was prepared at a ratio of Ani:Anis 75:25) is composed of dense crystalline rods about 3-10μm in diameter and length up to 70μm, which appears to form a majority phase. They almost certainly account for the strong crystalline peaks in the XRD, whereas the amorphous background is probably associated with the loose porous structure in the SEM. At a ratio (25:75) of Ani:Anis, the product Z-0052 shows of a two-phased amorphous structure, one phase being very loose and porous and the other dense and glassy.

## 4.2 Polymeric Blends

### 4.2.1 Conductive Polyaniline/Poly (Epichlorohydrin-co-Ethylene Oxide) Blends

#### *4.2.1.1 Solubility and Miscibility*

In order to achieve a good miscibility between PAni salt and a solvent, their solubility parameters clearly have to be comparable; the solubility parameter for THF is 20.3 $(J.cm^{-3})^{1/2}$ [190], whereas that calculated for PAni-DBSA is 20.8 [191]. The values are similar, so it is expected that PAni-DBSA would be soluble in THF. For Hydrin®, the solubility parameter is 19.9, which indicates that it is also quite compatible with PAni-DBSA.

In this study, determination of solubility parameters $\delta_p$ was based on the smallest repeat unit of each polymer. The solubility parameters of the polymers (elastomer and conducting polymer) are affected by variations in their chemical constituents such as the number of crosslinks and the distribution of chain branches or substituent groups along the polymer backbones. In this work, the group contribution method [192] was applied to estimate the solubility parameters of polymers using the equation below:

$$\delta_p = \rho(\ \sum F_i\ )/M_o$$

where $\rho$ is the density, $M_o$ is the formula weight of the polymer repeat unit and $\sum F_i$ is the sum of all groups' molar attraction constants in the polymer repeat unit. The structure of PAni-DBSA is represented as follows:

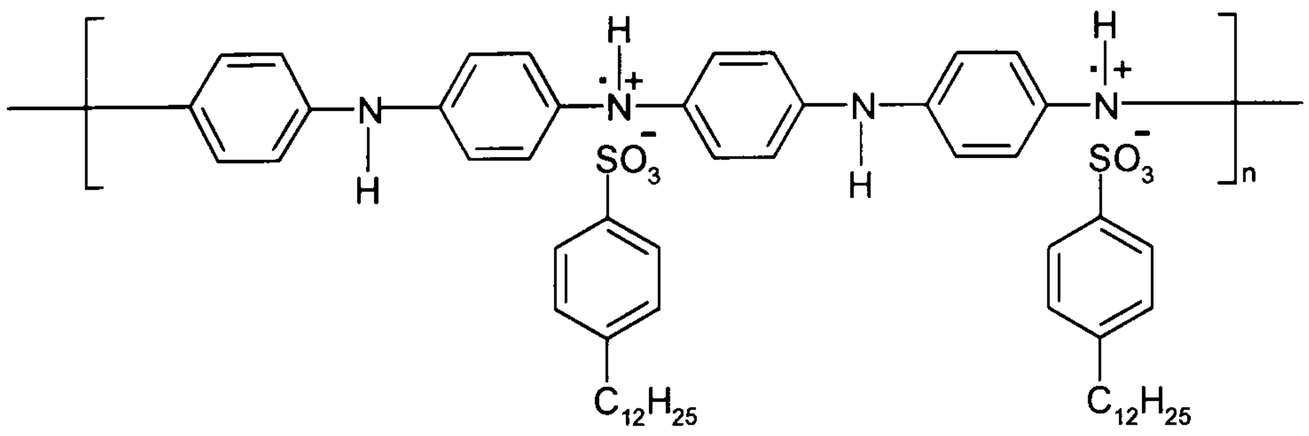


Figure 50 Structure of PAni-DBSA.

| Group | Molar attraction constant (Fi) | No. of each group | Total of group molar attraction constant (ΣFi) |
|---|---|---|---|
| 6C ring | -48 | 6 | -288 |
| -CH= aromatic | 239 | 20 | 4780 |
| >C= aromatic | 200 | 10 | 2000 |
| -CH= olefin | 249 | 4 | 996 |
| >C= olefin | 173 | 2 | 346 |
| -CH3 | 303 | 2 | 606 |
| -CH2- | 269 | 22 | 5918 |
| -OH | 462 | 2 | 924 |
| -O- epoxide | 360 | 4 | 1440 |
| -NH- | 368 | 2 | 736 |
| >N- | 125 | 2 | 250 |
| -S- | 428 | 2 | 856 |

Table 29 The number of functional groups present in PAni-DBSA and the corresponding molar attraction constants.

$\Sigma F_i$ of PAni-DBSA = 18564 $(J.cm^3)^{1/2}.mol^{-1}$; PAni-DBSA smallest repeat unit molecular weight = 1014 $g.mol^{-1}$; PAni-DBSA density (measured for pressed pellet) = 1.135 $g.cm^{-3}$.

Therefore using the equation above

$\delta\rho = (1.135 \times 18564) / 1014$ , $\delta\rho = 20.8\ (J.cm^{-3})^{1/2}$ or $20.8\ (MJ/m^{-3})^{1/2}$

The structure of Epi-EO is composed of the following groups

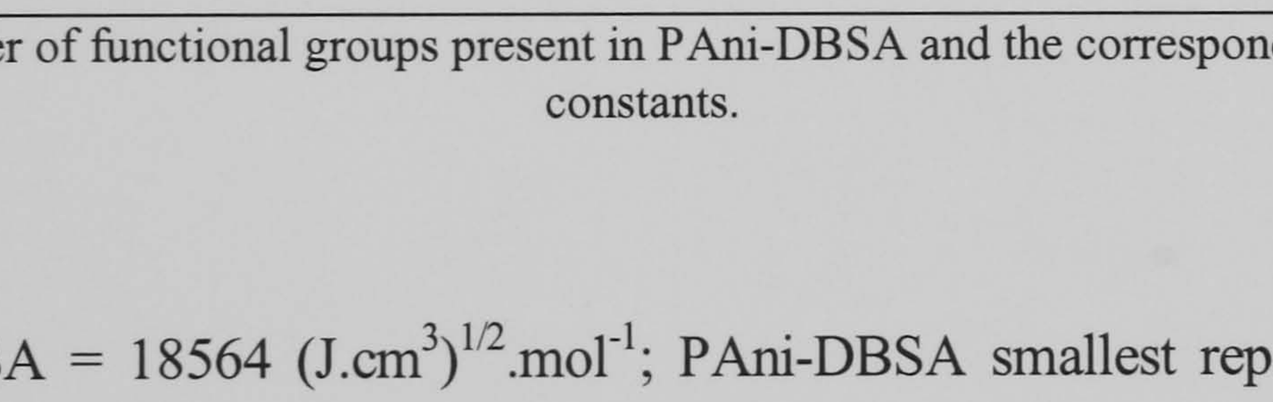


Figure 51 Poly(Epichlorohydrin-*co*-Ethylene Oxide) (Epi-EO).

| Group | Molar attraction constant (Fi) | No. of each group | Total of group molar attraction constant ($\Sigma F_i$) |
|---|---|---|---|
| -CH2 | 269 | 4 | 1076 |
| -CH | 176 | 1 | 176 |
| -O- ether | 235 | 2 | 470 |
| -Cl primary | 419 | 1 | 419 |

Table 30 The number of functional groups present in Epi-EO and the corresponding molar attraction constant.

$\Sigma F_i$ of Epi-EO = 2141 $(J.cm^3)^{1/2}.mol^{-1}$; Epi-EO smallest repeat unit molecular weight = 136.5 $g.mol^{-1}$; Epi-EO density (measured from a pressed pellet) = 1.270 $g.cm^{-3}$.

Therefore using the equation above:

$\delta_\rho = (1.270 \times 2141) / 136.5$, $\delta_\rho = 19.9\ (J.cm^{-3})^{1/2}$ or $19.9\ (MJ.m^{-3})^{1/2}$

### 4.2.1.2 Composition Dependence of the Electrical Conductivity of Rubber Blends

The dependence of electrical conductivity of various polyaniline blends on their PAni-DBSA content is illustrated in Figure 52. The conductivity of these films depended strongly on their composition. Pure Hydrin® rubber had insulating behaviour ($\sigma = 2 \times 10^{-10}$ S.cm$^{-1}$), but it was possible to obtain blends with greatly increased conductivities.

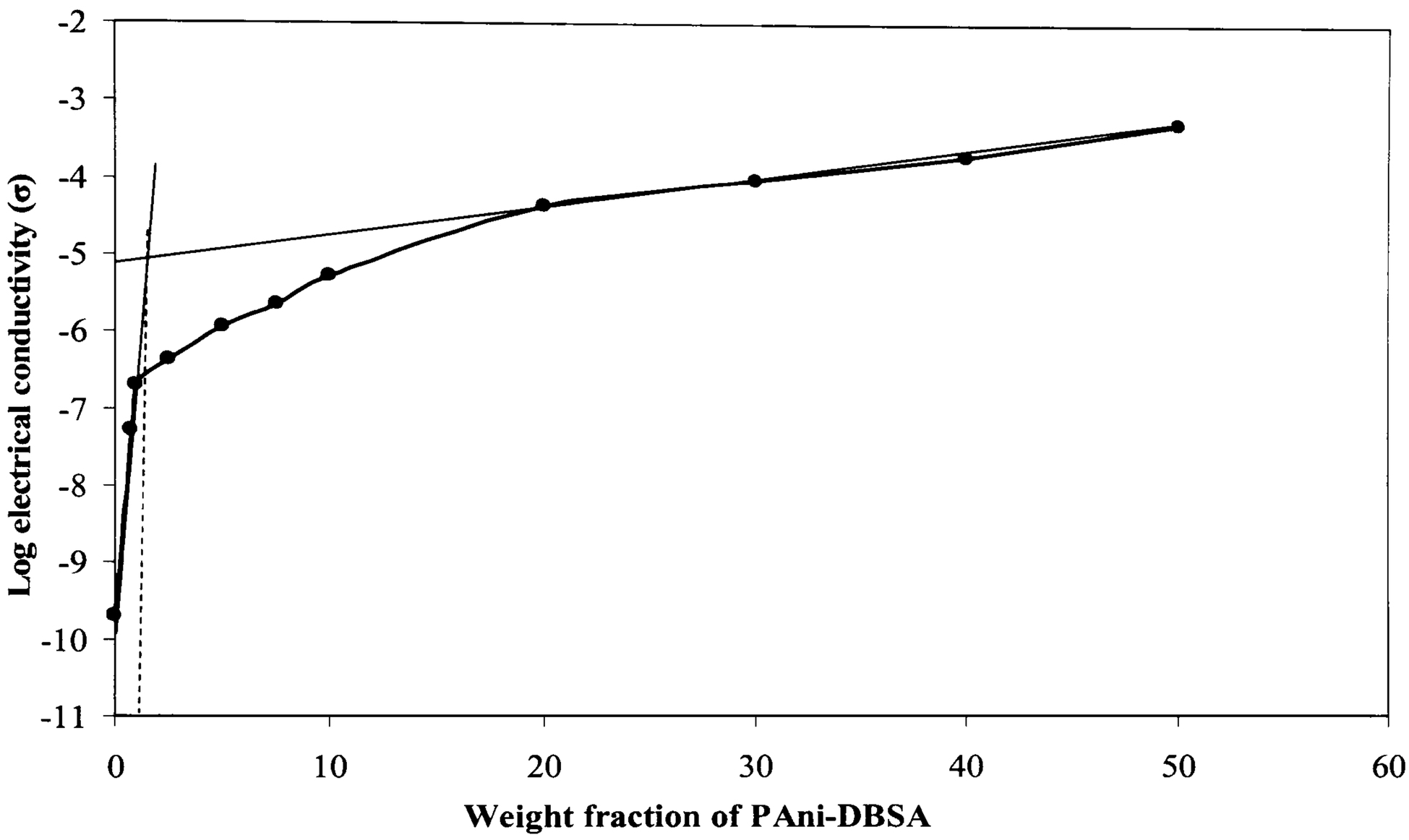


Figure 52 Variation of the electrical conductivity (σ) as function of PAni-DBSA content in the blend.

For blends containing 50% (w/w) of PAni-DBSA, conductivities of $5 \times 10^{-4}$ S.cm$^{-1}$ were obtained. These results are similar to those reported in the literature for comparable blends of polyanisidine and polyurethane [193].

The above results can be analysed in terms of standard percolation theory [194]. In accordance with the theoretical studies for spherical filler particles, the percolation threshold for bulk conduction occurs when the conductive filler occupies about 16% (v/v) of the volume in the mixture. Figure 52 shows a percolation threshold with 1% (w/w) [or 1.1% (v/v)] the electrical conductivity increases 1000 times , which may be due to the formation of an

interpenetrating network [195]. This indicates that the percolation threshold is at least 14 times smaller than that predicted for a spherical filler. The data presented in Figure 52 were found to fit to a simple percolation model as described below:

$$\sigma_f = c\,(f - f_p)^t$$

Where c is a constant, $t$ the critical exponent, $f$ the volume fraction of the conductive medium and $f_p$ the volume fraction at the percolation threshold.

By fitting the experimental data to a plot of log σ versus log ($f$-$f_p$), values of 1.1% (v/v) for $f_p$ and 2.4 for $t$ were obtained with a correlation coefficient (R) of 0.99. The conductivity of PAni-DBSA blends reached high values at PAni-DBSA concentrations close to 20% wt.

### *4.2.1.3 Thermal Analysis*

Thermogravimetric Analysis (TG)

In Figure 53, the thermogravimetric curves under $N_2$ atmosphere for pure PAni-DBSA, pure Hydrin® rubber and their blends are compared. The PAni-DBSA curve shows a small, intial mass loss (5%) at 90°C which could be assigned to the evaporation of small molecules such as water and solvent molecules, and a larger mass loss at 200-400°C (approximately 53%), attributable mainly to dopant loss and the beginning of main chain degradation [140, 165] . Above these temperatures, polyaniline shows a slower mass loss process assigned to main chain degradation. At 600°C, the polymer leaves a residue of about 29%, corresponding to heavily crosslinked materials. The curve for Hydrin® shows a large mass loss at 300-370°C (approximately 92%), corresponding to dehydrochlorination and polyether scission. At 600°C Hydrin® leaves a residue of 4%, probably largely carbonised material.

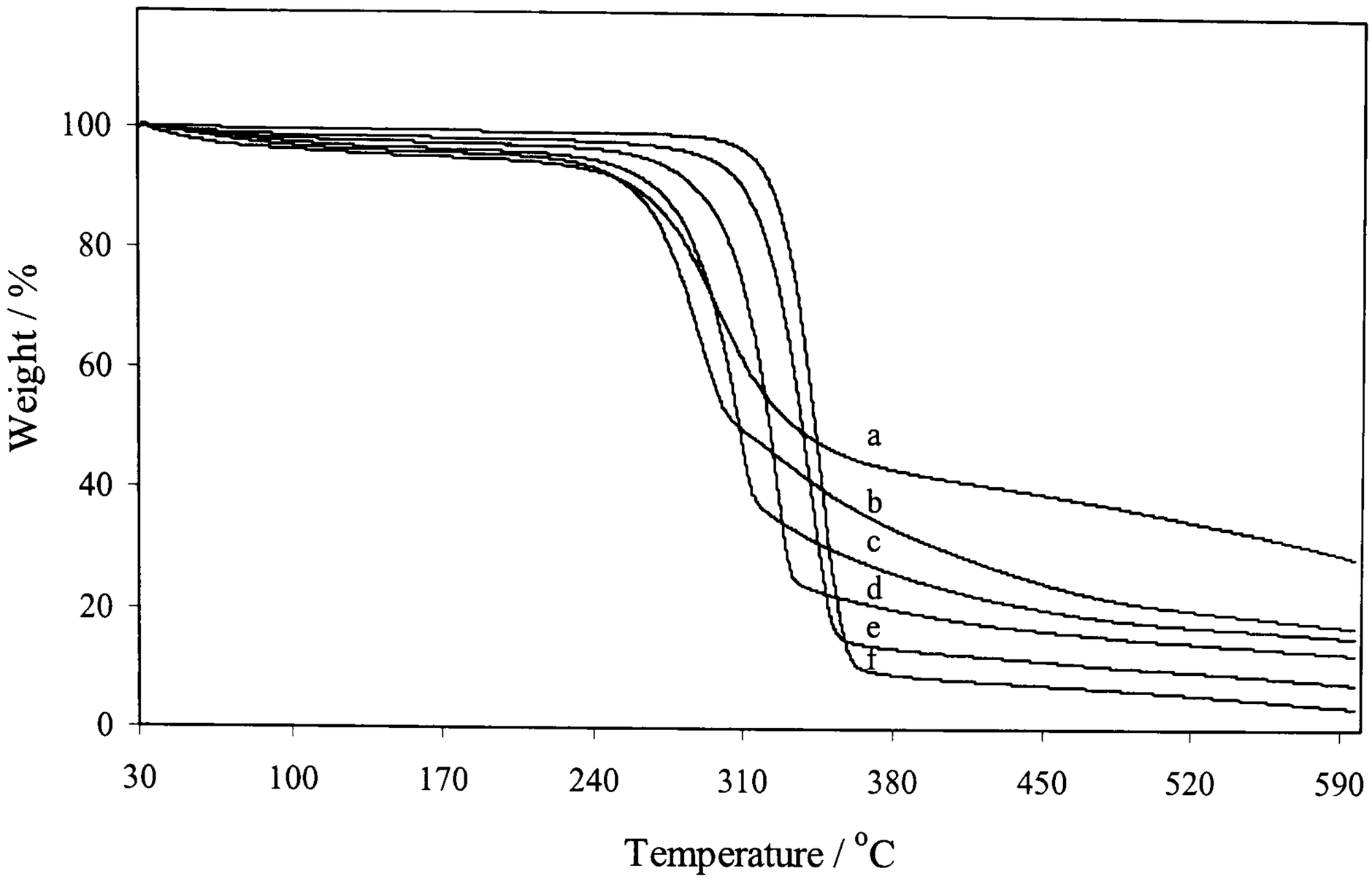


Figure 53Thermogravimetric curves at a heating rate of 10°C/min under $N_2$ for (a) pure PAni-DBSA, for blends containing (b) 50%, (c) 33.3%, (d) 20%, (e) 10% (w/w) of PAni-DBSA and (f) pure Hydrin®.

Different weight losses were observed, depending on the composition of the blends. Comparing the TG curves of blends containing 20 and 33.3% (w/w) of PAni-DBSA with those of pure Hydrin® and a blend containing 10%, it is possible to observe that these curves show a mass-loss process corresponding to the Hydrin® chain degradation at lower temperature: 290-355 °C in the blend containing 10% (w/w) PAni-DBSA compared to 280-335°C and 270-320°C for the blends containing 20 and 33.3% (w/w) of PAni-DBSA respectively. This indicates that the Hydrin® matrix hindered the degradation and evaporation of the dopant and therefore retarded the dedoping process.

## Differential Scanning Calorimetry (DSC)

Figure 54 represents the DSC thermograms for pure PAni-DBSA, pure Hydrin® and their blends. They show a decrease in the onset decomposition temperature of Hydrin® upon blending from 369°C to 348, 329 and 315 °C respectively, for the blends containing 10%, 20%, 33.3% (w/w) of PAni-DBSA. The blend PAni-DBSA/ Hydrin® 1:1 (w/w), Hydrin® does not exhibit a decomposition temperature. This means that conductive polyaniline encourages degradation for this material when there is sufficient dopant to promote scission in the elastomer chains, thereby accelerating the degradation process. No melting peak was observed for the conductive polymer.

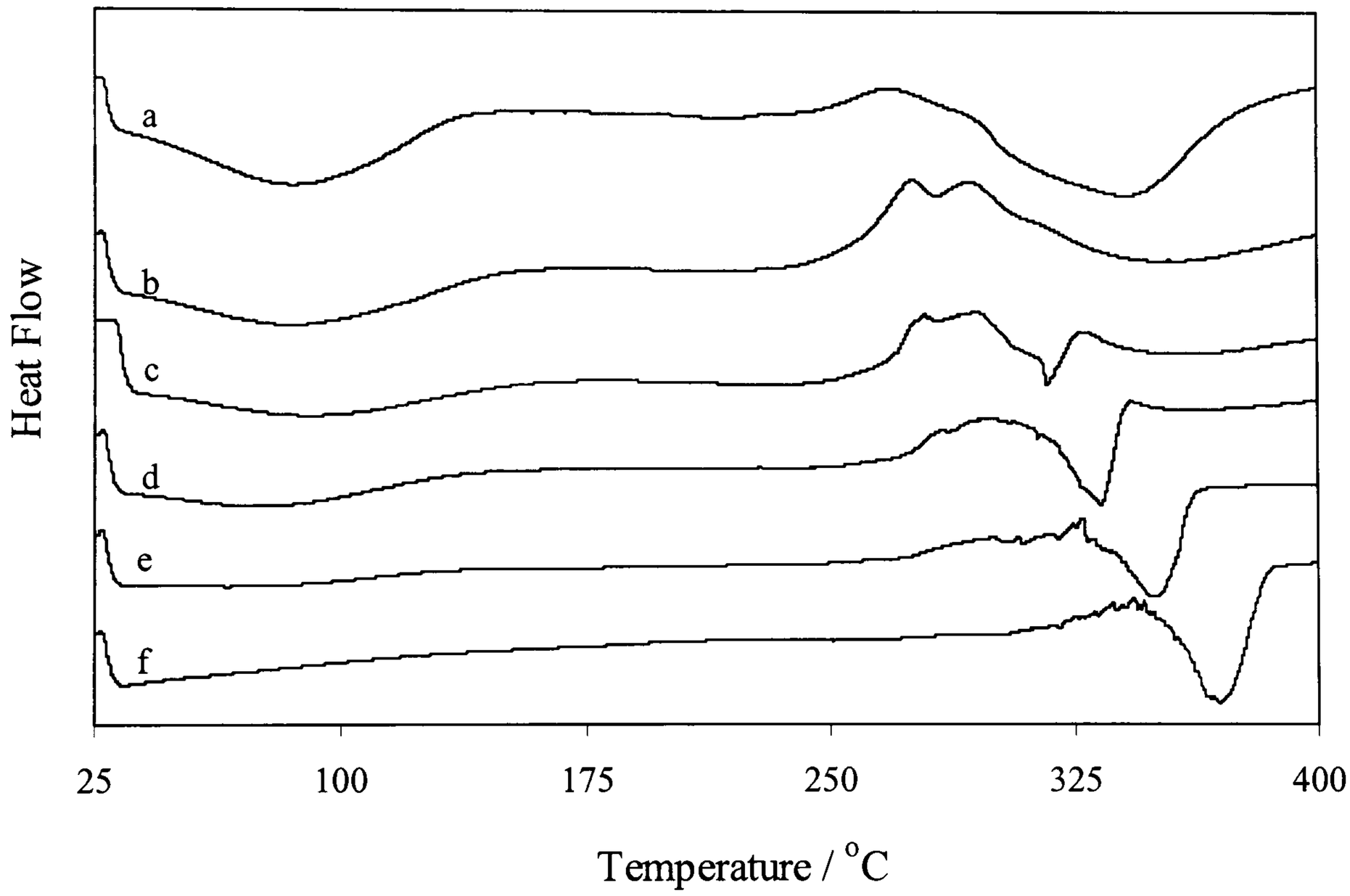


Figure 54 DSC thermograms ($10^{o}C.min^{-1}$, under $N_2$) of (a) pure PAni-DBSA, blends containing (b) 50%, (c) 33.3%, (d) 20%, (e) 10% (w/w) of PAni-DBSA and (f) pure Hydrin® rubber (C2000L).

The observed decrease in the decomposition temperature is consistent with some degree of miscibility of PAni-DBSA with Hydrin®. TGA analysis supports the DSC results.

### 4.2.1.4 *Infrared Spectroscopy*

ATR spectra obtained from pure Hydrin® C2000L and pure PAni-DBSA are shown in Figure 55 (a) and (b), respectively.

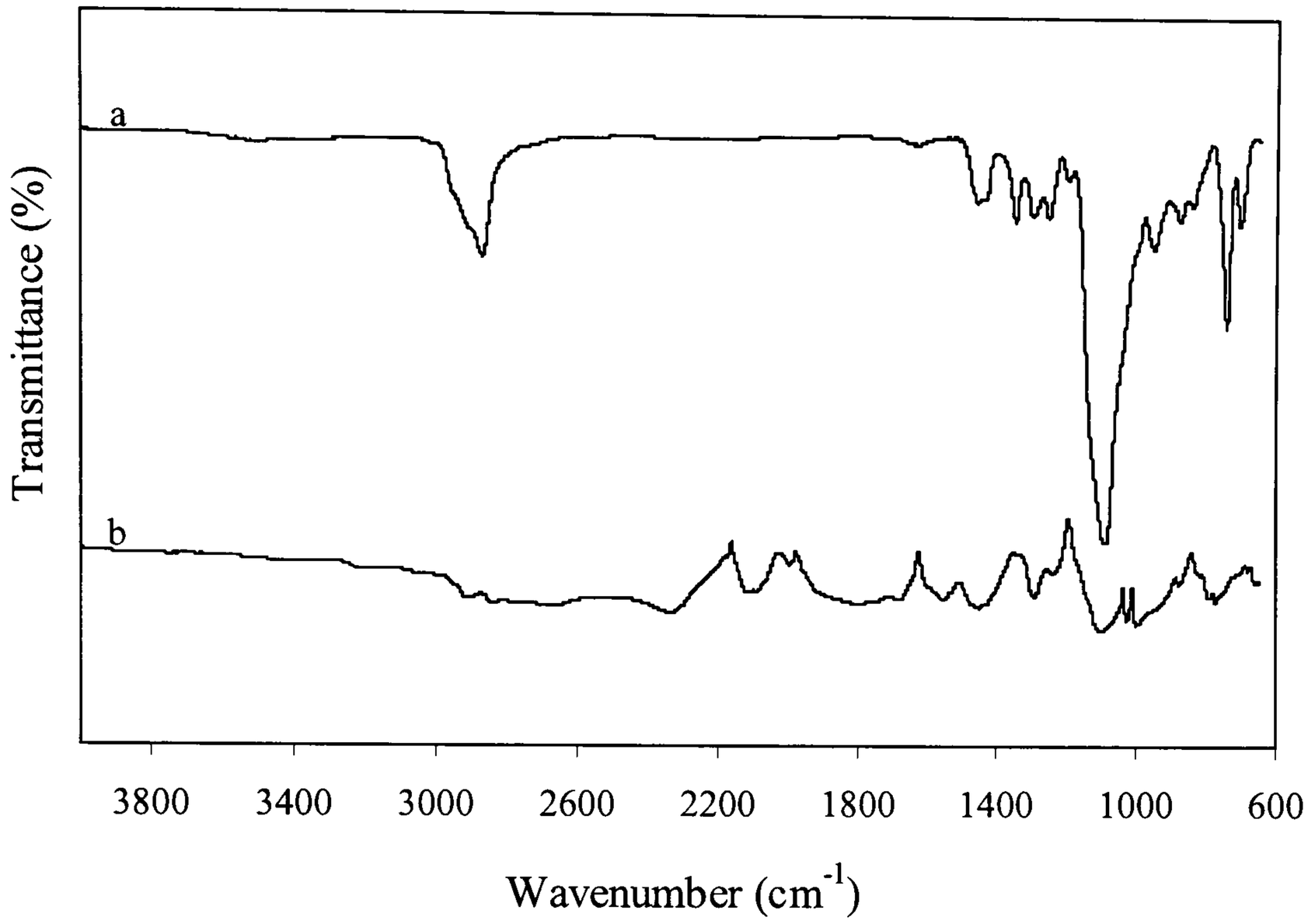


Figure 55 Infrared spectra of (a) pure Hydrin® and (b) pure PAni-DBSA.

The presence of quinoid and benzenoid vibrations indicates the emeraldine state of PAni. The band at 790cm$^{-1}$ was attributed to the out-of-plane bending of C-H and the 878cm$^{-1}$ band was considered to be evidence of the formation of para-linked polyaniline. Vibrational bands at 1000 and 1027cm$^{-1}$ correspond to the S=O stretching vibration. The band around 1102cm$^{-1}$, referred to as an electronic band by MacDiarmid and co-workers [152], was considered a measure of the degree of electron delocalisation in the polymer chain. The peak seen at 1291cm$^{-1}$ with the pronounced appearance of a shoulder at 1242cm$^{-1}$ [89] for C-N$^{+}$ stretching, is linked to conductivity. PAni-DBSA shows bands at 1451 and 1558cm$^{-1}$ and they can be attributed to the stretching vibration of the N-B-N and N=Q=N rings respectively [139]. The band at 2112cm$^{-1}$ was assigned to the overtones of C-H (out of plane) bending. The peak at

2916cm$^{-1}$ corresponds to aliphatic C-H stretching. Peaks in the region of 3212 and 3408cm$^{-1}$ are associated with N-H stretching, while the one at 2660cm$^{-1}$ is due to the iminium cation [138].

The IR spectrum of pure Hydrin® in Figure 55 (a) shows a band at 742cm$^{-1}$ due to C-Cl stretching. The band at 1088cm$^{-1}$ is assigned to C-O-C stretching, and peaks at 1253, 1296, 1347 and 1458cm$^{-1}$ correspond to aliphatic -$CH_2$- bending. The band at 2870cm$^{-1}$ is due to aliphatic -CH- stretching.

Figure 56 shows the IR spectra for PAni-DBSA/ Hydrin® blends. As can be seen from the spectra, the intensity of the C-Cl band decreases as the percentage of PAni-DBSA increases.

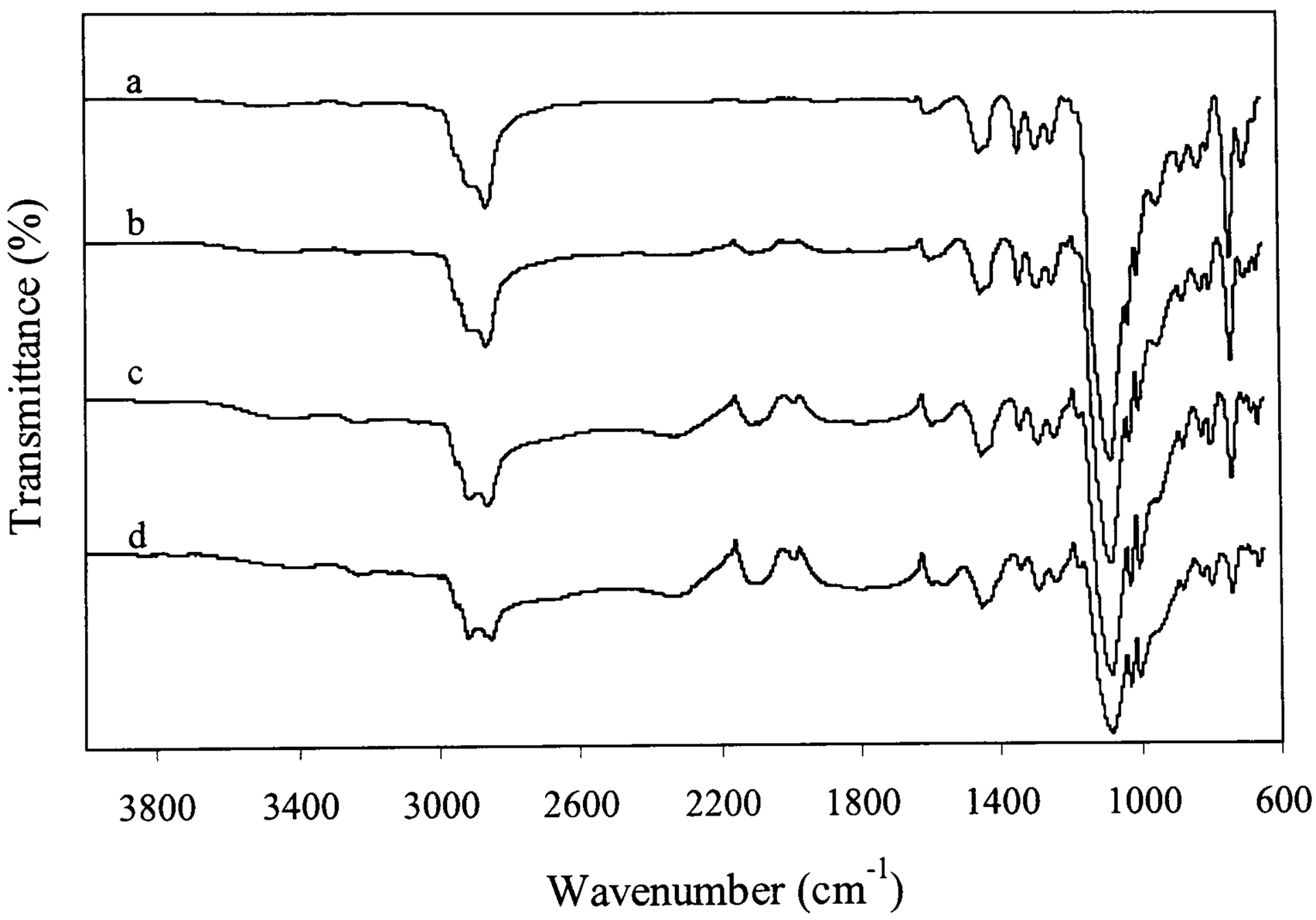


Figure 56 Infrared spectra of (a) PAni-DBSA/Hydrin® blends of the (a) 10%, (b) 20%, (c) 33.3% and (d) 50% (w/w) of PAni-DBSA.

The intensity of the S=O stretching bands occurring at 1000 and 1027cm$^{-1}$, which are characteristic of PAni-DBSA, noticeably increase as the percentage of PAni-DBSA increases in the polymer blend. The -CH- stretching vibration for the rubber was observed at 2870cm$^{-1}$.

With the initial addition of 10% of PAni-DBSA to the Hydrin®, one observes the emergence of individual -CH- aliphatic peaks comprising a well-defined band at 2870cm$^{-1}$ and a noticeable shoulder at 2912cm$^{-1}$. It is clear from the spectra that as the PAni-DBSA content increases, the shoulder becomes more defined, and the intensity of the N-H band at 3212-3233cm$^{-1}$ increases. Greater proportions of Hydrin® in the blend caused an increasing shift of the N-H stretching band position to a higher wavenumber. This is likely to have been caused by a reduction in hydrogen bonding between adjacent PAni-DBSA chains as it became more dispersed in the rubber.

### *4.2.1.5 Electronic (UV-Visible) Spectroscopy*

During the mixing of PAni-DBSA and Hydrin®, the colour of the blends remained green, indicating that PAni-DBSA remained in its doped state. In order to prove this, UV-Vis spectra of PAni-DBSA/Hydrin® blends were obtained, and compared with spectra of pure PAni-EB and PAni-DBSA. For the base polymer, N-methylpyrrolidone (NMP) was used as solvent and reference, while THF was used for the doped polymer. Figure 57 shows the UV-Vis spectra of the emeraldine base and PAni-DBSA solutions. In the EB spectrum (Figure 57) two characteristic bands were observed: one at 326nm due to the $\pi - \pi^*$ transition of the benzenoid ring and another at 628nm, corresponding to an $n - \pi^*$ transition between the HOMO of the benzenoid ring and the LUMO of the quinoid ring [196].

For the doped polymer (PAni-DBSA), the peak at 330nm was shifted to 347nm and two more absorptions were observed. The absorption at 420nm represents the protonation stage of the PAni chains. The band at 773nm was attributed to the presence of conductive polarons resulting from the doping process [197].

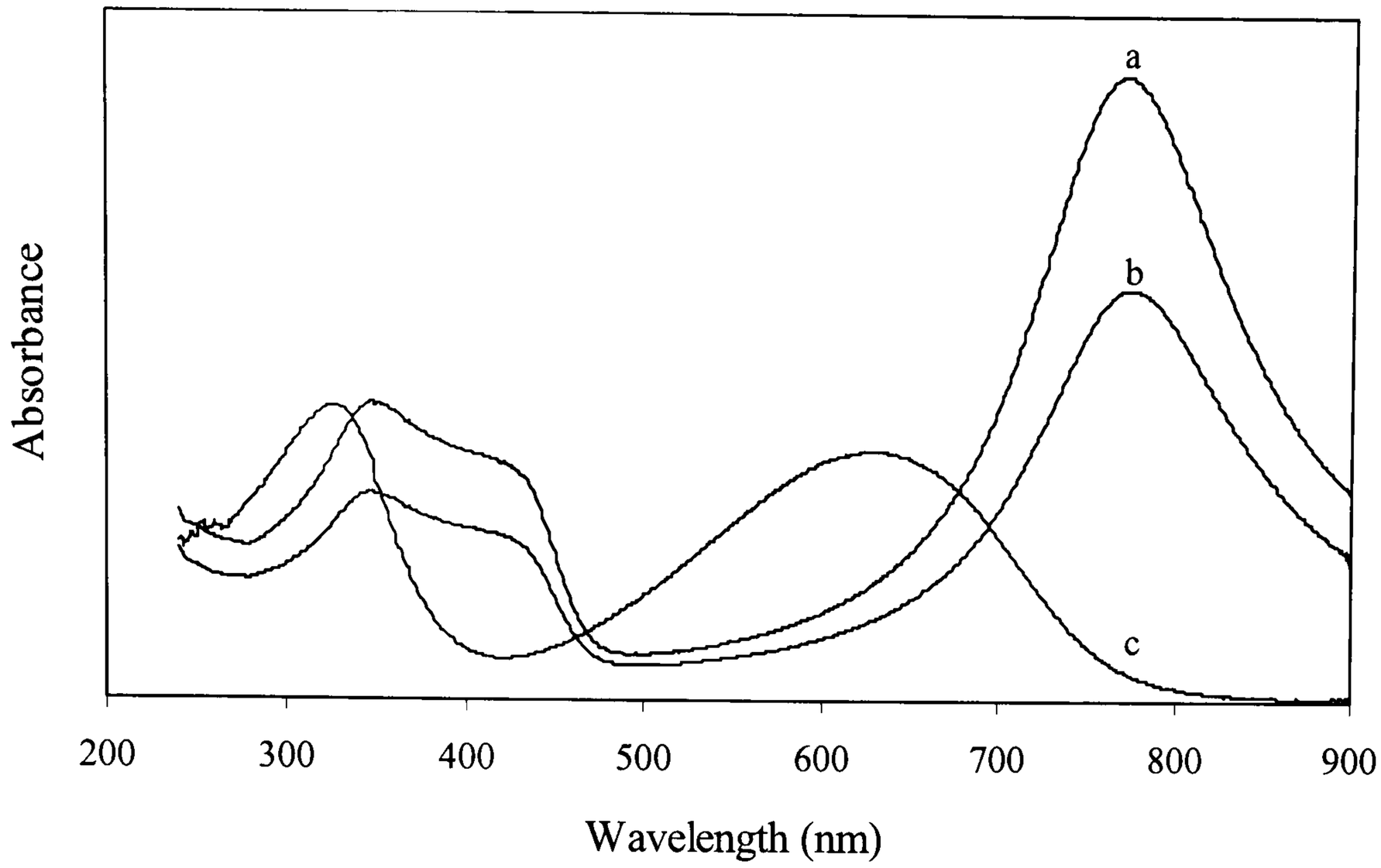


Figure 57 UV-Visible spectra of (a) PAni-DBSA, (b) PAni-DBSA/Hydrin® (20/80) and (c) PAni-EB.

Spectra of PAni-DBSA/ Hydrin® blends verified the initial assumption that PAni-DBSA remained in its doped state, since the characteristic peaks of the doped polymer are observed.

### *4.2.1.6 Morphological Structure*

The morphology of PAni-DBSA/Hydrin® blends was investigated by optical microscopy. The dark region was thought to be polyaniline chains in clusters, probably high molecular weight polyaniline, whilst the lighter region is likely to be related to PAni-DBSA oligomers forming a partial solution within the Hydrin®. A micrograph of the blend containing 1% of PAni-DBSA is shown in Figure 58 (a). It is possible to observe PAni-DBSA particles present in the form of large agglomerates. At this concentration it is postulated that a conducting pathway was formed due to the connection between high molecular weight polyaniline particles and dispersed oligomers in the rubber. This is in agreement with the calculated percolation threshold at 1% (w/w) of PAni-DBSA content, which was much lower than would be expected for percolation by direct contact between spherical particles of PAni-

DBSA in an insulating matrix. As the amount of the conducting polymer in the blends increased, the conducting pathways became denser and the conductivity increased.

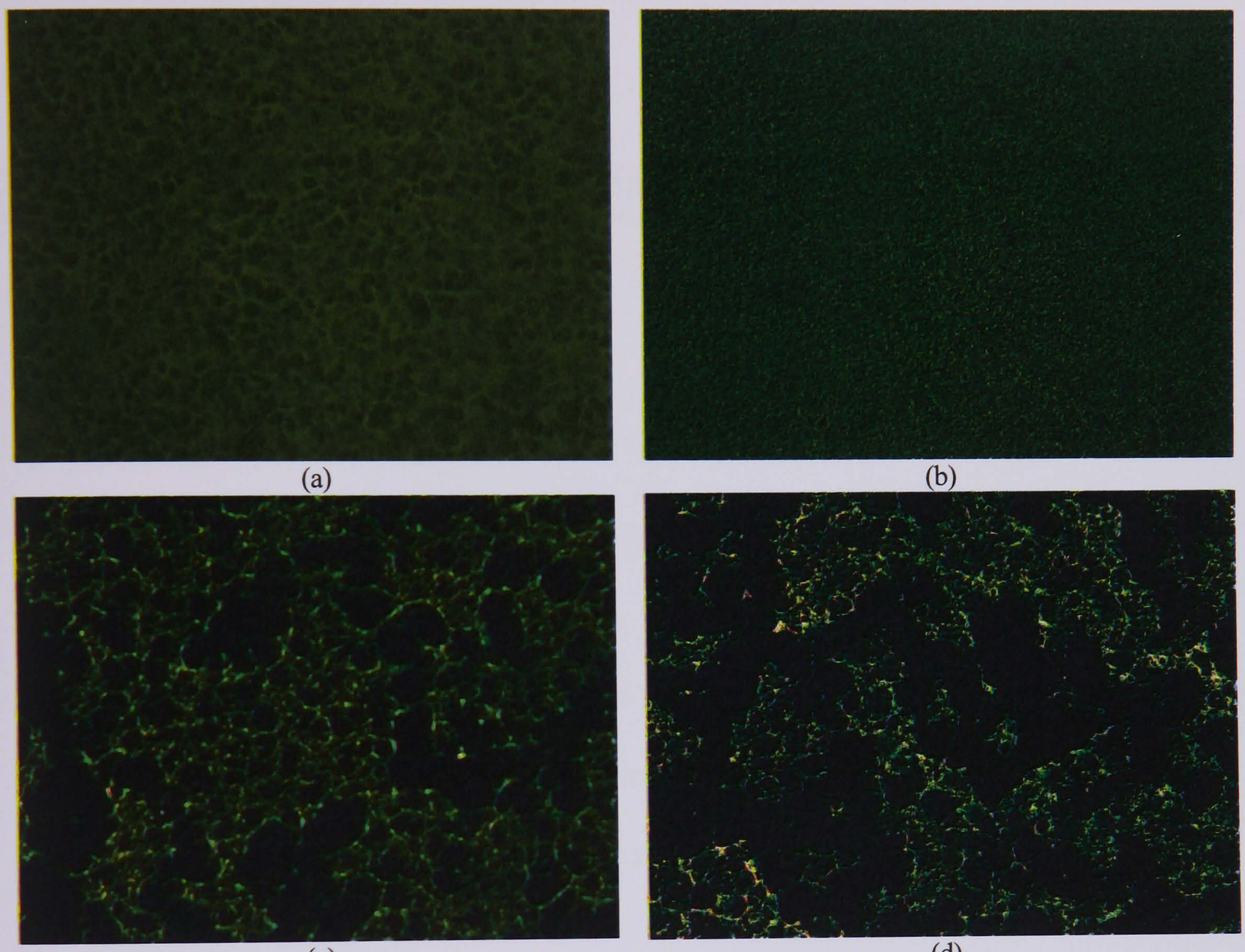


Figure 58 Optical micrographs of thin cast film of PAni-DBSA/Hydrin® blends prepared in solution. Blends contain (a) 1%, (b) 10%, (c) 30% and (d) 50% (w/w) of PAni-DBSA.

### 4.2.1.7 Thermomechanical analysis

Analysis by TMA was performed to characterise the miscibility of PAni-DBSA/Hydrin® blends further. The glass transition temperatures ($T_g$) of the pure materials and the blends are listed in Table 31.

| Blends | PAni-DBSA Content (wt%) | Tg(°C) |
|---|---|---|
| Hydrin® | 0 | -40 |
| PAni-DBSA/Hydrin® | 10 | -37 |
| | 20 | -36 |
| | 25 | -35 |
| | 33.3 | -33 |
| | 50 | -23 |

Table 31 Glass transition temperatures ($T_g$) of the pure materials and the blends.

It was found that there was only one Tg for each blend, and Tg values of various blends shifted to higher temperatures with increasing PAni-DBSA content. The glass transition behaviour indicates good compatibility between conductive polyaniline and the Hydrin®.

### 4.2.1.8 Measurement of vulcanisation behaviour of Zisnet FET-Vulcanised Hydrin rubber

Results from the Rheometer curves are summarised in Table 32. The slowest cure time ($t_{95}$) was identified as about 45min for sample B-001 with 1.6 wt% of added Zisnet-FET. A 38 minute vulcanisation time was therefore used for all blends as a reference, in order to achieve a vulcanising level of 95% or above. It was observed that the vulcanising times of all rubbers slightly decreased with increasing proportion of Zisnet-FET.

| Rheometer value | B-001 | B-002 | B-003 | B-004 |
|---|---|---|---|---|
| Scorch time min | 2.5 | 1.9 | 1.6 | 1.6 |
| Cure time ($t_{95}$) min | 45 | 42 | 40 | 38 |
| Minimum Torque ($M_L$) dNm | 14 | 14 | 11.5 | 12.5 |
| Maximum Torque ($M_H$) dNm | 21 | 40.5 | 41 | 43.5 |

Table 32 Vulcanisation behaviour of Zisnet FET-vulcanised Hydrin rubber.

It was found that each Rheometer curve also showed a constant value after its maximum torque. It is suggested that all rubbers reached their maximum vulcanisation level within the chosen test period i.e. 60 minutes.

### 4.2.1.9 Tensile properties measurement

Figure 59 shows the results of the stress-strain tests Young's modulus E of pure Hydrin and blends.

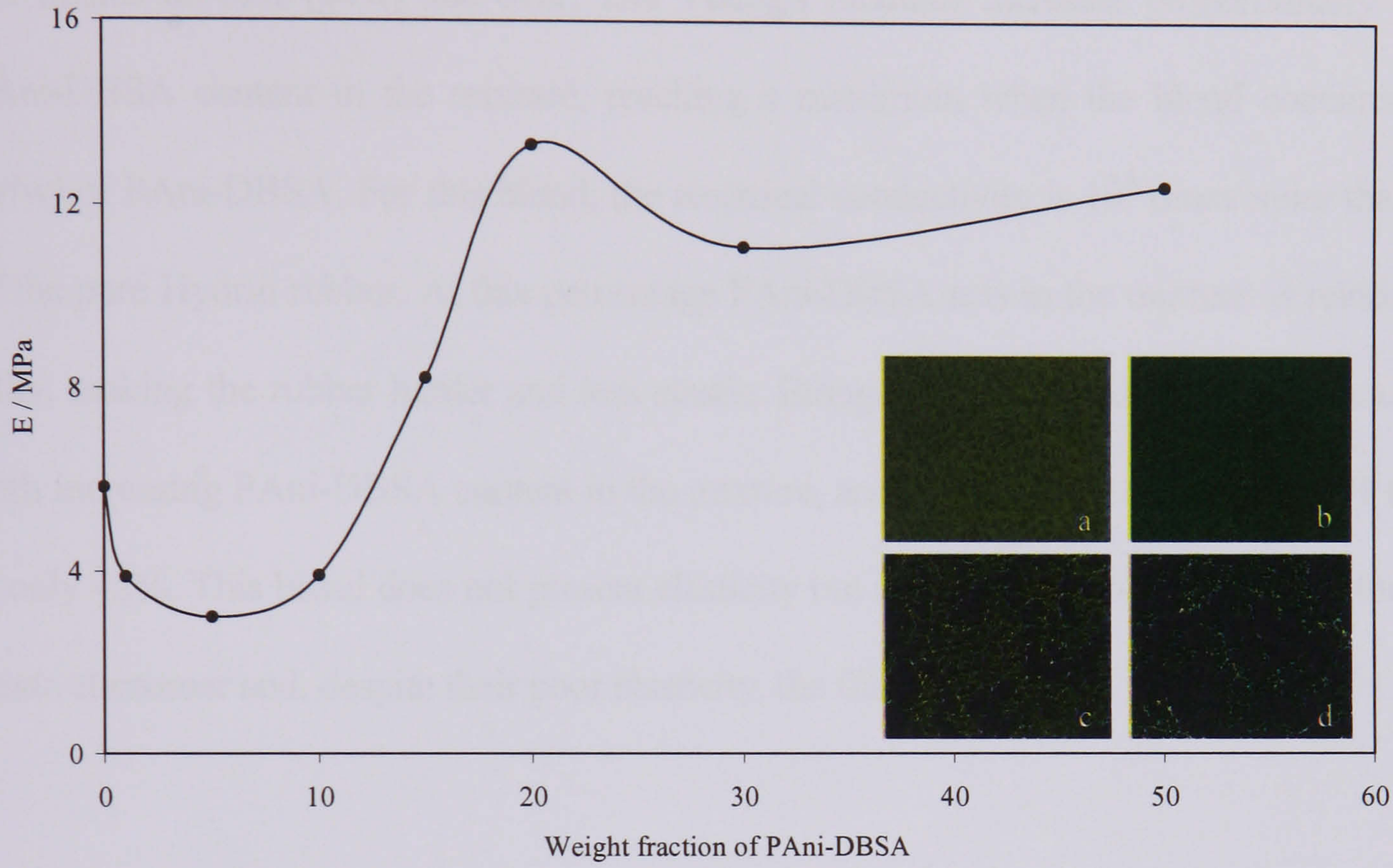


Figure 59 Young's modulus (E) as function of PAni-DBSA content in the mixture. Overlaid with optical micrographs of thin cast film of PAni-DBSA/Hydrin® blends prepared in solution. Blends contain (a) 1%, (b) 10%, (c) 30% and (d) 50% (w/w) of PAni-DBSA.

In the pure rubber, the existence of the highly electronegative chlorine on the backbone of the repeating unit of the monomer leads to dipoles along the polymer chain, resulting in secondary valence forces that reduce the flexibility of the individual molecule and consequently account for the greater rigidity of the rubber in comparison with rubbers like isoprene. However, with the addition of the conductive polymer up to about 10% (w/w), a decrease in Young's modulus is seen. This behaviour is common when a plasticiser is added to a polymer. When 'plasticiser' molecules are interposed between the chains of the polymer, the dipole forces are reduced, enabling the molecules to slide past one another easily and thus increase the flexibility. The changes in properties are due to the irregularity in molecular separation and the intermolecular forces brought about by the introduction of different

molecules in the matrix. This is supported by the optical micrographs of the prepared films which clearly illustrate the close molecular-level interface between the rubber and the conductive filler.

For blends of 10% (w/w) and over, The Young's modulus increases proportionally to the PAni-DBSA content in the mixture, reaching a maximum when the blend contains 20% (w/w) of PAni-DBSA. For this blend, the electrical conductivity is $10^5$ times more than that of the pure Hydrin rubber. At this percentage PAni-DBSA acts in the mixture as reinforcing filler, making the rubber harder and less elastic. Elongation at break decreases continuously with increasing PAni-DBSA content in the mixture, and for the blend containing 50% (w/w) is only 42%. This blend does not present elasticity but is $10^6$ times more conductive than the crude elastomer and, despite their poor elasticity, the films are flexible.

## 4.2.2 Conductive polyaniline/Poly [(acrylonitrile-co-butadiene) /poly vinylchloride] Blends

### *4.2.2.1 Solubility Parameter*

The solubility parameter of THF is known to equal 20.3 $(J.cm^{-3})^{1/2}$, however, in order to ascertain the likelihood of PAni-DBSA and pure grade Nipol® DN171 rubber dissolving in this solvent, their individual solubility parameters need to be similar to that of THF. The equation below was used to calculate their solubility parameters. The miscibility of PAni-DBSA and Nipol® DN171 rubber was rationalised by comparing their solubility parameters.

$$\delta_p = \rho(\Sigma F_i) / M_o$$

where $\delta_p$ represents the solubility parameter $(J.cm^{-3})^{1/2}$, $\Sigma F_i$ represents the total molar attraction constant of all the groups in the polymer repeat units $(J.cm^3)^{1/2}$ $.mol^{-1}$, ρ represents the density of the polymer $(g.cm^{-3})$ and $M_o$ represent the molar mass of polymers smallest repeating units $(g.mol^{-1})$.

Since, the structure of Nipol® DN171 rubber consist of a polyblend of poly(acrylonitrile-co-butadiene)/poly vinylchloride, the solubility parameters of each polymer constituents need to be calculated individually Table 33, shows a detailed composition of the individual polymers as contained in Nipol® DN171.

| (ACN –NBR) | (PVC) | Number of each group | | Molar attraction constant (Fi ) | | Total of group molar attraction constant ($\Sigma F_i$) | |
|---|---|---|---|---|---|---|---|
| A | B | A | B | A | B | A | B |
| -CH2 | -CH2 | 2 | 1 | 269 | 0 | 538 | 269 |
| -CH = | 0 | 4 | 0 | 249 | 0 | 996 | 0 |
| 0 | >CH- | 0 | 1 | 0 | 176 | 0 | 176 |
| 0 | Cl primary | 0 | 1 | 0 | 419 | 0 | 419 |
| -CN | 0 | 1 | 0 | 725 | 0 | 725 | 0 |

Table 33 The number of functional groups present in Nipol DN171 and the corresponding molar absorption constant.

Density of poly(acrylonitrile-*co*-butadiene) = 1.45 $g.cm^{-3}$

Molecular weight of poly(acrylonitrile-*co*-butadiene) = 160 $g.mol^{-1}$

$\delta p = (1.45 \times 2259) / 160 = (3276) / 106 = 20.5\ (J.cm^{-3})^{1/2}$ or 20.5 $(MJ.m^{-3})^{1/2}$

Density of poly vinylchloride = 1.34 $g.cm^{-3}$

Molecular weight of poly vinylchloride repeat unit = 62.5 $g.mol^{-1}$

$\delta p = 1.34\ (864) / 62.5\ g.mol^{-1} = (1157.76) / 62.5 = 18.5\ (J.cm^{-3})^{1/2}$ or 18.5 $(MJ.m^{-3})^{1/2}$

The closeness of the solubility parameters of both THF and PAni-DBSA indicates that they are miscible. Similarly, THF and Nipol DN171 were highly miscible, although there was a slight difference between the solubility parameters of the poly vinylchloride component of the Nipol® DN171 rubber and that of the solvent (THF). Conversely, PAni-DBSA and Nipol® DN171 rubber were highly miscible, due to the fact that their solubility parameters were almost equivalent.

### 4.2.2.2 Electrical Conductivity

The effects of increasing the weight fraction (or concentration) of PAni-DBSA on the electrical conductivity of each blend is illustrated in Figure 60.

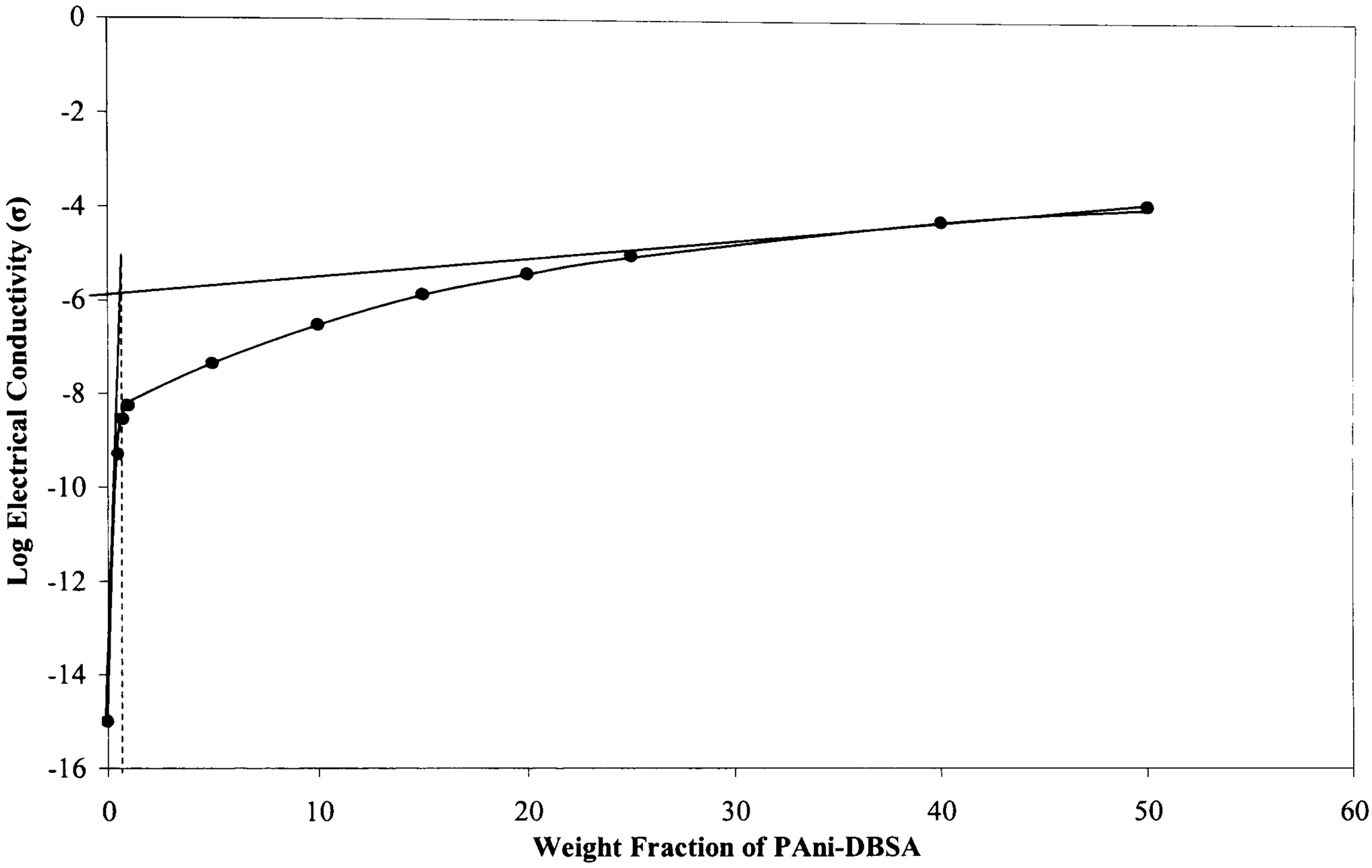


Figure 60 Logarithm of the electrical conductivity (σ) of PAni-DBSA/Nipol® DN171 rubber blends as a function of the weight fraction of PAni-DBSA.

Figure 60 shows a similar correlative trend to those of other polyaniline blends [119,198]. The electrical conductivity of the pure conducting PAni-DBSA was approximately 0.6 $S.cm^{-1}$, and that, of the pure grade Nipol® DN171 elastomer was about $5.4x10^{-16}$ $S.cm^{-1}$. It is immediately apparent that as the weight fraction (or concentration) of PAni-DBSA was decreased from 50 wt% to 0.5 wt%, the electrical conductivity also decreased, as would be expected.

The PAni-DBSA/Nipol® DN171 elastomeric blend consisting of 50wt% of PAni-DBSA exhibited an electrical conductivity of $1.21x10^{-4}$ $S.cm^{-1}$, while that at 0.5wt% was $5.35x10^{-10}$

$S.cm^{-1}$; hence the addition of 0.5wt% of PAni-DBSA to the pure rubber matrix, caused an increase in electrical conductivity of about six orders of magnitude, and a upsurge further in electrical conductivity ensued up to about 1wt% of PAni-DBSA ($4.32x10^{-8}S.cm^{-1}$), followed by a more gradual increase towards a plateau value. The importance of the dilute region is it shows the minimum amount of PAni-DBSA, that must be added to the rubber matrix in order to induce the inception (or onset) of electrical conductivity, which is technically, referred to as the percolation threshold. In addition, these blends exhibited enhanced mechanical properties, when compared with those at higher electrical conductivities [199].

The standard percolation theory (or scaling law of the percolation threshold) [194], in conjunction with the volumetric composition of the each blend (that is, the interaction between PAni-DBSA and the rubber matrix), can be utilised in order to explain the trend in Figure 60. Theoretical studies performed on spherical fillers indicate the occurrence of a percolation threshold at the point where the volume fraction of the filler is about 16% (v/v). However, Figure 60 shows that a percolation threshold of 0.9% (w/w) of PAni-DBSA in the blend [$d_{PAni\text{-}DBSA} = 1.135\ g.cm^{-3}$, $d_{rubber} = 2.83\ g.cm^{-3}$, therefore 0.9% (w/w) = 2.21% (v/v)], resulted in an increase in electrical conductivity of approximately eight orders of magnitude. Hence the percolation threshold is about seven times smaller than that predicated by the theory, suggesting that the formation of a interpenetrating network [199] may have resulted in such a decrease, or the finely dispersed nature of the PAni-DBSA particles within the rubber matrix, may have contributed to the bulk charge transport process [119]. The data in Figure 60 were sufficiently fitted by a simple scaling law based on percolation theory [119] as shown in the equation below:

$$\sigma f = c\,(f\text{-}fp)t$$

where $t$ is the critical exponent, $f$ is the volume fraction of the conductive medium, $f_c$ is the volume fraction at the percolation threshold and $c$ is a constant. Therefore, by plotting log electrical conductivity ($\sigma$) against log ($f - f_c$), the critical exponent (t) can be estimated. At a value of 2.21 v% ($f_c$), the critical exponent was 3.96, with a correlation coefficient (R) of 0.98, which is in good agreement with the percolation theory. Finally, since the size distribution of the conductive particles in the rubber matrix determines the percolation threshold, a non-homogeneous blend may possess a low percolation threshold, and thus, a higher electrical conductivity [200]. The presence of poly vinylchloride (PVC) in the Nipol® DN171 matrix may have contributed to the reduction of the percolation threshold, compared to that of the blend of pure nitrile butadiene rubber (without PVC), and the conducting polymer (PAni-DBSA) [119], as a result of the increase in the overall polarity of the elastomeric chain. This may have led to an improvement in the effective bulk charge transfer due to stronger intermolecular interaction between the conducting polymer particles.

### *4.2.2.3 Electronic Absorption Spectroscopic Analysis*

Figure 61, shows the UV-Visible spectra of pure grade PAni-DBSA and selected PAni-DBSA/Nipol® DN171 blends. The presence of the benzenoid fragments [49] is evident from the bands at 341-351nm, which are indicative of the transfer (or excitation) of electrons from the $\pi$ (bonding) orbital to the $\pi^*$ (anti-bonding) orbital of the benzenoid nitrogen atom. This is a direct consequence of the interaction of PAni-EB with the dopant (DBSA). According to similar studies, the bands at 341-351nm and 410-460nm may be attributed to the $\pi$-$\pi^*$ electronic transition involving both the benzenoid and quinoid fragments [51]. However, the group of bands (polaron lattice bands) at 778-840nm are characteristic of electromic transitions from the HOMO of the benzenoid fragment to the LUMO of the quinoid fragment

[52, 53]. Moreover, since these bands are related to the concentration of PAni-DBSA in each blend, the increase in their intensities (hyperchromic effect) can be rationalised from the expected presence of polarons, as a consequence of doping [201].

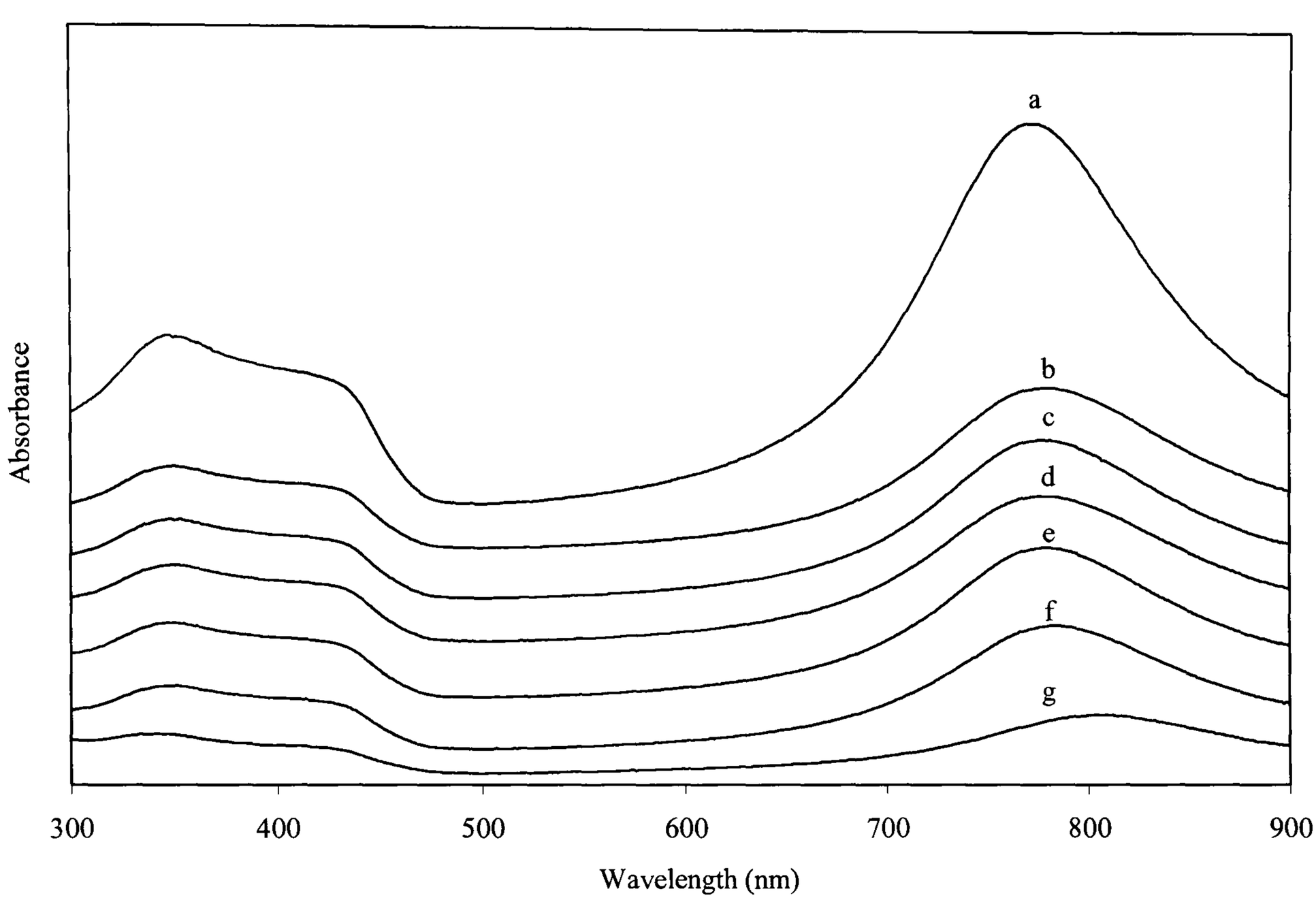


Figure 61 The UV-visible absorption spectra of (a) pure grade PAni-DBSA and selected blends of PAni-DBSA/Nipol® DN171 (b) 50:50, (c) 25:75, (d) 10:90, (e) 5:95 and (f) 1:99.

Furthermore, in this study, it was observed that an increase in the concentration of the conducting medium in each blend, reduced the hypsochromic shift of the polaron bands from 786 to 778nm, however, when the concentration was decreased, a bathochromic shift of the polaron bands from 804 to 840nm (the near IR region) occurred. Consequently, the bathochromic shifts may indicate an increased conjugation length, due to a reduction of the steric hindrance between the benzene fragment and the dopant (DBSA) [201]. It follows that the polarons absorbing at 804 to 840nm are extensively delocalised, while, those absorbing at 786 to 778nm are less delocalised, due to reduced conjugation lengths [148]. As a result, the blends absorbing at 786 to 778nm will exhibit higher conductivities than those absorbing at

804 to 840nm, and this is supported by the trend in the conductivity graph. Overall, the UV-visible spectra indicate that there was no deprotonation of PAni-DBSA by the Nipol® DN171 matrix.

### *4.2.2.4 Infrared Spectra Analysis*

The infrared (IR) spectra (Figure 62 and Figure 63) illustrate the characteristic absorption peaks of the cast films of each elastomeric blend and that of pure Nipol® DN171. By performing an IR spectra analysis, it is possible to establish any intermolecular interaction between the two components. The IR spectra of pure Nipol® DN171 (Figure 63) feature two distinctive absorption peaks at 2923cm$^{-1}$ and 2848cm$^{-1}$, attributed to the presence of aliphatic C-H symmetric and asymmetric stretching vibrations; the band at 2238cm$^{-1}$ is due to the presence of nitrile C-N stretching vibrations in the nitrile butadiene units (NBR). The band at 1637cm$^{-1}$ is due to C=C stretching, 1336 - 1437cm$^{-1}$ to the presence of out of plane C-H wagging, 967 cm$^{-1}$ and 917cm$^{-1}$, represent C-H stretching vibrations in the trans-1,3-butadiene and vinyl butadiene rubber fragments [202], and 690cm$^{-1}$ is ascribed to the C-Cl stretching vibration in poly vinylchloride [203, 37]. Recent reports [203 , 12] show the IR spectra of pure PAni-DBSA contain of unique absorption peaks at 3447cm$^{-1}$, representing free N-H stretching vibrations [10], 1000 and 1030cm$^{-1}$, due to S=O stretching vibrations, 1559cm$^{-1}$ and 1478cm$^{-1}$, representing N=Q=N and N-B-N functionalities [10], 1295cm$^{-1}$, attributed to Q=N-B stretching, 1240cm$^{-1}$, indicating the presence of aromatic C-N stretching, 1102cm$^{-1}$, ascribed to C-H stretching and finally, 797cm$^{-1}$, corresponding to para-substituted out of plane -C-H bending.

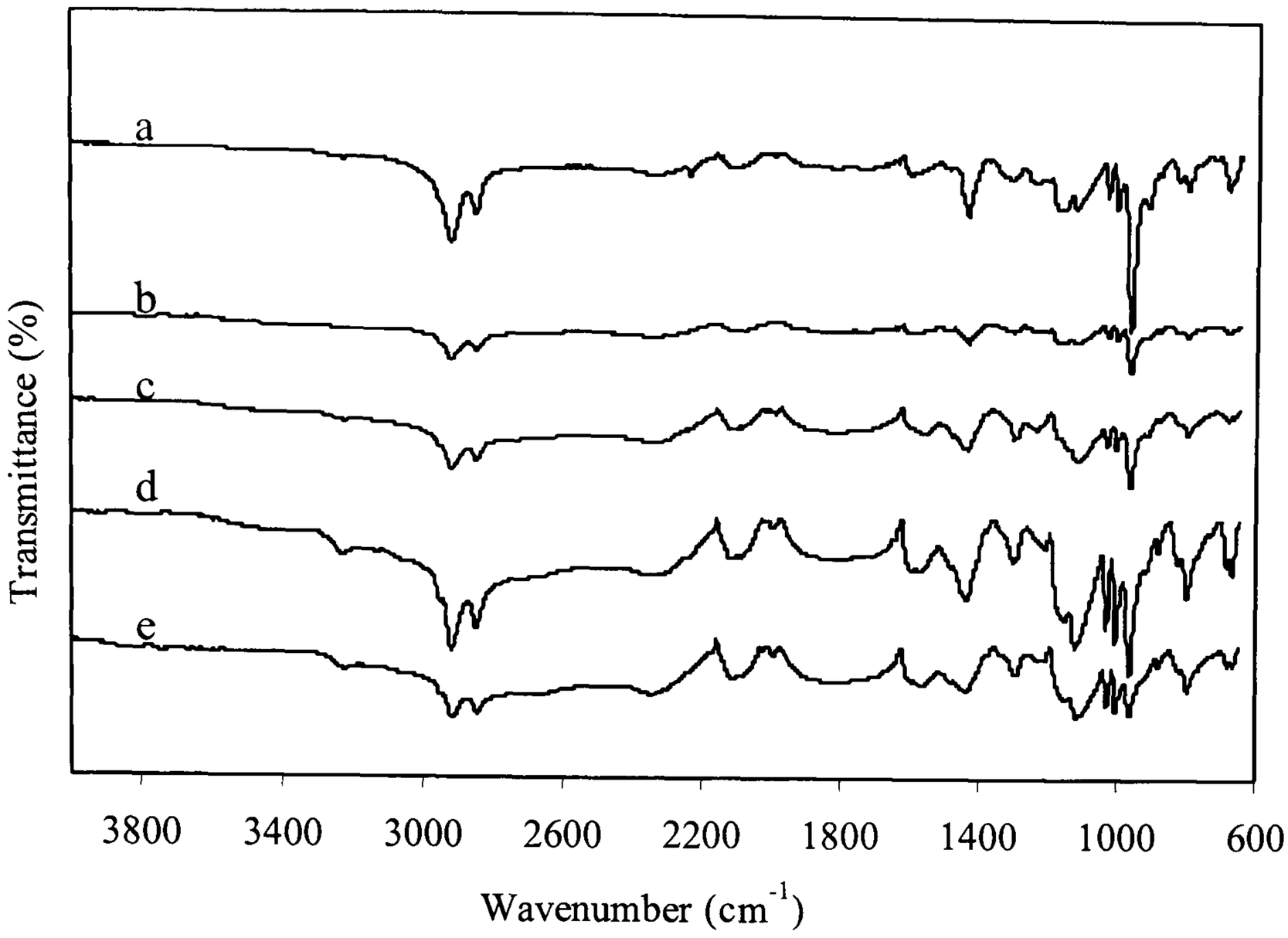


Figure 62 IR spectra of the PAni-DBSA/Nipol® DN171 elastomer blends (at varying ratios). (a) 50%:50%, (b) 40%:60%, (c) 25%:75%, (d) 20%:80%, and (e) 15%:85%.

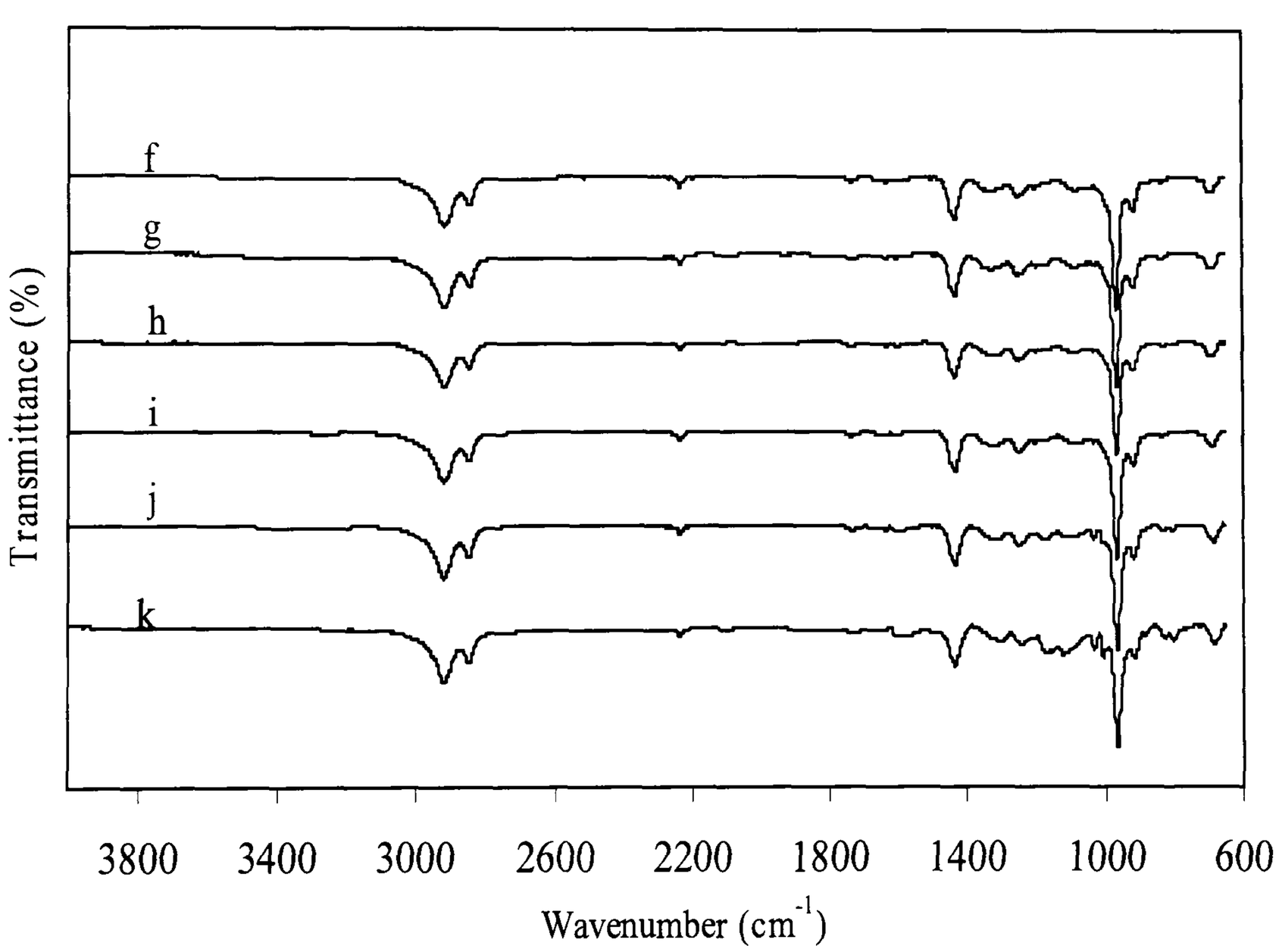


Figure 63 IR spectra of the PAni-DBSA/Nipol DN171 rubber blends (at varying ratios) and pure Nipol DN171 rubber. (f) 10%:90%, (g) 5%:95%, (h) 1%:99%, (I) 0.75%:99.25%, (J) 0.5%:99.5%, and (k) 100% rubber.

An in-depth study of the above IR spectra (Figure 62 and Figure 63) indicates some fundamental peak shifts and variations in peak intensities. It is assumed that the C-H

stretching band at 1102cm$^{-1}$ indicates the level of microscopic electrical conductivity in pure PAni-DBSA [203 ,12], thus, it is referred to as an electronic band and a measure of the degree of delocalization (or redistribution) of electrons along the polymer chain [14]. Inevitably, any changes in the position and intensity of this band are most likely to reflect the electrical conductivity of the conducting polymer. The blend (a) consisting of 50 wt% PAni-DBSA/50 wt% Nipol® DN171 showed a sudden shift in the electronic band (1102-1118cm$^{-1}$), and as the concentration of Nipol® DN171 was increased further (50- 99.5wt %), greater shifts in the electronic bands (1118-1177cm$^{-1}$) ensued. The observed trend is indicative of the increasing distance between the conducting particles in the rubber matrix, thereby, resulting in reduced electronic mobility (hence, a lower conductivity). This is supported by the optical micrographs (c) and (d) in Figure 66, which indicate an increased dispersion of the PAni-DBSA particles in correlation with higher Nipol® DN171 contents. Alterations in the observed positions of imine =N-H stretching (3447cm$^{-1}$) and S=O stretching (1000 and 1030cm$^{-1}$) bands in pure PAni-DBSA were also observed with variations in the concentration of Nipol® DN171. The 50:50wt% PAni-DBSA/Nipol® DN171 blend film showed a shift in the =N-H stretching band (3447-3227cm$^{-1}$) with a shoulder at 3247cm$^{-1}$. As the weight fraction of PAni-DBSA was decreased from 50wt% to 0.5wt%, the frequency of the =N-H stretching band increased further (3227–3267 cm$^{-1}$), accompanied by variations in the shoulder position (3453-3420cm$^{-1}$). Similarly, one of the S=O absorption peaks also shifted (1118-1177cm$^{-1}$), followed by variations in the other (1000-1007cm$^{-1}$); however, this was accompanied by a gradual disappearance of the shoulder, as the weight fraction of Nipol® DN171 reached its maximum. Furthermore, the intensities of the =N-H and S=O stretching bands in each blend film all decreased commensurately as the weight fraction of PAni-DBSA was carefully reduced. These observations suggest that the hydrogen bonding interactions between DBSA and PAni-EB may have been disrupted [203]. The observed variations in the

C-Cl and -CN bands confirm the existence of intermolecular interaction between the imine (=N-H) hydrogen atoms in PAni-DBSA, the highly electronegative chlorine atom ($Cl^-$) in PVC, and the negatively charged cyano ($CN^-$) group.

### *4.2.2.5 Thermal Analysis*

Thermogravimetric Analysis (TGA)

Figure 64 shows schematically, the thermogravimetric curves (or thermograms) of cast films of each blend from 30°C to 600°C.

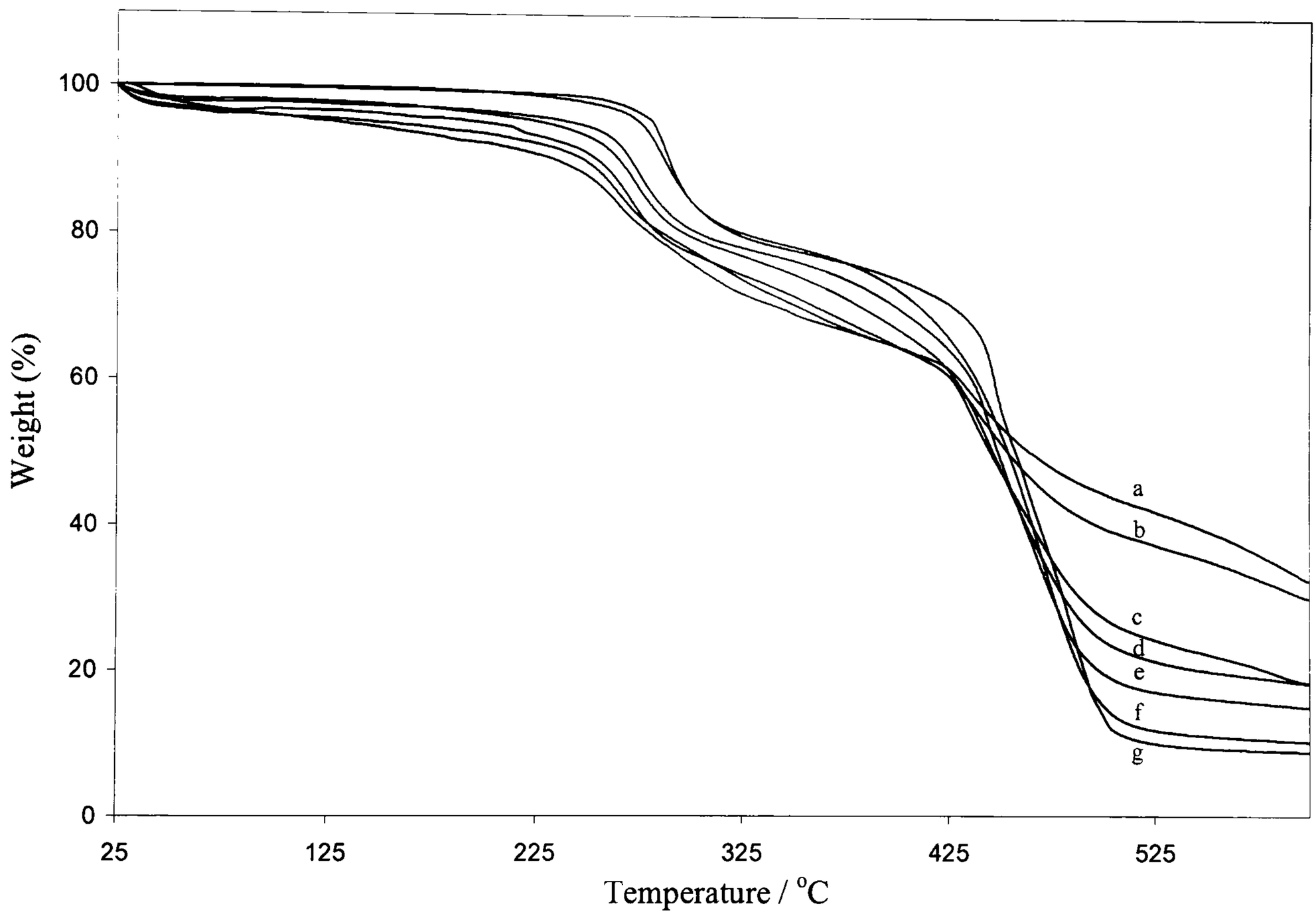


Figure 64 Thermogravimetric curves (at a heating rate of 10°C/min under $N_2$) of selected PAni-DBSA/ Nipol® DN171 blend films (a) 50:50%, (b) 40:60%, (c) 25:75%, (d) 20:80%, (e) 10:90%, (f) 1:99 and (g) pure grade Nipol® DN171.

The curve is divided into three segments, with each segment representing a decomposed or disintegrated fragment, and the corresponding temperature range. As previously stated, this technique gives an insight into the thermal stability of each conducting elastomer being analysed. In the above thermogravimetric curves, segment 1 shows the first change from

30°C to 260°C, which may be attributed to the evaporation of small molecules, such as water ($H_2O$), solvents and most importantly, HCl. The loss of HCl, at this early stage, suggests that, the PVC (thermoplastic) phase of the pure elastomer (Nipol® DN171) may have interacted with the backbone structure of the conducting polymer, thereby, acting as a decomposing-initiator (or a pro-degrading agent [12]). In addition, the thermogram (g) of the pure Nipol® DN171 elastomer correlates with this observation. However, in segment 2 the weight loss occurred at a significantly higher temperature range (from 260°C to 420°C) for each blend (consisting of PAni-DBSA at concentrations ranging from 50wt% to 1wt%). In this region by comparison to that of pure PAni-DBSA [12], the loss is probably attributable to the evaporation of the dopant or surfactant (DBSA) counter-ions, and also the commencement of main chain decomposition of the conducting polymer (PAni-DBSA)[12, 204,205].

The losses (approximately 42%) at segment 3 (420–600°C), are due to the continued disintegration of the main chain of the conducting polymer framework, accompanied by the decomposition of the remaining constituents of the Nipol® DN171 elastomer. In addition, it was observed that as the weight fraction of PAni-DBSA was reduced (from 50 wt% to 1 wt%), there was a corresponding increase in the decomposition temperatures, which supports the notion that the thermal stability of the conducting elastomeric blends is enhanced by the presence of an increasing concentration of Nipol® DN171 in each cast film. This is in accordance with the DSC results, which showed a similar trend.

## Differential Scanning Calorimetry (DSC)

The DSC thermogram (Figure 65) shows the onset temperatures of the major endothermic and exothermic peaks of the cast films of each blend (at specific ratios) and that of pure Nipol® DN171 rubber.

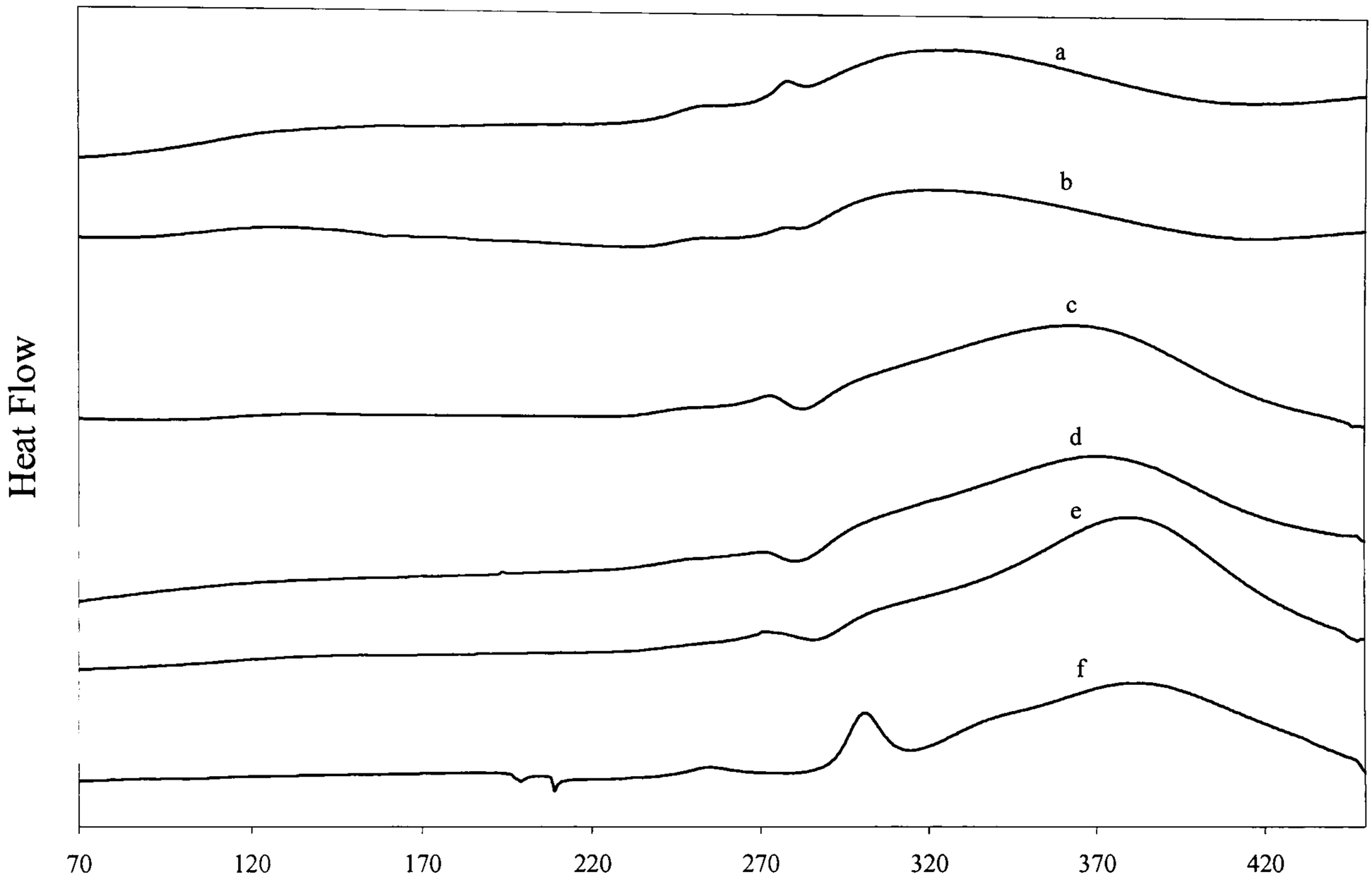


Figure 65 The DSC thermogram (at a heating rate of 10°C/min under $N_2$) of the cast films of the elastomeric blends PAni-DBSA and Nipol® DN171 (PAni-DBSA: rubber). (a) 20:80%, (b) 10:90%, (c) 1:99%, (d) 50:50%, (e) pure rubber, (f) 25:75%.

The thermogram (e) shows two endothermic, and exothermic peaks, which may be attributed to the presence of poly vinylchloride (PVC) and nitrile butadiene rubber (NBR). Recent literature reports [206,61], proposed that, the small exothermic peaks at 195°C and 206°C may be consistent with the process of melting of PVC. However, the exothermic peaks (283°C and 317°C) are associated with the oxidative decomposition of NBR (30wt% ACN) phase of the pure elastomer (Nipol® DN171).

The DSC thermogram (Figure 65), shows significant increases in the onset temperatures of the major endothermic peaks (from 75 to 251°C), as the concentration of the conducting polymer is reduced from 50 to 1wt%. The addition of 50wt% of PAni-DBSA to pure Nipol® DN171, induced a negative shift of the first endothermic peak (from 195°C to 75°C), accompanied by the disappearance of the second (at 206°C). This suggests even mixing of both components [206]. Similarly, a gradual disappearance of the second exothermic peak (at 317°C) was observed, with increasing concentration of PAni-DBSA.

Additionally, with 50wt% of PAni-DBSA added to the rubber matrix, a decrease in the temperature of the first exothermic peak (from 283°C to 232°C) was observed; however, as this amount was gradually reduced (down to 1wt%), the onset temperature of this peak increased (from 231°C to 296°C). This signifies that, as the weight fraction of PAni-DBSA in each blend film is reduced, there was enhancement of the thermal stability [119, 198, 207].

### 4.2.2.6 Morphological Analysis by Optical Microscopy

The optical micrographs (Figure 66) shows the PAni-DBSA/Nipol® DN171 blends at 20x magnification. The light regions in (a) and (b), are thought to represent the mixture of PAni-DBSA oligomers and Nipol® DN171 rubber in each film, while the darker regions may be attributed to the presence of polymeric PAni-DBSA clusters.

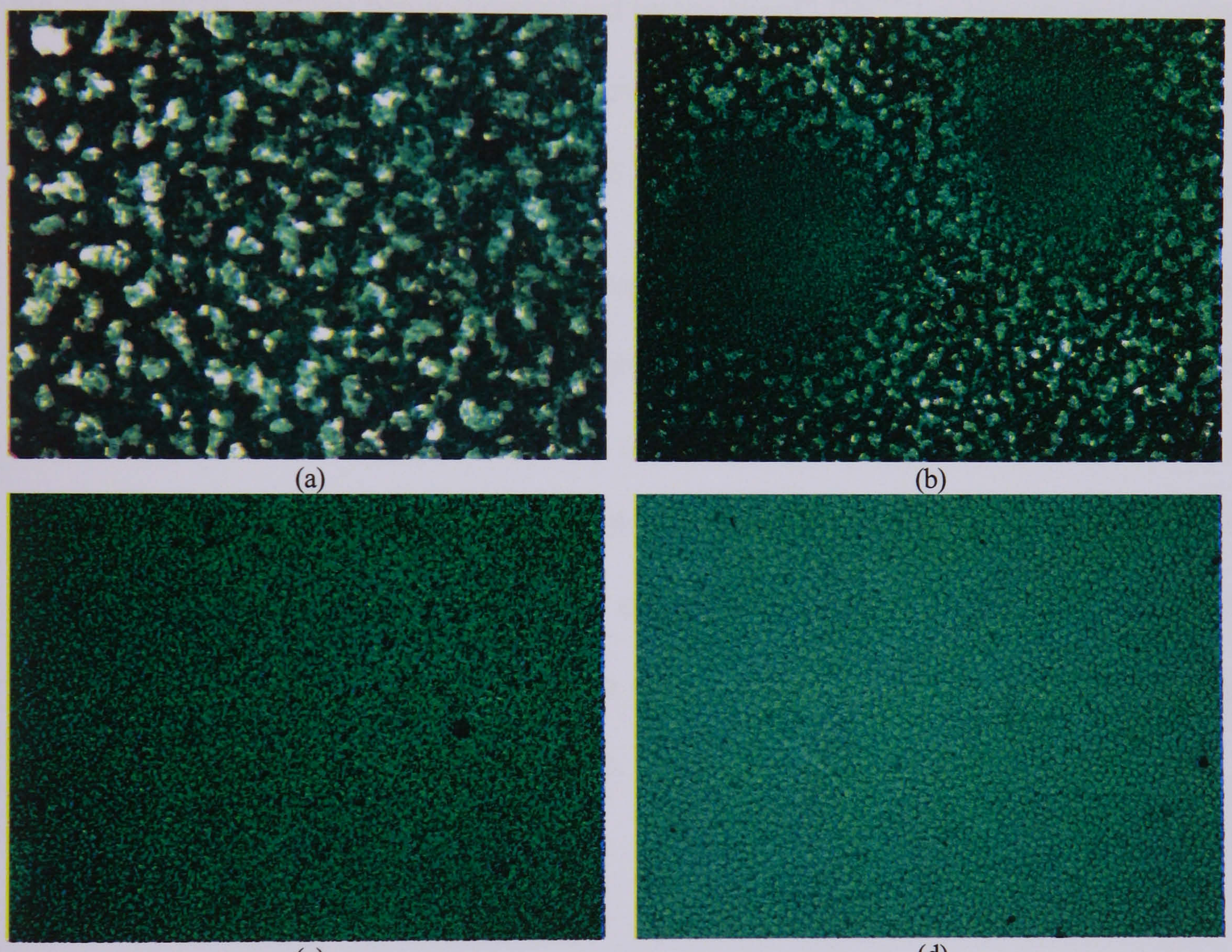


Figure 66 Optical micrographs of selected PAni-DBSA/Nipol® DN171 blend films consisting of (a) 25 wt%, (b) 25 wt%, (c) 20 wt% and (d) 10 wt% PAni-DBSA.

The blend consisting of 25 wt% of PAni-DBSA shows the presence of bulky conductive particles and their interconnected agglomerates, as a consequence of partial phase separation. The networks formed by the agglomerates may act as a conducting pathway, facilitating efficient bulk charge transfer. This explains why the electrical conductivity of this particular

film was higher than those of lower PAni-DBSA content. On the contrary, as the weight fraction of PAni-DBSA is decreased an interesting phenomenon is noticed.

In the micrograph (c) consisting of 20wt% of PAni-DBSA, larger agglomerates with no interconnections are noticeable, with minimal phase separation (but, high isolated particle dispersion), which depicts a reasonably homogeneous phase. This may be a result of some of the PAni-DBSA particles being encapsulated by the Nipol® DN171 rubber matrix, and may have been facilitated by the effect of plasticization/plastification due to the presence of the poly(vinyl chloride). Consequentially, there is reduction in electrical conductivity.

In addition, the insulating and elastomeric properties of the rubber may be partly responsible for the occurrence of such phenomena, which is evidently persistent in the blend films with lower PAni-DBSA concentration. This may result in a high level of isolated dispersion and encapsulation of the conducting particles within the rubber matrix. It can be postulated, that the conducting pathway may have been altered, thereby resulting in a low electrical conductivity. However, the low percolation threshold may be due to the interpenetrating networks formed by the PAni-DBSA clusters.

# CHAPTER 5

# CONCLUSION

*This chapter concludes the findings of the present work. A thorough survey of conducting polyaninline, polyaniside and copolymeres of the latter two, have been presented in this thesis. There were noticeable differences in the behaviour of the two families of polymers. In this work, various polyaniline blends have been prepared and their properties were investgated.*

# 5 Conclusion

Several aniline or anisidine based conducting polymers have been synthesised through suitably tailored synthetic routes. Some of these were later decommissioned due to the insolubility or low conductivity of the doped polymers. DBSA doped polyaniline was successfully synthesised via a controlled oxidation method. Spectral, electrical and thermal measurements were performed to characterise this polymer; it was reasonably soluble in organic solvents such as tetrahydrofuran and chloroform.

Conducting polyanilines and its derivatives were synthesised using two distinct pathways which led to a broad range of morphologies.

When solution polymerisation was employed, the products exhibited non-uniform fibrillar and globular morphologies, and the use of *o*-anisidine as (co-)monomer influenced their morphological characteristics. This co-monomer induced changes in the physical and chemical properties of the final polymer. Having an electron donor attached to the ring, the doped polymer PoAnis displayed lower conductivities than that of pure PAni due to the lower mobility of the charge carriers. Thermogravimetric measurements showed a substantial difference in heat resistance properties for the two polymers. PoAnis degraded more quickly owing to its less ordered structure, and since it was more susceptible to radical cross linking upon oxidation by air due to its higher reactivity, complete degradation was achieved at a lower temperature than for PAni.

With the aim of producing polyaniline particles having homogeneous sizes, shapes, elongation and crystallinity, a wide variety of conducting polyanilines was synthesised. This was achieved *in-situ* by means of sulfonic acid surfactants. These surfactants have the property of thickening the reaction media. They also prevent the growing polymer chains from aggregating and precipitating during the synthesis as in the conventional preparation

method. The sulfonic acids were used during the polymerisations to protonate the aniline monomers prior to their oxidation by APS. When low molecular weight sulfonic acids such as TSA were used, the resulting polymers had similar characteristics to those of PAni-HCl because of the latter's inability to thicken the reaction medium. When larger molecules such as DBSA, CSA, or β- NSA were used, thickening took place. In an aqueous medium, their lipophilic tails attracted one another and self-organised micelles were formed. On the outer part of the micelles, anilinium cations reacted with each other upon addition of the oxidant. This specific arrangement of the monomer units prior to the polymerisation led to various conformational changes in the resulting polymers.

PAni-DBSA/Hydrin® composite films were obtained by solution casting. The PAni-DBSA used to prepare the solution blends was synthesised by a three-step chemical polymerisation method. The theoretically calculated solubility parameters for both the conductive polymer and the Hydrin® were comparable, leading one to expect at least partial miscibility. This was confirmed by studies of the structure and morphology of the blends using ATR-IR spectroscopy and optical microscopy. The IR spectra indicated changing intermolecular interaction with concentrations, shown especially by a shift of the amine (PAni-DBSA) absorption peak to a higher wavenumber.

The electrical conductivity of the blends increased with the proportion of PAni-DBSA, and the percolation threshold was recorded as 1 wt% of the conductive polymer. UV-Visible spectroscopic analysis was used to confirm that the PAni-DBSA remained in the doped state upon blending with Hydrin®. The concentration of PAni-DBSA had a significant influence on the thermal stability of the blends. TMA spectra of the polymer blend exhibited a single Tg, indicating homogeneous single-phase behaviour.

Very promising results were obtained for cast films of the electrically conducting elastomeric blends formed by the co-dissolution of PAni-DBSA and poly(acrylonitrile-co-butadiene) /(poly vinylchloride) or Nipol® DN171 rubber in differing ratios. Electrical conductivity measurements indicate a correlation between the concentration (or weight fraction) of the conducting polymer (PAni-DBSA) and the electrical conductivity. An increase in the concentration of PAni-DBSA, by 50 wt%, was accompanied by an increase in electrical conductivity, from $5.4x10^{-16}$ $S.cm^{-1}$ (for the pure grade Nipol® DN171 rubber) to $1.24x10^{-4}$ $S.cm^{-1}$. In addition, a percolation threshold of 0.9% (v/v) was determined at 2.21% (w/w) of the conducting PAni-DBSA. Morphological or structural analysis of each blend (by optical microscopy) suggested that the increase in electrical conductivity may be due to the formation of interconnected agglomerates with just 20 wt% of PAni-DBSA, which increased with increasing PAni-DBSA content; however, a decline in electrical conductivity was observed for blends with less than 20 wt% of PAni-DBSA, which was attributed to the highly dispersed nature of the PAni-DBSA particles (the discontinuous phase) and the lack of interconnectivity in the rubber matrix (the continuous phase). Analysis of the UV-visible spectra of each blend, indicated the presence of bands due to PAni-DBSA, which showed the retention of its doped form during blending with Nipol DN171 rubber. This was supported by the IR spectra, which showed some characteristic functional groups, attributable to both PAni-DBSA and Nipol® DN171 rubber.

Thermal analysis performed by DSC and TGA, showed that the thermal stability increased with increasing concentration of rubber. The DSC also revealed the compatibility of both PAni-DBSA, and Nipol® DN171 rubber, as result of mixing at ambient temperatures. This observation is in accordance with the solubility parameter calculations, which established the miscibility (or compatibility) of the conducting polymer and the rubber matrix.

The blending of Nipol® DN171 with PAni-DBSA has brought about an advance in the field of electrically conducting polymers, due to a combination of useful properties (that is, high electrical conductivity, chemical, environmental, and thermal stabilities). This electrically conducting elastomer could potentially be used in the automobile industry, alongside various fluoropolymers, which are the main constituents of the gaskets found in motor engines.

## References


1 J. M.G. Cowie, *Polymers: Chemistry and Physics of Modern Materials*, Chapman and Hall, New York, 2nd edition, (1991).

2 V. Schmidt, S. C. Domenech, M. S. Soldi, E. A. Pinheiro and V. Soldi, *Polym. Degrad. Stab.*, **83** (2004) 519.

3 R. J. Young and P. A. Lovell, *Introduction to Polymers*. Chapman and Hall, 2nd edition, (1991).

4 D. R. Rebecca and B. C. Mary, *Mech. Mater.*, **39** (2006) 39.

5 S. Nikolov, R. A. Lebensohn, and D. Raabe, *J. Mech. Phys. Solids*. **54** (2006) 1350.

6 R. Jacques, *J. non-cryst. solids*, **235-237** (1999) 737.

7 G. Odian, *Principles of Polymerisation*. 3rd edition. New York (1991).

8 A. F. Garito and A. J. Heeger, *Acc. Chem. Res.*, **7** (1974) 232.

9 J. H. Perlstein, Angew. *Chem. Int. Ed.*, **16** (1977) 519.

10 M. Aldissi, M. Hou, J. Farrell, *Synth. Met.*, **17** (1987) 229.

11 M. Aldissi, *Polym. Plast. Technol. Eng.*, **26** (1987) 45.

12 M. R. Bryce, A. Chissel, P. Kathirgamanathan, D. Parker, *J. Chem. Soc., Chem. Commun.*, (1987) 466.

13 J. H. Edwards, W. J. Feast, D. C. Bott, *Polym.*, **25** (1984) 395.

14 M. A. De-Paoli, R. J. Waltman, A. F. Diaz, J. Bargon, *J. Polym. Sci. Polym. Chem.*, **23** (1985) 1687.

15 B. Scrosati, *Applications of Electroactive Polymers*, Chapman and Hall, London (1993).

16 S. Etemad, *Ann. Rev. Phys. Chem.*, **33** (1982) 443.

17 M. Nechtstein, *Phys. Rev. Lett.*, **44** (1980) 356.

18 H. Shirakawa and S. Ikeda, *J. Polym.*, **2** (1971) 231.

19 Y. Ito, H. Shirakawa and S. Ikeda, *J. Polym. Sci. Polym. Chem.*, **12** (1974) 11.

20 G. Natta, P. Corradini, G. Mazzanti, *Atti. Accad. Naz. Lincei Cl. Sci. Fis. Mat. Nat. Rend.*, **25** (1958) 3.

21 M. Hatano, S. Kambara, S. Okamoto, *J. Polym. Sci.*, **51** (1961) S26.

22 R. B. Kaner, A. G. MacDiarmid, *Sci. Am.*, **258** (1988) 60.

23 H. Shirakawa, E. J. Louis, A.G. MacDiarmid, C. K. Chiang, A. J. Heeger, *J. Chem. Soc., Chem. Commun.*, (1977) 578.

24 J. Margolis, *Conductive Polymers and Plastics*, Chapman and Hall, New York (1989).

25 I. M. Cambell, *Introduction to Synthetic Polymers*, Oxford Science Publications, (1994) 196.

26 K. Seeger, *Angew. Makromol. Chem.*, **109/10** (1982) 227.

27 X. Z. Yang, J.C.W. Chien, *J. Polym. Sci. Polym. Chem. Ed.*, **23** (1985) 859.

28 H. Naarmann, *Electronic Properties of Conjugated Polymers*, (H. Kuzmany, M. Mehring and S. Roth (Eds.), Springer-Verlag, *Solid State Sci.*, **76** (1987) 12.

29 C. K. Chiang, C. R. Fincher, A. J. Heeger, H. Shirakawa, A.G. MacDiarmid, *Phys. Rev. Lett.*, **39** (1977) 1089.

30 A. F. Diaz, *J. Electrochem. Soc.*, **123** (1989) 115.

31 R. J. Waltman, *Can. J. Chem.*, **64** (1986) 76.

32 A. F. Diaz, J. A. Logan, *J. Electroanal. Chem.*, **111** (1980) 111.

33 G. Tourillon, F. Garnier, *J. Electroanal. Chem.*, **135** (1982) 173.

34 A. F. Diaz, K. K. Kanazawa, G. P. Gardini, *J. Chem. Soc., Chem. Commun.*, (1979) 635.

35 J. L. Bredas, R. R. Chance and R. Silbey, *Phys. Rev.*, Part B., **B26(10)** (1982) 5843.

36 C.Rebbi, *Sci. Am.*, **240** (1979) 92.

37 J. L. Bredas and G. B. Street, *Acc. Chem. Res.*, **18** (1985) 309

38 R. Qian and J. Qiu, *J. Polym.*, **19** (1987) 157.

39 J. Roncali, F. Garnier, M. Lemaire and R. Garreau, *Synth. Met.*, **15** (1986) 323.

40 S. Sadki, P. Schottland, N. Brodie, G. Sabouraud, *Chem. Soc. Rev.*, **29** (2000) 283.

41 R. B. Kaner and A. G. MacDiarmid, *Sci. Am.*, **258** (1988) 106.

42 C.E. Tang, *Appl. Phys. Lett.*, **48** (1986), 183.

43 J. Jaglarz, A. Kassiba, P. Armatys, M. Pokladko, E. Gondek, J. Sanetra, *Mater. Sci.*, **22**(2004) 389.

44 D. W. Berry, *J. Electrochem. Soc.*, **132** (1985) 1022.

45 W. K. Lu, R. L. Elsenbaumer, and B. Wessling, *Synth. Met.*, **71** (1995) 2163.

46 S. Sathiyanarayanan, S. Muthkrishnan, G. Venkatachari, *Prog. Org. Coat.*, **53** (2005) 297.

47 C. Y. Lee, H. G. Song, K. S. Jang, E. J. Oh, A. J. Epstein, and J. Joo, *Synth. Met.*, **102** (1999) 1346.

48 D. Cottevieille, A. Le Mehaute, C. Challioui, P. Mirebeau, J. N. Dernay, *Synth. Met.*, **101** (1999) 703.

49 A. A. Syed, M. K. Dinesan, *Talanta*, **38** (1991) 815-837.

50 J. Fritzche, *J. Prakt. Chem.*, **20** (1840) 453.

51 M. Smith and O. Meth-cohn, *J. Chem. Soc., Perkin Trans* **1** (1994) 5.

52 A. S. Travis and O. Meth-Cohn, *Chem. Br.*, **31** (1995) 547.

53 H. Letheby, *J. Chem. Soc.*, **15** (1862) 161

54 H. S. Nalwa, *Handbook of Organic Conductive Molecules and Polymers*, John Wiley and Sons, Chichester, **2** (1997) 506.

55 R. Willstatter, C. W. Moore, *Chem. Ber.*, **40** (1907) 2665.

56 R. Willstatter, S. Dorogi, *Chem. Ber.*, **42** (1909) 4118.

57 A. G. Green, A. E. Woodhead, *J. Chem. Soc.*, **97** (1910) 2388.

58 A. G. MacDiarmid, J. C. Chiang, W. S. Huang, S. L. Mu, N. L. D. Somasiri, W. Wu, S. I. Yaniger, *Mol. Cryst. Liq. Cryst.*, **121** (1985) 173.

59 A. G. MacDiarmid, A. J. Epstein, *Faraday Discuss. Chem. Soc.*, **88** (1989) 317.

60 A. G. MacDiarmid, J. C. Chiang, *Synth. Met.*, **13** (1986) 193.

61 E. M. Geniès, A. Boyle and M. Lapkowski, *Synth. Met.*, **36** (1990) 139.

62 X. Andrieu, L. Josset, J. F. Fauvarque, *J. Chem. Phys.*, **92** (1995) 879.

63 T. Matsunaga, H. Daifuku, T. Nakajima, T. Kawagoe, *In Polymers for Advanced Technologies*, John Wiley & Sons, New York, **1** (1990) 33.

64 R. V. Gregory, W. C. Kimbrell, H. H. Kuhn, *Synth. Met.*, **28** (1989) C823.

65 A. G. MacDiarmid, A. Ray, A. F. Richter, *Synth. Met.*, **29** (1989) E151-E156.

66 A. G. MacDiarmid, , J. C. Chiang, A. F. Richter, A. J. Epstein, *Synth. Met.*, **18** (1987) 285.

67 K. G. Noeh, E. T. Kang, K. L. Tan, *Synth. Met.*, **40** (1991) 341.

68 E. M. Genies, M. Lapkowski, *J. Electroanal. Chem.*, **220** (1987) 67.

69 A. G. MacDiarmid, *Synth. Met.*, **125** (2002) 14.

70 F. Lux, *Polym.*, **35** (1994) 2915.

71 J. Stejskal, P. Kratochvil, A. D. Jenkins, *Polym.*, **37** (1996) 367.

72 E. T. Kang, K. G. Neoh, K. L. Tan, *Prog. Polym. Sci.*, **23** (1998) 277.

73 W. S. Huang, B. D. Humphrey, A. G. MacDiarmid, *J. Chem. Soc., Faraday Trans.*, **1** (1986) 2386.

74 A. J. Heeger, *Angew. Chem. Int. Ed. Engl.*, **40** (2001) 2591.

75 A. J. Epstein, A. G. MacDiarmid, *Mol. Cryst. Liq. Cryst.*, **160** (1988) 165.

76 F. Wudle, R. O. Angus, F. L. Lu, P. M. Allemand, D. J. Vachon, M. Nawok, Z. X. Liu, A. J. Heeger, *J. Am. Chem. Soc.*,**109** (1987) 3677.

77 A. G. MacDiarmid, A. J. Epstein, *in Science and applications of conducting polymers* W. R Salaneck, D. T. Clark, E. J. Samuelsen, Editors. Adam Hilger, Bristol (1990).

78 Z. H. Wang, C. Li, E. M. Scherr, A.G. MacDiarmid, A. J. Epstein, *Phys. Rev. Lett.*, **66** (1991) 1745.

79 S. P. Armes, J. F. Miller, *Synth. Met.*, **22** (1988) 385.

80 Y. Cao, A. J. Heeger, P. Smith, *Polym.*, **30** (1989) 2309.

81 L. M. Abrantes, J. P. Correia, M. Savic, G. Jin, *Electrochim. Acta.*, **46** (2001), 3181-3187.

82 G. J. Cruz, J. Morales, M. M. Castillo-Ortega, R. Olayo, *Synth. Met.*, **88** (1997) 213-218.

83 R. Noufi, A. J. Frank, A. J. Nozik, *J. Am. Chem. Soc.*, **103** (1981) 1849-50.

84 R. Noufi, D. Tench, *J. Electrochem. Soc.*, **127** (1980) 188-90.

85 D. M. Mohilner, R. N. Adams ,W. J. Argersinger, *J. Am. Chem. Soc.*, **84** (1962) 3618.

86 M. Doriomedoff, F. H. Cristofini, R. De. Surville, M. Josefowiez, L. T. Yu, R. Buvet, *J. Chem. Phys.*, **68** (1971) 1055.

87 L.T. Yu, M. S. Borredon, R. Buvet, G. Belorgey, *J. Polym. Sci.*, **10** (1987) 2931.

88 C. Y. Yang, P. Smith, A. J. Heeger, Y. Cao, and J. E. Osterholm, *Polym.*, **35** (1994) 1142-1147.

89 H. Morgan, P. J. S Foot, N. W. Brooks, *J. Mater. Sci.*, **36** (2001) 5369-77.

90 A. J. Motheo, J. R. Santos, E. C. Venancio, L. H. C. Mattoso, *Polym.*, **39** (1998) 6977-82.

91 B. Beau, J. P.Travers, E. Banka, *Synth. Met.*, **101** (1999) 772-75.

92 I. J. Ball, S. C. Huang, R. A. Wolf, J. Y. Shimano, and R. B. Kaner, *J. Membr. Sci.*, **174** (2000) 161-176.

93 Show-An Chen, Hsun-Tsing Lee, *Macromol.*, **28** (1995) 2858-2866.

94 L. H. Dao, M. Leclerc, J. Guay, J. W. Chevalier, *Synth. Met.*, **29** (1989) E377-E382.

95 J. Yue, A. J. Epstein, A. G. MacDiarmid, *Mol. Cryst. Liq. Cryst.*, **189** (1990) 255-61.

96 F. Cataldo, P. Maltese, *Eur. Polym. J.*, **38** (2002)1791-803.

97 S. C. Ng, H. S. O. Chan, H. H. Huang, and P. K. H. Ho, *Chem. Commun.*, (1995) 1327-1328.

98 K. G. Neoh, E. T. Kang, K. L Tan, *Polym. Degrad. Stab.*, **43** (1994)141-47.

99 Show-An Chen, Gue Wuu Hwang, *Polym.*, **38** (1997) 3333-46.

100 Ali Al Ghamdi, Al Saigh, Y. Zeki, *J. Chromatogr. A*, **969** (2002) 229-243.

101 L. Ding, X. Wang, R. V. Gregory, *Synth. Met.*, **104** (1999) 73-78.

102 Yen Wei, Hsueh, F. Kesyin, *J. Polym. Sci.*, Part A: *Polym. Chem.*, **27** (1989) 4351-63.

103 L. S. Tan, S. R. Simko, S. J. Bai, R. A. Vaia, B. E. Taylor, M. D. Houtz, M D. Alexander, R. J. Spry, *J. Polym. Sci.*, Part B: *Polym. Phys.*, **39** (2001) 2539-48.

104 R. Mathew, B.R. Mattes, M. P. Espe, *Synth. Met.*, **131** (2002) 141-47.

105 J. A. Conklin, S. C. Huang, S. M. Huang, T. Wen, R. B. Kaner, *Macromol.*, **28** (1995) 6522.

106 J. Lippe, R. Holze, *J. Electroanal. Chem.*, **339** (1992) 411-422.

107 A. Pron, P. Rannou, *Prog. Polym. Sci.*, **27** (2001) 135-90.

108 G. M. Morales, M. C. Miras, C. Barbero, *Synth. Met.*, **101** (1999) 686.

109 B. Wang, J. Tang, F. Wang, *Synth. Met.*, **18** (1987) 323-28.

110 G. Zotti, S. Cattarin, N. Comisso, *J. Electroanal. Chem. Interfac. Electrochem.*, **239** (1988) 387-96.

111 J. Desilvestro, W. Scheifele, *J. Mater. Chem.*, **3** (1993) 263-72.

112 P. Nunziante, G. Pistoia, *Electrochim. Acta*, **34** (1989) 223-28.

113 L. J. Duic, Z. Mandic, F. Kovacicek, *J. Polym. Sci.*, Part A: *Polym. Chem.*, **32** (1994) 105.

114 H. Tang, A. Kitani, M. Shiotani, *Electrochim. Acta*, **41** (1996) 1561-67.

115 D. Warren, Brazil and the struggle for Rubber: A study of environmental history. Cambridge: Cambridge University press (1987).

116 M. Russell, V. Pool, J. M. Kelso and V. J. Tomazic-Jezic, *Vaccine*, **23** (2004) 664-667.

117 K. Cornish, *J. Photochem.*, **57** (2001) 1123-1134.

118 M. A. De Paoli, W. A. Gazotti, E. M. Girotto, M. A. S. Spinace, *Solids State Ionics*, **130** (2000) 281.

119 K. C. Yong, P. J. S. Foot, H. Morgan, S. Cook and A.J. Tinker, *Eur. Polym. Soc.*, **42** (2006) 1716-1727.

120 J. A. Manson, L. H. Sperling, *Polym. Blen. Compos.*, Plenum Press, New York, 1976.

121 D. R. Paul, S. Newman (Eds.), *Polymer Blend*s, Academic Press, New York, 1978.

122 H. Scher, R. Zallen, *J. Chem. Phys.*, **53** (1970) 3759 -3761.

123 M. J. Powell, *Phys. Rev. B*, **20** (1979) 4194-4198.

124 R. H. Norman, *Conductive Rubbers and Plastics*. England; Elsevier, (1970) 3-4.

125 R. H. Norman, *J. European Rubber*, **20** (1981) 169.

126 E. K. Sichel, *Carbon Black-Polymer Composites: The Physics of Electrically Conducting Composites (Plastics engineering)*, Marcel Dekker Inc, New York, (1982).

127 G. Jiang, M. Gilbert, D. J. Hitt, G. D. Wilcox, and K. Balasubramanian, *Compos. Part A-Appl. Sci.*, **33** (2002)745.

128 S. K. Bahattacharya, and R. P. Kusy. Metal-Filled Polymers: Properties and Applications. New York:Marcel Dekker.(1986).

129 L. Rupprecht, *Conductive Polymers and Plastics in Industrial Applications*, Plastics Design Library, USA, 1999.

130 J. E. Österholm, et al., *Synth. Met.*, **55** (1993) 1034.

131 J. D. Macinnes and D. B. L. Funt, *Synth. Met.*, **25** (1988) 235-242.

132 A. Srivastava, V. Singh, A. Chandra, K. Witte, U. W. Scherer and T. V. Singh, *Nuclear Instruments and Methods in Physics Research Section B: Beam Interactions with Materials and Atoms*, **245** (2006) 277-280.

133 Y. Haba, et al., *Synth. Met.*, **110** (2000) 189.

134 M. Wan and J. Li , *J. Polym. Sci. A*, **38** (2000) 2359.

135 S. Quillard, et al., *Synth. Met.*, **50** (1992) 525.

136 N.V. Bhat, D.T. Seshadri, and R.S. Phadke, *Synth. Met.*, **130** (2002)185.

137 F.Cataldo, *Polym. Degrad. Stab.*,**75** (2002) 93.

138 A.A. Athawale, M.V. Kulkarni, and V.V. Chabukswar, *Mater. Chem. Phys.*, **73** (2002) 106.

139 J. Tang, et al., *Synth. Met.*, **24** (1988) 231.

140 X. Lu, et al., *Synth. Met.*, **128** (2002)167.

141 Y. Cao, et al., *Synth. Met.*, **16** (1986) 305.

142 X. Lu, et al., *Synth. Met.*, **138** (2003) 429.

143 X.-R. Zeng, and T.-M. Ko, *Polym.*, **39** (1998)1187.

144 L.H.C. Mattoso, A.G. MacDiarmid, and A.J. Epstein, *Synth. Met.*, **68** (1994)1.

145 W.A.J. Gazotti and M.-A. De Paoli, *Synth. Met.*, **80** (1996) 263.

146 A.Gruger, et al., *J. Mol. Struct.*, **328** (1994) 153.

147 Z. Ping, H. Neugebauer, and A. Neckel, *Electrochim. Acta*, **41** (1996) 767.

148 D.C. Trivedi, *Handbook of Organic Conductive Molecules and Polymers,* John Wiley & Sons Ltd., ed. H. S. [Nalwa]Vol. **2** (1997).

149 K.G. Neoh, E.T. Kang, and K.L. Tan, *Polym.*, **34** (1993) 3921.

150 M.G. Han, et al., *Synth. Met.*,**126** (2002) 53.

151 J. E. Osterholm, et al., *Polym.*, **35** (1994) 2902.

152 W. R. Salaneck, B. Liedberg Inganas, R. Enandsson, A.G. MacDiarmid, M. Halpem, L. Lundstrom, N.L.D. Somasim, *Mol. Cryst. Liq. Cryst.*, **121**(1985) 191.

153 W. H. Jang, et al., *Colloid and Polymer Science*, **279** (2001) 823.

154 M. Trchova, J. Prokes, and J. Stejskal, *Synth. Met.*, **101** (1999) 840.

155 J. W. Kim, H. J.C., K. To, *Polym. Eng. Sci.*, **39** (1999)1493.

156 A. N. Aleshin, et al., *Synth. Met.*, **99** (1999) 27.

157 A. J. Motheo, M. F. Pantoja, and E. C. Venancio, *Solid State Ionics*, **171** (2004) 91.

158 H. H.Wieder, *Materials Science Monographs*. Vol. 2. 1979, Amsterdam: Elsevier.

159 M. Cochet., et al., *Synth. Met.*, **84** (1997) 757.

160 Y. Cao and P. Smith, *Polym.*, **34** (1993) 3139.

161 P. Rannou, A. Pron, and M. Nechtschein, *Synth. Met.*, **101** (1999) 827.

162 J. Y. Shimano and A.G. MacDiarmid, *Synth. Met.*, **123** (2001) 251.

163 S. Kim, J. M. Ko and I. J. Chung, *Polym. Adv. Technol.*, **7** (1996) 559.

164 O. T. Ikkala, L. O. Pietla, P . Passiniemi, T. Vikki, H. Osterholm, *Synth. Met.*, **84** (1997) 55.

165 K. Pielichowski, *Solid State Ionics*, **104** (1997) 123.

166 T. L. A. Campos, D. F. Kersting, and C. A. Ferreira, *Surface and Coatings Technology*, **122** (1999) 3.

167 P. Ghosh, et al., *Synth. Met.,* **123** (2001) 83.

168 H.Q. Xie, , Y. M. Ma, and D. S. Feng, *Eur. Polym. J.*, **36** (2000) 2201.

169 P. C. Rodrigez, et al., *Polym.*, **43** (2002) 5493.

170 M. K. Traore, W. T. K. Stevenson, B. J. McCormick, R. C. Dorey, Shao Wen, D. Meyers, *Synth Met.*, **40** (1991)137.

171 H. S. O. Chan, M. Y. B. Teo, E. Khor, C. N. Lim, *J. Therm. Anal.*, **35** (1989) 765.

172 H. Wu-Song, B. D. Humphrey, and A. G. MacDiarmid, *J. Chem. Soc.*, Faraday Transactions, **82** (1986) 2385.

173 S. P. Armes and J.F. Miller, *Synth. Met.*, **22** (1988) 385.

174 S. P. Armes, et al., *Langmuir*, **7** (1991) 1447.

175 M. Wan and J. Li, *J. polym. sci.* part A, **38** (2000) 2359.

176 D. Chattopadhyay and B.M. Mandal, *Langmuir*, **12** (1996) 1585.

177 J. Joo, et al., *Phys. Rev. B*, **57** (1998) 9567.

178 J. P. Pouget, et al., *Macromol.*, **24** (1991) 779.

179 M.C. Gupta, S.S.Umare, *Macromol.*, **25** (1992) 138.

180 L. H. C. Mattoso, et al., *Synth. Met.*, **52** (1992) 171.

181 Z. Wei, Z. Zhang, and M. Wan, *Langmuir*, **18** (2002) 917.

182 A. R Hopkins, R. A. Lipeles, and W. H. Kao, *Thin Solid Films*, **447-448** (2004) 474.

183 M.Wan, et al., *Synth. Met.*, **135-136** (2003)175.

184 S. Li, Y. Cao, and Z. Xue, *Synth. Met.*, **20** (1987) 141.

185 Z. Zhang and M. Wan *Synth. Met.*, **132** (2003) 205.

186 W. Luzny, et al., *Synth. Met.*, **90** (1997) 19.

187 E. Bankaand, W. Luzny, *Synth. Met.*, **101** (1999) 715.

188 D. Djurado, et al., *Synth. Met.*, **84** (1997 ) 121.

189 M. J. Winokur, H. Guo, and R. B. Kaner, *Synth. Met.*, **119** (2001) 403.

190 E. A. Collins, J. Bares, F. W. Billmeyer, *Experiments in Polymer Science*, Wiley-Interscience, New York, (1973).

191 M. Zilberman, G. I. Titelman, A. Segmann, Y. Haba, M. Narkis, D. Alperstein, *J. Appl. Polym. Sci.*, **66** (1997) 243.

192 K. L. Hoy, *J. Paint Technol.*, **42** (1970) 76.

193 D. Goncalves, A. Waddon, F. E. Karasz, L. Akcelrud, *Synth. Met.*,**74** (1995) 197.

194 R. Zallen, *The Physics of Amorphous Solids*, Wiley, New York.(1983).

195 Y. Cao, P. Smith, A. J. Heeger, *Synth. Met.*, **48** (1992) 91.

196 W. S. Huang, A. G. MacDiarmid, *Polym.*, **34** (1993) 1833.

197 Y. Xia, Wie singer, A. G. MacDiarmid, A. J. Epstein, *Chem. Mater.*,**7** (1995) 443.

198 Z. K. Abbas, S. J. Barton, P. J. S. Foot, and H. Morgan, *Polym. Polym. Compos.*, **15** (2007) 1.

199 W. A. Gazotti, Jr., R. Faez and M. De Paoli, *Eur. Polym. J.*, **35** (1999) 35-40.

200 W. J. Bae, W. H. Jo and Y. H. Park, *Synth. Met.*, **132** (2003) 239-244.

201 E. M. Geniès, A. Boyle and M. Lapkowski, *Synth. Met.*, **36** (1990) 139.

202 W. Zheng, M. Angelopoulos, A. J. Epstein and A.G. MacDiarmid, *Macromol.*, **30** (1997)2953– 2955.

203 T.A. Skotheim, *Handbook of Conducting Polymers*, Marcel Dekker, New York **1- 2** (1986).

204 J. Stejskal, I. Sapurina, M. Trchová, E. N. Konyushenko and P. Holler, *Polym.*, **47** (2006) 8253–8262.

205 I. M. Campbell, *Introduction to Synthetic Polymers*, Oxford University Press, Oxford (1994).

206 G. Broza, K. Piszczck, K. Shulte, and I. Sterzynski, *Compos. Sci. Technol.*, **67** (2007) 890 – 894.

207 R. K. Paul and C. K. S. Pillar, *Synth. Met.*, **114** (2000) 27-35.